

VOLATILE FATTY ACID METABOLISM IN THERMOPHILIC AEROBIC
DIGESTION OF SLUDGE

by

ANGUS CHU

B.Sc., The University of British Columbia, 1988
M.Sc., The University of British Columbia, 1990

A THESIS SUBMITTED IN PARTIAL FULFILLMENT OF
THE REQUIREMENTS FOR THE DEGREE OF
DOCTOR OF PHILOSOPHY

in

THE FACULTY OF GRADUATE STUDIES

(Department of Civil Engineering)

We accept this thesis as conforming
to the required standard

THE UNIVERSITY OF BRITISH COLUMBIA

July 1995

© Angus Chu, 1995

In presenting this thesis in partial fulfilment of the requirements for an advanced degree at the University of British Columbia, I agree that the Library shall make it freely available for reference and study. I further agree that permission for extensive copying of this thesis for scholarly purposes may be granted by the head of my department or by his or her representatives. It is understood that copying or publication of this thesis for financial gain shall not be allowed without my written permission.

(Signature)

Department of CIVIL ENGINEERING

The University of British Columbia
Vancouver, Canada

Date July 6, 1995

Abstract

The efficacy of Volatile Fatty Acid (VFA) production in Thermophilic Aerobic Digestion (TAD) of primary sludge was investigated. This research program was carried out in a pilot scale, TAD process, located in the wastewater treatment pilot plant site, at the University of British Columbia. Preliminary results showed that the highest accumulation of VFA (950 mg/L as acetate) had occurred, under microaerobic conditions (air flow rate of between 0-0.17 V/V-h), in the first stage of the 150 L, 2-stage process. The two other aeration conditions examined (transition-air flow rate of 0.28 V/V-h and aerobic-air flow rate of 0.6 V/V-h) accumulated negligible amounts of VFA. Therefore, the subsequent research concentrated on the first stage of the TAD process, under microaerobic conditions. The two independent variables examined were air flow rates and solids retention times (SRT). The three SRTs tested were 3, 4.5 and 6 days. The four air flow rates examined were assigned the labels true anaerobic, low flow microaerobic, medium flow microaerobic and high flow microaerobic conditions. Net VFA production was found to be a function of both aeration and SRT. In general, as SRT and air flow rates decreased, net VFA production increased (specifically acetate and propionate). The measured concentration of any species of VFA, at any given time, was a function of both the relative rates of its synthesis and biodegradation. Decreasing or increasing the aeration rate and/or SRT resulted in a proportional change in VFA accumulation. The maximum measured acetate accumulation rate occurred under the 4.5 d SRT and the true anaerobic condition.

A biochemical model was developed in order to explain the process of VFA metabolism in TAD. In this process, under strict anaerobic conditions, bacteria must achieve oxidation/reduction balance by diverting the catabolic flow of carbon to fermentative end products (eg. propionate) that will consume NADH (Nicotinamide Adenine Dinucleotide). The key issue in fermentation is the recycling of NADH by the conversion of specific intermediates to different fermentation products which regenerate NAD^+ . The oxidation of intermediates that required the net reduction of NAD^+ cannot proceed under fermentative conditions. Consequently, these catabolic intermediates added under batch test conditions, using TAD sludge, under anaerobic conditions, remained in their unoxidized form and persisted in the medium. The oxidation of intermediates which required no net reduction of NAD^+ can and did proceed under fermentative conditions. Under strict anaerobic conditions, the VFA profiles in the pilot scale TAD process were similar to fermentation type processes (eg. an even distribution of VFA between acetate and propionate).

When the bioreactors were operated under microaerobic conditions (ie. oxygen demand is greater than oxygen supply), metabolism resulted in a characteristic VFA distribution profile with acetate as the predominant VFA produced (up to 80% of the total VFA). Propionate constituted the second largest fraction at 11%. Under this microaerobic condition, the NADH produced during oxidation of substrates could be reoxidized by operation of the respiratory chain. Therefore, the carbon flow could be uncoupled from the necessity to maintain redox balance via fermentative means. This separation would presumably allow the organisms in a TAD process to maximize ATP (adenosine triphosphate) production by increasing the flux of

intermediates to acetate. The majority of the substrates examined under batch test conditions, with TAD process biomass, under microaerobic conditions, were oxidized to an acetate intermediate.

Table of Contents

ABSTRACT	ii
TABLE OF CONTENTS	v
LIST OF FIGURES	viii
LIST OF TABLES	xiii
ACKNOWLEDGMENTS	xiv
1. INTRODUCTION	1
2. LITERATURE REVIEW	3
2.1 Autothermal Thermophilic Aerobic Digestion	3
2.1.1 The Autothermal Process	4
2.1.2 Process Development	7
2.2 Enhanced Biological Phosphorus Removal Process Model	8
2.3 Acetate Production in ATAD	11
2.4 Thermophilic Pre-Stage Process (Dual Digestion)	13
2.4.1 Anaerobic Digestion: Substrate Specificity During Phase Separation	15
2.4.2 Phase Separation	16
2.5 Thermodynamics and Metabolism	18
2.5.1 Energy Production (ATP)	21
2.5.2 Bacterial Energetics	22
2.5.3 NADH	26
3. METHODS AND MATERIALS	29
3.1 Thermophilic Aerobic Digester	29
3.1.1 Preliminary Operational Phase	29
3.1.2 Second Phase of Operation	31
3.2 Aeration	33

3.2.1 Preliminary Operational Phase	34
3.2.2 Second Phase of Operation	34
3.3 Volatile Fatty Acids	35
3.4 Ethanol and Propanol Determination	36
3.5 Pyruvic and Lactic Acid Determination	36
3.6 Total and Inorganic Carbon	36
3.7 Solids	37
3.8 On Line Data	37
3.9 Batch Experiment	38
4. RESULTS AND DISCUSSION	41
4.1 Batch Experiments	41
4.1.1 Fermentative and Oxidative VFA Metabolism in TAD	41
4.1.2 Substrate Addition Experiments	45
4.1.2.1 Valerate and Butyrate Addition Experiments	49
4.1.2.2 Isobutyrate, Isovalerate and 2-Methylbutyrate Addition Experiments	54
4.1.2.3 Pyruvate and Lactate Addition Experiments	60
4.1.2.4 Ethanol and Propanol Addition Experiments	66
4.1.2.5 Effects of Different Classes of Macromolecules on VFA Metabolism	72
4.1.3 2, 4-Dinitrophenol Addition Experiment	81
4.1.4 Response of Biomass from a Fermenter Process to Anaerobic and Microaerobic Conditions	86
4.1.5 Fermentative TAD Experiments	95
4.1.6 Salmon Arm ATAD Performance	99
4.2 Preliminary Pilot Scale TAD Experiments	105
4.3 3 x 3 Pilot Scale TAD Experiments	115
4.3.1 Temperature Variation of Pilot Scale TAD experiments	116
4.3.2 On Line ORP Measurements as State Variable	121
4.3.3 VFA Accumulation in TAD	123
4.3.3.1 Variability of VFA Measurements	123
4.3.3.2 VFA Accumulation in Pilot Scale TAD Experiments	129
4.3.3.3 Kendall's Tau-b and Analysis of Variance of VFA Data	137
4.3.3.4 Response Surface Plots of VFA Production in Pilot Scale TAD	140
4.3.4 TAD Pilot Scale Process pH	143
4.3.5 Total and Volatile Solids Reduction of the Pilot Scale TAD Process	146

4.3.5.1 Role of Enzymes in Solids Destruction	152
4.3.5.2 Solids Destruction Variability Discussion	153
4.3.6 Salmon Arm ATAD	154
5. OVERVIEW AND SUMMARY	159
5.1 Biochemical Model of Substrate Metabolism in TAD	159
5.2 Acetate Accumulation Phenomenon in TAD	165
5.3 ¹⁴C-Acetate Label Experiment	167
5.4 Acetate Production in Microorganisms	168
6. CONCLUSIONS AND RECOMMENDATIONS	174
6.1 Conclusions	174
6.2 Recommendations	176
7. REFERENCES	180
APPENDIX A: BATCH TEST RESULTS	190
APPENDIX B: 3X3 PILOT SCALE TAD RESULTS	250
APPENDIX C: PRELIMINARY PILOT SCALE TAD RESULTS	293
APPENDIX D: TEST CHEMICALS	299

List of Figures

2. 1	Heat balance schematic of a thermophilic aerobic digester (adapted from EPA, 1990).	6
2. 2	Biochemical model of phosphate accumulation the a) anaerobic and b) aerobic zones of a Bio-P process (from Comeau, 1988).	10
2. 3	Variations in the concentrations of VFA during the biodegradation of yeast cells by aerobic thermophilic bacteria under oxygen limiting conditions (from Mason, 1986).	12
2. 4	Principal sequences of anaerobic digestion (Fox and Pohland, 1994).	17
2. 5	Overall organization of electron transport and oxidative phosphorylation (adapted from Lehninger, 1982).	25
2. 6	Pathways involved in the fermentation of glucose (adapted from Boyd, 1984).	28
3. 1	Schematic of the UBC pilot scale TAD process a) operating in series (1st and 2nd phases) and b) under the parallel mode of operation (A and B sides).	30
4. 1	Comparison of acetate and propionate concentrations between the anaerobic and microaerobic conditions. a) acetate response and b) propionate response.	42
4. 2	Comparison of butyrate and 2-methylbutyrate concentrations between the anaerobic and microaerobic conditions. a) butyrate response and b) 2-methylbutyrate response.	43
4. 3	Comparison of isovalerate and valerate concentrations between the anaerobic and microaerobic conditions. a) isovalerate response and b) valerate response.	44
4. 4	VFA response in batch TAD experiment to propionate addition. a) microaerobic control b) microaerobic with propionate addition c) anaerobic control d) anaerobic with propionate addition.	47
4. 5	Difference plots of the propionate addition experiment under a) microaerobic and b) Anaerobic conditions.	50
4. 6	Difference plots of the valerate addition experiment under a) microaerobic and b) anaerobic conditions.	51
4. 7	Difference plots of the butyrate addition experiment under a) microaerobic and b) anaerobic conditions.	52

4. 8 β -oxidation of butyric and valeric acids (adapted from Lehninger, 1982).	53
4. 9 Difference plots of the isobutyrate addition experiment under a) microaerobic and b) anaerobic conditions.	55
4. 10 Difference plots of the isovalerate addition experiment under a) microaerobic and b) anaerobic conditions.	56
4. 11 Difference plots of the 2-methylbutyrate addition experiment under a) microaerobic and b) anaerobic conditions.	57
4. 12 Reactions for the oxidation of the branched chain amino acids by bacteria (adapted from Sokatch <i>et al.</i> , 1968).	58
4. 13 Difference plots of the pyruvate addition experiment under a) microaerobic and b) anaerobic conditions.	61
4. 14 Difference plots of the lactate addition experiment under a) microaerobic and b) anaerobic conditions.	62
4. 15 Formation of propionate and acetate from DL-lactate via the acrylate pathway (Gottschalk, 1986).	65
4. 16 Difference plots of the ethanol addition experiment under a) microaerobic and b) anaerobic conditions.	67
4. 17 Difference plots of the propanol addition experiment under a) microaerobic and b) anaerobic conditions.	68
4. 18 VFA difference profiles under anaerobic conditions for a) linoleic acid and b) glucose addition experiments.	73
4. 19 VFA difference profiles under anaerobic conditions for the a) dextrin and b) peptone addition experiments.	74
4. 20 VFA difference profiles under microaerobic conditions for the a) linoleic acid and b) glucose addition experiments.	75
4. 21 VFA difference profiles under the microaerobic condition for the a) dextrin and b) peptone addition experiments.	76
4. 22 Fermentation of pyruvate to propionate via the succinate-propionate pathway (Gottschalk, 1986).	78

4. 23 Formation of CO₂, lactate and ethanol from glucose by the heterofermentative pathway. (Gottschalk, 1986). 79
4. 24 2, 4-Dinitrophenol addition experiment under a) anaerobic and b) microaerobic conditions. 83
4. 25 VFA, pH and ORP profiles in the 2, 4-dinitrophenol addition experiment under microaerobic conditions. a) control condition and b) 2,4-dinitrophenol addition condition.84
4. 26 Fermenter process sludge response to increasing primary sludge addition under anaerobic conditions. a) acetate profiles and b) propionate profiles. 87
4. 27 Fermenter process sludge response to increasing primary sludge addition under microaerobic conditions. a) acetate profiles and b) propionate profiles. 88
4. 28 TAD process sludge response to increasing primary sludge addition under anaerobic conditions. a) acetate profiles and b) propionate profiles. 89
4. 29 TAD process sludge response to increasing primary sludge addition under microaerobic conditions. a) acetate profiles and b) propionate profiles. 90
4. 30 Comparison of maximum rate of VFA production between TAD and fermenter process biomass under a) anaerobic and b) microaerobic conditions. 93
4. 31 Comparison of maximum achievable concentration of VFA between TAD and fermenter process biomass under a) anaerobic and b) microaerobic conditions. 94
4. 32 VFA profiles of fermentative TAD biomass response to increasing primary sludge addition under a) microaerobic and b) anaerobic conditions. 97
4. 33 VFA profiles of control side TAD biomass response to increasing primary sludge addition under a) microaerobic and b) anaerobic conditions. 98
4. 34 VFA difference plots of Salmon Arm ATAD sludge under anaerobic conditions to a) primary and b) waste activated sludge additions. 101
4. 35 VFA difference plots of Salmon Arm ATAD sludge under anaerobic conditions to a) propionate and b) a mixture of primary and waste activated sludge additions. 102
4. 36 VFA difference plots of Salmon Arm ATAD sludge under microaerobic conditions to a) primary and b) waste activated sludge additions. 103

4. 37 VFA difference plots of Salmon Arm ATAD sludge under microaerobic conditions to a) propionate and b) a mixture of primary and waste activated sludge additions. 104
4. 38 The transition condition in the first stage of the TAD process (air flow rate of 0.28 V/V-h). a) An example of one cycle of ORP and temperature profiles. b) VFA profiles of the same cycle. 107
4. 39 ORP and VFA profiles in the first stage of the TAD process under a) microaerobic (air flow rate of 0 V/V-h) and b) aerobic conditions (0.6 V/V-h). 108
4. 40 ORP and VFA profiles in the first stage of the TAD process during a switch from a) microaerobic to aerobic conditions and from b) aerobic to microaerobic conditions. 109
4. 41 Comparison of the net acetate and net total VFA production in the first stage of the TAD process under the three aeration conditions. 110
4. 42 Examples of on line temperature measurements during pilot scale TAD experiments 118
4. 43 Temperature effects in TAD reactors from changing Turborator rotational speed. 119
4. 44 Examples of on line ORP measurements during pilot scale TAD experiments. a) ORP variation of both sides over a period of 12 days and b) an extract of the same period showing shark tooth pattern. c) Fast Fourier transform of this ORP data. 120
4. 45 Variation of acetate concentrations over time in the pilot scale TAD experiments with a 3 d SRT. a) A side and b) B side. 124
4. 46 Variation of acetate concentrations over time in the pilot scale TAD experiments with a 4.5 d SRT. a) A side and b) B side. 125
4. 47 Variation of A side propionate concentrations over time for all 10 runs. 126
4. 48 Variation of B side propionate concentrations over time for all 10 runs. 127
4. 49 Acetate accumulation in pilot scale TAD experiments on the a) A and b) B sides. 130
4. 50 Propionate accumulation in pilot scale TAD experiments on the a) A and b) B sides. 131
4. 51 Isobutyrate accumulation in pilot scale TAD experiments on the a) A and b) B sides. 132
4. 52 Isovalerate accumulation in pilot scale TAD experiments on the a) A and b) B sides. 133

4. 53 VFA accumulation normalized to their respective control values. a) acetate and b) propionate.	135
4. 54 VFA accumulation normalized to their respective control values. a) isobutyrate and b) isovalerate.	136
4. 55 Response surface plots of daily VFA accumulation normalized to their respective control values for a) acetate and b) propionate.	141
4. 56 Response surface plots of daily VFA accumulation normalized to their respective control values for a) isobutyrate and b) isovalerate.	142
4. 57 Experimental reactor (B side) pH values over time for all 10 runs.	144
4. 58 Average pH values of the a) A side and b) B side bioreactors.	145
4. 59 Total solids destruction capacity in pilot scale TAD experiments on the a) A (control) and b) B (experimental) sides.	148
4. 60 Total volatile solids destruction capacity in pilot scale TAD experiments on the a) A (control) and b) B (experimental) sides.	149
4. 61 Total and volatile solids destruction capacities normalized to their control values. a) Total solids and b) volatile solids.	150
4. 62 District of Salmon Arm ATAD process schematic.	155
4. 63 District of Salmon Arm ATAD reactor temperatures during the a) March, 1993 visit and b) May, 1994 visit.	156
4. 64 Salmon Arm ATAD VFA profiles in all three cells during the a) March, 1993 visit and b) May, 1994 visit.	157
5. 1 Biochemical model of acetate production in TAD under a) microaerobic and b) anaerobic conditions.	160
5. 2 Summary of carbon flow from substrate addition experiments under a) microaerobic and b) anaerobic conditions.	161
5. 3 Comparison between oxygen demand and oxygen supply of any aerobically metabolizing culture.	164

List of Tables

3. 1 Comparison of pilot scale TAD parameters and recommended values (EPA, 1990; Kelly, 1990).	31
3. 2 Combination of aeration and SRT for each experimental run.	32
4. 1 Selected acetogenic reactions.	69
4. 2 Duration of microaerobiosis during the three aeration conditions in the first stage of the TAD process.	111
4. 3 Comparison of VFA distribution between 2 thermophilic aerobic digestion processes and 2 fermentation processes.	112
4. 4 Descriptive statistics of air flow rates and SRTs of pilot scale TAD experiments.	116
4. 5 Matrix of Kendall's tau-b correlation coefficients for both acetate and propionate accumulation values versus time.	138
4. 6 Analysis of variance table for acetate and propionate accumulation.	140

Acknowledgments

I would like to express my gratitude to all the individuals involved in the completion of this thesis:

I would first like to thank my supervisor, Dr. D. S. Mavinic, Head of the Environmental Engineering Group at UBC, for his encouragement, understanding and unwavering support throughout the completion of this research. I am grateful to Dr. W. K. Oldham, Dr. W. D. Ramey, Dr. E. Hall and H. G. Kelly for serving on my supervisory committee and for their constructive criticisms and valuable suggestions through both the research phase and the preparation of the final report.

I would also like to acknowledge the excellent technical support of the staff of the Environmental Engineering Lab. Special thanks goes to the District of Salmon Arms wastewater treatment plant operators, Hart Frese and Lee Robinson, for their assistance and cooperation during the final phase of the research program.

Financial support for the study was provided by both grants and in kind contributions from the Natural Sciences and Engineering Research Council of Canada (NSERC), Dayton and Knight Ltd. and Turborator Technologies Inc.

1. Introduction

The widespread application of sewage treatment processes to satisfy increasingly stringent legislation concerning aqueous discharges into surface waters has resulted in increased sludge production and exacerbated problems of sludge disposal. Throughout the world considerable attention is being directed into the treatment and ultimate disposal of sludge resulting from the purification of domestic wastewaters.

In 1991, a research program was undertaken, in the Civil Engineering Department, at the University of British Columbia, to investigate specific aspects of a process known as Thermophilic Aerobic Digestion (TAD). This thesis is specifically concerned with the phenomenon of Volatile Fatty Acid (VFA) metabolism in TAD process biomass, as well as the factors that affect VFA production. The purpose for studying VFA metabolism in TAD will be introduced and reviewed in the following section. This literature review briefly introduces the various topics of interest which specifically deals with the autothermal thermophilic aerobic digestion process.

The objectives of the research were two fold. The first research goal was to map the metabolic pathways of various carbon substrates in a mixed culture biomass. A batch test apparatus was used to examine the biochemistry involved in substrate metabolism in TAD, specifically acetate metabolism (Results and Discussion, section 4.1). The second objective was to maximize VFA production by optimization of two independent variables (ie. Solids Retention

times [SRT] and aeration rates). The effects of varying these two parameters were studied on a pilot scale TAD process, located in the wastewater treatment pilot plant site, at the University of B.C. (sections 4.2 and 4.3).

The overview and summary section covers the proposed biochemical model of substrate metabolism in TAD as well as some aspects of acetate production in microorganisms. The final section deals with the main conclusions and subsequent recommendations which arose from this research program.

2. Literature Review

The following literature review is only meant as a brief introduction to the various phases of the research program. A more detailed and comprehensive review of some of the subjects are included within the results and discussion section under many of the subheadings.

Since the main topic of this thesis deals with the production of VFA in TAD, the potential augmentation of other processes, with the VFA rich effluent, must be addressed. The two processes that have the potential to complement TAD are the biological phosphorus removal process and the second phase of anaerobic digestion. A brief critique of each of these processes is included in the literature review.

2.1 Autothermal Thermophilic Aerobic Digestion

Bacteria are an abundant natural resource, but the only way they can be utilized in effective technological processes is through a comprehensive understanding of their physiology and biochemistry. Temperature is one very important factor affecting the physiology and biochemistry of microorganisms. Largely out of convenience, microbiologists have classified bacteria according to their optimum growth temperatures, thereby introducing the three artificial categories we see today. These categories include psychrophiles, mesophiles and thermophiles. There is still considerable debate concerning the temperature cutoffs between these three groups. In general, psychrophilic organisms have an optimal growth temperature of $<10^{\circ}\text{C}$, mesophilic organisms have optimal growth temperatures ranging from 15 to 40°C and thermophilic organisms have optimum growth temperatures of $>45^{\circ}\text{C}$.

The study of high temperature aerobic digestion of sludge began in the 1960's with Woodley (1961) and Kambhu and Andrews (1969). The development of these plants was initially limited by the belief, by some, that pure oxygen was necessary to achieve the needed elevated operating temperatures. However, Fuchs and Fuchs (1980) and Hoffman and Crauer (1973) reported developmental work which used air in laboratory scale and in prototype facilities. The 1980's saw the emergence of many full scale plants in Europe, but the few operating in North America were confined to western Canada.

Autothermal Thermophilic Aerobic Digestion (ATAD) systems are aerobic sludge digestion processes that operate under temperature conditions in the thermophilic range (40 to 80° C) without externally supplied supplemental heat. The process relies on the conservation of heat released during operation to generate and sustain the desired temperatures. The heat generated originates from both the bacterial metabolic activity and the mixing/aeration system. The two major advantages associated with the ATAD process are pasteurization of the sludge which reduces pathogen loads, and higher biological reaction rates. Although advances have been made in ATAD technology from an engineering perspective (since its original development 20 years ago), little is known concerning the microbial ecology and thermodynamics of this system.

2.1.1 The Autothermal Process

Autothermal aerobic digestion is capable of degrading complex organic substances into end products including carbon dioxide and water. To achieve this outcome, an adequate supply

of biodegradable organic matter, oxygen and nutrients are required. A fraction of the energy released by microbial degradation is consumed to form new cellular material. The other fraction is released as heat energy. Typical biological heat production values reported in the literature range from 14,190 to 14,650 kJ/kg O₂ (Andrews and Kambhu, 1973; Cooney *et al.*, 1968). The oxygen requirements vary (eg. from 1 to 3 kg O₂/kg Volatile Suspended Solids [VSS] oxidized) but are often considered to fall within the values of mesophilic digestion which is 1.42 kg O₂/kg of VSS oxidized. According to the EPA report on ATAD technology, the heat released by the digestion process is the major heat source used to achieve the desired operating temperature (Kambhu and Andrews, 1969). However, it is not yet clear as to what fraction biologically produced heat contributes to the total heat input of the system. Figure 2. 1 shows the various inputs, outputs and heat production items to be included in a heat balance.

Autothermal conditions require an “adequately thickened” sludge to provide the needed substrate, a suitably insulated reactor to minimize conductive heat loss, good mixing and an efficient aeration device which minimizes heat loss due to aeration. Sufficient heat should be generated and sustained in the process such that heat exchangers between feed and effluent, to warm the incoming sludge, are not normally required, unless the temperature of the incoming feed sludge is low (eg. 8-9° C).

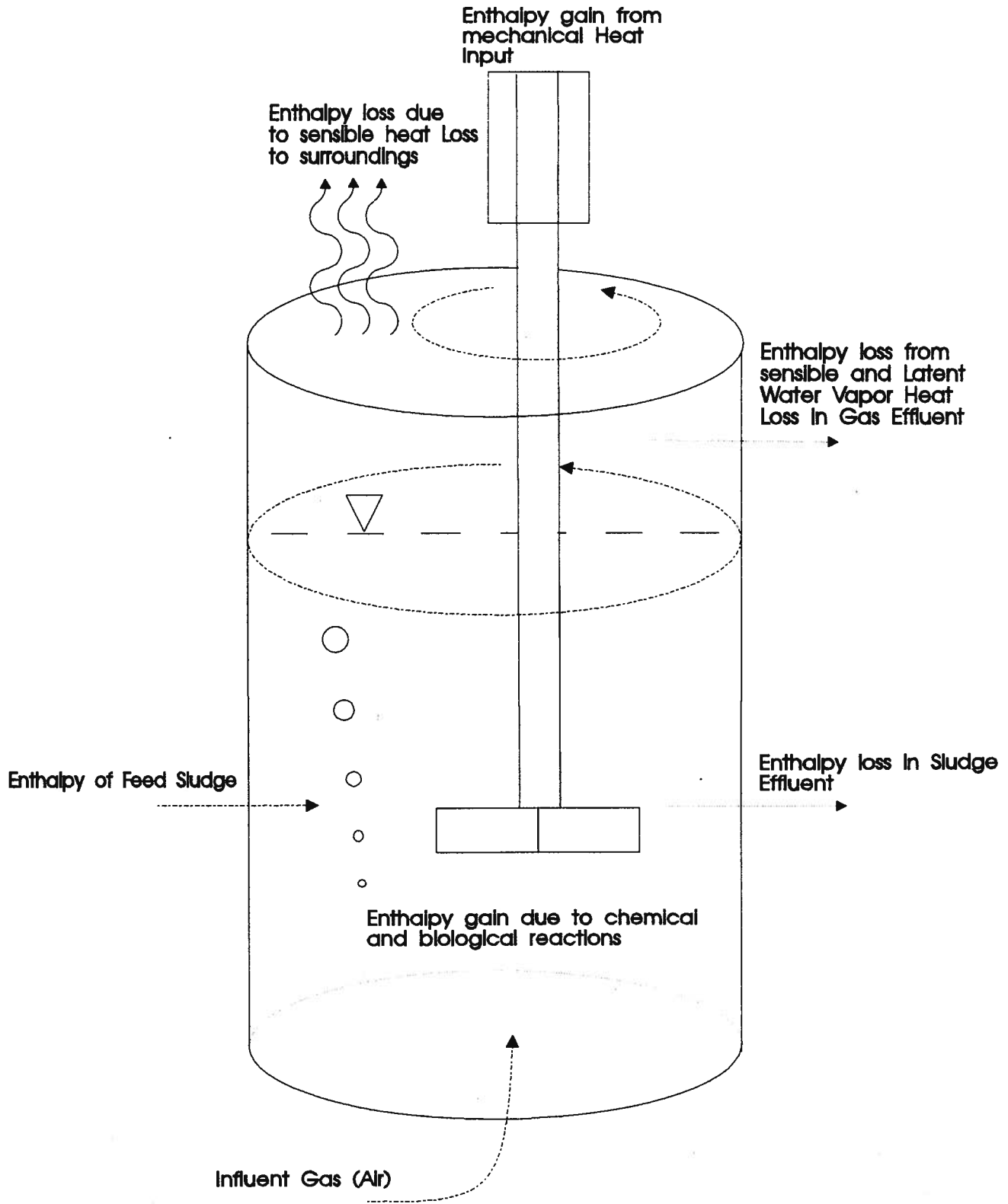


Figure 2.1: Heat Balance Schematic of a Thermophilic Aerobic Digester (adapted from EPA, 1990)

2.1.2 Process Development

Much of the developmental work leading to the ATAD process occurred in Germany and has been described by Popel (Popel and Ohnmacht, 1972). The early studies on ATAD used a self-aspirating aeration device manufactured by DeLaval, Inc. They were marketed in the U.S. for the treatment of high strength industrial and liquid manure waste in the 1970s, in a patented process called the LICOM (Liquid Composting) system. Several batch tests with various industrial and animal wastes were reported. Thermophilic temperatures of 50°C to 60°C were achieved (DeLaval Separation Company). Other studies on dairy, beef and swine wastes demonstrated that autoheating to thermophilic temperatures was possible (Hoffman and Craver, 1973; Terwilleger and Craver, 1975). High purity oxygen systems were also investigated, at the pilot scale, in the early 1970s, by Union Carbide (Matsch and Drnevich, 1977). The most extensive U.S. study of ATAD using air was conducted at Binhampton, New York, in 1977 and 1978 (Jewell *et al.*, 1982). Currently, the only known ATAD systems for municipal sludge stabilization in North America are in Canada, where four systems have been installed in British Columbia and one in Alberta (Kelly, 1989; Kelly, 1990).

Today the Germans and Swiss are the leaders in this technology with over 80 operating plants between them. Other countries using ATAD include Norway, Britain and South Africa (EPA, 1990). All reported ATAD facilities in the FRG (Federal Republic of Germany) have been reported easy to operate and require very little process control and maintenance. In most cases, process control consists of performing periodic suspended solids tests and pH analysis, monitoring reactor temperatures and controlling the pumping of specific volumes of sludge to

the ATAD reactors on a batch basis. The normal control parameter for sludge volume management is the filling levels of the tanks. At present, there is no comprehensive real time, on line monitoring method for reactor performance. The two most common on line parameters are temperature and pH.

Dissolved oxygen levels in several reported ATAD studies have varied from 0.7 mg/L to more than 3 mg/L (EPA, 1990). Other measurements in a single stage ATAD system have shown negligible dissolved oxygen concentrations, ranging between 0 and 0.2 mg/L. These measurements suggest that oxygen concentrations can be a limiting factor for a portion of the batch cycle after initial sludge feed has been introduced.

Oxidation Reduction Potential (ORP) has been proposed as a tool to assess reactor conditions (Kelly, 1990). It was concluded that ORP was a useful indicator for determination of poor oxygen transfer, odor potential, thin sludge, over aeration and over feeding. When used in conjunction with pH and temperature measurements, ORP monitoring permits the identification of operational problems and the evaluation of possible corrective actions.

2.2 Enhanced Biological Phosphorus Removal Process Model

The process of biological phosphorus removal (Bio-P) is a modification of a conventional activated sludge process. This process usually consists of an anaerobic zone followed by an aerobic zone. The anaerobic zone induces the recycled biomass to release phosphorus into solution, while accumulating intracellular substrate reserves, to be used later in

the aerobic zone. In the aerobic zone, the biomass recovers the phosphorus released in the anaerobic zone, as well as the initial phosphorus present in the incoming wastewater, by oxidizing the stored carbon reserves, thus resulting in the accumulation of phosphorus. The biomass of an enhanced Bio-P plant is capable of accumulating up to 3% (or greater) phosphorus by dry weight, in comparison to conventional activated sludge biomass which typically contains 1%. In the model proposed by Comeau *et al.* (1986) and Wentzel *et al.* (1986), the bacteria responsible for phosphate accumulation are believed to derive an advantage over other bacteria by exchanging polyphosphate for the accumulation and storage of polyhydroxyalkanoate (PHA) in the anaerobic zone. This stored carbon, in turn, provides energy to drive the accumulation of phosphate under aerobic conditions where carbon availability is limited. This model explains the beneficial effects of simple acetate and propionate additions to the anaerobic zone, since these short chain fatty acids favor the accumulation of PHA which would in turn, favor the aerobic accumulation of phosphorus (Potgieter and Evans, 1983; Siebritz *et al.*, 1983; Arvin and Kristensen, 1985). A simplified representation of the model is shown in Figure 2. 2. Therefore, the key to efficient performance lies in the adequate supply of low molecular weight VFA (specifically acetate) in the anaerobic step.

In practice, this VFA prerequisite has been achieved in a number of ways. These methods include increasing the solids retention times in the primary clarifiers to promote fermentation to produce the needed VFA, and/or fermenting the primary sludge in a separate reactor that feeds the VFA rich fermented sludge directly into the anaerobic zone (Comeau *et al.*,

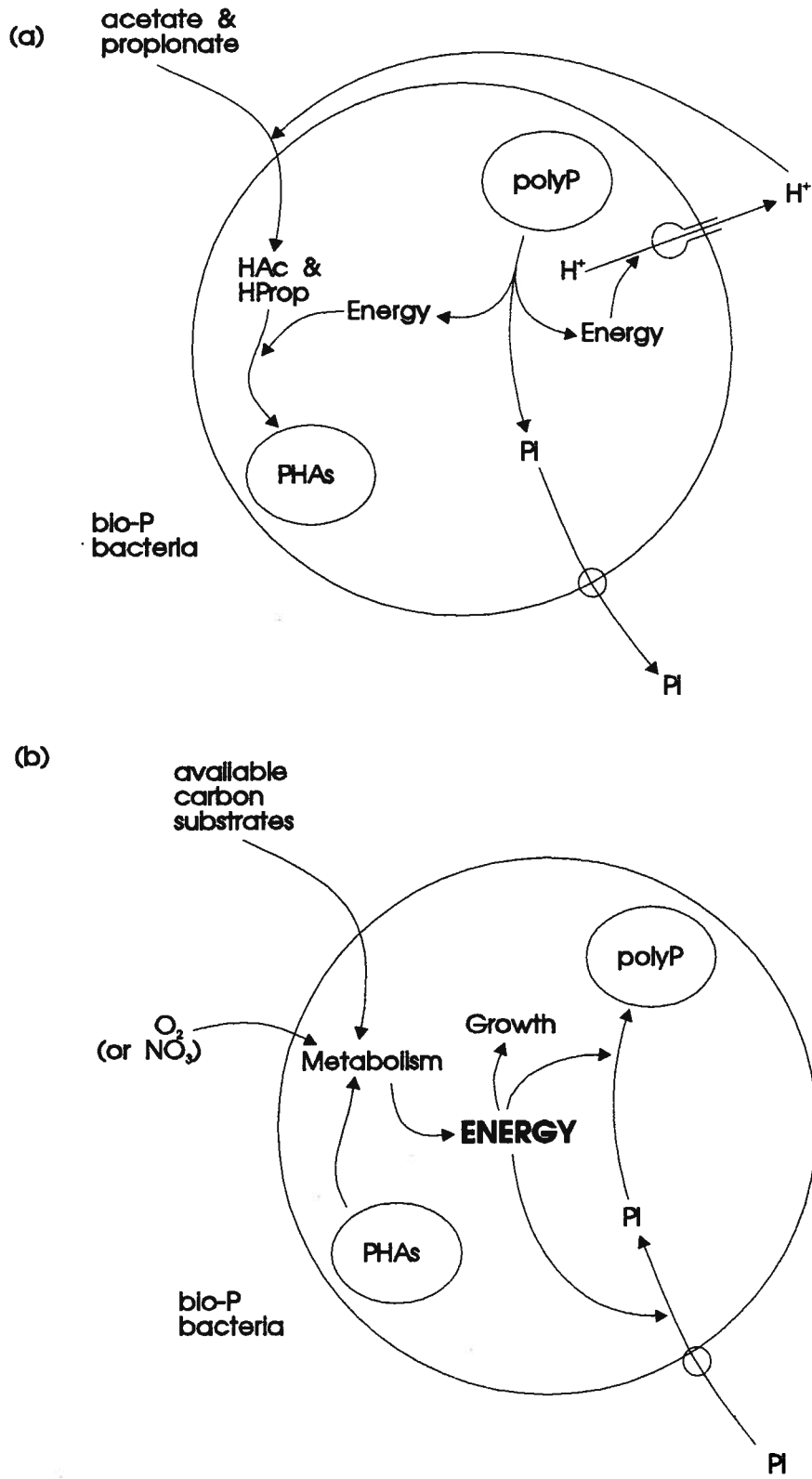


Figure 2.2: Biochemical model of phosphate accumulation (adapted from Comeau, 1988)
 (a) anaerobic zone (b) aerobic zone

1987; Rabinowitz and Oldham, 1985). These methods all rely on the process of fermentation to produce the VFA needed for efficient phosphorus removal.

2.3 Acetate Production in ATAD

The ATAD process has the potential to provide the acetate required in Bio-P but this alternative has not been systematically evaluated. Mason *et al.* (1987) had reported that acetate formation in ATAD greatly exceeded all other carboxylic acids and, at 2000 to 2500 mg/L, was 5 to 10 times the concentration of other VFA. Hamer (1987) also conducted ATAD experiments involving the solubilization and biodegradation of yeast cells, by thermophilic bacterial populations in a laboratory scale bioreactor, operating in a fill and draw mode (ie. semi-continuous). The mixed culture of process bacteria used was obtained from a full scale, thermophilic aerobic waste sludge pre-treatment process. The results showed an accumulation of up to 6000 mg/L acetate. The next highest VFA concentration was propionate at 800 mg/L. The results from this study are shown in Figure 2.3.

Kelly (1990) also conducted experiments on VFA production at a full scale ATAD process in Salmon Arm, B.C. Sludge treatment in the digester was found to produce up to 10,000 mg/L (personal communication). However, the proportion of acetic acid out of the total is not known. In each of these studies, fermentation was assumed to be responsible for the measured VFA.

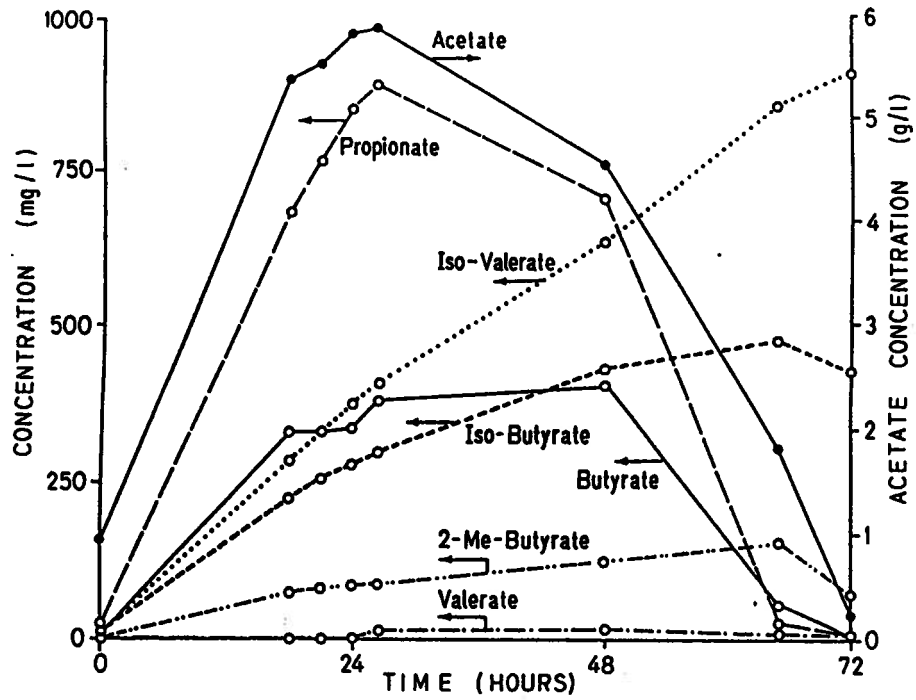


Figure 2. 3: Variations in the concentrations of VFA during the biodegradation of yeast cells by aerobic thermophilic bacteria under oxygen limiting conditions (Mason, 1986).

Experience in Salmon Arm, B.C. (Kelly, 1990) had shown that VFA concentrations in ATAD were related to pH and ORP. By changing the rate of supplied air and mixing effectiveness, changes in VFA concentrations did occur. Since the Salmon Arm facility operates as a biological phosphorus removal plant, the potential for augmenting the supply of VFA to the process via the digesters would be attractive. Sludge stabilization and VFA production could ultimately be accomplished in one operation and, as such, was examined at Salmon Arm. This potential could also be extended to applications in other communities that have Bio-P processes. The initial batch experiments were done by diverting the contents of one ATAD reactor into the anaerobic zone. The results showed only modest increases in both phosphorus release and uptake rates for respective anaerobic and aerobic periods, when compared to the control. Although these batch tests showed that biological phosphorus removal was slightly improved, further investigation was not carried out. A more detailed discussion is presented in section 5 (ie. Overview and Summary).

2.4 Thermophilic Pre-Stage Process (Dual Digestion)

A thermophilic, pre-stage process is an aerobic thermophilic pretreatment system applied prior to conventional mesophilic anaerobic digestion (Zwiefelhofer, 1985). Pre-stage systems differ from ATAD systems in several respects. There is normally only one pre-stage reactor prior to anaerobic digestion. The residence time in the thermophilic reactor is normally between 18 and 24 hours. Pre-stage systems are not autothermal and require supplemental heating. Heat exchangers are normally used in these systems. For raw sludge heating, a sludge to sludge heat

exchanger is included in the thermophilic pre-treatment step. This exchanger recovers heat from the hot sludge prior to introduction into the mesophilic anaerobic digester. Waste gas from the reactor is often recirculated into the air injection device to minimize vent gas heat loss.

Although pre-stage systems are referred to as aerobic, "aerated" is probably a more appropriate descriptor. Air input into the system is typically less than the stoichiometric demand for oxygen, and there is no measurable dissolved oxygen residual. Because of the limited oxygen supply, the concentration of soluble degradable organic compounds such as VFA is normally very high (Baier and Zwiefelhofer, 1991) and sludge leaving the process has not been fully stabilized.

Aerobic thermophilic treatment of sewage sludge has been successfully applied to pretreatment prior to a mesophilic anaerobic digestion process. When this thermophilic process is incorporated ahead of mesophilic anaerobic digestion, the benefit of stimulation of VFA production becomes evident. The acetate, in particular would be beneficial to the direct metabolism of methanogenic organisms in the following stage. Some authors have described TAD as a possible acidification stage (Keller and Berninger, 1984). Bomio *et al.* (1989) investigated this possible beneficial nature of TAD sludge. Cultivations carried out at very low aeration rates (0.1V/V-h), with a bench scale bioreactor configuration fed with a mixture of primary and waste activated sludges from a full scale waste water treatment plant, showed little production of VFA.

2.4.1 Anaerobic Digestion: Substrate Specificity During Phase Separation

Anaerobic digestion consists of a complex sequence of biological reactions, during which the products of one group of organisms are utilized as substrates by another group. The principal reaction sequences can be classified into three or four major groups. The first reaction sequence is the hydrolysis of complex, insoluble organic substrates into simpler more soluble intermediates.

The second reaction is the fermentation/acidification of soluble substrates into more oxidized intermediates, primarily VFA, by fermentative organisms. In the past, anaerobic conversion of particulate, biodegradable organic compounds to methane and carbon dioxide was thought to comprise three steps: hydrolysis, acid formation and methane production. On the basis of this model, methanogenesis from fatty acids was considered the rate limiting step in the digestion of dissolved organic compounds (Ghosh and Pohland, 1974; Novac and Carlson, 1970) and the hydrolysis of insoluble particulate organics was regarded as rate limiting for the overall process of sludge digestion (Ghosh *et al.*, 1975). Kaspar and Wuhrmann (1978) were among the first to suggest that the degradation of acetate, rather than methanogenesis from fatty acids, was the rate limiting reaction in the anaerobic degradation of dissolved organic matter. This carbon flow model based on percentage of total flow of theoretical chemical oxygen demand, suggested that 54% of the total methane produced in anaerobic digestion is evolved from acetogenic reactions that produce hydrogen and acetate from more reduced compounds (eg. propionate, other VFA).

In the third major reaction, VFA and hydrogen are converted into methane and carbon dioxide by two coupled reactions, mediated by acetogenic and methanogenic bacteria. Acetogenic organisms convert the products of fermentation into acetate, formate and hydrogen, which serve as substrates which methanogens convert to methane and CO₂. A distinction between acetogenic and acidification reactions is not always clear. Acetate and hydrogen are produced by both acidification and acetogenic reactions, and both acetate and hydrogen are substrates for methanogenesis. The syntrophic coupling of many acetogenic reactions to methanogenic reactions is critical, because the conversion of VFA to acetate and hydrogen is only thermodynamically favorable in the presence of methanogens (Fox and Pohland, 1994). If the conversion is energetically unfavorable, as it is in the case of butyrate, propionate and ethanol, the concentration of products must be maintained at low levels in order for acetogenesis to occur. These low concentrations can be accomplished by the utilization of the acetate and hydrogen by methanogens as the intermediates are produced. In this case, it is the interspecies transfer of reducing equivalence that is essential for the conversion of these substrates to their corresponding products (Thiele and Ziekus, 1988).

2.4.2 Phase Separation

The goal of a two phase digestion system is to enhance the anaerobic biodegradation by controlled separation of the major reactions. Figure 2. 4 illustrates the single phase as well as the two phase digestion process. The principle of two phase digestion is to separate the hydrolysis and fermentation/acidification reactions from the acetogenic /methanogenic reactions.

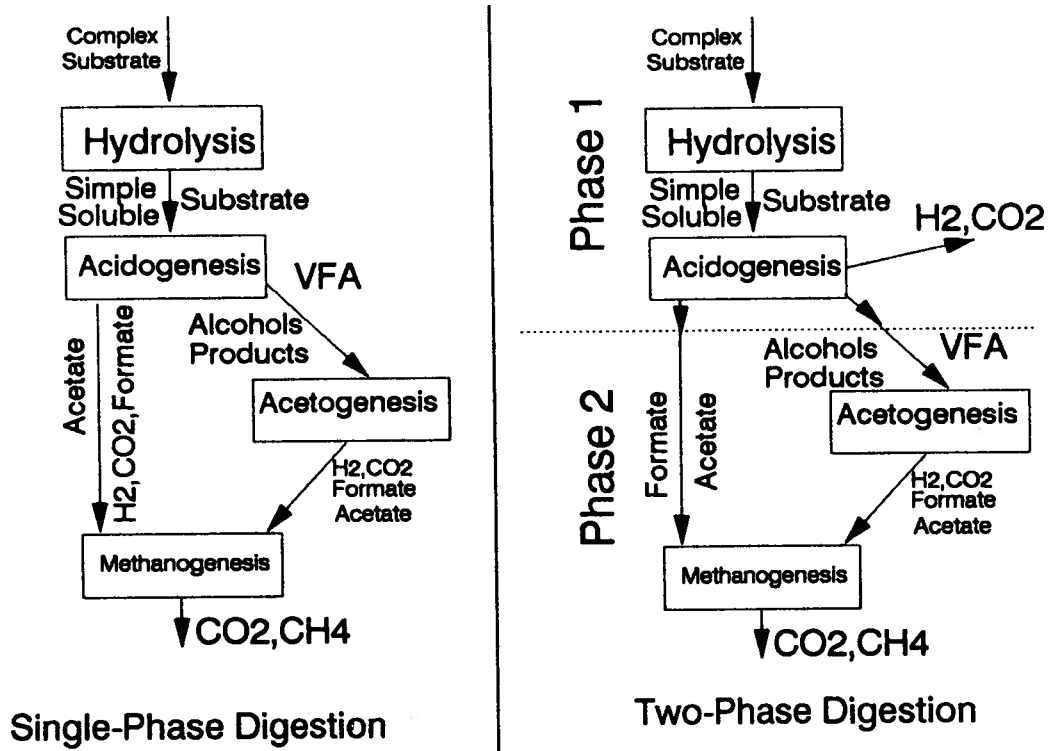


Figure 2. 4 Principal sequences of anaerobic digestion (Fox and Pohland, 1994).

Because of this separation, the syntrophic effects involving acidogenesis and methanogenesis will be altered. From an operational point of view, enhancing anaerobic digestion by phase separation is accomplished by providing optimal environments (eg. SRT, HRT, pH) for each major group of bacteria and their associated biological reactions.

The two steps commonly cited as rate limiting in the process of anaerobic digestion are the hydrolysis of complex substrates and methanogenesis (Wuhrman, 1978; Ghosh *et al.*, 1975).

Two phase digestion isolates each potential rate limiting step and thereby allows the optimization of each. However, the syntrophy between acetogenesis and methanogenesis must still exist in two phase separation. In order for acetate to be produced in the second phase, the products of acetogenesis (eg. acetate and H_2), must be maintained at extremely low levels. These levels are achieved by utilizing these products as substrate by methanogenic organisms. This syntrophic couple could potentially be broken by introducing a process upstream of anaerobic digestion that could produce acetate as its major by-product (eg. Thermophilic Pre-stage Process).

2.5 *Thermodynamics and Metabolism*

To understand the details of the biochemical model which describes substrate metabolism in the TAD process, some fundamental aspects of thermodynamics and metabolism must be addressed. The following sections review some of the basic central pathways involved in the oxidation of substrate molecules (eg. Glycolysis, Citric Acid Cycle and the Electron Transport

Chain) which are integral to understanding the mechanisms of the model. The introduction of the molecules responsible for energy production and electron transport (eg. ATP and NADH) must also be considered in order to develop a comprehensive understanding of the basic fundamentals of the proposed biochemical model.

Metabolism is the sum total of all the biochemical reactions that take place within an organism and like other chemical reactions is governed by the laws of thermodynamics. Energy transformation from one form to another is the basis of the science of thermodynamics and observations made by physicists and chemists have led to two fundamental laws, which may be stated simply as follows:

First Law: In any physical or chemical change the total amount of energy in the universe remains constant.

Second Law: All spontaneous physical or chemical changes tend to proceed such that useful energy (ie. free energy) undergoes irreversible degradation into a random, disordered form; this is called entropy.

Biochemical reactions, in which reactants are converted to products, can be described thermodynamically since there is a change in their energy contents. Gibbs explained the changes in the energy content of such a system with the following equation (Lehninger, 1982):

$$\Delta G = \Delta H - T\Delta S$$

ΔG refers to the change in free energy of the reacting system, ΔH is the change in its heat content (ie. Enthalpy), T is the absolute temperature at which the process is taking place and ΔS

is the change in entropy of the universe. In most cases ΔH is nearly equal to ΔG and the two are often used interchangeably. If ΔH of a reaction is positive, it is referred to as an endergonic reaction, which means that the forward reaction cannot proceed unless energy is put into the system. The reverse reaction will however proceed spontaneously. If the ΔH is negative, this is referred to as an exergonic reaction and tends to proceed spontaneously in the forward direction with the release of free energy.

The form of energy that cells can and must use is free energy, which can do work at constant temperature and pressure. Heterotrophic cells obtain their free energy from energy rich nutrient molecules. Thousands of metabolic reactions occur in the cell; some are exergonic while others are endergonic. Exergonic reactions such as the oxidative reactions involving carbohydrates, fats and proteins, as well as the hydrolysis reactions involving energy rich molecules such as ATP release free energy. Endergonic reactions require the addition of energy, for example some of the biosynthetic reactions that are involved in the synthesis of proteins, lipids and carbohydrates. Every chemical reaction has a standard free energy change, ΔG° . This standard free energy change is a constant for any given reaction and can be calculated from the equilibrium constant of the reaction under standard temperature (25° C) and pressure (1 atmosphere). For example the equilibrium constant for the reaction $A+B \leftrightarrow C+D$ is given by,

$$K_{eq} = \text{Product of [Products] / Product of [Reactants]} = [C][D] / [A][B]$$

Once the equilibrium constant (ie. K_{eq}) of a reaction is determined its standard free energy change (ie. ΔG°) can then be calculated by the following expression,

$$\Delta G^{\circ} = -RT \ln K_{\text{eq}}$$

R is the gas constant (1.987 cal/mol*degree), T is the absolute temperature and $\ln K_{\text{eq}}$ is the natural log of the equilibrium constant. If, for example the equilibrium constant is high, a large amount of product has been produced, the reaction tends to go to completion and the free energy change is negative. If the equilibrium constant is low, little product is formed, the reaction does not go to completion, and the free energy change is positive. In this scenario, the conversion of reactants to products requires that energy be supplied to the system. High energy compounds, such as ATP, are responsible for supplying most of the energy required for completion of endergonic reactions (Boyd, 1984).

2.5.1 Energy Production (ATP)

Energy production in any organism is based on oxidation reduction reactions in which a molecule donates electrons (ie. thus becoming oxidized) and another molecule accepts electrons (ie. thus becoming reduced). Electrons will flow from a compound with a higher potential energy to a compound with lower potential energy with a decline in free energy (ie. $-\Delta G$) Some of the energy is lost as heat but much of the free energy released from cellular fuels during their catabolism is conserved by the coupled synthesis of phosphorylated compounds such as the nucleoside triphosphates (eg. ATP and GTP). Most of the energy supplied to endergonic reactions (ie. reactions that require energy input) is provided by ATP. Heterotrophs, depending on the species of electron acceptor, can produce ATP using different or modified metabolic pathways.

Fermentation is an oxidation/reduction reaction in which the electron donors and electron acceptors are organic. It is an incomplete oxidation process in which the end products formed possess considerable amounts of extractable free energy. These compounds are usually various acids and alcohols excreted by the organism into the environment. Molecular oxygen is not involved. Respiration, on the other hand, is a process in which either an organic or inorganic electron donor is oxidized and the final electron acceptor is oxygen. The substrates or products from fermentation can serve as electron donors in respiration. Fermentation end products can serve as substrates in respiration since this process results in a complete oxidation and extraction of all biologically available energy from the donor molecule. Complete oxidation of organic molecules are characterized by the formation of CO₂ and H₂O.

2.5.2 Bacterial Energetics

Glycolysis is an almost universal central pathway of glucose catabolism, not only in animals and plants, but also in a great many microorganisms. The glycolytic sequence of reactions differs from one species of bacteria to another only in how its rate is regulated and in the subsequent metabolic fate of the pyruvate produced. During glycolysis, much of the free energy produced is conserved in the form of ATP. The conversion of glucose into two molecules of pyruvate is shown by the equation:



Thus, for each molecule of glucose degraded, two molecules of ATP are generated from ADP and Pi. The conversion of glucose to pyruvate is catalyzed by 10 enzymes acting in

sequence. Glycolysis is an essential set of reactions driven to completion by the large decrease in free energy.

When cells catabolize glucose to lactate, this compound contains approximately 93% of the available energy of the original glucose molecule. This is because lactic acid is almost as complex a molecule as glucose and has undergone no net oxidation. The free energy released on complete combustion of organic molecules is in approximate proportion to the ratio of hydrogen bound carbon atoms to the total number of carbons. Only by the removal of all the hydrogen atoms from the carbon atoms of organic substrates and their replacement with oxygen to yield CO_2 , can all their biological free energy be realized. Carbohydrates, fatty acids and most of the amino acids are ultimately oxidized to CO_2 and H_2O via the citric acid cycle (ie. Krebs cycle). First however, before these nutrients can enter the Krebs cycle their carbon backbones must be degraded so that they yield the acetyl group of acetyl-CoA, the form in which the Krebs cycle accepts most of its fuel input. Under aerobic conditions, the next step in the generation of energy from glucose is the oxidative decarboxylation of pyruvate to form acetyl-CoA. The equation for this is as follows:



The formation of acetyl-CoA from pyruvate is a key irreversible step in metabolism. Acetyl-CoA and NADH, which are the products of the oxidation of pyruvate, inhibit the enzyme complex that mediates this reaction (ie. pyruvate dehydrogenase complex). These inhibitory effects are reversed by CoA and NAD^+ .

Figure 2. 5 shows the overall organization of electron transport and oxidative phosphorylation. One cytochrome system is considered in this figure. In each turn around the citric acid cycle, four pairs of hydrogen atoms are removed from isocitrate, α -ketoglutarate, succinate and malate by the action of specific dehydrogenases. These hydrogen atoms donate their electrons to the electron transport chain and become H^+ ions, which escape into the aqueous medium. The electrons are then transported along a chain of electron carrying molecules until they reach cytochrome oxidase, which promotes the transfer of the electrons to oxygen, the final electron acceptor in aerobic metabolism. In addition to the four pairs of electrons arising from the citric acid cycle, others come from the dehydrogenases that act upon pyruvate, fatty acids and amino acids during their degradation to acetyl-CoA and other intermediate products. In aerobic cells virtually all the hydrogen atoms derived by the action of dehydrogenases on substrate molecules ultimately donate their electrons to the respiratory chain, the final common pathway leading to the terminal electron acceptor, oxygen. As each pair of electrons passes down the respiratory chain from NADH to oxygen, the coupled synthesis of three molecules of ATP from ADP and P_i takes place.

In carbohydrate catabolism, there are three energy yielding stages, glycolysis, the citric acid cycle and oxidative phosphorylation. Each is so regulated by its own set of controls that it proceeds at a rate just sufficient to satisfy the minute to minute needs of the cell for its products. These three stages are coordinated with each other so that they function together in an economic and self regulating manner, like a smoothly running piece of machinery, to produce ATP and

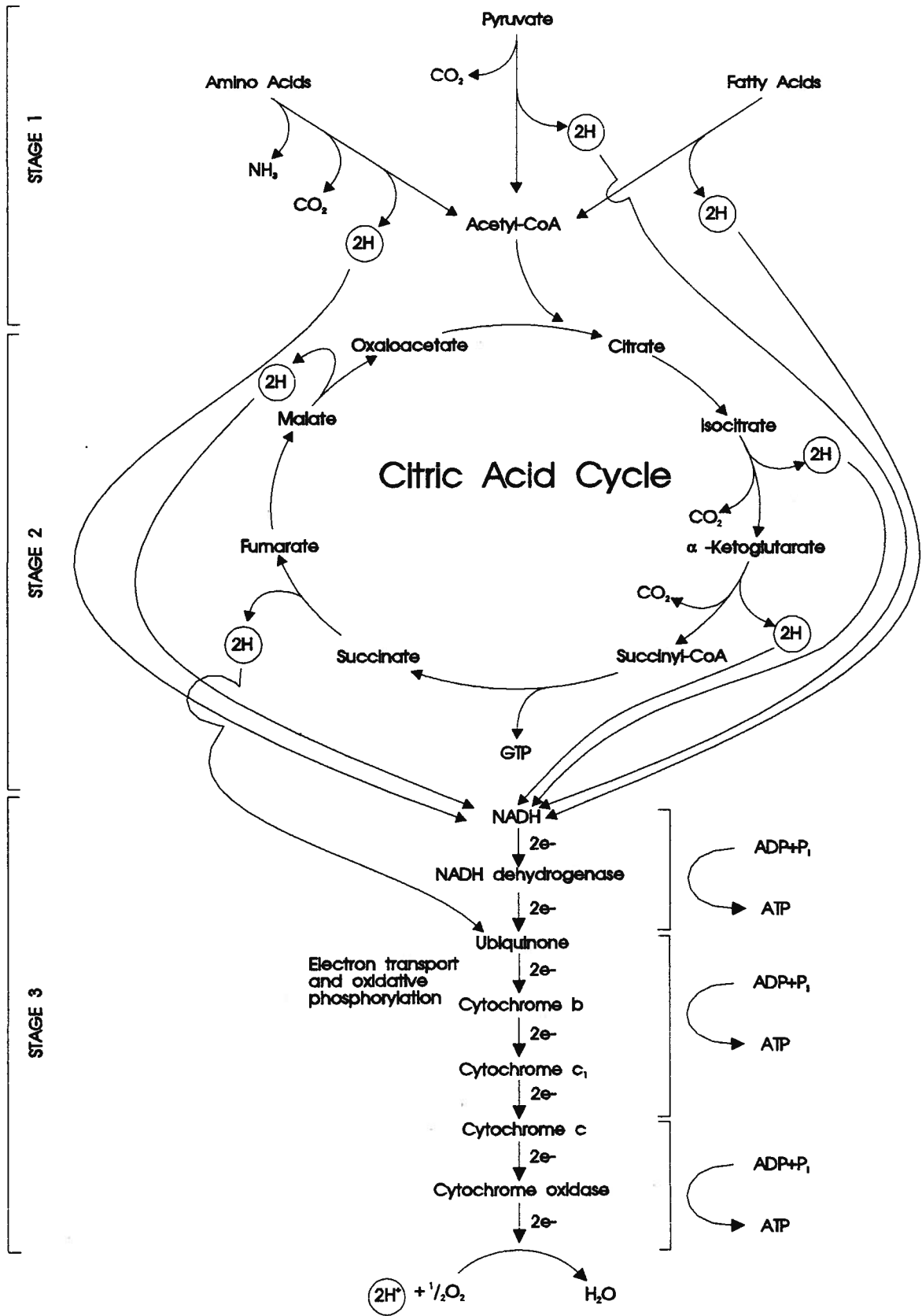


Figure 2. 5 Overall organization of electron transport and oxidative phosphorylation. (Lehninger, 1982)

specific intermediates such as pyruvate and citrate which are required as precursors in the biosynthesis of other cell components. The integration of these 3 stages is made possible by interlocking regulatory mechanisms. For example the relative concentrations of ATP and ADP not only control the rate of electron transport and oxidative phosphorylation, but also the rates of the citric acid cycle and glycolysis.

2.5.3 NADH

All living cells contain nicotinamide adenine dinucleotides [NADH], which serve as cofactors in many metabolic reactions. The reduced form [NADH] is a high energy molecule, which supplies reducing equivalence to many intracellular redox reactions. The level of NADH in cultures is a function of the number of cells, the energy balance within those cells and the level of metabolic activity. The central role played by NADH in oxidative reactions within organisms inevitably implicates it in the regulation of respiration, since NADH is, after all, the main immediate electron donor to the respiratory chain. As a substrate for respiration, NADH must exert some type of influence on its rate.

One important feature of fermentative metabolism is an even hydrogen balance. Since there is no external electron acceptor such as oxygen, NADH producing and NADH consuming reactions have to balance. Since the amount of NADH to be recycled varies with the nature of the substrate, so must the compositions of the mixture of fermentation products. Hexoses such as glucose or fructose, produce two NADH per C₆ molecule upon conversion to pyruvate; however, hexitols (eg. sorbitol or manitol) produce three NADH per C₆ molecule. To achieve a

proper fermentation balance, it is necessary to match the NADH produced with the NADH consumed by the excretion of specific fermentation end products. In practice, *E. coli* uses a mixture of ethanol, lactate and acetate, all of which consume different amounts of protons per C6 molecule. By varying the proportions of each of these products it is possible to match the substrate to achieve redox balance (Clarke, 1989). In the presence of oxygen, NADH generated during glycolysis, the TCA cycle and associated reactions is reoxidized by operation of the respiratory chain (Ingeldew and Poole, 1984). During fermentation, neither the respiratory chains linked to oxygen nor those linked to alternative electron acceptors (eg. nitrates, sulfates) are functional. The TCA cycle and pyruvate dehydrogenase reactions which generate NADH in large amounts are largely inoperative under anaerobic conditions (Spencer and Guest, 1985; Smith and Neidhardt, 1983). However NADH produced by glycolysis must be reoxidized to NAD^+ so that the glycolytic sequence can proceed. Thus, the key issue in fermentation is the recycling of reducing equivalence by conversion of substrate to specific fermentation end products. Figure 2. 6 shows the necessary sequence of reactions of fermentative organisms to maintain redox balance (Boyd, 1984).

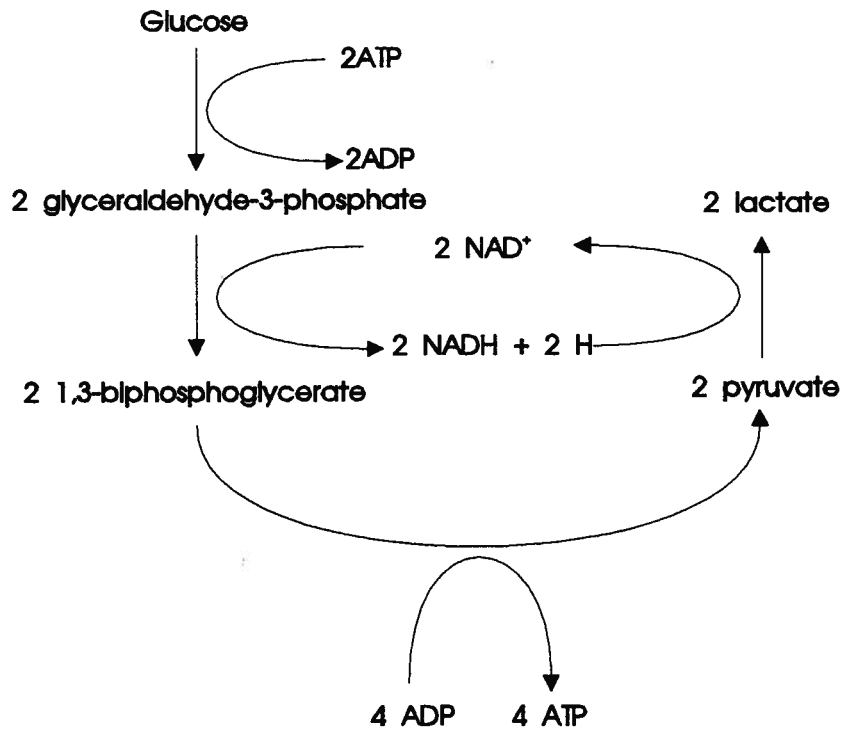


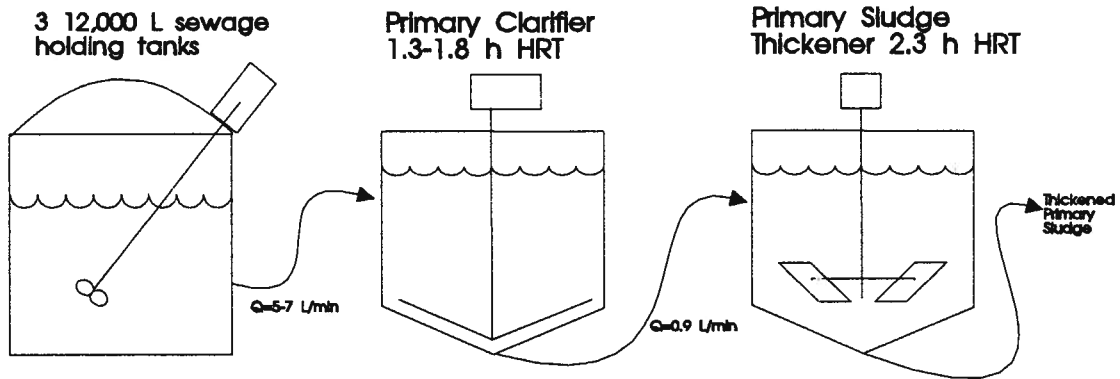
Figure 2. 6 Pathways involved in the fermentation of glucose.
(Boyd, 1984)

3. Methods and Materials

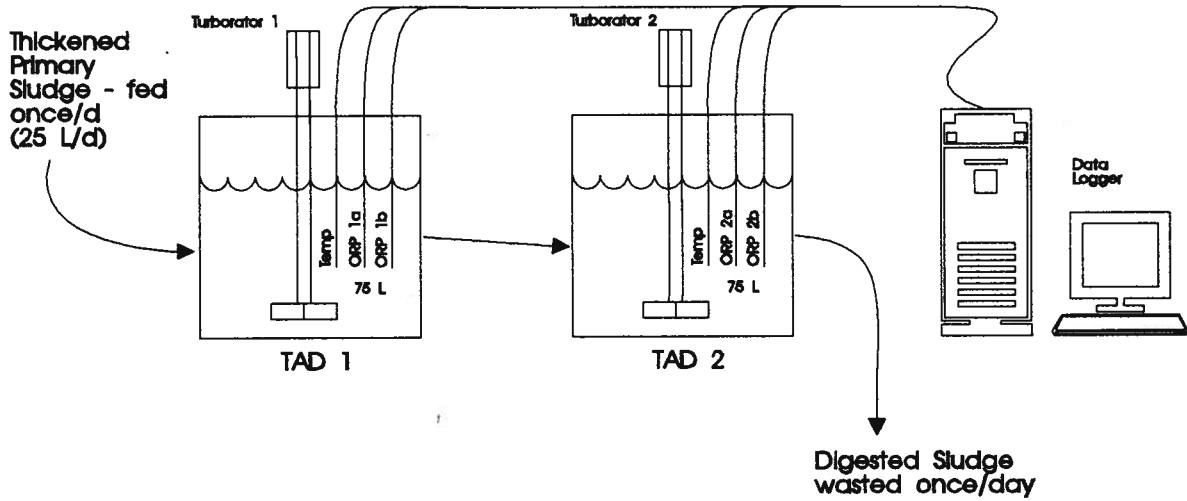
3.1 Thermophilic Aerobic Digester

3.1.1 Preliminary Operational Phase

The sludge feed source for all pilot scale and batch experiments originated from the sewer that connects the University of B.C. campus residences to the sewage collection system. The raw sewage was pumped into three, 12,000 L sewage holding tanks. This sewage diversion was done twice daily during peak flows (ie. from 10:00 to 12:00 and from 17:00 to 19:00) to maximize the solids content of the subsequent primary sludge. From these tanks the sewage was pumped at a constant rate into a primary clarifier. The primary sludge was then pumped into a primary thickener. The thickened sludge was then metered and fed into the first stage of the TAD process. A 2-stage, 150 L, pilot scale TAD (Figure 3. 1a), located in the Wastewater Treatment Pilot Plant site at the University of B.C., was used in this preliminary study. Each 75 L reactor was equipped with a 250 mm foam breaker. Aeration and mixing were supplied with the Turborator aerator designed by Turborator Technologies Inc.(Guarnaschelli and Elstone, 1987). This aerator is a self aspirating type of aerator-mixer. Heat was supplied by biological activity and the mechanical mixing energies from the aerator/mixer. The reactors operated in series under daily batch feed conditions. Table 3. 1 is a comparison of operating conditions and solids destruction efficiencies achieved in the pilot scale TAD units to those recommended for full scale practice (EPA, 1990; Kelly, 1990). The pilot scale TAD feed was approximately 1/3



a) Preliminary phase of operation (series configuration)



b) Second phase of operation (parallel configuration)

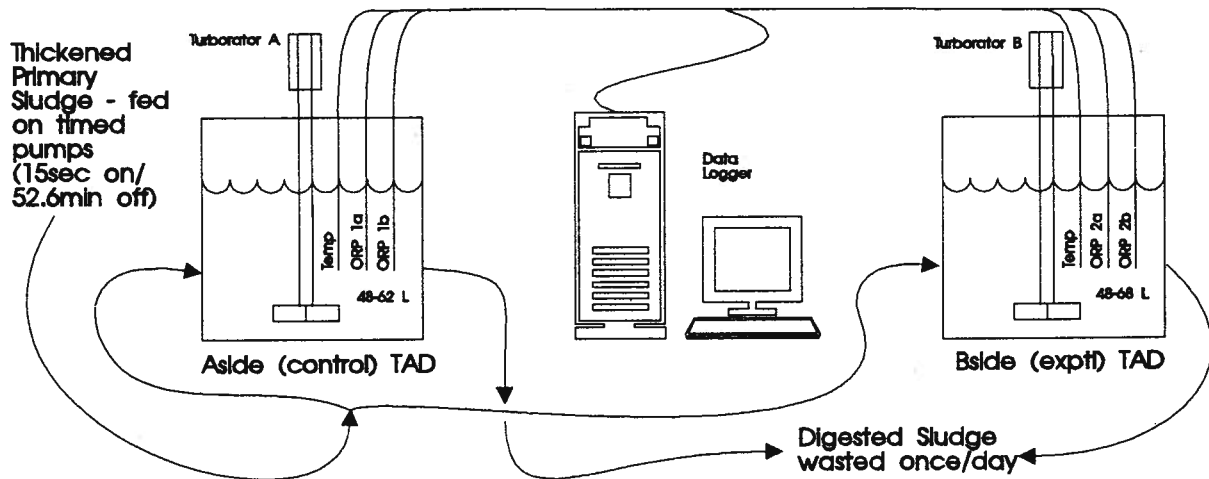


Figure 3. 1 Schematic of the UBC pilot scale TAD process a) operating in series (1st and 2nd phases) and b) under the parallel mode of operation (A and B sides).

of the recommended concentration. The operating degree day product was below the recommended range of 400-500.

Table 3. 1 Comparison of pilot scale TAD parameters and recommended values (EPA, 1990; Kelly, 1990).

Variables	Pilot scale TAD values	Recommended values
Number of stages	2	2
Temperature range of 1st stage (°C)	37-47	35-50
Temperature range of 2nd stage (°C)	54-60	55-65
Total SRT (d)	6(3/stage)	5-10
Total solids in feed (%)	1.7	4-6
Total solids destruction (%)	29	40
Power Density (W/m ³)	3000	100-250
Degree-day product	294	400-500

3.1.2 Second Phase of Operation

Based on preliminary results, the first stage of the 2 stage pilot scale TAD process produced the highest measured concentrations of VFA (up to 950 mg/L as acetate). The second phase of operation explored this stage in detail. The series configuration of the reactors was changed to a parallel mode of operation (Figure 3. 1b). This scheme resulted in a control side (A side) and an experimental side (B side). Each side received an identical primary sludge feed. The feeding regime was also changed from once per day to approximately once per hour. The sludge within each TAD reactor was allowed to accumulate throughout the day and was wasted once per day.

Table 3. 2 Combination of aeration and SRT for each experimental run.

Air flow rate (mL/min.)	Aeration	SRT (days)		
		3	4.5	6
True anaerobic	0	n/d	run 10	n/d
0	Low	run 2	run 1	run 3
117	Medium	run 5	run 4	n/d
164	High	run 6	runs 7, 9	run 8

n/d- not done

A 3x3 factorial experiment was conducted under this new mode of operation. The two independent variables examined were aeration and SRT. The range of air flows was from 0-165 mL/min and the SRT range was 3-6 days. This 3 level factorial design was made up of 9 individual cells or runs and is shown in Table 3. 2. Within all 9 runs, the A side control independent variables were maintained at their respective medians (ie. 4.5 d SRT and medium aeration), while the B side experimental variables were adjusted to their appropriate values. This experimental design facilitated the comparison of the test condition (B side) to its corresponding control condition (A side) within each run. This would alleviate the variability of primary sludge feed characteristic and external environmental condition effects on the measured responses, since both reactors were fed from the same sludge source and were operated over the same time period. As can be seen from Table 3. 2 not all the combinations of SRT and aeration were done. Under the true anaerobic condition (run #10) only one run was attempted (eg. 4.5 d SRT) and the combination of medium aeration and 6 d SRT was not done. Prior to each individual run, the sludge contents of both control and test sides were thoroughly mixed, to ensure that both sides would start with an identical sludge composition, and allowed to acclimate

at their respective set conditions for one SRT. Samples for analysis were collected for a further two SRTs, after which the contents were thoroughly mixed in preparation for subsequent runs. A tenth experiment was conducted which compared the median control condition for both aeration and SRT (A side) to a fully fermentative TAD. To achieve a fully anaerobic environment the test side reactor (B side) was purged with an anaerobic gas mixture instead of air (eg. 90% N₂, 5% CO₂ and 5% H₂).

3.2 Aeration

Clean water aeration experiments performed earlier on the aerators indicated that significant amounts of oxygen were entrained by mixing alone (Boulanger, 1994). These results suggested that the standard oxygen transfer rate was 28 mg/L-h at an ambient water temperature of 15° C and rotational turborator speed of 964 rpm. Surface entrainment of oxygen is an interface phenomenon between the bulk liquid and the overlying gas phase. The gas in the head space in the pilot scale TAD reactor, under clean water aeration conditions, contains approximately 20% O₂ by volume. The oxygen percentage in the gas within the head space of an operating TAD process is a function of the aeration conditions employed. Under Boulanger's (1994) oxygen deficient condition, the oxygen content in the headspace was as low as 4% by volume. The oxygen satisfied condition resulted in a 12 -15% oxygen in the gas within the head space. Consequently, the standard oxygen transfer rates, due to surface entrainment, would invariably change depending on the percentages of the head space gases. Temperature and turborator rotational speed would also effect the standard oxygen transfer rates due strictly to surface entrainment.

3.2.1 Preliminary Operational Phase

For the purpose of this study, the tested air flow rate for the aerobic condition was 0.6 Volume of air/Volume of sludge-hour, the rate for the intermediate transition condition at 0.28 V/V-h and the rate for the microaerobic condition at 0 V/V-h. The air flow rates in all 3 conditions were measured with an inline rotameter (Cole Parmer model 044-40C). The flow rate for the third condition as measured by the flow meter was zero. A 0.126 V/V-h maximum flow rate for the microaerobic condition may be calculated by extrapolating a value using standard oxygen transfer rate data. Since a zero air flow rate correlated to a measurable transfer rate of 28 mg/L-h, extrapolation of the transfer rate back to zero resulted in a calculated maximum air flow rate of 0.126 V/V-h. However, it must be remembered that this flow rate is based on clean water aeration tests at ambient temperatures. Under these conditions the percentage of oxygen within the head space of the TAD units was 20%. Under the microaerobic condition in which the oxygen percentage in the head space is considerably less, the calculated flow rate of 0.126 V/V-h is probably a gross overestimate of the actual air flow rate due to mixing alone.

3.2.2 Second Phase of Operation

Since the TAD sludge was fed with thickened primary sludge once/hour and was allowed to accumulate throughout the day within the reactor, the retention volume of each reactor was continuously increasing until wastage was achieved (once/day). For this reason, the air flow rates cannot be normalized to the reactor volume. Instead, the rates are reported as flow rates (eg. Volume/Time). A much narrower range of air flow rates were used in the second phase of operation (0-165 mL/min or approximately 0-0.17 V/V-h). This entire range resulted in a

microaerobic environment within the bioreactors. For the purposes of this study, the microaerobic environment was divided up into 3 subconditions. The low flow microaerobic condition corresponded to an air flow rate of 0 mL/min as measured by an in line rotameter (Cole Parmer models FM032-15, FM012-10). This corresponded to a calculated flow rate of 0.126 V/V-h. The medium air flow microaerobic condition represents a mean air flow rate of 117 mL/min and the high flow microaerobic condition corresponds to a mean air flow rate of 164 mL/min (Table 3. 2).

3.3 Volatile Fatty Acids

Samples of TAD sludge taken at various times after feeding were centrifuged in a microcentrifuge (IEC Micro-MB centrifuge) for 10 minutes. One mL of supernatant was put into a sealed glass container with 100 μ L of 3% phosphoric acid to drop the pH to 3. The containers were then stored at 4 $^{\circ}$ C until analysis was done. The VFA determination was conducted using a Hewlett-Packard 5880A gas chromatograph, equipped with a Flame Ionization Detector (FID). Helium was used as the carrier gas. The packing material was 0.3% Carbowax 20M/0.1% H₃PO₄ on Supelco Carbopak C 2 mm ID. The column was conditioned according to the procedures described in Supelco Bulletin 751E (1989). The operating parameters were: (a) Injector temperature of 150 $^{\circ}$ C; (b) Detector Temperature of 200 $^{\circ}$ C; (c) Oven temperature of 120 $^{\circ}$ C for 1 minute and then ramped up 5 $^{\circ}$ C/min. to 150 $^{\circ}$ C for 5 minutes; and d) Helium flow rate of 20 mL/min. Quantitation of response peaks were done by comparison to external reagent grade standards.

3.4 Ethanol and Propanol Determination

Ethanol and propanol analysis was done in a similar manner to VFA determination except that the oven temperature was set at 80° C in contrast to VFA determination which was carried out at 120° C.

3.5 Pyruvic and Lactic Acid Determination

Samples of TAD sludge were taken and centrifuged in a microcentrifuge for 10 minutes (IEC Micro-MB centrifuge). One mL of supernatant was put into a sealed glass container with 100 μ L of 0.3 M oxalic acid. The containers were then stored at 4° C until analysis could be performed. Pyruvic and lactic acid determination were performed by injecting 1 μ L of sample into an HP 5880A gas chromatograph, equipped with an Flame Ionization Detector. The column packing material was 4% Carbowax 20M on Supelco Carbowax B-DA 2 mm ID. The operating parameters were: (a) Injector temperature of 175° C; (b) Detector temperature of 200° C; (c) Isothermal oven temperature of 175° C, and (d) Helium flow rate of 24 mL/min. Quantitation of response peaks were done by comparison with reagent grade standards.

3.6 Total and Inorganic Carbon

Samples of TAD sludge were taken and centrifuged in a microcentrifuge (IEC Micro-MB centrifuge) for 10 minutes. Approximately 1 mL of supernatant was taken with a disposable plastic pipette. The liquid within the pipette was forced to the base of the pipette before sealing the end of the pipette by passing it over an open flame. The samples were then frozen and stored at -17° C until analysis could be conducted. The samples were thawed at room temperature and

subjected to the appropriate dilution. A 40 μL aliquot was then injected into a Shimadzu Total Carbon Analyzer (Model TOC-500), using a series of low and high standards (Shimadzu corporation, 1987). Each sample was analyzed 3 times and a standard deviation and coefficient of variation were calculated.

3.7 Solids

Total and volatile solids were determined by evaporating a known volume of sample in a Fisher Isotemp (Model 350) forced draft oven at 104°C and igniting the residue at 550°C in a Lindberg muffle furnace (type 51828), respectively. Both analyses were performed as outlined in *Standard Methods* (A.P.H.A. *et al.*, 1989).

3.8 On Line Data

Each reactor contained two Oxidation Reduction Potential (ORP) combination electrode probes using Ag-AgCl reference half cells and one thermocouple temperature probe. Two ORP probes were used to ensure the accuracy of the values obtained. During the preliminary operational phase (3.1.1), both ORP and temperature measurements were logged at 1 minute intervals on an on-line data acquisition package (Labtech Notebook/XE). The two ORP values were then averaged and graphed as a moving average, with an interval of 10 data points. During the second phase of operation, both ORP and temperature measurements were taken every 10 seconds and logged at 5 minute intervals. Each logged value was the result of the average value of the previous 30 measurements (ie. 10 seconds x 30 measurements = 5 minutes).

3.9 Batch Experiment

A batch test apparatus was commissioned in order to examine the biochemistry involved in VFA metabolism in TAD, specifically acetate metabolism. The basic principle of this experiment was to test specific substrates and inhibitor compounds for their effect on VFA metabolism. The tested substrates were:

- | | |
|---------------------|----------------------------------|
| 1. Propionate | 10. n-Propanol |
| 2. Butyrate | 11. Peptone |
| 3. Isobutyrate | 12. Glucose |
| 4. 2-Methylbutyrate | 13. Dextrin |
| 5. Valerate | 14. Linoleic acid |
| 6. Isovalerate | 15. Primary sludge |
| 7. Lactate | 16. Primary sludge supernatant |
| 8. Pyruvate | 17. Primary sludge washed pellet |
| 9. Ethanol | |

The inhibitor agents tested were:

1. Sodium cyanide
2. Sodium fluoride
3. 2,4-Dinitrophenol

These inhibitor compounds were used with primary sludge as substrate. Concentrated stock solutions of acidic compounds 1-8 were made and adjusted to pH 7 before addition to the batch reactors.

The tested sludges included:

1. TAD sludge from the pilot scale control side (A side, medium air and 4.5 d SRT).
2. TAD sludge from the pilot scale experimental side (B side, 0 air and 4.5d SRT).
3. Fermenter sludge from a side stream fermentation process (PhD candidate Al Gibb's FGR-SGR pilot plant located at BC Research Inc. [FGR-Fixed Growth Reactor, SGR-Suspended Growth Reactor]).
4. Salmon Arm full scale ATAD sludge from the first and third cells of the process.

The batch test reactors were one L Erlenmeyer flasks. Each compound was tested under 2 conditions. The anaerobic condition was achieved by filling the Erlenmeyer flasks with process sludge to within 2 cm from the brim of the flask. The microaerobic condition was achieved by filling a one L flask to the 300 mL gradation with process sludge. Surface aeration in the microaerobic condition and mixing in the anaerobic condition were maintained by using 30 mm stir bars driven by a stirring platform. Rotational speed was kept between 120-150 rpm. TAD sludge experiments were conducted at the average 45° C operating temperature of the pilot scale units. The temperatures of the Salmon Arm ATAD batch sludge experiments were maintained at their respective full scale reactor temperatures (Appendix A). These temperatures were controlled by submerging the flasks and their contents into a Haake circulating water bath

(modelE8) set at specific isothermal temperatures. The fermenter sludge experiments were conducted at ambient room temperature.

Each compound tested had its respective anaerobic and microaerobic control, so that there were 2 anaerobic flasks and 2 microaerobic flasks for each compound tested. Each experiment lasted for approximately 50 h. Over the duration of each experiment, grab samples were taken to perform VFA and TOC determination. pH and ORP measurements were also made.

4. Results and Discussion

4.1 Batch Experiments

4.1.1 Fermentative and Oxidative VFA Metabolism in TAD

The batch experiments with spiked substrates and inhibitors were done to investigate VFA metabolism in TAD. The two batch experimental conditions tested were anaerobic and microaerobic. For a description of the physical apparatus, refer to Section 3.9. The anaerobic condition was selected in order to investigate the strict fermentative metabolism of the TAD process biomass. Under this condition (which lacks oxygen as the terminal electron acceptor), the oxidative metabolism of organisms in the process should be completely inhibited. The microaerobic condition was chosen in order to investigate the shift in metabolic activity when oxygen was introduced as a terminal electron acceptor. Figures 4. 1 to 4. 3 are results comparing the baseline accumulation of each VFA in terms of their response to both anaerobic and microaerobic conditions. The process biomass source was from the A side pilot scale TAD unit. The substrate was thickened primary sludge. Under the anaerobic condition, each VFA tended to increase, suggesting that only fermentative type reactions were occurring. It is interesting that propionate concentrations increased in the same proportion to that of acetate. This observation is consistent with results that show fermentation processes produce roughly the same equivalence of acetate to propionate (Elefsiniotis, 1993; Rabinowitz and Oldham, 1985). Under strict anaerobic conditions, complex organics would be oxidized to simple organics, resulting in the accumulation of fermentative end products in the medium. The accumulation of VFA in the

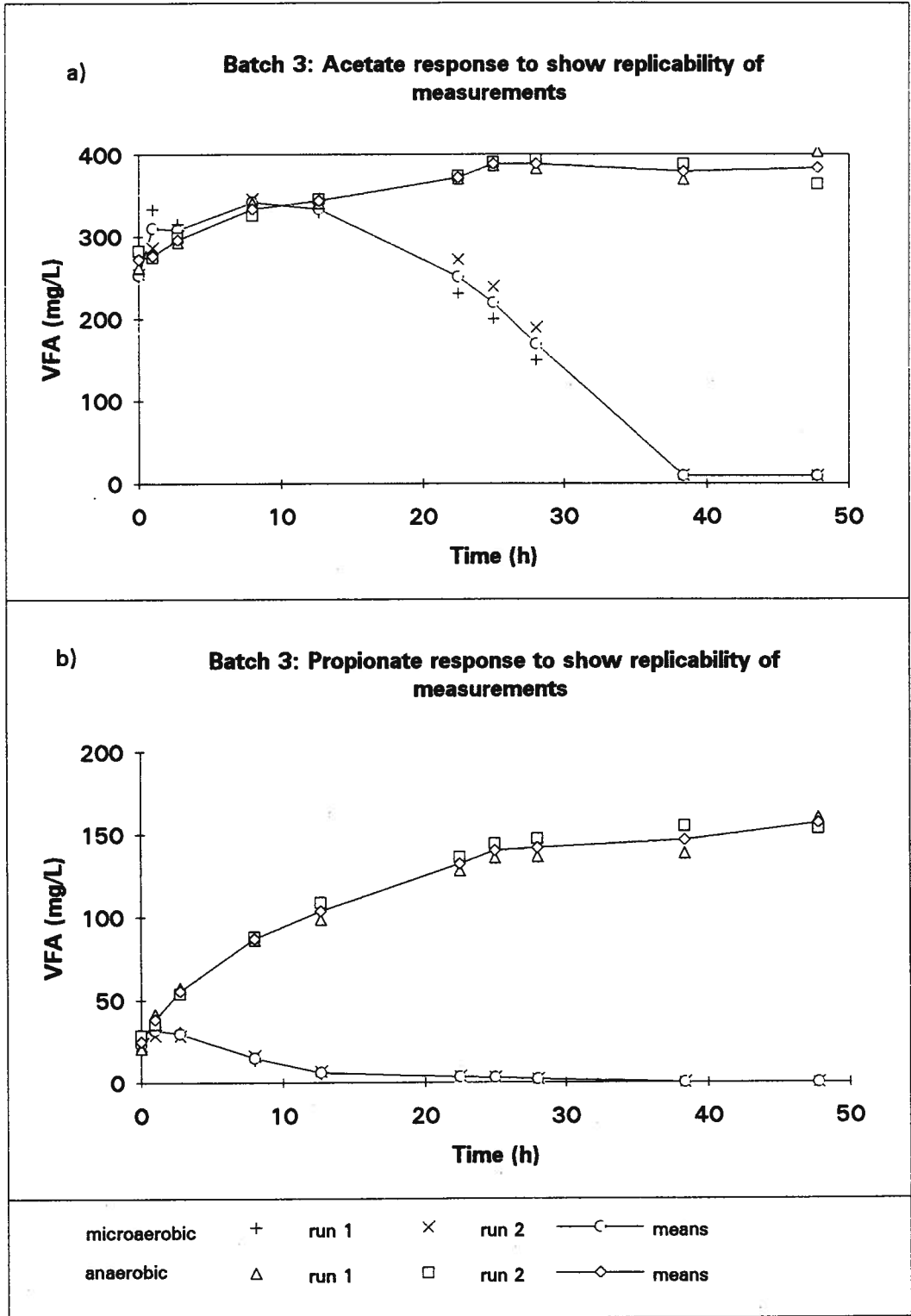


Figure 4. 1 Comparison of acetate and propionate concentrations between the anaerobic and microaerobic conditions. a) Acetate response and b) Propionate response.

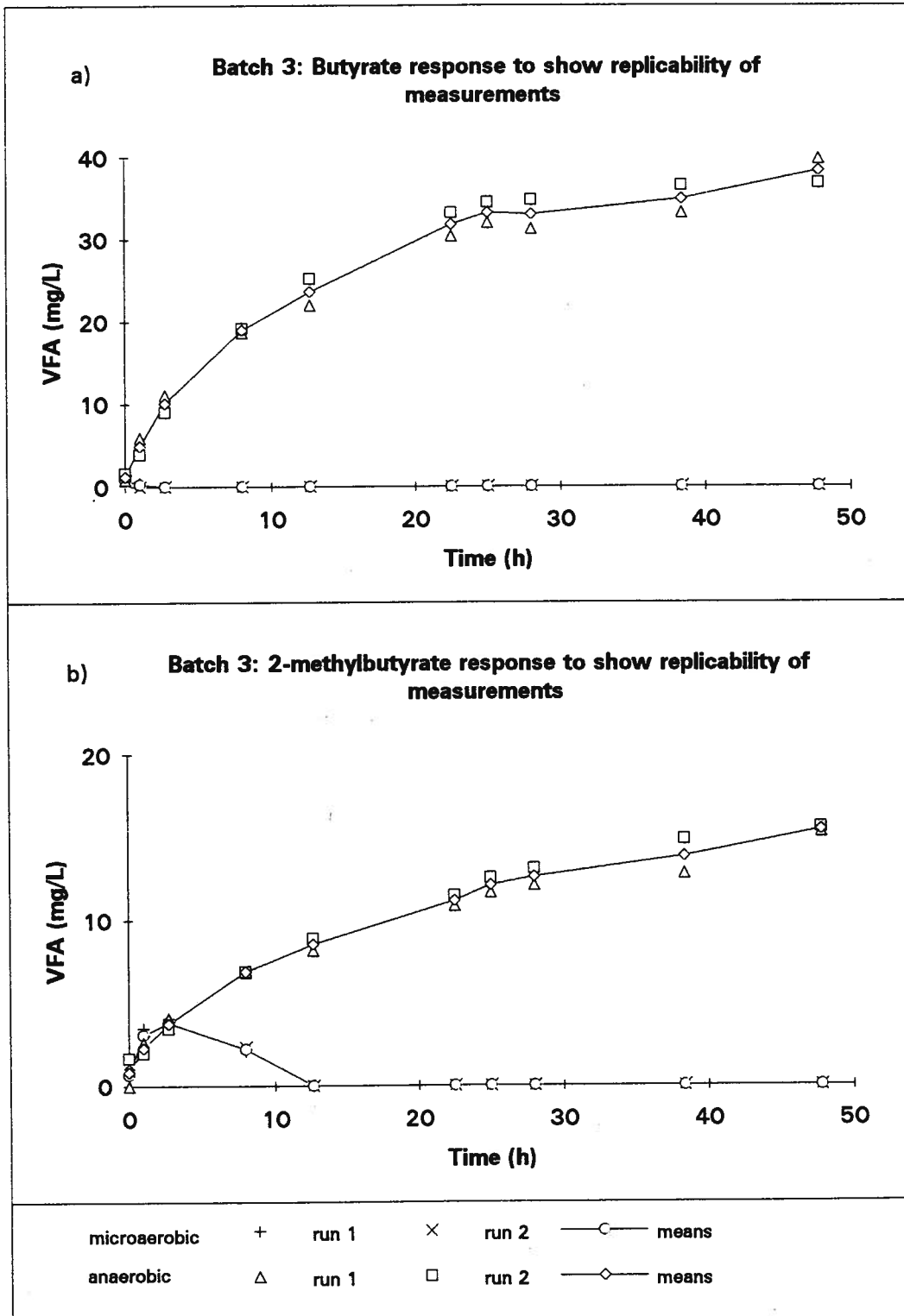


Figure 4. 2 Comparison of butyrate and 2-methylbutyrate concentrations between the anaerobic and microaerobic conditions. a) Butyrate response and b) 2-methylbutyrate response.

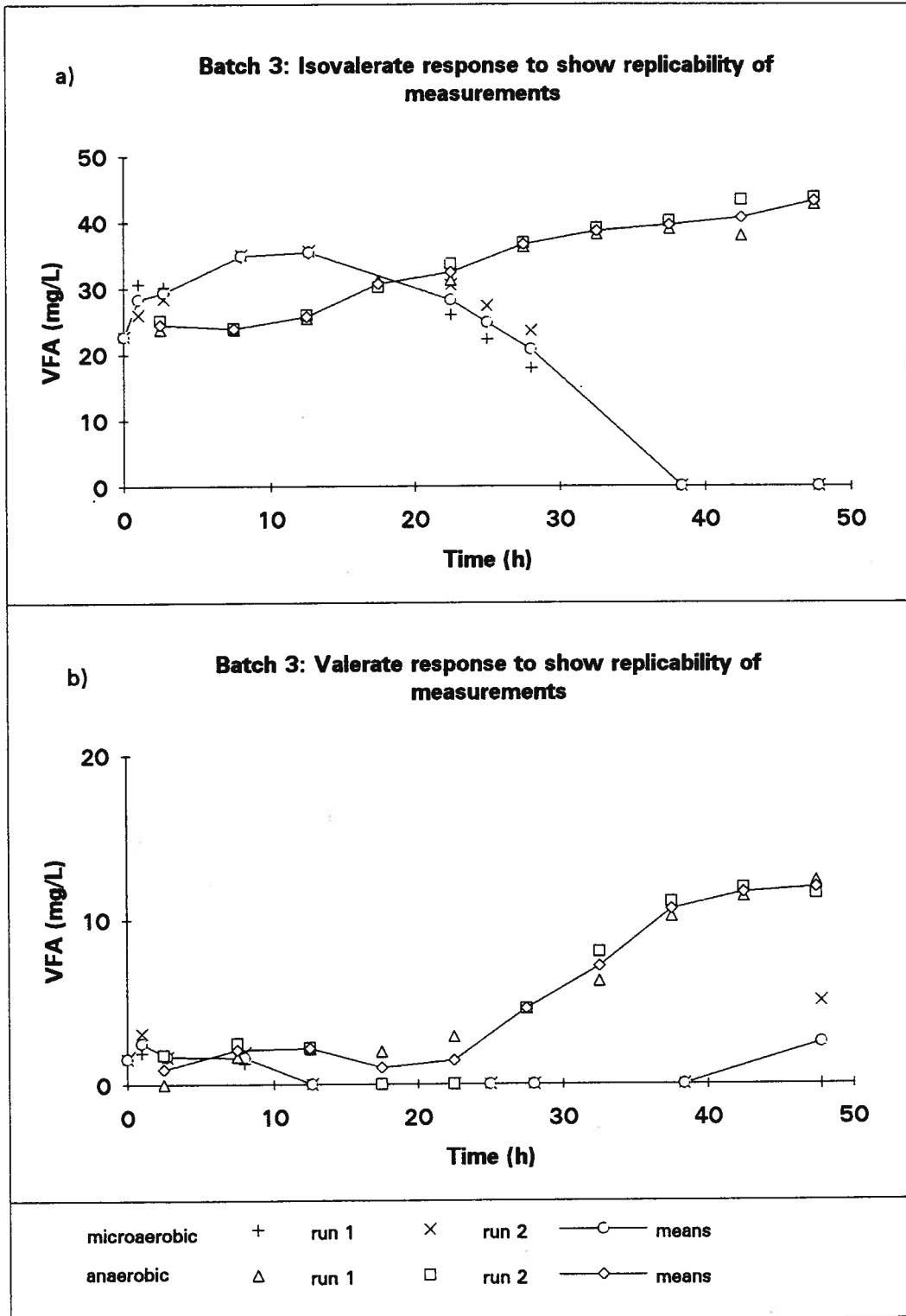


Figure 4. 3 Comparison of Isovalerate and valerate concentrations between the anaerobic and microaerobic conditions. a) Isovalerate response and b) Valerate response.

reactor indicates that these end products have been made. However, under microaerobic conditions, the trends of VFA metabolism are completely different. During the first 15 h, acetate concentrations increased while propionate concentrations decreased. This is similar to the response of these two VFA during the preliminary operation of the pilot scale TAD process under the transition condition (See Section 4.2). Over the next 25 h, net acetate concentrations decreased until 40 h into the study, when measurable acetate disappeared. It is clear from these results that the introduction of a terminal electron acceptor (eg. O₂), under the microaerobic condition, could account for the disappearance of VFA (ie. oxidation of VFA to CO₂ and H₂O). These trends in VFA metabolism define the baseline response of TAD sludge biomass to these two environmental conditions.

4.1.2 Substrate Addition Experiments

A range of substrates were tested for their effect on altering the baseline response of VFA accumulation under both the anaerobic and microaerobic conditions. The substrates tested were:

- | | |
|---------------------|----------------|
| 1. Propionate | 2. Valerate |
| 3. Isovalerate | 4. Butyrate |
| 5. 2-methylbutyrate | 6. Isobutyrate |
| 7. Pyruvate | 8. Lactate |
| 9. Ethanol | 10. Propanol |
| 11. Linoleic acid | 12. Glucose |
| 13. Dextrin | 14. Peptone |

The process biomass came from the control (A) side bioreactor. Substrates 1 through 10 were spiked and measured within each reactor during the course of the batch experiments. Substrates 11 to 14 were spiked to a concentration of approximately 1000 mg/L. The individual substrates were added at the beginning of each experiment. Figure 4. 4 shows results from the propionate addition experiment. Figures 4. 4a and 4. 4b show VFA trend data for the microaerobic control and propionate spiked reactors, respectively. These trends suggest that propionate consumption occurs concurrently with acetate production above that observed for the control. Net acetate concentrations started to decrease following the exhaustion of propionate.

Figures 4. 4c and 4. 4d show the VFA trend for the anaerobic control and propionate spiked reactors, respectively. Under this condition, propionate concentrations did not significantly change over the course of the experiment. The resulting acetate concentrations did not significantly deviate from that of the control reactor. The results from Figure 4. 4 suggest that under anaerobic conditions, propionate cannot be further oxidized while under the microaerobic condition, propionate can be oxidized to an acetate intermediate on its way to complete oxidation to CO₂ and H₂O.

The metabolism of propionate is initiated by its activation to propionyl-CoA. For the further metabolism of propionyl-CoA, several different pathways have been found which may be involved. A likely pathway for the catabolism of propionate occurs in both *E. coli* and *Acinetobacter* (formerly *Moraxella*) *lwoffi* (Gottschalk, 1986). These organisms convert

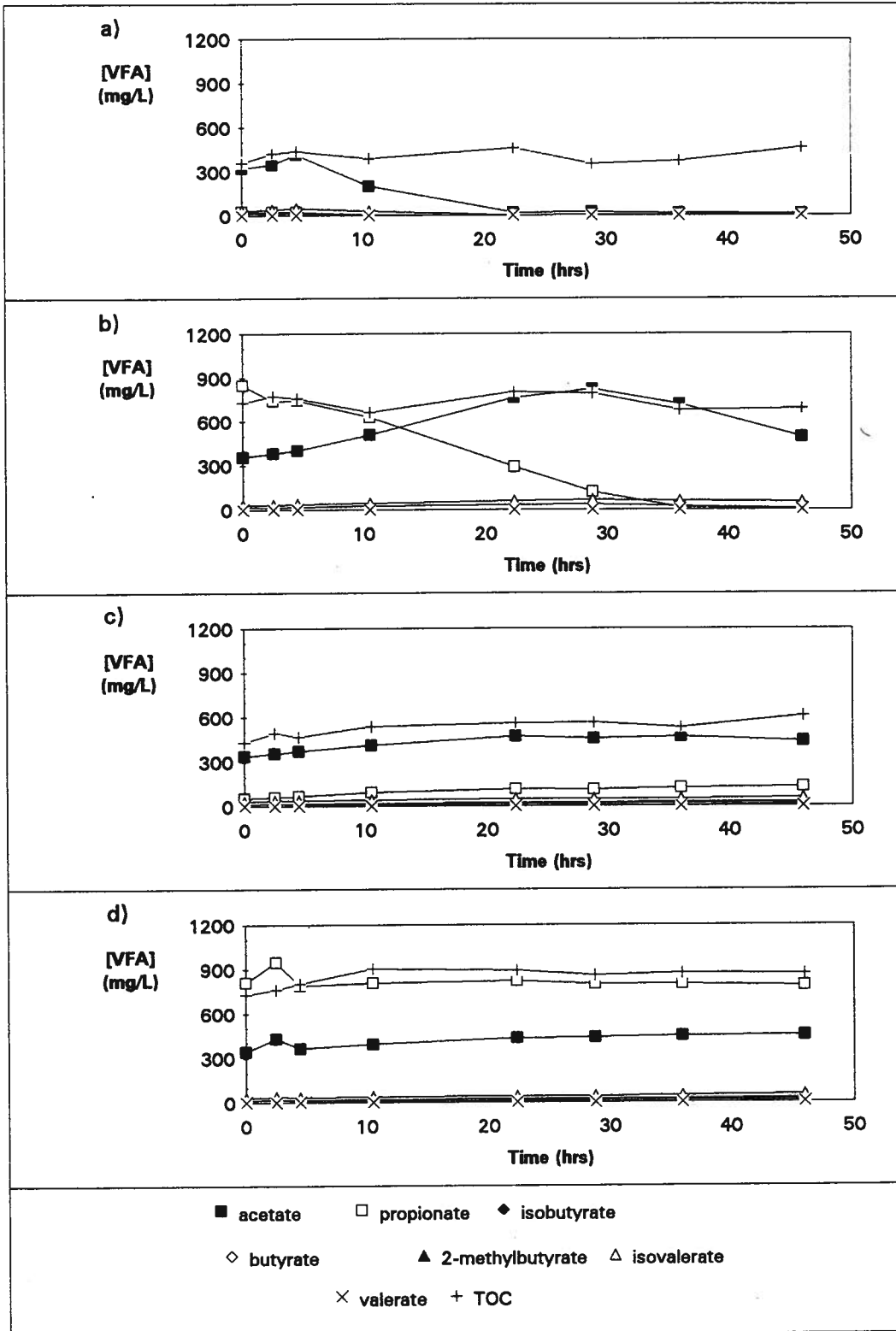
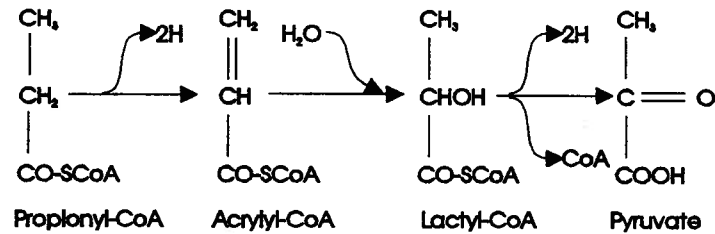


Figure 4. 4 VFA response in batch TAD experiment to propionate addition.
a) Microaerobic control b) Microaerobic with propionate addition
c) Anaerobic control d) Anaerobic with propionate addition.

propionyl-CoA to pyruvate by the following reactions,



According to these reactions, the conversion of propionyl-CoA to pyruvate liberates hydrogen and electrons, which are then carried in the form of $\text{NADH} + \text{H}^+$. This reduced form requires reoxidation if the conversion of propionate to pyruvate is to continue. Under strict fermentative conditions, the cells are unable to recycle the pool of NAD^+ , resulting in the accumulation of propionate (Figure 4. 4d). The introduction of oxygen results in a functional electron transport chain which can potentially regenerate NAD^+ , thus replenishing the pool of oxidized electron carrier, allowing the conversion to proceed. Only the conversion of propionate to pyruvate is addressed in this section, since the catabolism of pyruvate to acetate will be addressed in a subsequent section. In order to minimize the number of figures, difference plots between the substrate addition reactors and its corresponding control reactor were constructed. Figures 4. 5 - 4. 10 show this type of VFA profile in response to the addition of individual VFA at high concentrations at the start of each experiment (ie. substrates 1 through 6 from list). Individual reactors, with substrate added, were compared to the corresponding control reactor which had no external VFA added. The trends seen in these figures plot the difference between the experimental flask and the corresponding control flask. Each point on the plots is the difference between a concentration of measured compound in the substrate addition reactor and

the corresponding value in the control reactor at each sampling time point ($[\Delta]=[\text{experimental}]-[\text{control}]$). A trend that is localized to the zero line suggests no difference in VFA response between the control and test conditions.

Figure 4. 5 shows the same results as Figure 4. 4, except that the data are expressed using this new format. As can be seen from Figure 4. 5, most of the observations from Figure 4. 4 also show up in these figures. Under the microaerobic condition (Figure 4. 5a), acetate shows the greatest deviation from its control value and as propionate concentrations approach that of the control value, which is zero by 30 h, acetate concentrations start to fall. Under the anaerobic condition (Figure 4. 5b), propionate is not consumed so the difference between the addition reactor value and its control value remains constant over the length of the experiment.

4.1.2.1 Valerate and Butyrate Addition Experiments

Figures 4. 6 and 4. 7 show the results of the valerate and butyrate addition experiments, respectively. The results are similar to that of the propionate addition experiment, with the exception of the valerate addition experiment. Under the microaerobic condition, the consumption of valerate seems to stimulate the production of acetate and propionate but to a lesser extent. This anomaly is consistent with known biochemical properties of bacteria. These VFA can be degraded by the aerobic β -oxidation process (Lehninger, 1982) known to occur in a number of microorganisms (eg. *Pseudomonads*, *Acinetobacter*, *Bacilli* and *E. coli*). The first step in the oxidation of these VFA is the conversion to their corresponding CoA esters by acyl-

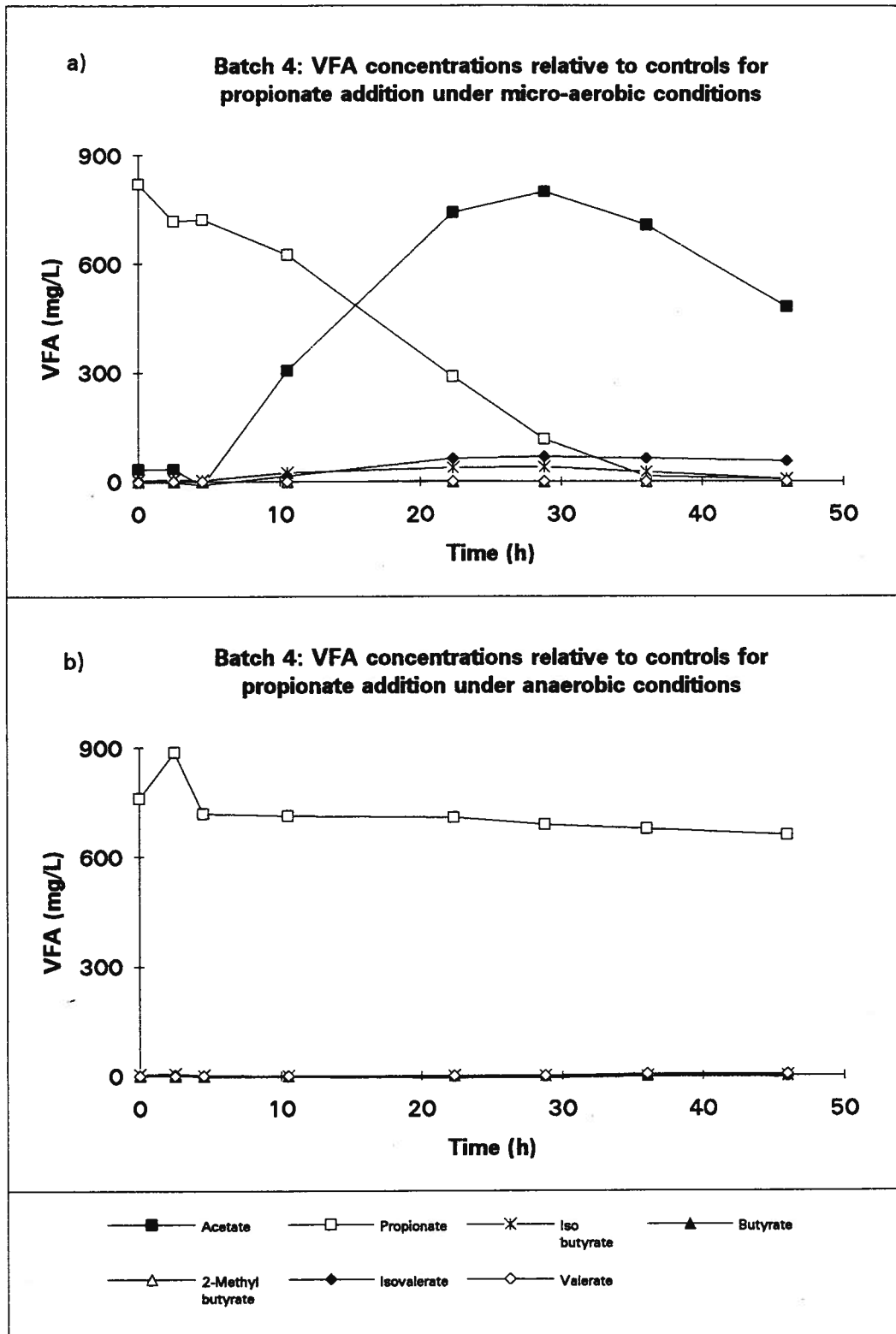


Figure 4. 5 Difference plots of the propionate addition experiment under a) microaerobic and b) anaerobic conditions.

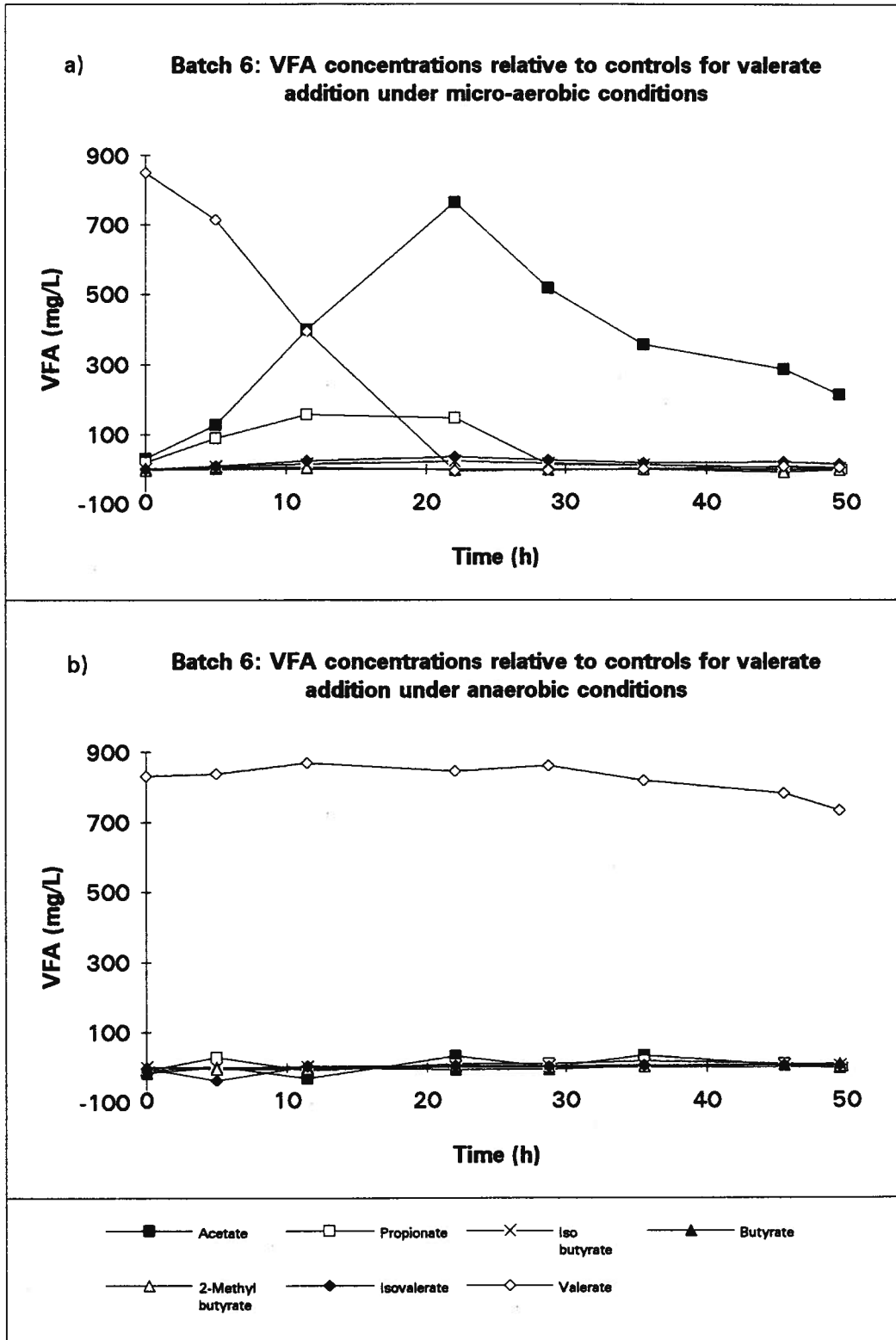


Figure 4. 6 Difference plots of the valerate addition experiment under a) microaerobic and b) anaerobic conditions.

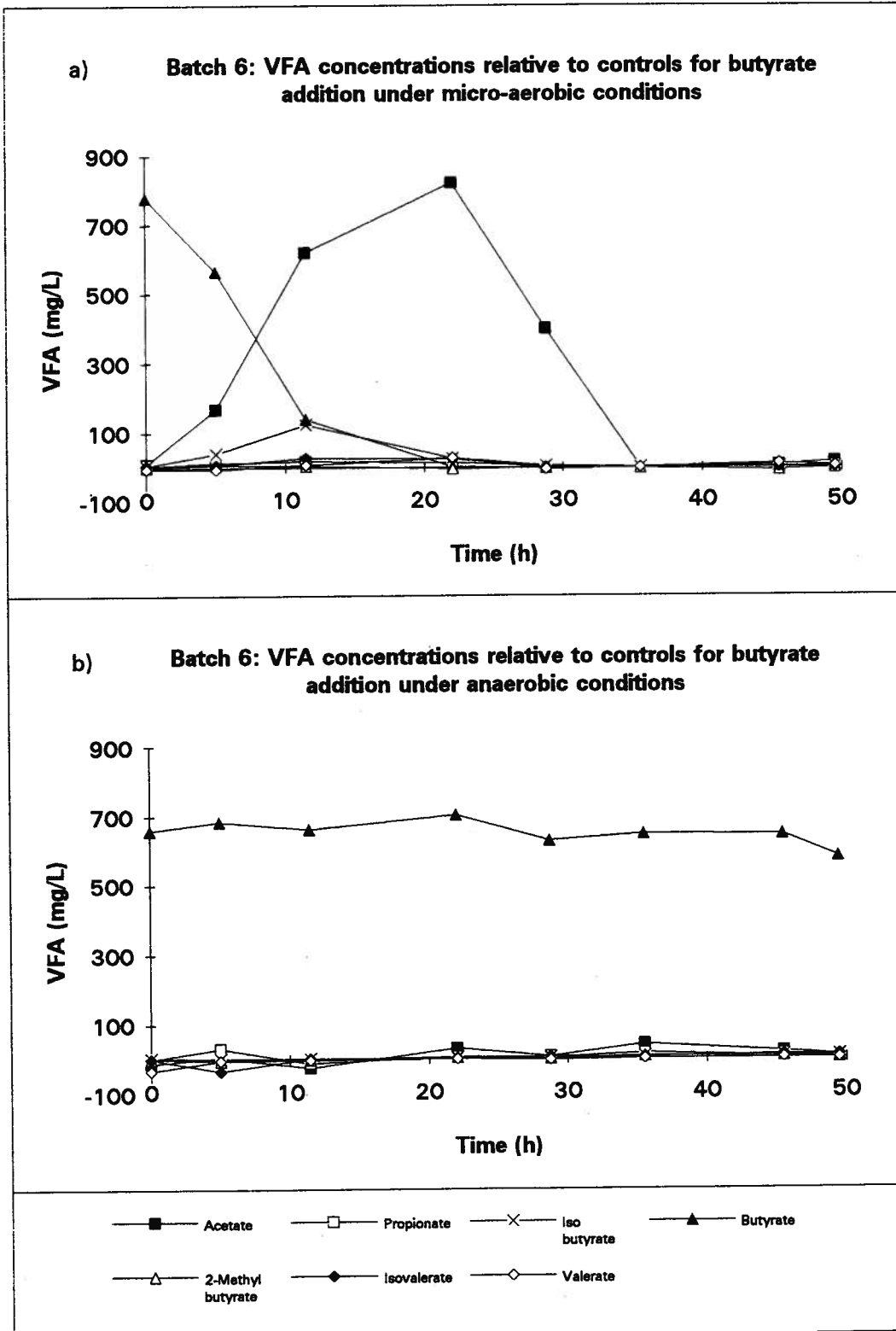
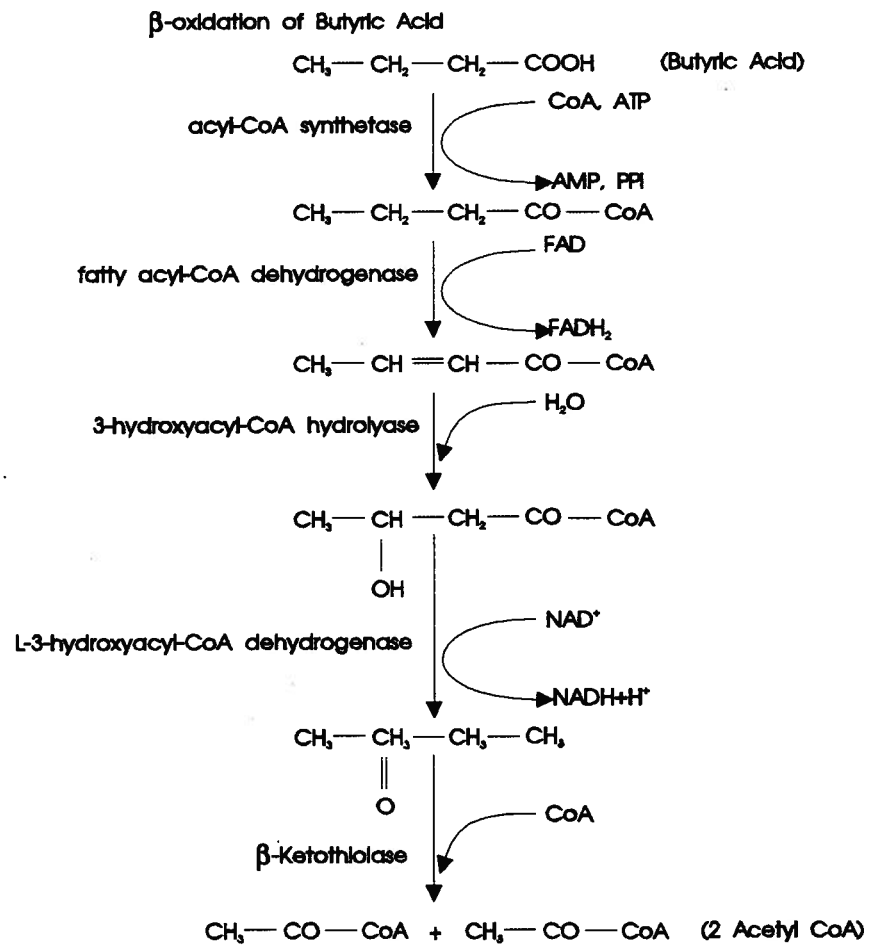


Figure 4. 7 Difference plots of the butyrate addition experiment under a) microaerobic and b) anaerobic conditions.



β -oxidation of Valeric Acid

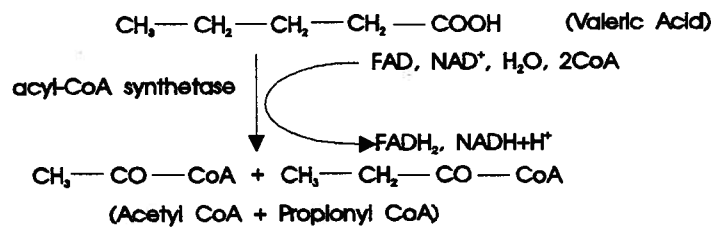


Figure 4. 8 β -oxidation of butyric and valeric acids.
(adapted from Lehninger, 1982)

CoA synthetase. The CoA esters are then oxidized in the β position and subsequently cleaved to yield acetyl-CoA and the CoA ester of the fatty acid shortened by 2 carbon atoms. This process required the concerted action of four enzymes, as illustrated in Figure 4. 8. In the case of butyrate, β -oxidation yields two acetyl-CoA. With valerate, β -oxidation yields acetyl-CoA and propionyl-CoA in equimolar amounts. Figure 4. 6a shows that acetate and propionate are not produced in equimolar proportions. This is expected since propionate, under microaerobic conditions, can be further oxidized to acetate. For each molecule of butyrate or valerate oxidized, there is a corresponding consumption of one molecule each of FAD and NAD^+ (Lehninger, 1982). In order for β -oxidation to continue, as is the case for propionate oxidation, there must be an operating mechanism to recycle the oxidized form of these electron carriers. Under microaerobic conditions, the electron transport chain can serve this purpose.

4.1.2.2 Isobutyrate, Isovalerate and 2-Methylbutyrate Addition Experiments

Figures 4. 9 to 4. 11 show the difference trends in VFA metabolism for the isobutyrate, isovalerate and 2-methylbutyrate addition experiments. Under the anaerobic condition, each of these spiked VFA behaved similarly to the other VFA tested. They remained in the medium and were not further oxidized to any intermediate products. Under microaerobic conditions, the disappearance of these VFA seemed to stimulate a transient acetate production. The available evidence in the literature suggests that bacterial catabolism of these 3 VFA converges with the

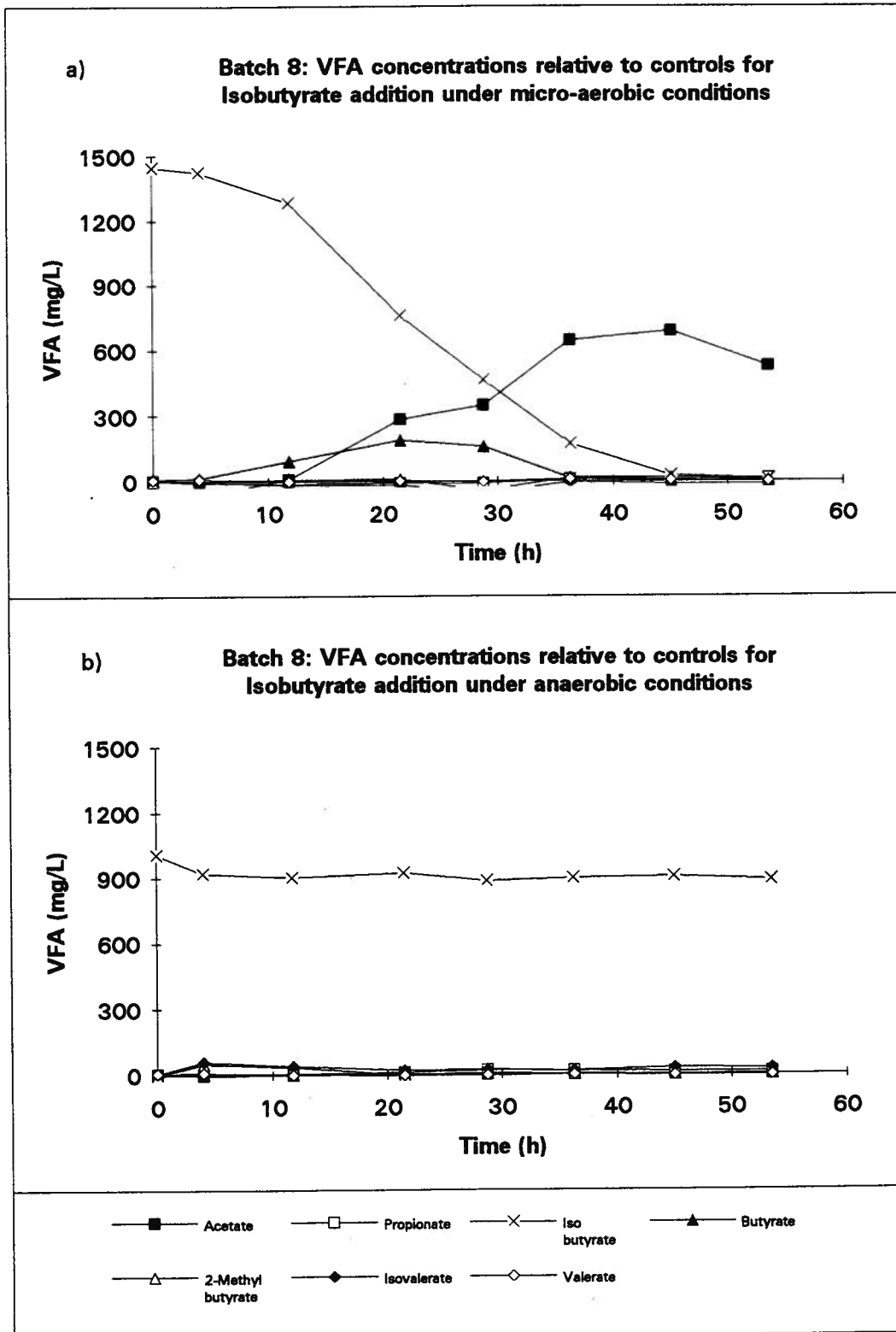


Figure 4. 9 Difference plots of the isobutyrate addition experiment under a) Microaerobic and b) anaerobic conditions.

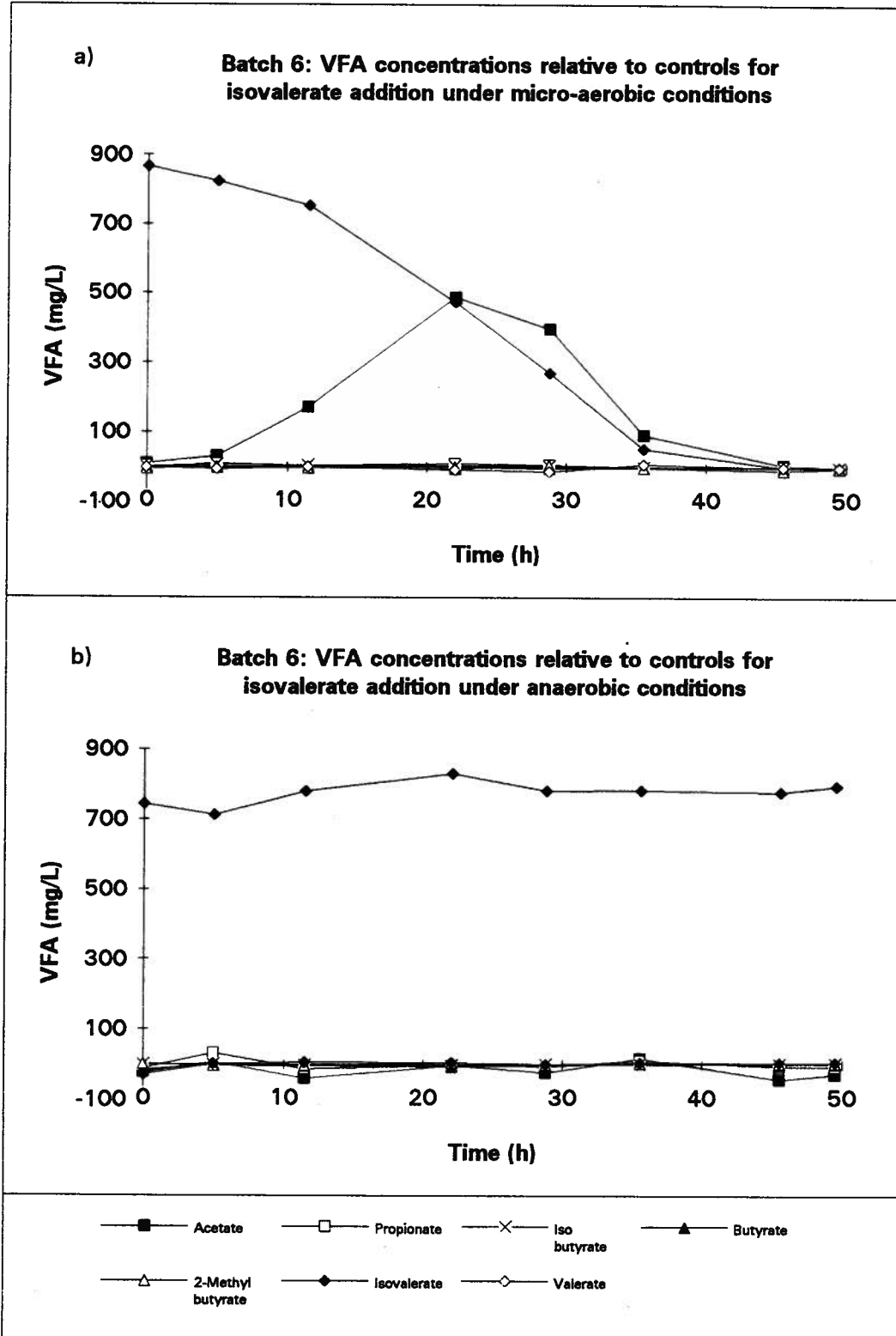


Figure 4.10 Difference plots of the isovalerate addition experiment under a) microaerobic and b) anaerobic conditions.

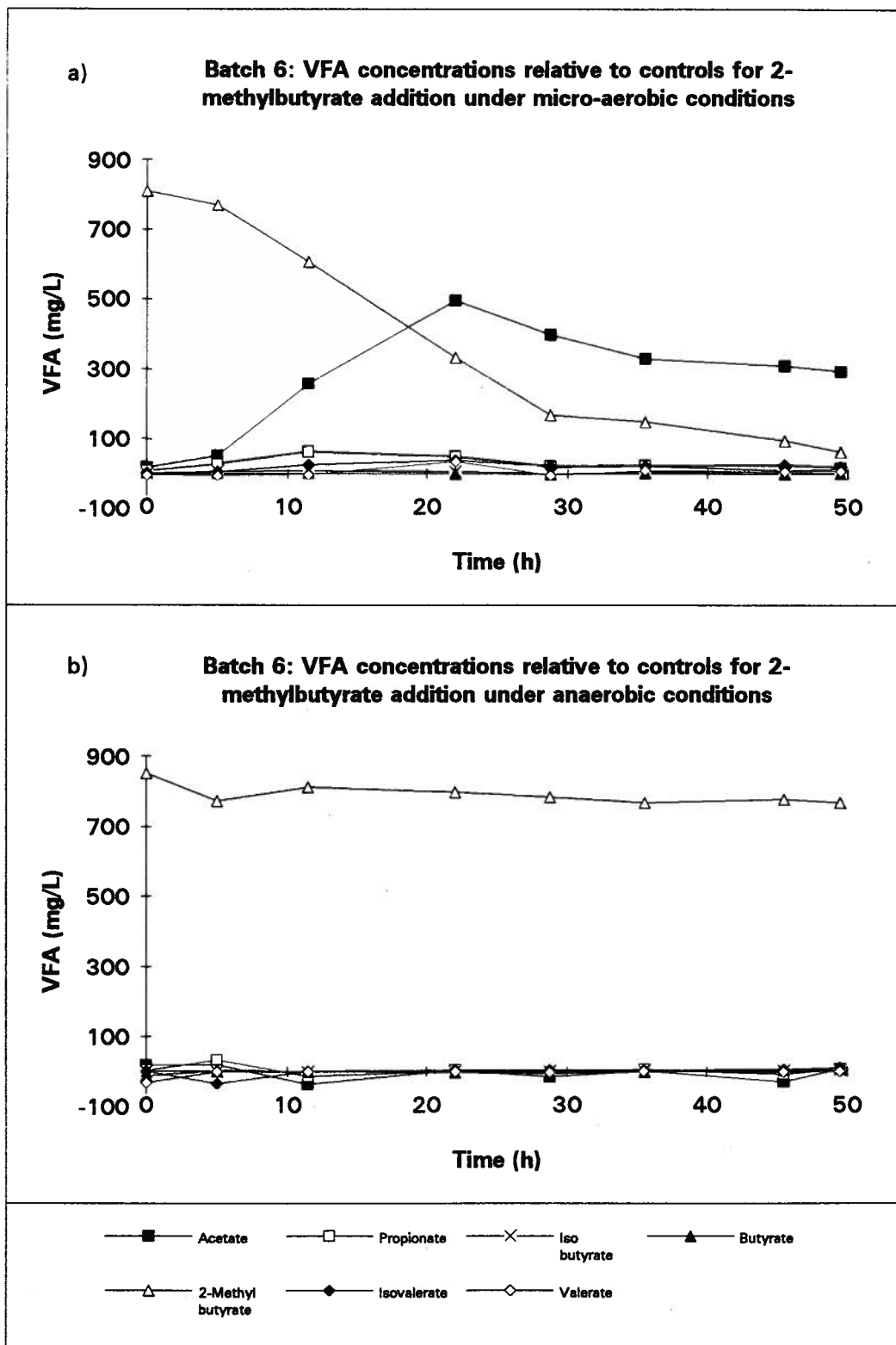


Figure 4.11 Difference plots of the 2-methylbutyrate addition experiment under a) microaerobic and b) anaerobic conditions.

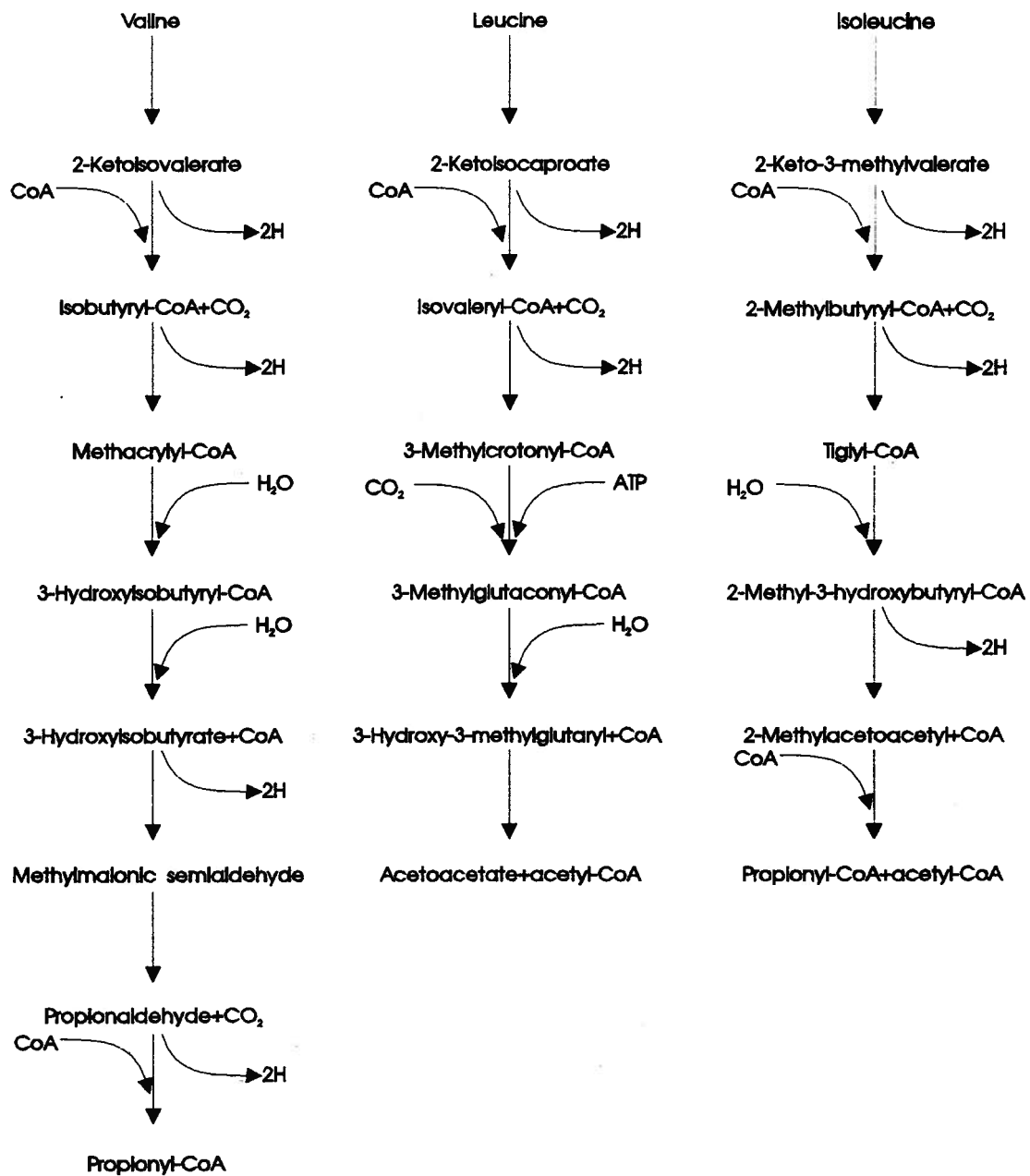


Figure 4. 12 Reactions in the oxidation of the branched chain amino acids by bacteria (adapted from Sokatch et al., 1968).

oxidative pathways of branched chain amino acids, valine, leucine and isoleucine (Figure 4. 12).

The enzymatic conversions necessary for the catabolism of branched chain amino acids shown in Figure 4. 12 have been reported to occur in a variety of organisms. However, most studies have been done using several species of *Pseudomonas* (Massey *et al.*, 1976).

Growth of *P. aeruginosa* on valine results in simultaneous development of the ability of whole cells to oxidize isobutyrate and propionate (Sokatch *et al.*, 1968). The enzymes involved in the catabolism of leucine were first discovered in species of *Mycobacterium* and *Alcaligenes* (formerly called *Achromobacter*) isolated from soil, using a selective culture medium with isovaleric acid as the sole carbon source (Sokatch, 1969). The bacterial oxidation of isoleucine to acetyl-CoA and propionyl-CoA was first described by Conrad *et al.* (1974). The synthesis of these enzymes was induced by growth on either isoleucine or 2-methylbutyrate.

The complete catabolism of each branched chain amino acid requires the cooperation of two sequential series of reactions. The enzymes of the first series comprise a common pathway catalyzing the conversion of isoleucine, leucine and valine to their respective acyl-CoA derivatives. However, the branched chain metabolites formed subsequent to this common pathway are catabolised by three separate enzyme series, one specific for each amino acid.

The first step in the oxidation of isobutyrate, isovalerate and 2-methylbutyrate are the conversion to their respective CoA esters. From this point in the reaction sequence, these intermediates can feed directly into the catabolic pathways of the branched chain amino acids. From these sequential series of reactions (Figure 4. 12), it is clear that isobutyryl-CoA is oxidized to propionyl-CoA; isovaleryl-CoA is oxidized to acetoacetate and acetyl-CoA and 2-

methylbutyryl-CoA are oxidized to acetyl-CoA and propionyl-CoA. The results from Figures 4. 9 to 4. 11 suggests that the catabolism of these VFA lead only to acetate as an intermediate metabolite. However, it must be remembered that, under microaerobic conditions, propionyl-CoA will be further metabolized to pyruvate and ultimately to acetate via acetyl-CoA. Therefore, it is reasonable to observe no accumulation of propionate in the batch reactors. As is the case for all other VFA tested, the catabolic pathways of the branched chain amino acids evolve hydrogen (ie. consume NAD^+). Consequently, operation of these pathways can only take place when a terminal electron acceptor, such as oxygen, is available (ie. microaerobic condition).

4.1.2.3 Pyruvate and Lactate Addition Experiments

Figures 4. 13 and 4. 14 show the pyruvate and lactate addition experiments, respectively. What makes these results different from the VFA addition experiments is the apparent consumption of both of these substrates under anaerobic conditions. Under this condition, pyruvate consumption was followed by acetate production. Since there is no acetate catabolic activity under anaerobic conditions, acetate accumulated and persisted in the medium. Under the microaerobic condition, pyruvate disappearance was followed by only a slight short term accumulation of acetate.

The Enterobacteriaceae are able to synthesize two different enzyme systems for the breakdown of pyruvate to acetyl-CoA. The pyruvate dehydrogenase multienzyme complex is

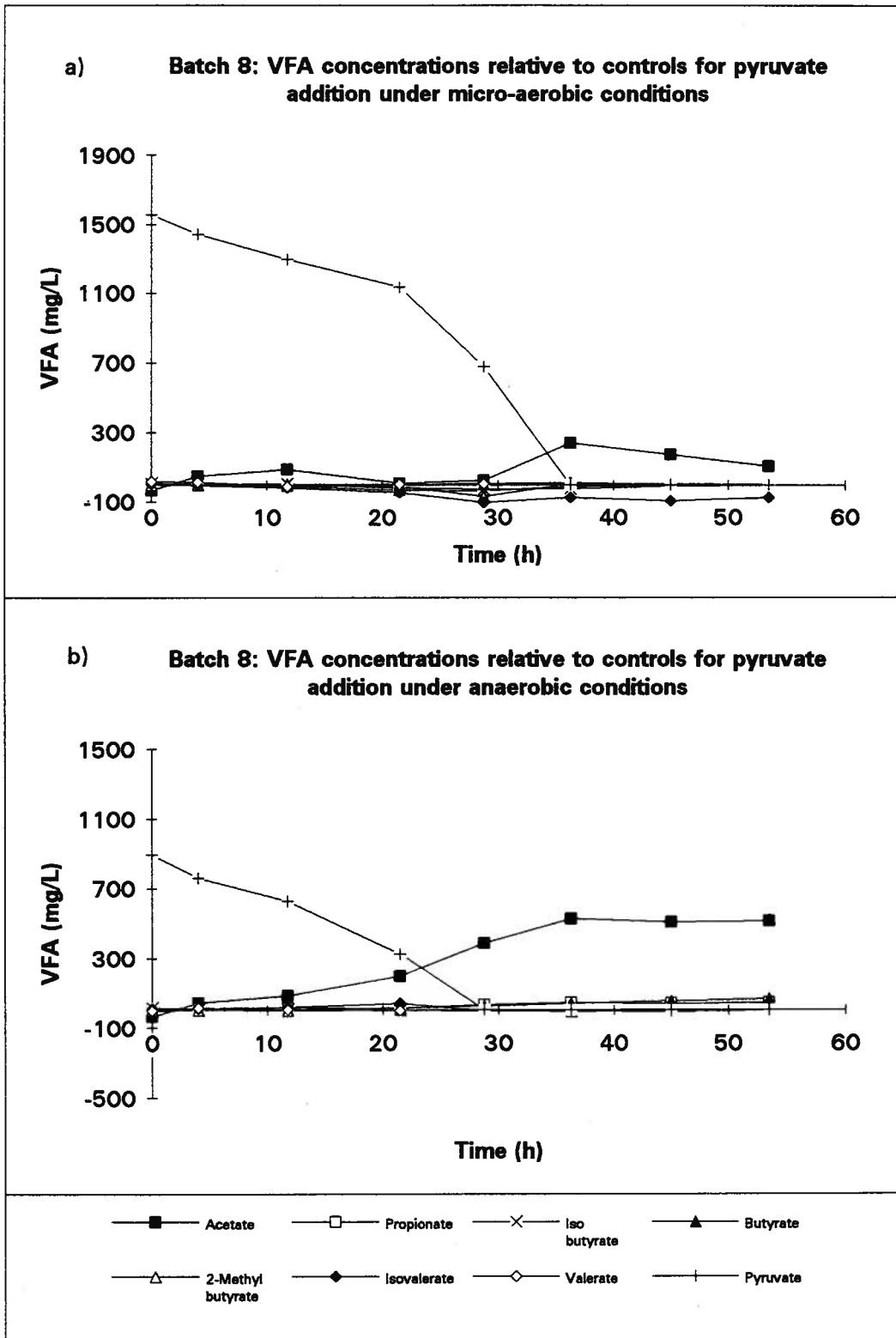


Figure 4.13 Difference plots of the pyruvate addition experiment under a) microaerobic and b) anaerobic conditions.

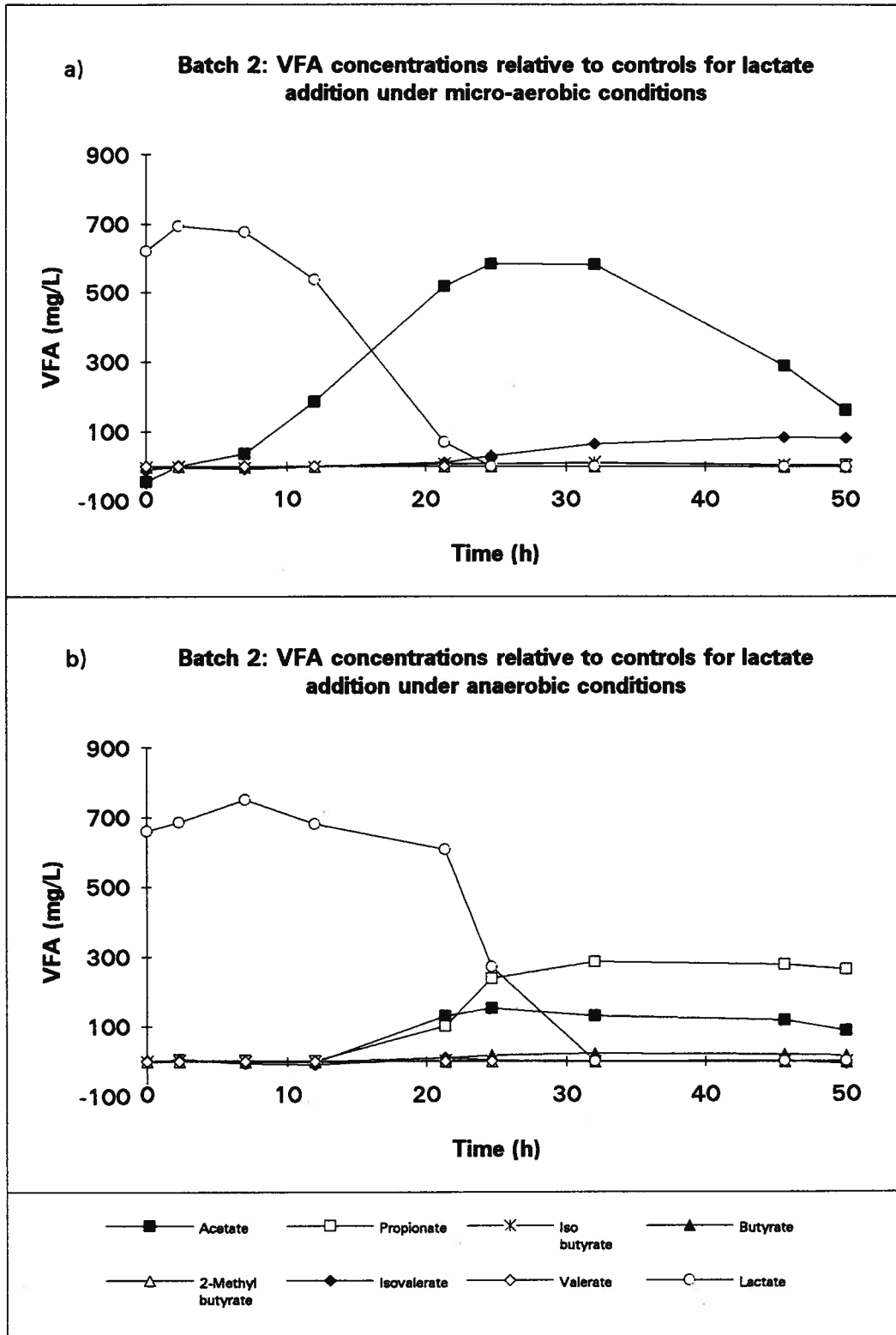
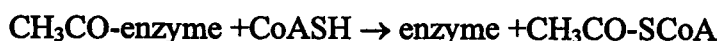


Figure 4.14 Difference plots of the lactate addition experiment under a) microaerobic and b) anaerobic conditions.

involved in the aerobic metabolism of this compound. Under anaerobic conditions, these enzymes are no longer synthesized and the enzyme still present is inhibited by NADH. Instead, the synthesis of pyruvate formate lyase is induced under fermentative conditions (Pecher *et al.*, 1982). The reactions catalyzed by this enzyme proceed in two steps, with an acyl-enzyme intermediate and acetyl-CoA and formate as products.



Pyruvate formate lyase is irreversibly and rapidly inactivated in the presence of air so that it functions only in fermentative metabolism. Even under anaerobic conditions, the enzyme is not very stable. At low concentrations of pyruvate, it is converted to an inactive form which can be reactivated. Upon a shift to anaerobic conditions, the inactive form of pyruvate formate lyase is converted to the active enzyme by a complicated reaction series involving reduced flavodoxin, S-adenosyl methionine and an activating enzyme (Knappe and Schmitt, 1976; Conradt *et al.*, 1984; Pascal *et al.*, 1981). The major advantage of pyruvate formate lyase over the pyruvate dehydrogenase complex is that the formation of acetyl-CoA is not accompanied by the reduction of NAD^+ . The functional nature of this enzyme is consistent with the observations from Figure 4. 13, that pyruvate consumption, under anaerobic conditions, is accompanied by acetate production. The criteria for balancing reducing equivalence had been met by producing formate instead of CO_2 .

Under anaerobic conditions, the consumption of lactate is followed by the accumulation of both propionate and acetate in an approximate 2 propionate: 1 acetate molar ratio. The most

likely sequence of reactions for this type of conversion is the acrylate pathway. This pathway is generally associated with a few anaerobic microorganisms (eg. *Clostridium propionicum*, *Megasphaera* [formerly *Peptostreptococcus*] *elsdenii*). Figure 4. 15 illustrates this pathway, which converts lactate to propionate and acetate in a molar ratio of 3:2:1 with CO₂ and H₂O as by products. This figure shows that L, D or DL-lactate may serve as substrate; an enzyme is present which interconverts the isomers (#1). L-lactate is converted to L-lactyl-CoA in a CoA transferase reaction (#2). By reactions not yet established in detail, acrylyl-CoA is produced (#3). This intermediate is then reduced to propionyl-CoA (#4) and propionate is produced by the above mentioned CoA transferase (#2). The hydrogen donor for the reduction of acrylyl-CoA to propionyl-CoA is a reduced electron transferring flavoprotein. These oxidized carriers become reduced by the conversion of D-lactate to acetate, thus achieving redox balance without the necessity of an external process to regenerate the pool of electron carriers (eg. respiratory chain). Under microaerobic conditions, with a functioning electron transport chain, only the accumulation of acetate is seen. These results are consistent with the previous results obtained for the VFA addition experiments under microaerobic conditions. Specifically, when oxygen is introduced into the bioreactor, propionate (which accumulated in the lactate addition experiment under anaerobic conditions) may either not be produced or be further oxidized to a transient acetate intermediate under microaerobic conditions.

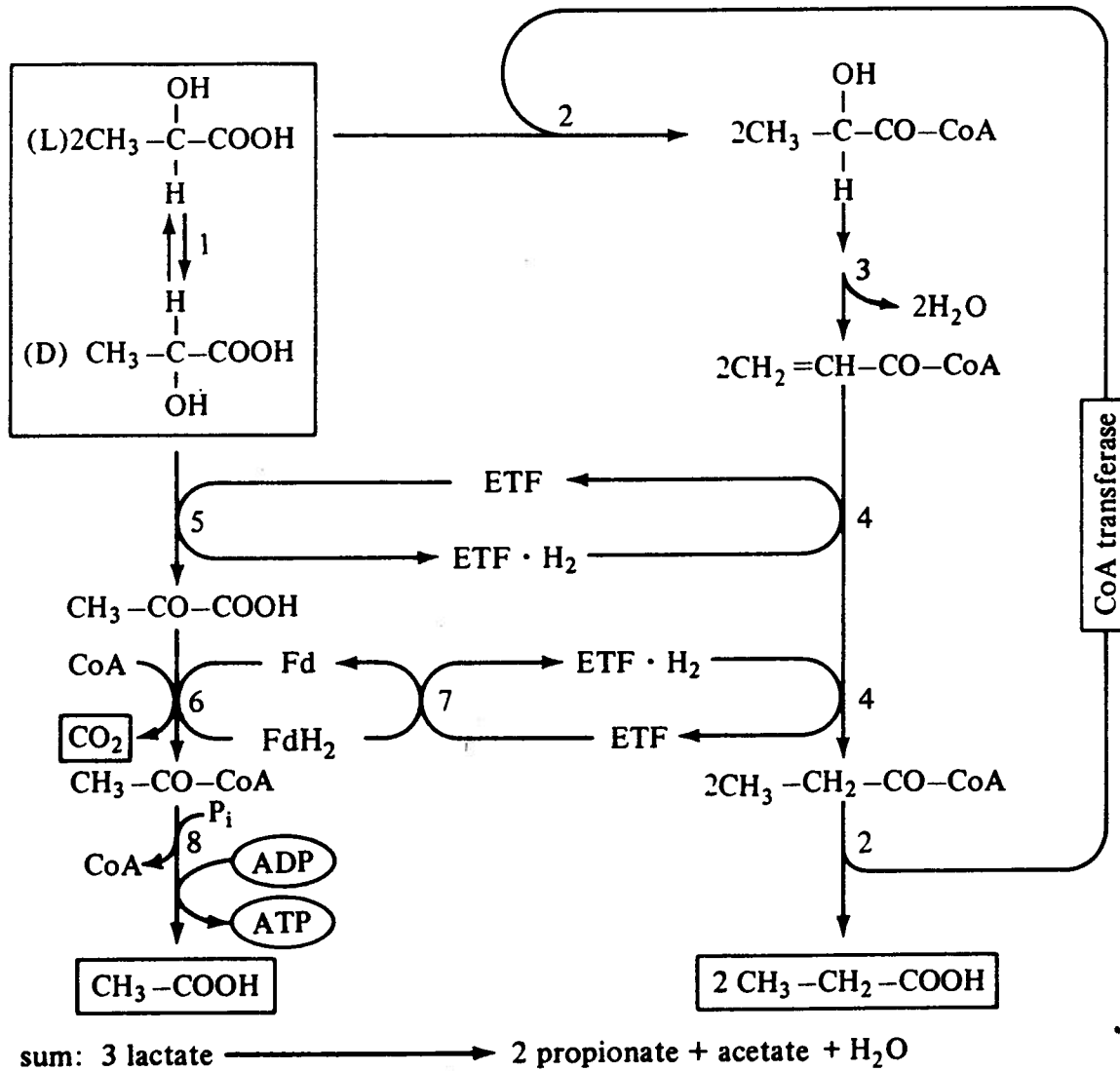


Figure 4. 15: Formation of propionate and acetate from DL-lactate via the acrylate pathway (Gottschalk, 1986).

4.1.2.4 Ethanol and Propanol Addition Experiments

Figures 4. 16 and 4. 17 show the results of the ethanol and propanol addition experiments. Under anaerobic conditions, ethanol consumption was concomitant with the production of acetate. Under this same condition, propanol consumption corresponded to the production of propionate. This is a somewhat surprising result since ethanol and propanol are more reduced compounds than acetate and propionate, respectively. Therefore, the oxidation of these compounds to their corresponding acids necessitates the production of reduced electron carriers, and since the oxidative chain is not functional under fermentative conditions, there must be an alternative mechanism for recycling the oxidized pool of these electron carriers.

A mechanistic process to explain anaerobic consumption of ethanol and production of acetate are found in the anaerobic digestion literature (Harper and Pohland, 1986). In order for catabolism of glucose to proceed, the NADH produced during substrate level phosphorylation of glyceraldehyde-3-phosphate must be regenerated to NAD^+ . This function is accomplished by the reduction of protons to form hydrogen gas, which is subsequently removed by the hydrogenotrophs (eg. methanogens). Microbial associations, in which an H_2 producing organism can grow only in the presence of an H_2 consuming organism, are called 'syntrophic associations'. The coupling of formation and use of hydrogen is called 'interspecies hydrogen transfer'. The thermodynamics of reactions in which some compounds yield acetate and H_2 (and CO_2 in the cases of propionate and lactate) are illustrated in Table 4. 1. The free energy changes are positive for propionate, butyrate and ethanol. Therefore, the reactions will not proceed from

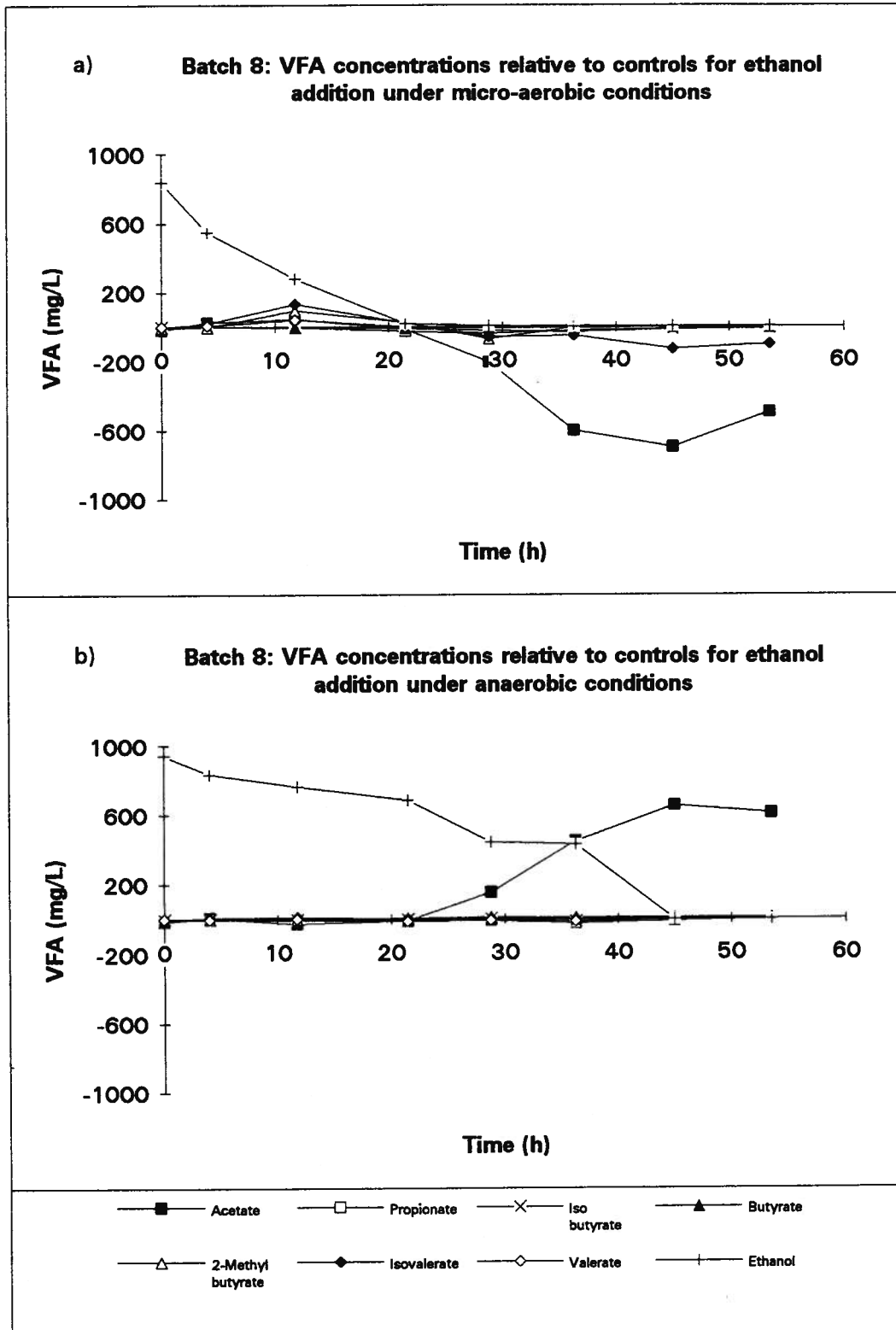


Figure 4.16 Difference plots of the ethanol addition experiment under a) microaerobic and b) anaerobic conditions.

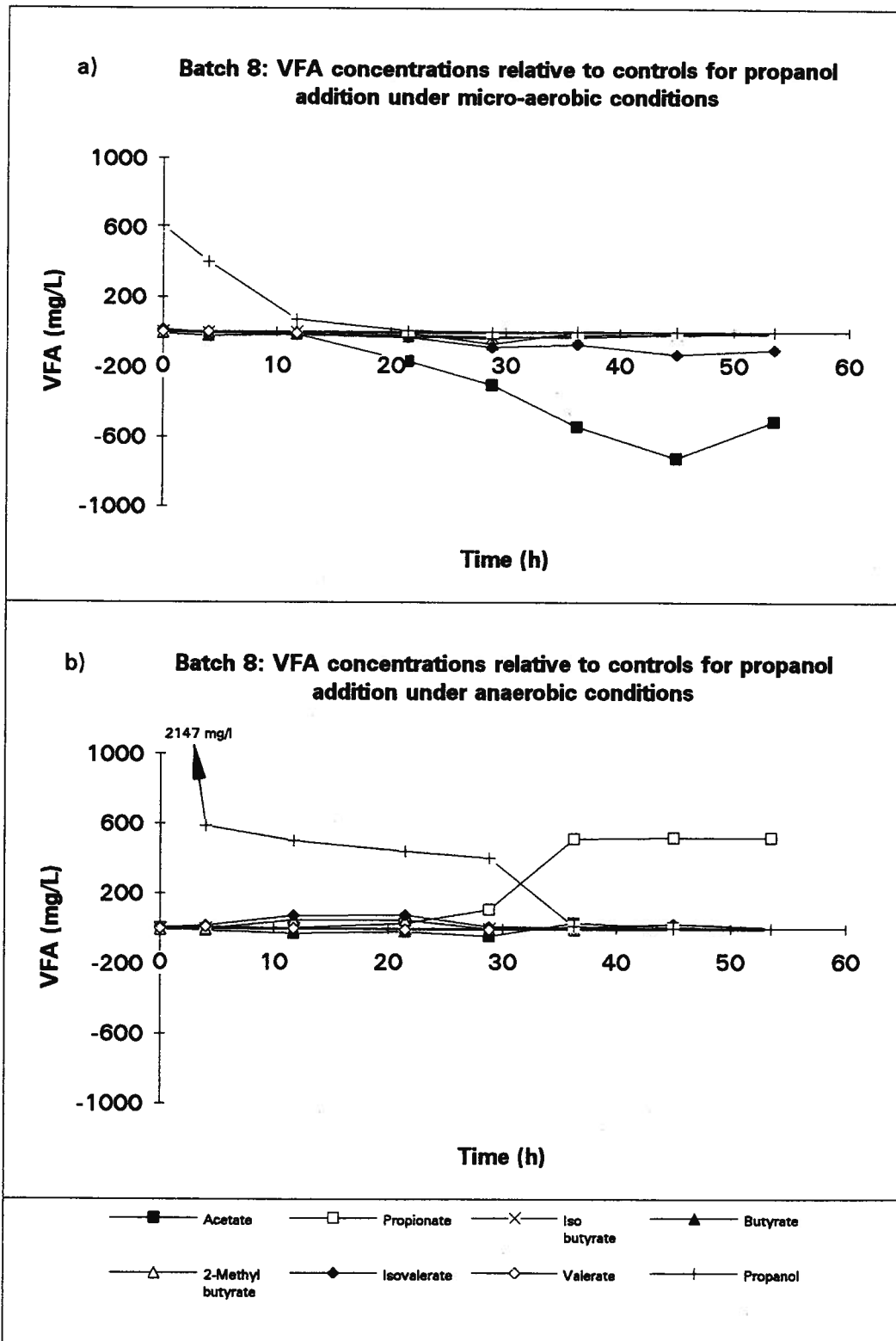


Figure 4.17 Difference plots of the propanol addition experiment under a) microaerobic and b) anaerobic conditions.

left to right except under conditions in which a product is kept at an extremely low concentration. Due to the high affinity of the methanogenic organisms towards H_2 , the partial pressure of H_2 , which is a product in the catabolism of these compounds, is maintained as low as 10^{-4} atmospheres in the presence of these bacteria. This concentration is low enough to allow the formation of H_2 by oxidizing NADH to regenerate NAD^+ as well as allowing thermodynamically unfavorable reactions feasible (ie. reactions having a $+\Delta G^{\circ}$)(Wolin, 1976). What must be remembered about the previous results shown is that both propionate and butyrate remain unmetabolized in the medium under anaerobic conditions. These results seem to be contradictory to the ethanol catabolic results that suggest ethanol catabolism under fermentative conditions. However, this free energy change is much more positive for both propionate and butyrate conversion to acetate than for ethanol (ie. +76.1 and +48.1 kJ versus +9.6 kJ).

Table 4. 1 Selected acetogenic reactions.

Acetogenic reactions	ΔG° (KJ) ^a
Propionate → acetate	
$CH_3CH_2COOH + 2H_2O \rightarrow CH_3COOH + CO_2 + 3H_2$	+76.1
Butyrate → acetate	
$CH_3CH_2CH_2COOH + 2H_2O \rightarrow 2CH_3COOH + 2H_2O$	+48.1
Ethanol → acetate	
$CH_3CH_2OH + H_2O \rightarrow CH_3COOH + 2H_2$	+9.6
Lactate → acetate	
$CH_3CHOHCOOH + 2H_2O \rightarrow CH_3COOH + CO_2 + H_2O$	-4.2
Hydrogen + carbon dioxide → acetate	
$4H_2 + 2CO_2 \rightarrow CH_3COOH + 2H_2O$	-107.1
Hydrogen + carbon dioxide → methane	
$4H_2 + CO_2 \rightarrow CH_4 + H_2O$	-135.6

^a Adapted from Thauer *et al.*(1977) and Gottschalk (1986)

Table 4. 1 lists the free energy changes for each of the reactions listed above. According to Harper and Pohland (1986), thermodynamic calculations associated with these reactions indicate that propionic acid oxidation to acetate becomes favorable only at hydrogen partial pressures below 10^{-4} atm, while butyric acid oxidation becomes favorable at 10^{-3} atm H_2 or below. In contrast, ethanol oxidation to acetate is not inhibited until the hydrogen partial pressure approaches 1 atm. Therefore, if the hydrogen partial pressure can be maintained between 10^{-3} and 10^{-1} atm., this would theoretically favor the oxidation of ethanol to acetate but not the oxidation of propionate or butyrate. The mechanism by which the partial pressure of hydrogen can be maintained within this range under the experimental conditions of the batch tests is not well understood. The syntrophic association between acetogenic and methanogenic reactions under TAD conditions probably does not occur since methanogens are typically not associated with the TAD process. There is, however, another group of organisms which may play a role in the process of hydrogen utilization.

We have seen that acetate, so far, is an important product in a number of fermentations. There is a group of organisms, however, by which acetate is formed as the predominant nongaseous product. Knowledge of this very small group of acetogenic organisms has grown in recent years to include a number of thermophilic organisms, including *Clostridium thermoautotrophicum*, *C. thermoaceticum* and *Acetogenium kivui* (Gottschalk, 1986). These species of bacteria are able to live at the expense of acetate formation from H_2 and CO_2 , according to the equation illustrated in Table 4. 1. The free energy change is slightly less

negative than the free energy change for methanogenic conversion of CO_2 and H_2 to methane. According to Harper and Pohland (1986), the range of hydrogen partial pressures that encompasses the methanogenic "niche" (ie. H_2 partial pressure range of methanogenic activity) is between 10^{-4} and 10^{-6} atm. Presumably, acetogenic conversion of H_2 and CO_2 to acetate operates in a higher partial pressure range, since the free energy change of this reaction is less negative than the free energy change of the corresponding methanogenic conversion. It may be possible that the types of acetogenic organisms associated with a TAD process could maintain a range of hydrogen partial pressures that could allow ethanol conversion to acetate and propanol conversion to propionate, but inhibit both oxidation of propionate and butyrate.

Under the microaerobic condition, both ethanol and propanol were catabolized (Figures 4. 16a and 4. 17a). The complete consumption of both of these compounds occurred within 20 h, compared to their anaerobic catabolic rates which were much slower. The catabolism of these compounds was followed by an apparent suppression in acetate production, which resulted in the acetate concentrations being lower in the experimental reactor than the concentrations were in the corresponding control reactor (which had no external ethanol or propanol added). The results of these figures suggest that a switch to aerobic ethanol or propanol catabolism seems to either stimulate the catabolic rate of acetate consumption or suppress the rate of acetate anabolism, thus resulting in a quicker disappearance of acetate from the medium.

4.1.2.5 Effects of Different Classes of Macromolecules on VFA Metabolism

In order to investigate the effects of different classes of compounds on VFA metabolism in TAD, examples of representative lipids, carbohydrates and proteins were chosen and tested under batch TAD conditions. The molecules selected were linoleic acid (fatty acid), glucose, dextrin (carbohydrates) and peptone (protein). Linoleic acid is a polyunsaturated fatty acid and is a major constituent of many vegetable oils (eg. soybean, peanut, corn and sunflower oils). Dextrin is a hydrolysis product formed when starch is heated at low temperatures for a short period of time in the presence of large amounts of acid. Starch consists of chains of D-glucose residues that are connected by $\alpha(1\rightarrow4)$ linkages and at branch points by $\alpha(1\rightarrow6)$ linkages (Windholz, 1983). Starch is a storage material and as such is structured to be degraded. It is therefore not surprising that powerful starch decomposing enzymes are produced and excreted by microorganisms.

Two important enzymes in this process are α -amylase and pullulanase. α -amylase is produced by bacteria and it cleaves the $\alpha(1\rightarrow4)$ glycosidic linkages in the starch molecule at random. Pullulanases are called debranching enzymes, because they hydrolyze the $\alpha(1\rightarrow6)$ linkages in starch. Grueninger *et al.* (1984) prepared crude α -amylase extracts from a subspecies of *Bacillus stercorophilus* isolated from an ATAD pilot plant in Altenrhein, SG, Switzerland. Sonnleitner and Fiechter (1983) over a two year period isolated thermophilic microorganisms from an aerobic thermophilic, continuously operated sewage sludge treatment process.

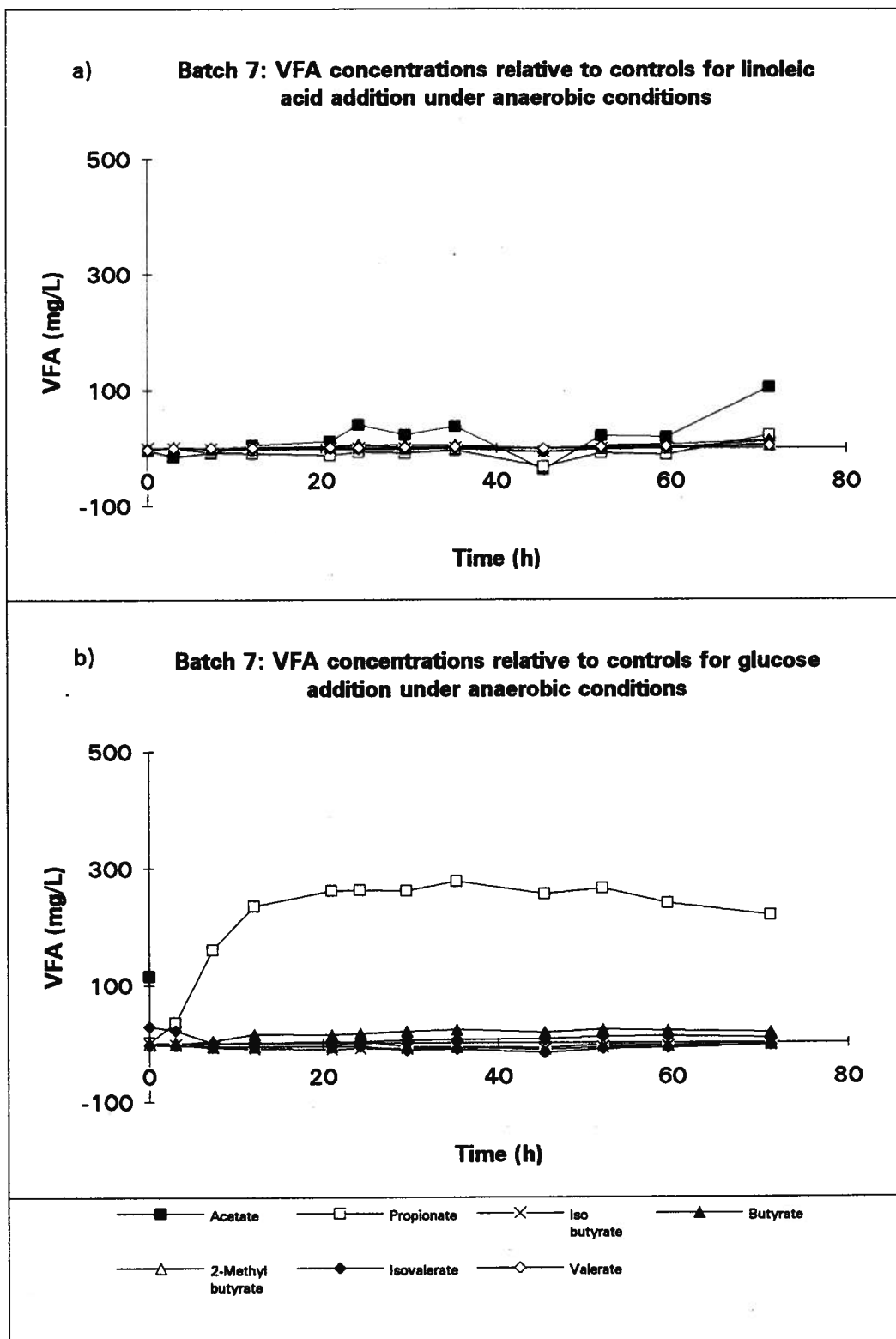


Figure 4.18 VFA difference profiles under anaerobic conditions for a) linoleic acid and b) glucose addition experiments.

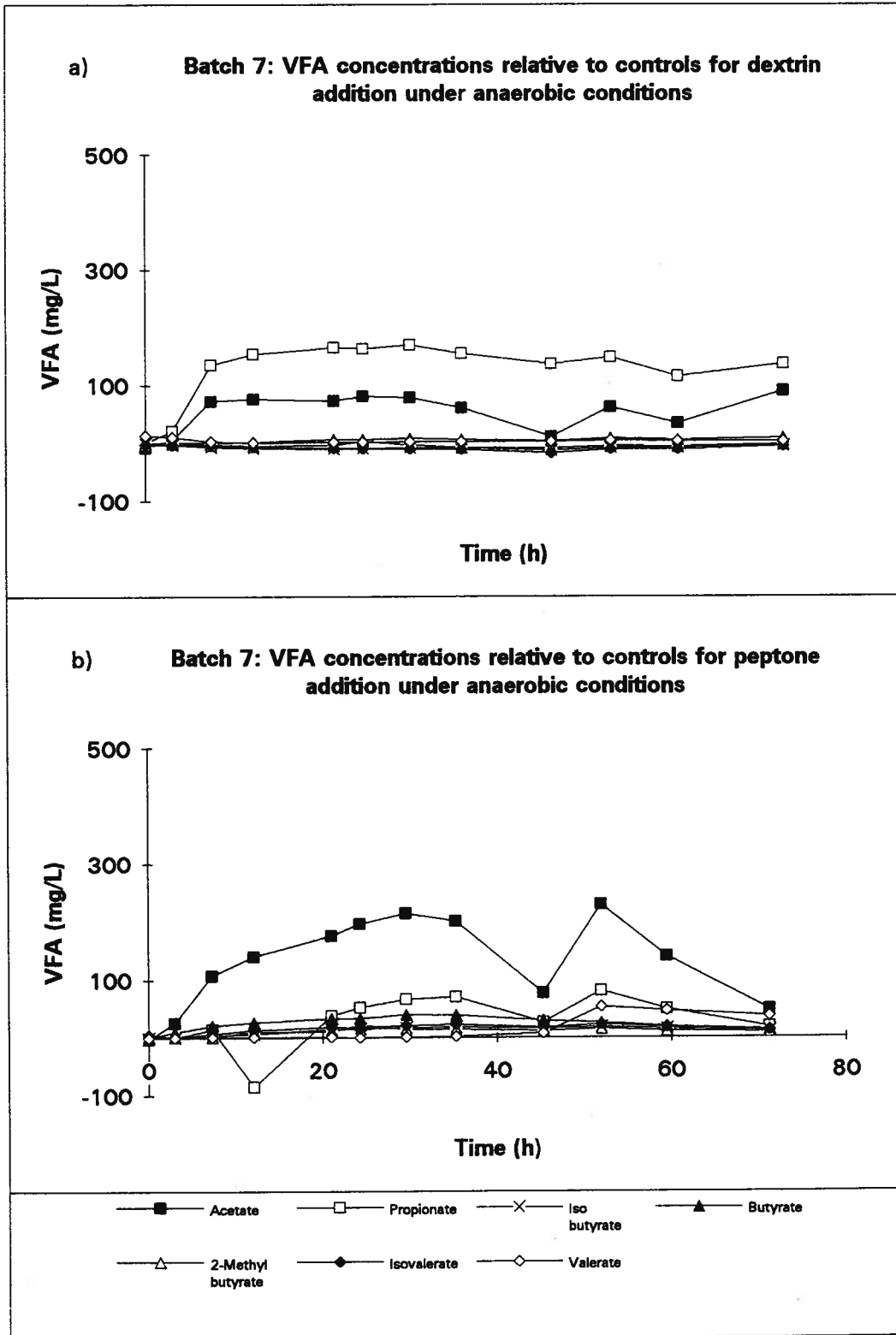


Figure 4.19 VFA difference profiles under anaerobic conditions for the a) dextrin and b) peptone addition experiments.

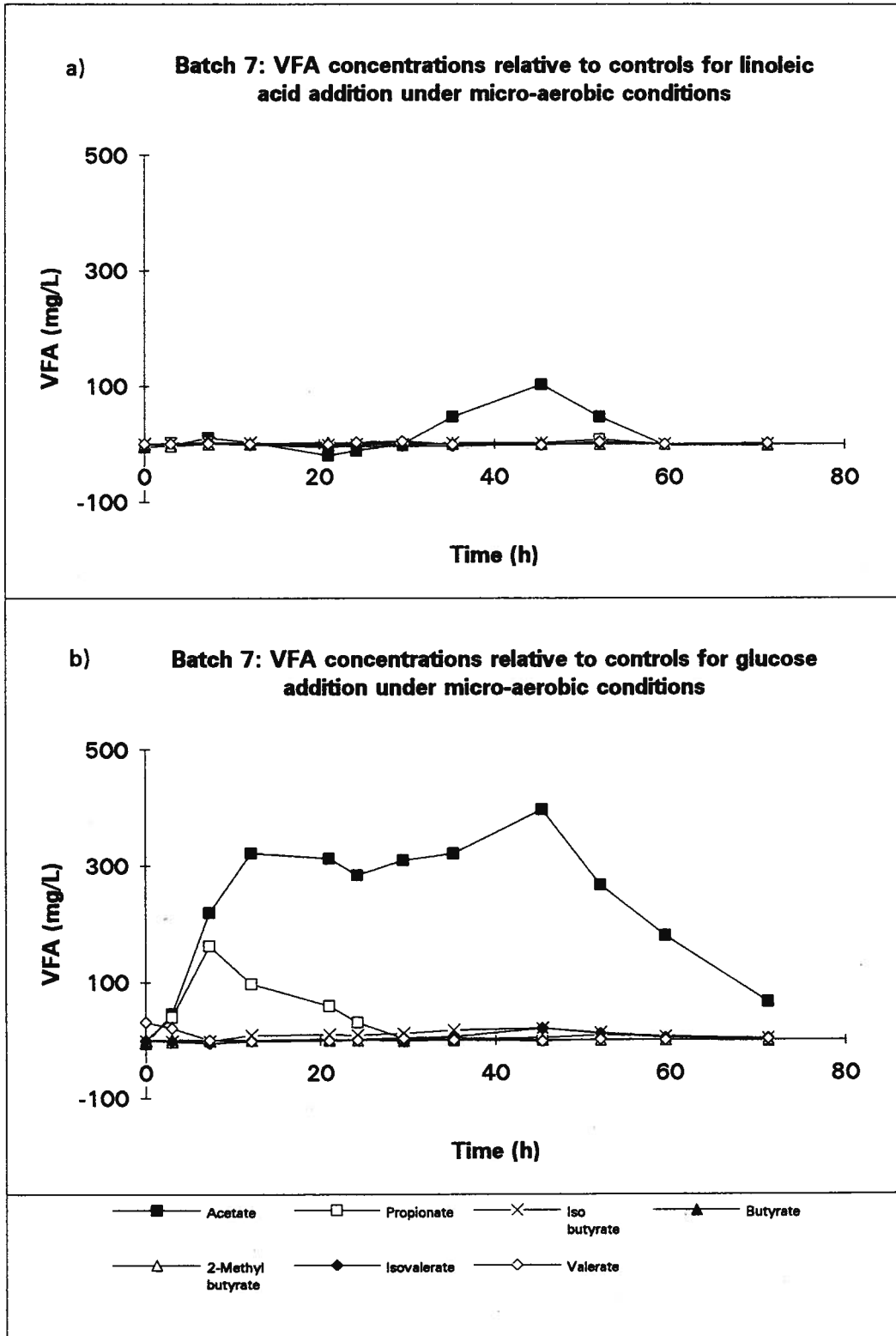


Figure 4.20 VFA difference profiles under microaerobic conditions for the a) linoleic acid and b) glucose addition experiments.

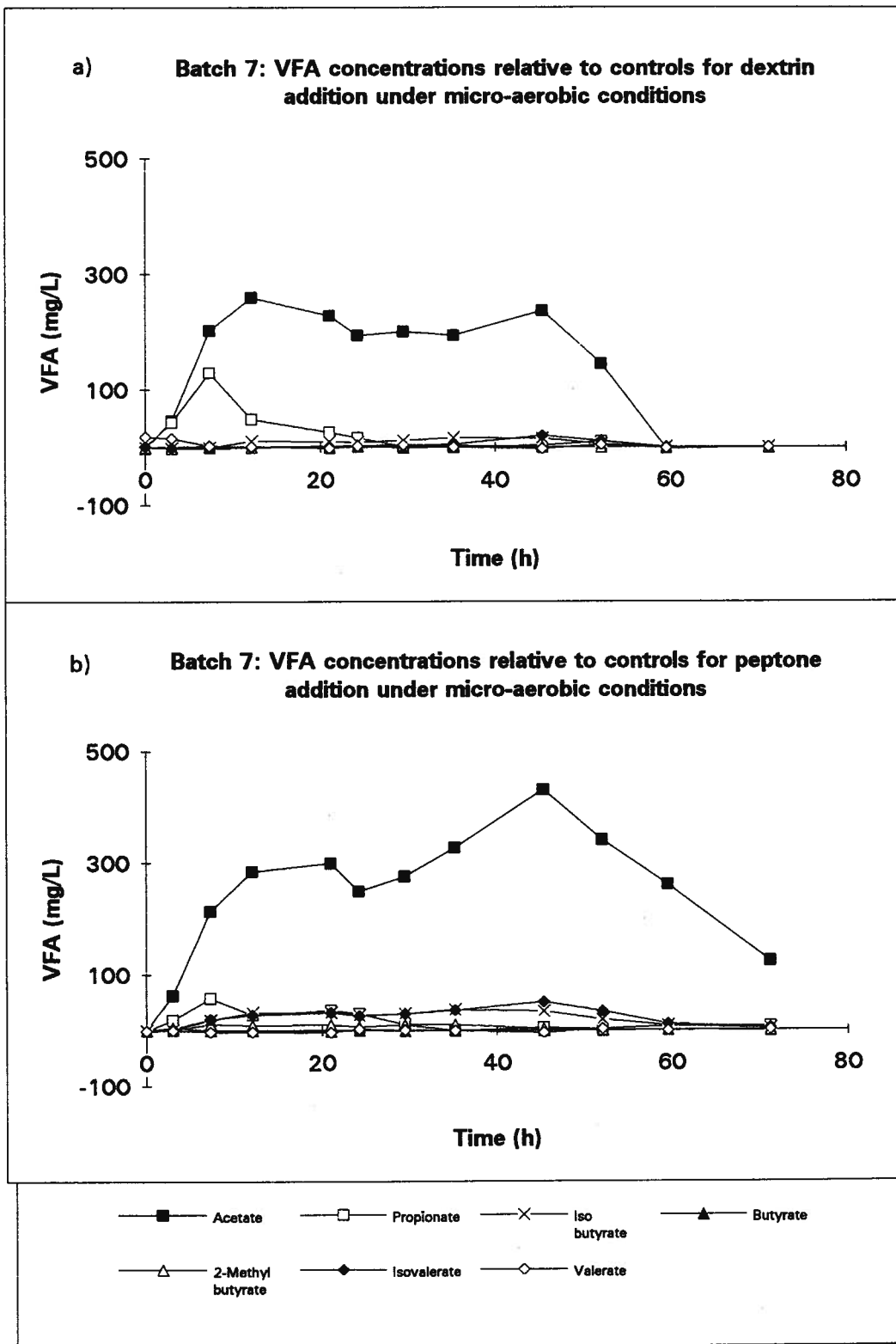


Figure 4.21 VFA difference profiles under the microaerobic condition for the a) dextrin and b) peptone addition experiments.

A representative set of isolates were characterized for microbiological and biochemical properties. More than 90% of the isolates could degrade starch and grew on gummi arabicum as a sole carbon source. Amylases and proteases were formed in media containing complex compounds, but were not found in significant amounts in growth media containing simple carbon substrates. Peptone is high in amino acid content and contains a negligible quantity of proteoses and more complex nitrogenous constituents.

Figures 4. 18 to 4. 21 show the results of the macromolecule addition experiments. Peptone was the only one of the four tested substrates to stimulate only acetate production under fermentative conditions. Glucose and dextrin stimulated predominantly propionate production. A somewhat surprising result was that linoleic acid did very little in terms of VFA stimulation in either the anaerobic or microaerobic environments. The β -oxidation of long chain fatty acids did not seem to readily occur, although this degradation had been proposed in a previous section (4.1.2.1) as the model pathway for the catabolism of butyrate and valerate. Possible explanations for this anomaly lie in the fact that linoleic acid is a much larger molecule than the other VFA tested and would therefore have different transport characteristics across the cytoplasmic membrane. Under microaerobic conditions, the other three macromolecules predominantly stimulated the production of acetate. Whether or not each of these compounds was being actually consumed is not known since these macromolecules were not assayed.

The most likely sequence of reactions for the anaerobic catabolism of glucose and dextrin to propionate is the succinate-propionate pathway. This pathway is employed by most propionate producing organisms. Succinate is an intermediate but is also produced as an end

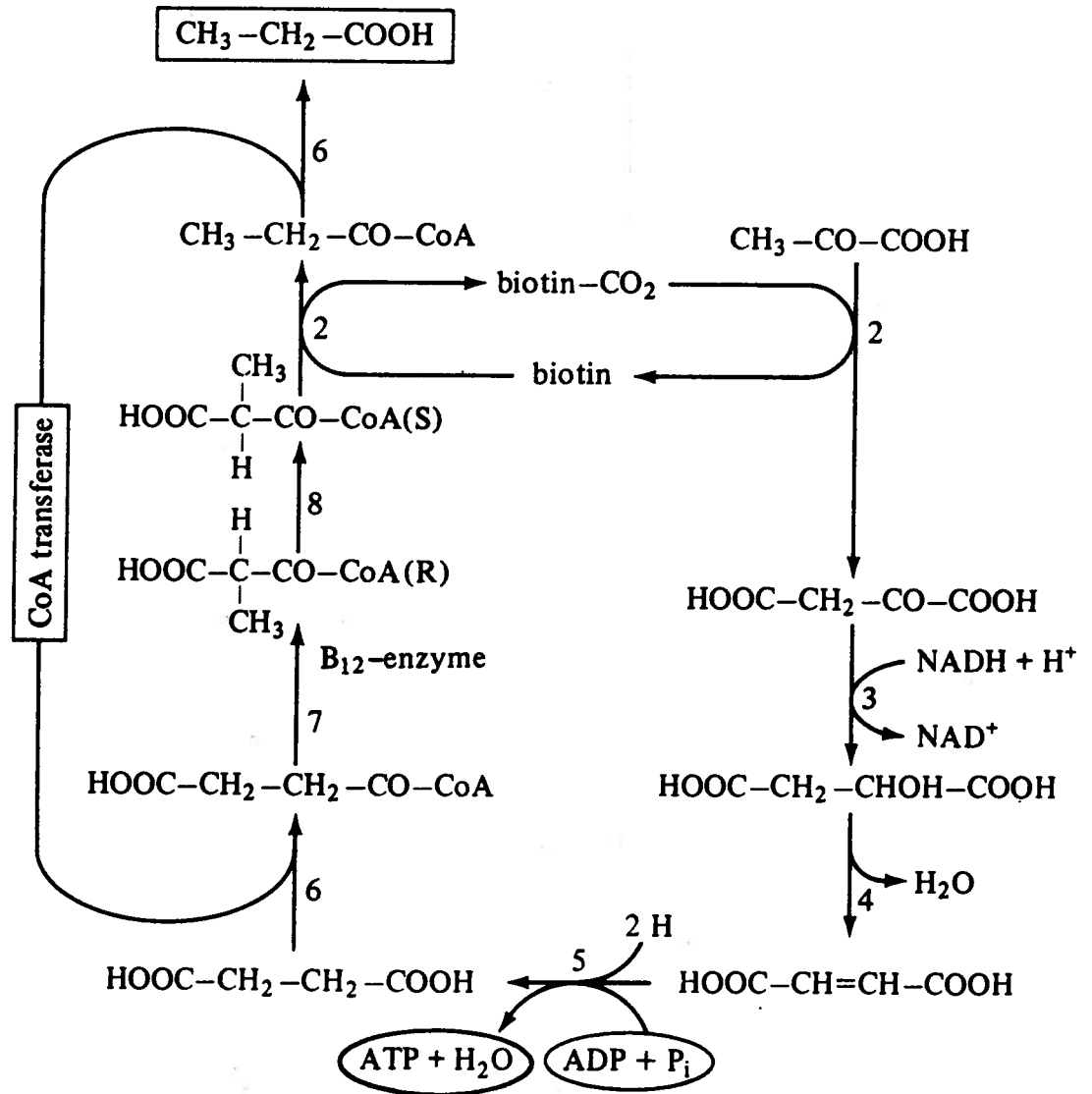


Figure 4. 22: Fermentation of pyruvate to propionate via the succinate-propionate pathway (Gottchalk, 1986).

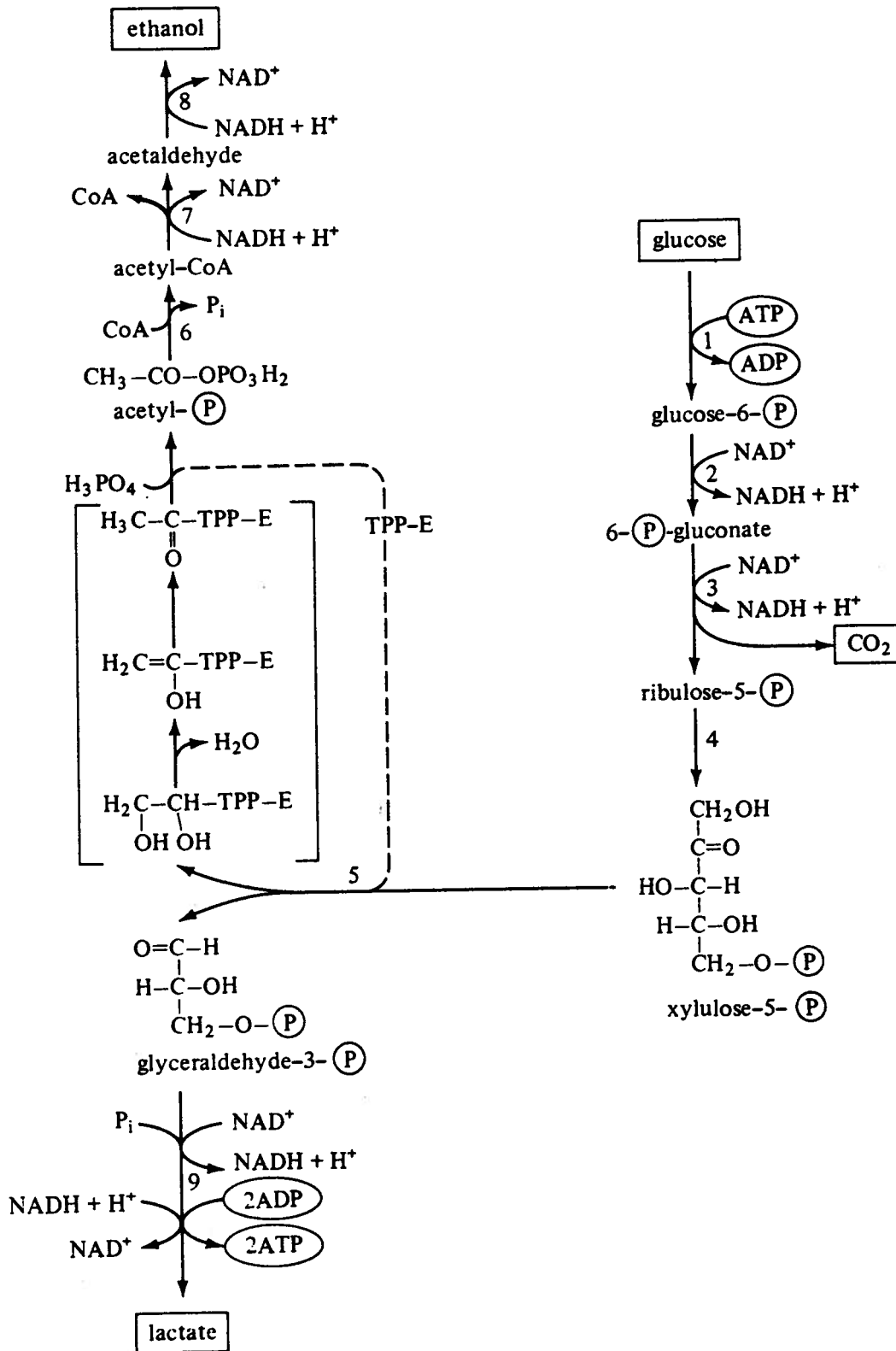
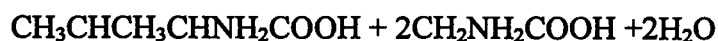


Figure 4. 23: Formation of CO₂, lactate and ethanol from glucose by the heterofermentative pathway. The numbers refer to the sequence of enzymes involved in this pathway (Gottchalk, 1986).

product in small or large amounts. The sequence of reactions involved in this pathway are illustrated in Figure 4. 22 (Gottschalk, 1986). The NADH produced during substrate level phosphorylation of glyceraldehyde-3-phosphate during glycolysis must be regenerated to NAD^+ , in order for the catabolism of glucose to proceed. This regeneration requirement can be met by the fermentation of pyruvate to either propionate or butyrate which consume NADH to produce NAD^+ . Since butyric acid was not detected in these experiments, this results in the succinate-propionate pathway as a likely candidate. Another potential pathway is the heterofermentative process which results in the production of lactate or ethanol and is illustrated in Figure 4. 23. Either of the two pathways shown in these figures (4. 22 and 4. 23) will balance the redox. The lactate accumulation in the heterofermentative pathway can further be metabolized to propionate and acetate in an approximate 2 propionate: 1 acetate molar ratio and could account for the observed occurrence of both propionate and acetate. The results from the dextrin addition experiment, under anaerobic conditions (Figure 4. 19a), suggest that the heterofermentative sequence of reactions was the model pathway. The discrepancies between the glucose and dextrin addition results may possibly be explained in terms of the relative efficiencies of the acquisition of these substrates by different subpopulations of bacteria. This type of kinetic rate argument could account for the discrepancies seen in the VFA profiles.

Although a number of bacterial species grow with some single amino acids, many prefer to ferment mixtures of amino acids. They carry out coupled oxidation-reduction reactions between pairs of amino acids. One amino acid is oxidized and a second one is reduced. This allows the amino acids that cannot be fermented individually to be used as a source of energy.

These reactions are carried out by many proteolytic species of Clostridia (eg. *C. stickandii*, *C. sporogenes*, *C. histotiticum*) (Barnard and Akhtar, 1979; Barker, 1981). For example, the coupling of valine (hydrogen donor) and glycine (hydrogen acceptor) results in the formation of isobutyric and acetic acids. These reactions were first demonstrated by Cohen-Bazire *et al.* (1948).



In a similar manner, isoleucine, acting as a hydrogen donor can be oxidized to 2-methylbutyric acid (Elsden and Hilton, 1978).

Under microaerobic conditions, it is no longer necessary to maintain redox balance by shuttling substrates to specific reduced end products. This change allows the stimulation of acetate as the predominant by product. Acetyl-CoA is converted to acetate via a two step reaction. This pathway produces acetic acid and generates an ATP for every acetyl-CoA. Although only a single ATP is produced, this level is significant when compared with a net gain of two ATP/glucose realized from the glycolytic pathway.

4.1.3 2, 4-Dinitrophenol Addition Experiment

The purpose of this section is to investigate the effect of inhibitor compounds on substrate metabolism in TAD. In aerobic metabolism, the oxidation of NADH and the phosphorylation of ADP are coupled reactions. *In vivo*, the uncoupling of these two reactions

can be achieved by the addition of certain compounds to the cells. These agents make the cytoplasmic membrane permeable to protons. As a consequence, a ΔpH gradient cannot be established and ATP cannot be synthesized by oxidative phosphorylation. Because of their mode of action, uncouplers are also known as 'protonophores'. One such compound is 2,4-dinitrophenol (Gottschalk, 1986; Lehninger, 1982). Figure 4. 24 shows the results of the addition of this compound and its subsequent effect on VFA metabolism in the TAD batch experiment with primary sludge as substrate. Since fermentative reactions do not utilize oxidative phosphorylation to produce ATP, this agent should have no effect in an anaerobic environment. Under this condition, the expected results are seen.

However, there is an unexpected result under the microaerobic condition, which is the accumulation of acetate far in excess of its control values. It is also apparent from these results that the anabolic activity of acetate consumption may be suppressed since there is no net oxidation of this intermediate (ie. acetate accumulation in the medium). Normally, in *E. coli* cells growing on glucose, approximately 50% of the original carbon is released as CO_2 , with the remaining 50% being converted into cellular material (Gottschalk, 1986). In the presence of 2, 4-dinitrophenol, glucose is oxidized almost completely to CO_2 with virtually no anabolic intermediates.

The results from Figures 4. 24 and 4. 25 suggest that, under microaerobic conditions, the process bacteria are able to switch from generating ATP via oxidative means to employing substrate level phosphorylation reactions. This results in the production of acetate, since acetate production from acetyl-CoA yields ATP. The ORP and pH profiles also support this

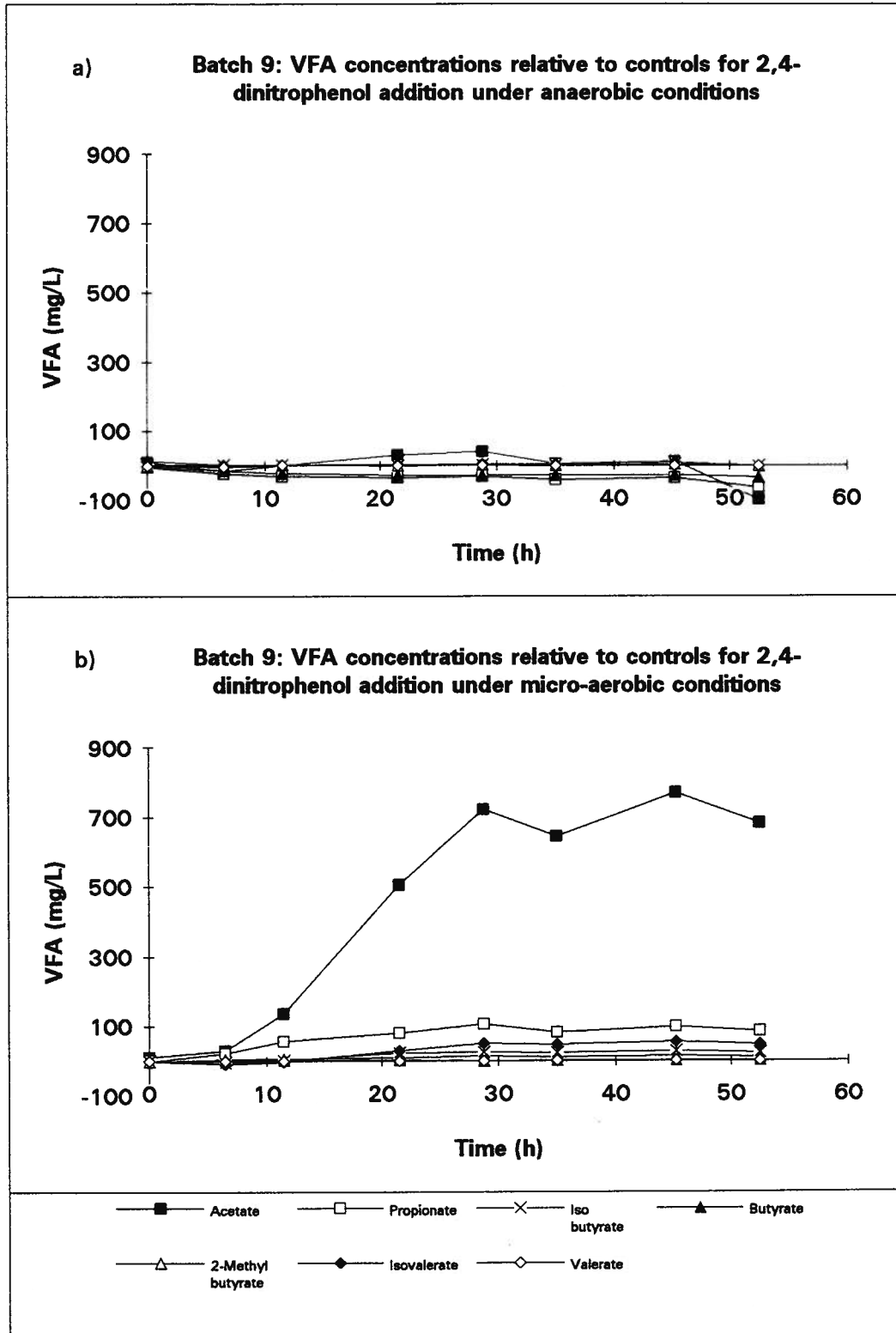


Figure 4.24 2, 4-dinitrophenol addition experiment under a) anaerobic and b) microaerobic conditions.

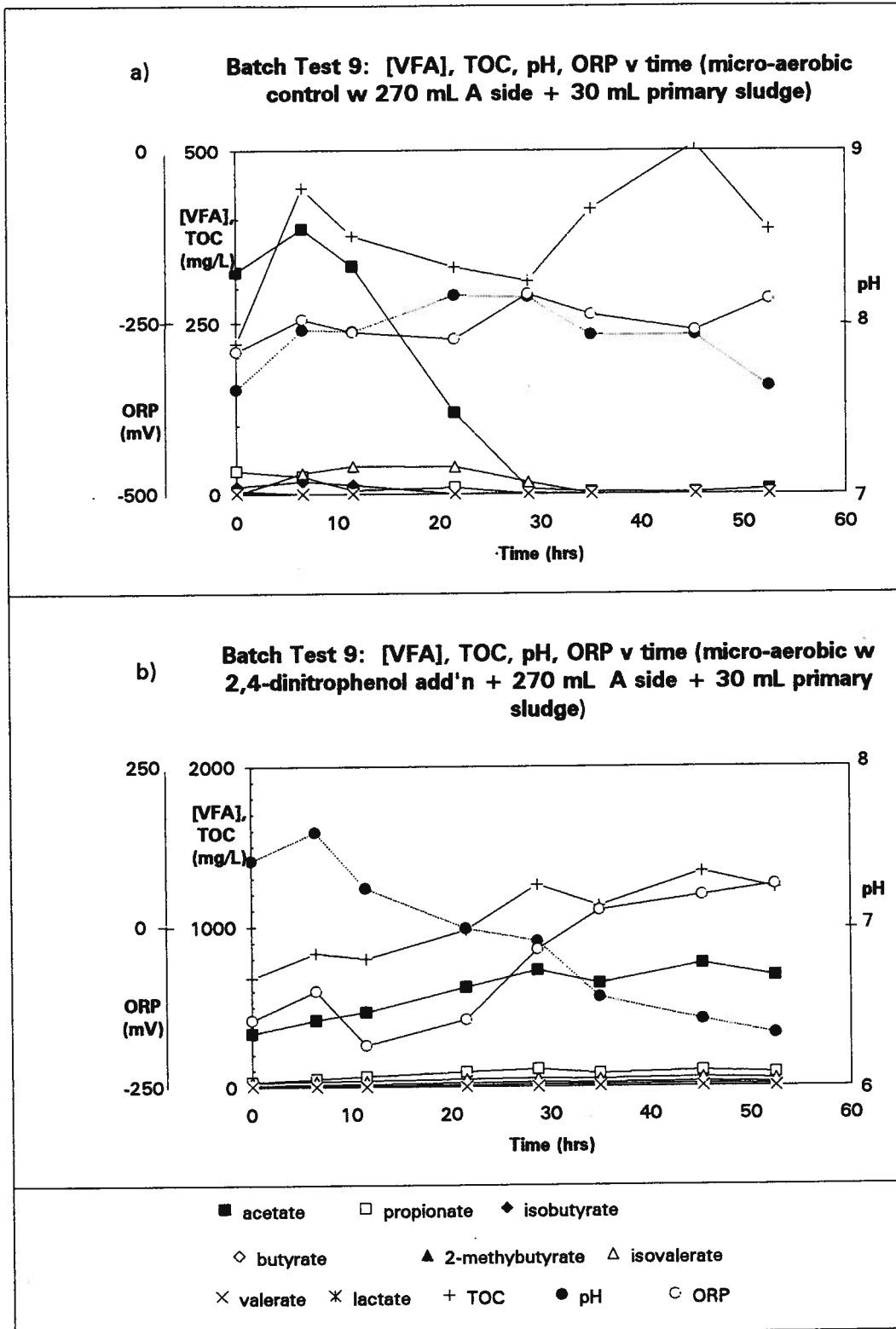


Figure 4.25 VFA, pH and ORP profiles in the 2, 4-dinitrophenol addition experiment under microaerobic conditions. a) control condition and b) 2,4-dinitrophenol addition condition.

hypothesis (Figure 4. 25). Under the control microaerobic condition, the ORP remains relatively constant at approximately -250 mV, suggesting a relatively constant baseline oxygen demand. In the 2,4-dinitrophenol addition reactor, the ORP increases until, by the end of the experiment, the reactor has a slightly positive ORP, suggesting that oxidative metabolism had been suppressed. This may represent some cellular damage from long term energetic poisoning. The large decrease in pH was consistent with the accumulation of acidic end products.

The catabolic flow of complex substrates in the primary sludge feed source to a predominant acetate end product, generates NADH, which must be reoxidized by operation of the electron transport chain. Therefore, these results suggest that, although the oxidative metabolism may be suppressed, a basal level of activity of the respiratory chain must be maintained to regenerate oxidized electron carriers (ie. NAD^+).

In addition to uncouplers, the respiratory chain can be impaired by inhibitors of electron transport. Cyanide is one such inhibitor. This compound blocks the reduction of oxygen catalyzed by the terminal electron carrier in the transport chain. However, this compound had no effect on the metabolism of VFA under both anaerobic and microaerobic batch test conditions. Neither did the anion fluoride. The physiological effect of this compound is to inhibit glycolysis by blocking the enzyme enolase to prevent the production of phosphoenolpyruvate from 2-phosphoglycerate (Lehninger, 1982).

4.1.4 Response of Biomass from a Fermenter Process to Anaerobic and Microaerobic Conditions

Experiments with fermenter process sludge were conducted in order to understand the complex interactions at work in a fermentation process. This section describes the behavior of fermenter sludge subjected to both the anaerobic and aerobic conditions. The sludge used in these batch experiments came from a side stream fermentation process located at B. C. Research (Al Gibb, PhD thesis, in progress). This sidestream fermentation process fed its VFA rich mixed liquor into an FGR-SGR biological phosphorus removal process.

Figure 4. 26 shows the acetate and propionate response trends to increasing amounts of added primary sludge (0-80% by volume) under anaerobic conditions. Within a fermentation type system, propionate concentrations started out approximately equal to that of acetate. Over the course of the experiment, which in this case lasted for 70 h, propionate concentrations, in all cases, increased at a slightly higher rate than that of acetate. Under microaerobic conditions (Figure 4. 27) both acetate and propionate curves are similar to the response of these VFA under TAD batch conditions. Specifically, under high primary sludge feed rates, over time, propionate concentrations decrease as acetate concentrations increase. These trend results suggest that the effector is the aeration conditions employed. Therefore, it should not be highly process specific.

When the increasing primary sludge addition experiment was repeated with TAD sludge, some interesting observations and similarities appear (Figures 4. 28 and 4. 29). Under microaerobic conditions, the maximum transient acetate concentrations and maximum acetate production rates within the batch reactors increased with increasing primary sludge addition

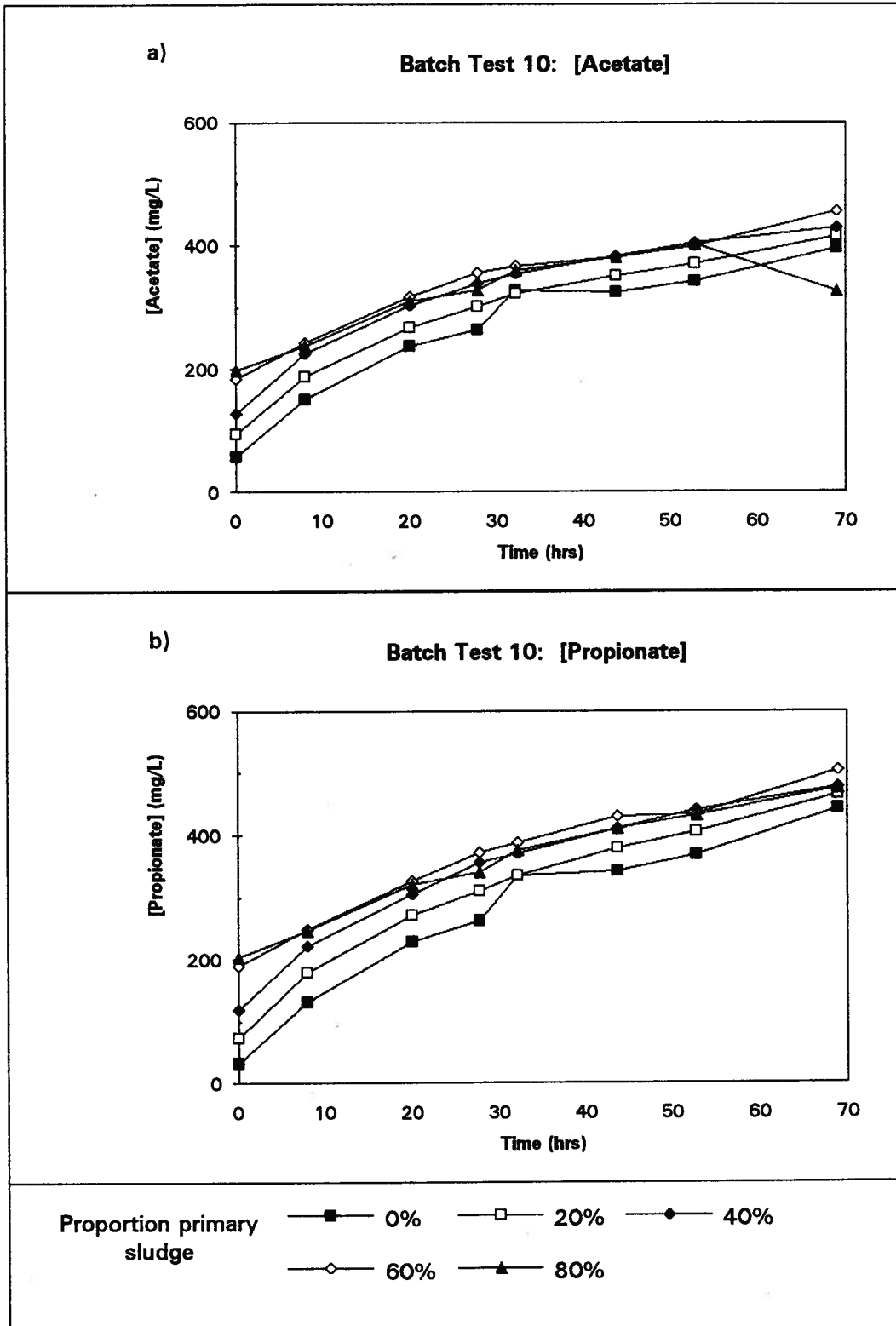


Figure 4.26 Response of fermenter sludge to primary sludge addition under anaerobic conditions. a) Acetate profiles and b) Propionate profiles.

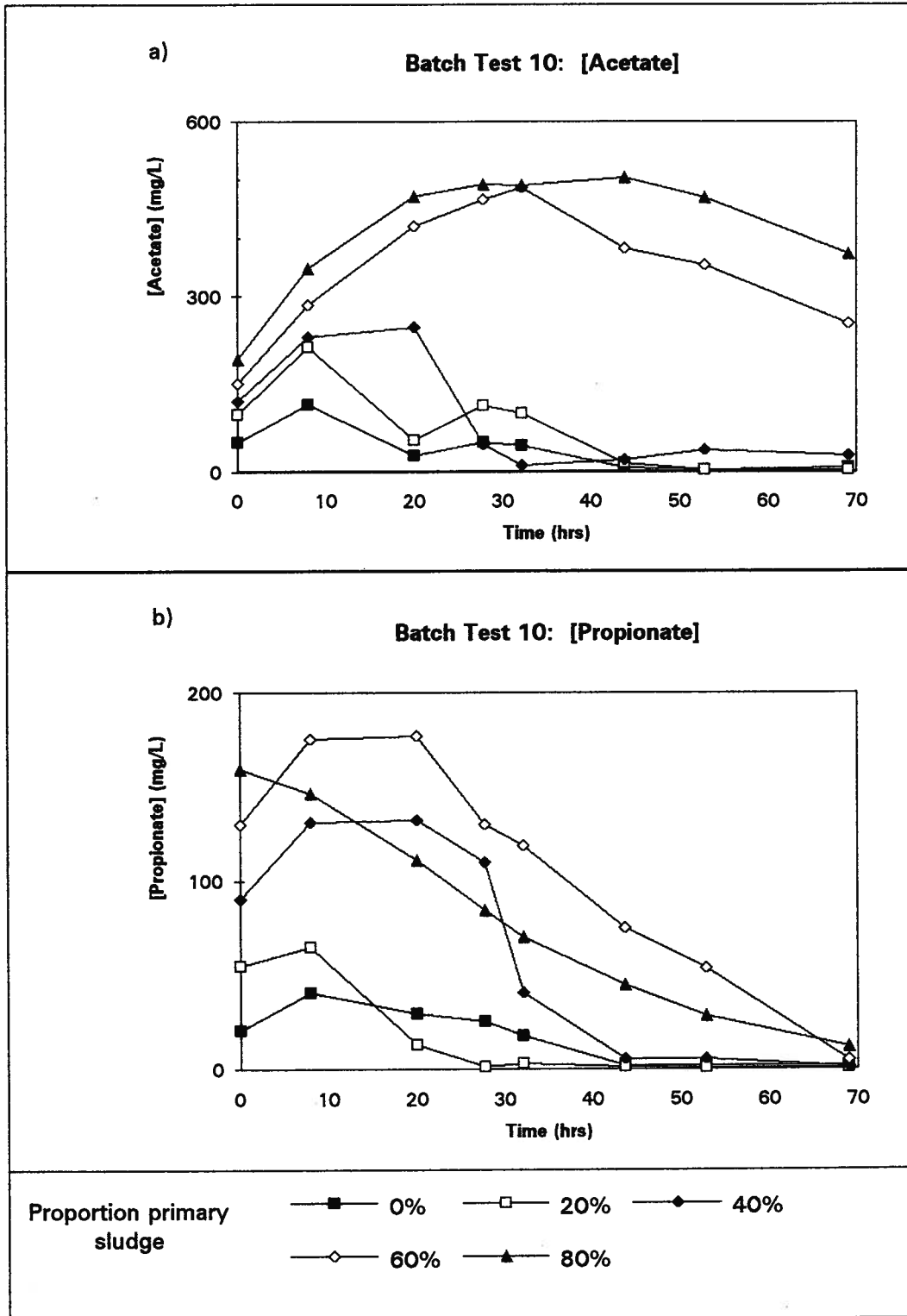


Figure 4.27 Response of fermenter sludge to primary sludge addition under microaerobic conditions. a) Acetate profiles and b) Propionate profiles.

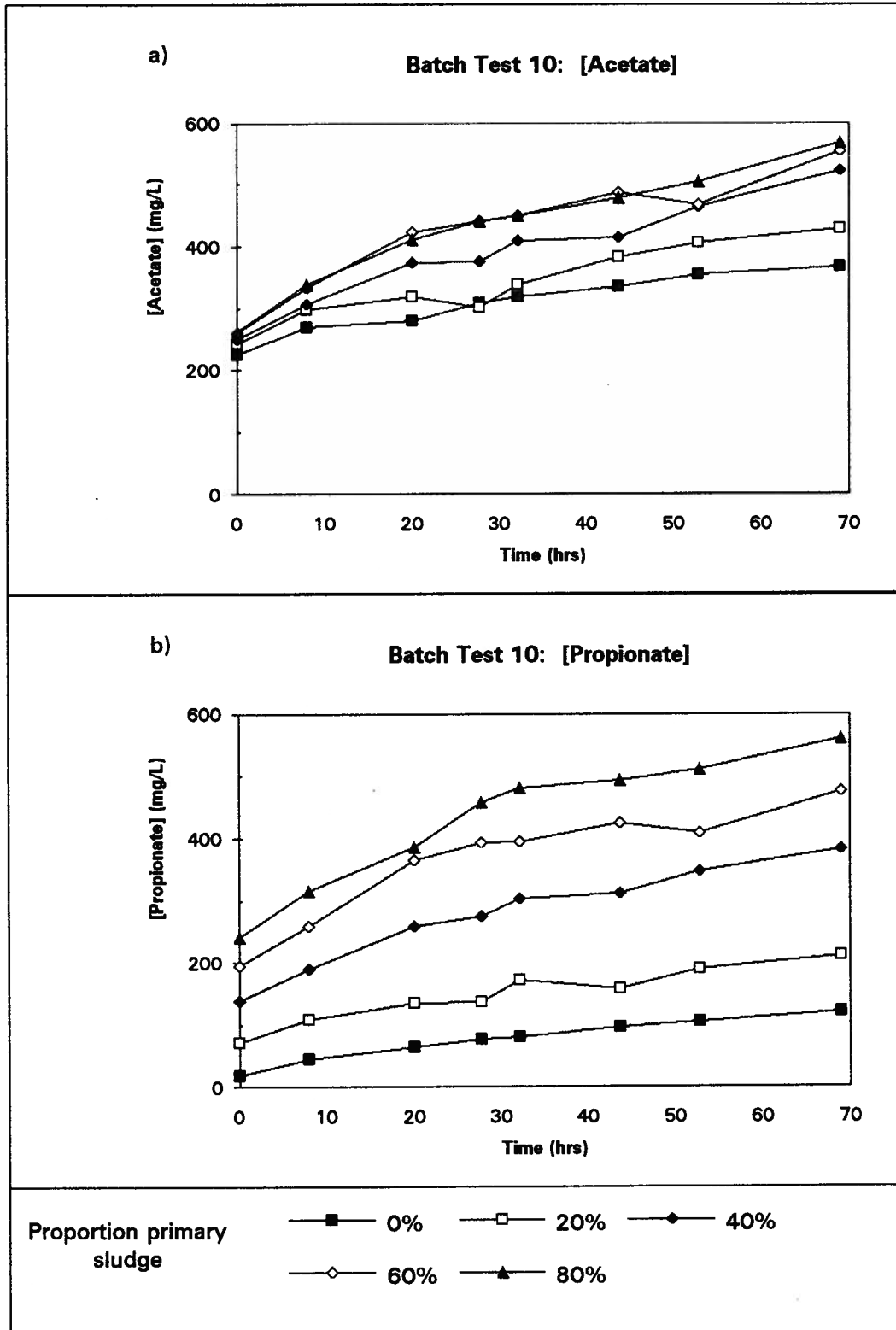


Figure 4.28 Response of TAD sludge to increasing primary sludge addition under anaerobic conditions. a) acetate profiles and b) propionate profiles.

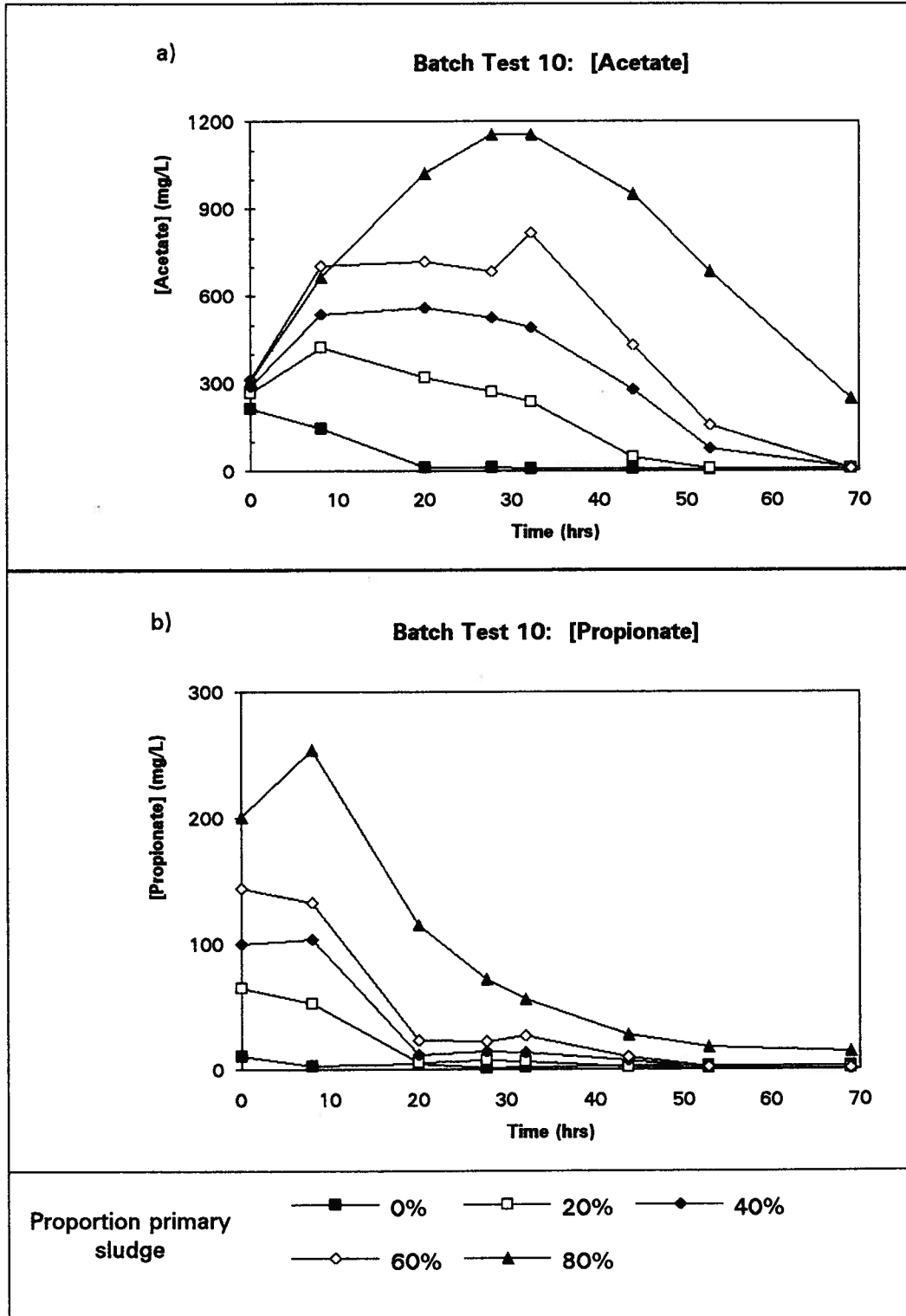


Figure 4.29 Response of TAD sludge to increasing primary sludge addition under microaerobic conditions. a) acetate profiles and b) propionate profiles.

rates. These increases in maximum concentrations and production rates were apparent at even the highest volume of primary sludge added (ie. 80% primary and 20% TAD sludges by volume). If 80% of the volume of a full scale TAD bioreactor were replaced each day, this would correspond to a 1.25 d SRT for that reactor. Therefore, these results suggest that solids retention times that could potentially maximize VFA production could be somewhere in the range of 1 d, which is the recommended value for thermophilic prestage systems.

Like the pattern for fermenter sludge both acetate and propionate profiles for TAD increased in proportion to each other during anaerobic incubation conditions. Both VFA trends under the microaerobic condition had less similarity to the VFA trends of fermenter sludge. The most obvious differences are that propionate concentrations decreased more rapidly and that acetate concentrations increased more rapidly, resulting in higher transient concentrations when comparing TAD sludge to fermenter sludge performance. However, it is interesting that these results suggest that fermenter sludge, upon aeration, can behave in a similar manner to TAD sludge. This observation suggests that the oxidative metabolism of facultative anaerobes within the fermenter sludge biomass, upon the introduction of oxygen as the terminal electron acceptor, is capable of selectively shuttling complex substrates to an acetate end product, presumably in order to maximize ATP production. These results imply that these 'acetate overflow' systems are ubiquitous over a large spectrum of microorganisms.

Figures 4. 30 and 4. 31 show the maximum net rate of VFA production and the maximum concentrations achieved with both fermenter and TAD biomass. Each point represents a batch experiment with varying amounts of added primary sludge (0-80% by

volume). The maximum rate of acetate production in most cases occurred within the first 20 h of each experiment. Figures 4. 30b and 4. 31b show that, in a microaerobic environment under high primary sludge addition rates, the maximum rate of acetate production and the maximum transient acetate concentrations of TAD sludge was 2.5x higher than the maximum rate and maximum acetate concentrations of fermenter sludge. Figure 4. 30a shows that under anaerobic conditions, fermenter sludge performance was superior to TAD sludge performance under low primary sludge addition rates.

When comparing fermenter sludge performance under both anaerobic and microaerobic conditions, some interesting results can be seen (Figure 4. 30). Under fermentative conditions, over the entire range of primary sludge addition rates, propionate production was similar to that of acetate and decreased as the primary sludge added was increased. The acetate production rate was highest when no primary sludge was added (14 mg/L-h). Under microaerobic conditions, acetate production increased as the volume of primary sludge added increased. Although the production rate was only 8 mg/L-h when no primary sludge was added, it increased to 18 mg/L-h with the highest added volume of primary sludge. By slightly aerating fermenter sludge, it was possible to improve acetate production during high primary sludge addition rates. Under ambient room temperatures, it is difficult to differentiate the relative effects of substrate (ie. primary sludge) and active biomass (ie. fermenter sludge) under such high primary sludge addition rates. Under TAD conditions, the biomass in the primary sludge would be considered predominantly substrate since incubation temperatures of the batch experiments were 45° C. Therefore, if production rate calculations were normalized to the active biomass, the resulting

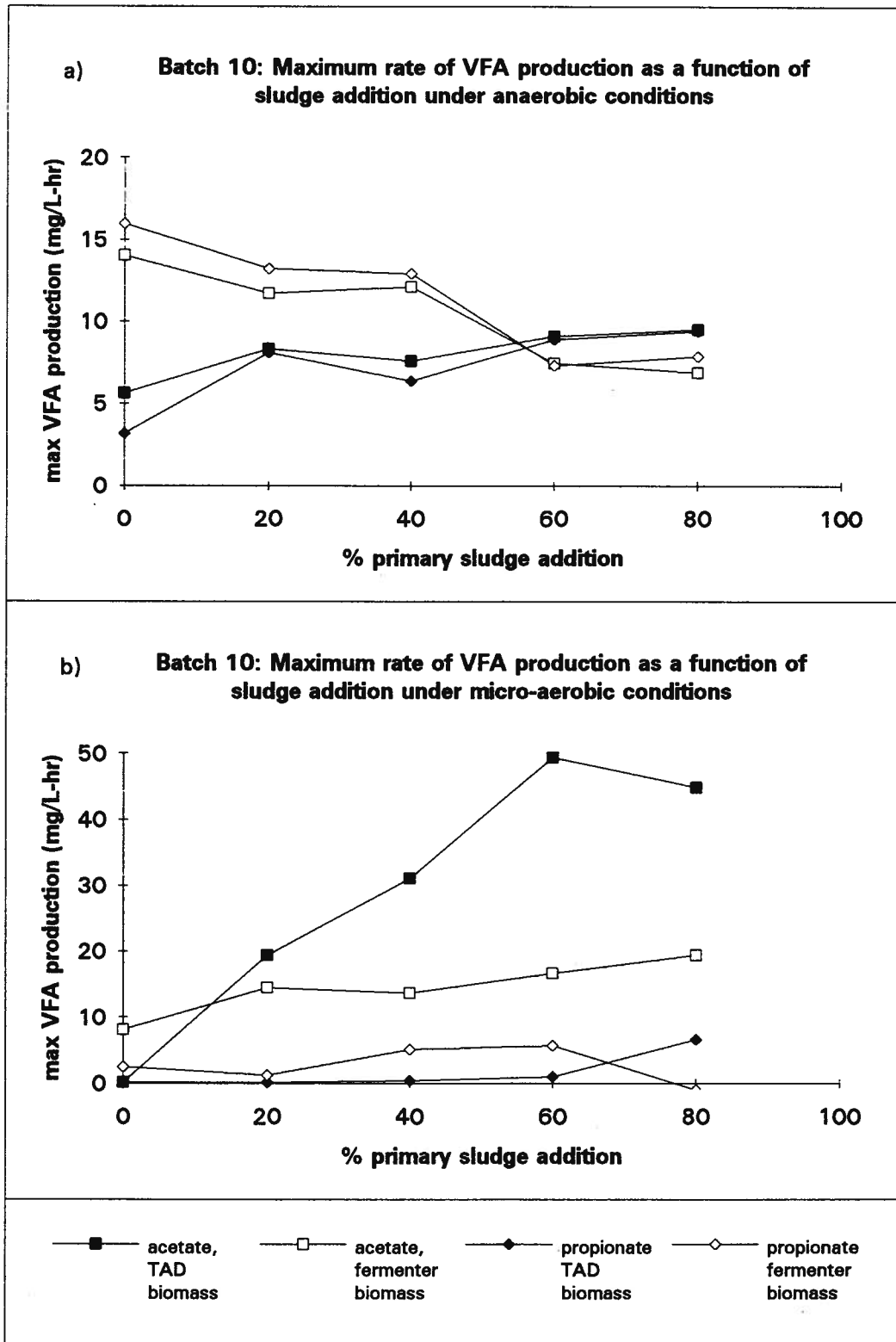


Figure 4.30 Comparison of maximum rate of VFA production between TAD and fermenter process biomass under a) anaerobic and b) microaerobic conditions.

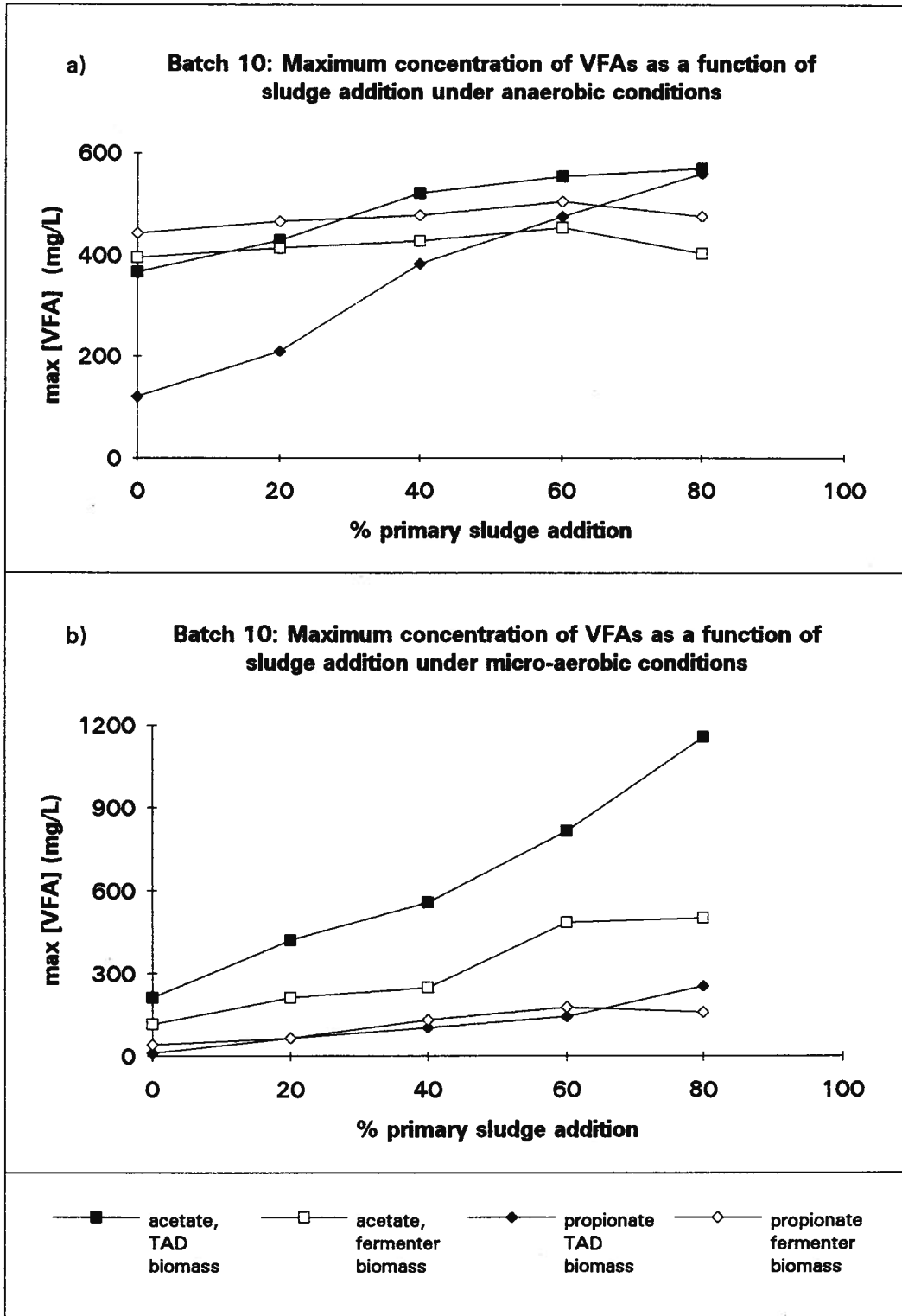


Figure 4.31 Comparison of maximum achievable concentration of VFA between TAD and fermenter process biomass under a) anaerobic and b) microaerobic conditions.

TAD sludge performance would be far superior to fermenter sludge.

4.1.5 Fermentative TAD Experiments

The purpose of this section is to address the difficulties that arise when trying to compare TAD and fermenter biomass performance. The most obvious confounding factor is that these sludges originate from 2 distinctly different processes. Since TAD sludge came from a process operating at 45° C and fermenter sludge came from a process at ambient temperatures (approximately 20° C), the batch experiments on each corresponding biomass were thus conducted at different temperatures. One system is acclimated to the presence of oxygen while the other process was strictly fermentative. TAD SRTs and Hydraulic Retention Times (HRT) are equal while fermenters usually have a much longer SRT than HRT.

In order to address these discrepancies, one parallel side of the pilot scale TAD process was run under strict fermentative conditions under a thermophilic temperature regime. To achieve a true anaerobic environment, one of the reactors was purged with an anaerobic gas mixture (ie. 90% N₂, 5% CO₂ and 5% H₂). Batch experiments were then performed with sludge drawn from this side as well as the control side. This type of comparison would eliminate the preceding confounding independent variable effects, except for the effect of oxygen.

Figure 4. 32 shows the VFA profiles of the true fermentative TAD sludge under both anaerobic and microaerobic batch conditions. These results show, that under microaerobic conditions, propionate and acetate trends were divergent and the decrease in propionate

concentrations was much slower compared to a TAD process acclimated to small amounts of oxygen (Figure 4. 33). These results have a striking similarity to the VFA response of fermenter sludge under microaerobic conditions. The experiment, in which 25% (by volume) primary sludge was added, yielded a maximum acetate production rate of 5.5 mg/L-h under anaerobic conditions and 18.0 mg/L-h under microaerobic conditions and resulted in a higher acetate concentration under microaerobic conditions by the end of the experiment (Figure 4. 32).

Another interesting result is that, under the microaerobic condition, the fermentative TAD sludge exhibited an ORP profile which was consistently less negative than that of the control side TAD sludge (Fermentative TAD ORP > -250 mV, control TAD ORP < -250 mV). This observation is consistent with the hypothesis that TAD biomass acclimated to small amounts of oxygen have a more efficient O₂ scavenging system than a fermentative TAD process, resulting in a more reduced environment under microaerobic conditions. These results suggest that the systems responsible for acetate metabolism in TAD, under microaerobic conditions, are ubiquitous in nature and are not a function of the aeration rate employed, since fermentative TAD biomass can behave in a similar manner to TAD biomass acclimated to small amounts of O₂.

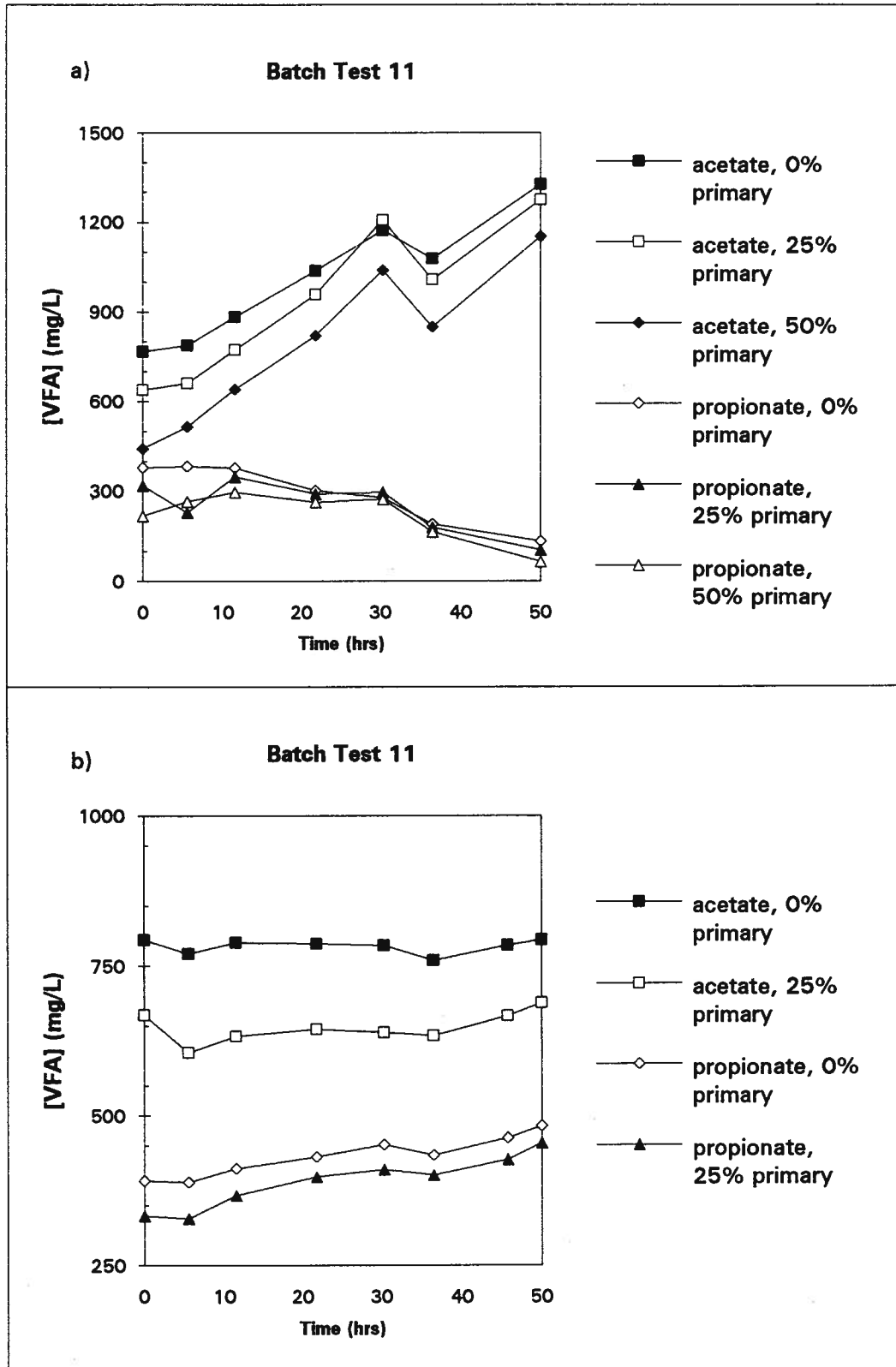


Figure 4.32 VFA profiles of fermentative TAD biomass response to increasing primary sludge addition under a) microaerobic and b) anaerobic conditions.

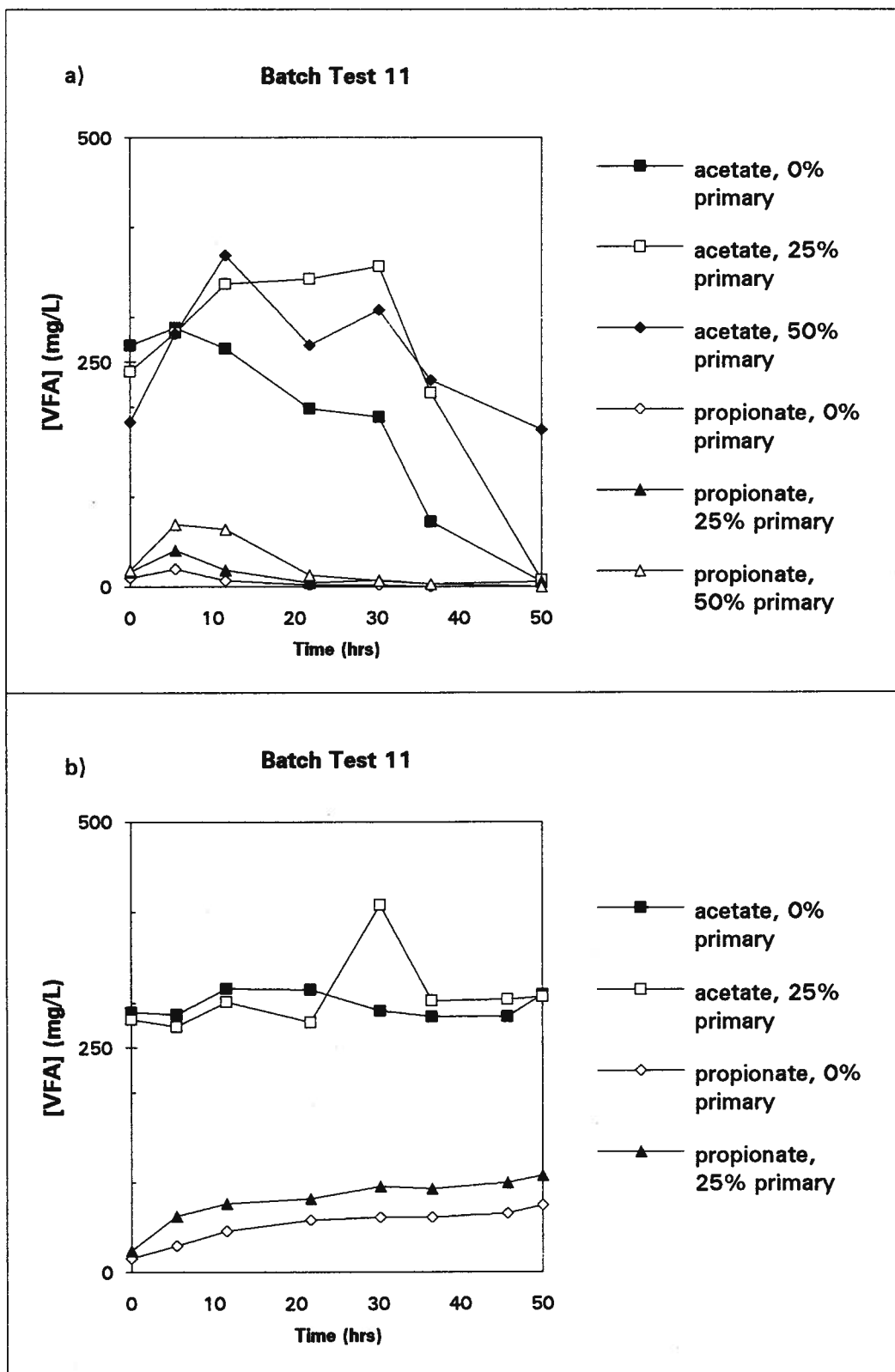


Figure 4.33 VFA profiles of control side TAD biomass response to increasing primary sludge addition under a) microaerobic and b) anaerobic conditions.

4.1.6 Salmon Arm ATAD Performance

Since most of the experiments were conducted with pilot scale TAD biomass, confirmation of these results with full scale ATAD biomass was necessary. In 1985, the District of Salmon Arm chose a biological phosphorus removal process to replace their existing trickling filter process. This novel Bio-P system employs fixed and suspended growth reactors to achieve phosphorus removal (Gibb *et al.*, 1989). To replace their existing sludge digestion system, aerobic mesophilic digesters were retrofitted for ATAD operation. This system uses the same Turborator Inc. designed aerator/mixer as the UBC pilot scale TAD process. The digesters operate in series and are fed with a mixture of primary and waste activated sludges in an approximate 1:1 ratio. Since the majority of the batch experiments were conducted with pilot scale TAD sludge, confirmation of a few of these batch experiments on full scale Salmon Arm ATAD sludge was necessary.

Figures 4. 34 to 4. 37 illustrate the response of individual VFA in the Salmon Arm ATAD sludge taken from the third cell relative to their control values, under both anaerobic and microaerobic batch test conditions. The substrates tested were primary sludge, waste activated sludge, a mixture of primary and waste activated sludges and propionate. The results are similar to those obtained using the pilot scale TAD process biomass. There are, however, a few discrepancies between pilot and full scale VFA trends. In the propionate addition experiment under anaerobic conditions (Figure 4. 35a), there was little deviation of acetate concentrations from its control value until 45 h into the experiment. At this point, acetate concentrations

increased very rapidly until, by the end of the experiment, the concentration was approximately 800 mg/L higher than the corresponding control value. The difference between the propionate concentrations of the addition reactor and the control reactor remained constant over the course of the experiment, suggesting that the added propionate was not consumed under anaerobic conditions. Under microaerobic conditions (Figure 4. 37a), propionate consumption occurred but was not concomitant with acetate production. There was however a transient increase in isovalerate concentrations relative to control values.

An interesting observation was that under microaerobic conditions, primary sludge was superior to waste activated sludge in terms of its ability to stimulate acetate production (Figure 4. 36). However, a mixture of primary and waste activated sludges seemed to be better at stimulating acetate production than primary sludge alone (Figure 4. 37). This result seems contradictory. It must be remembered that the Salmon Arm ATAD process is acclimated to a feed stream consisting of both primary and waste activated sludges. Although waste activated sludge cannot stimulate acetate production alone, there must be some necessary components provided by this fraction to the digestion process.

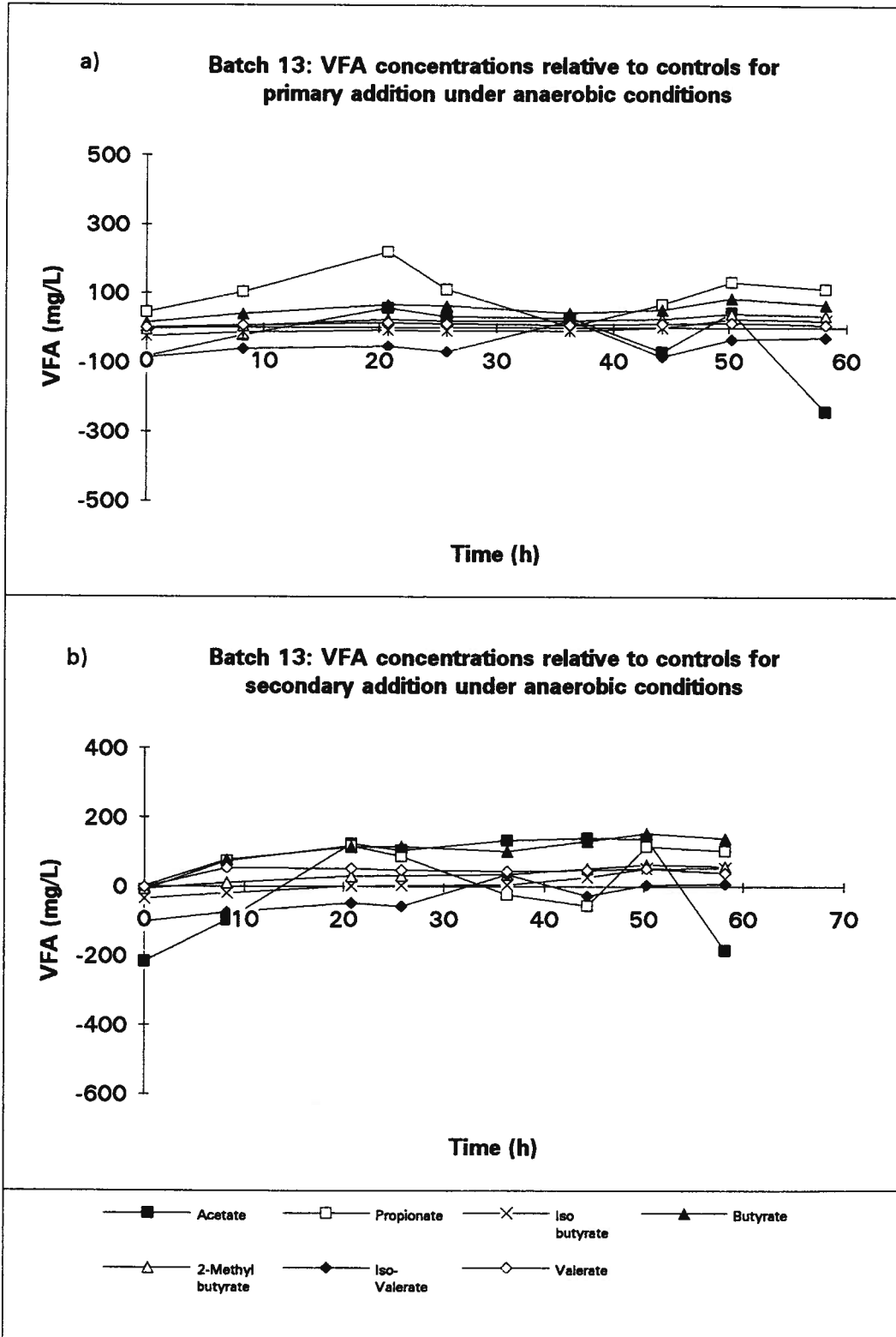


Figure 4.34 VFA difference plots of Salmon Arm ATAD sludge under anaerobic conditions to a) primary and b) waste activated sludge additions.

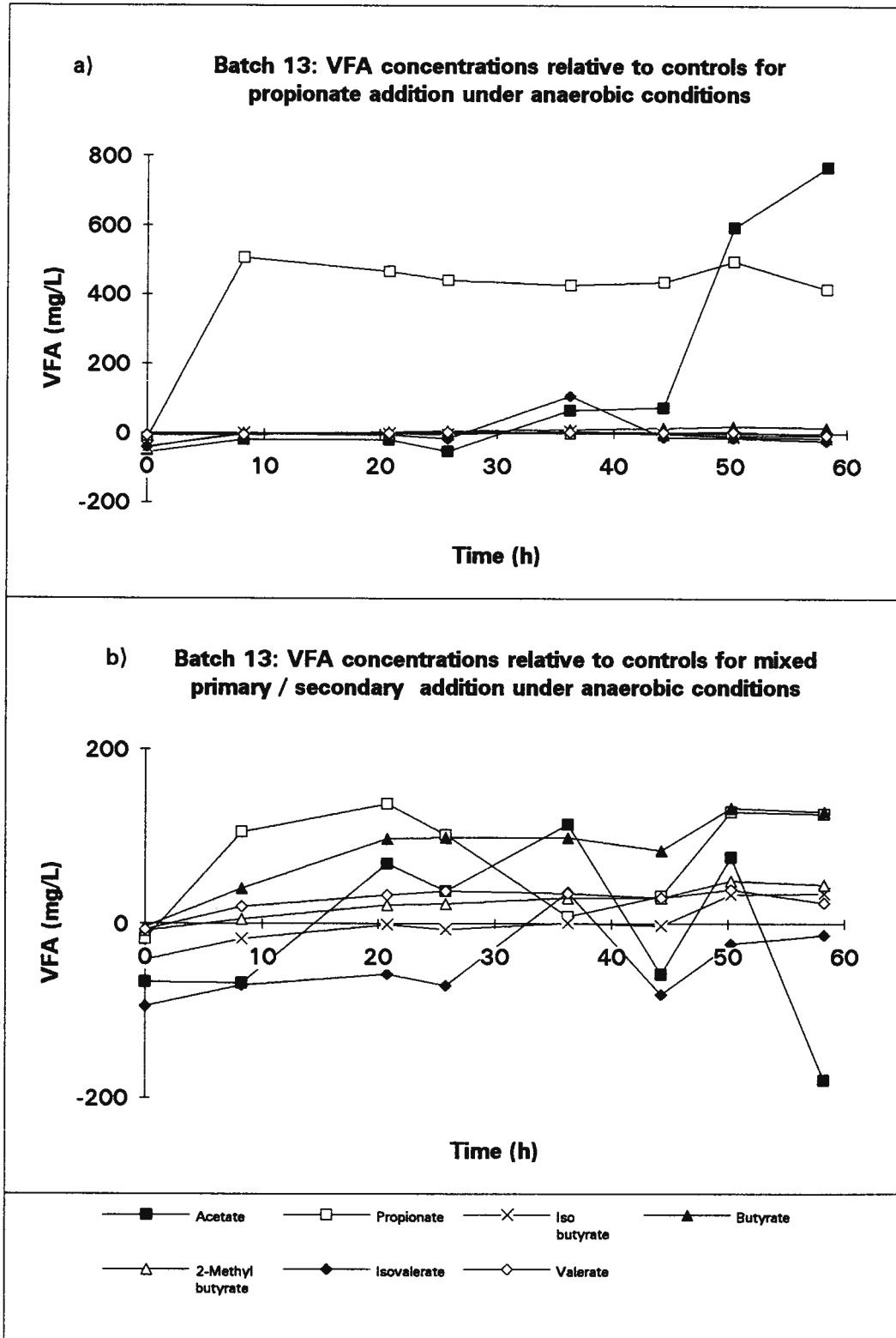


Figure 4.35 VFA difference plots of Salmon Arm ATAD sludge under microaerobic conditions to a) propionate and b) a mixture of primary and waste activated sludge additions

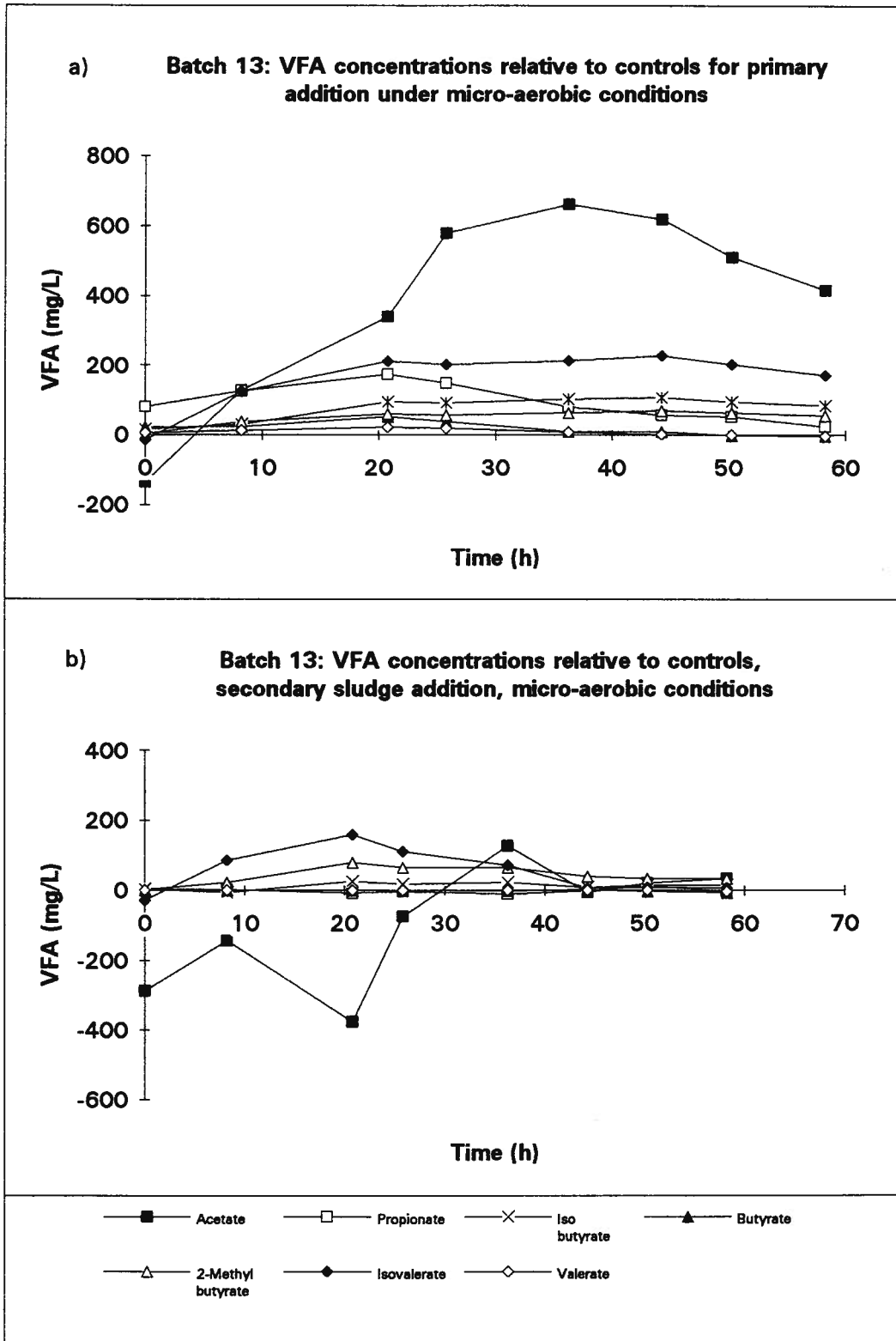


Figure 4.36 VFA difference plots of Salmon Arm ATAD sludge under microaerobic conditions to a) primary and b) waste activated sludge additions.

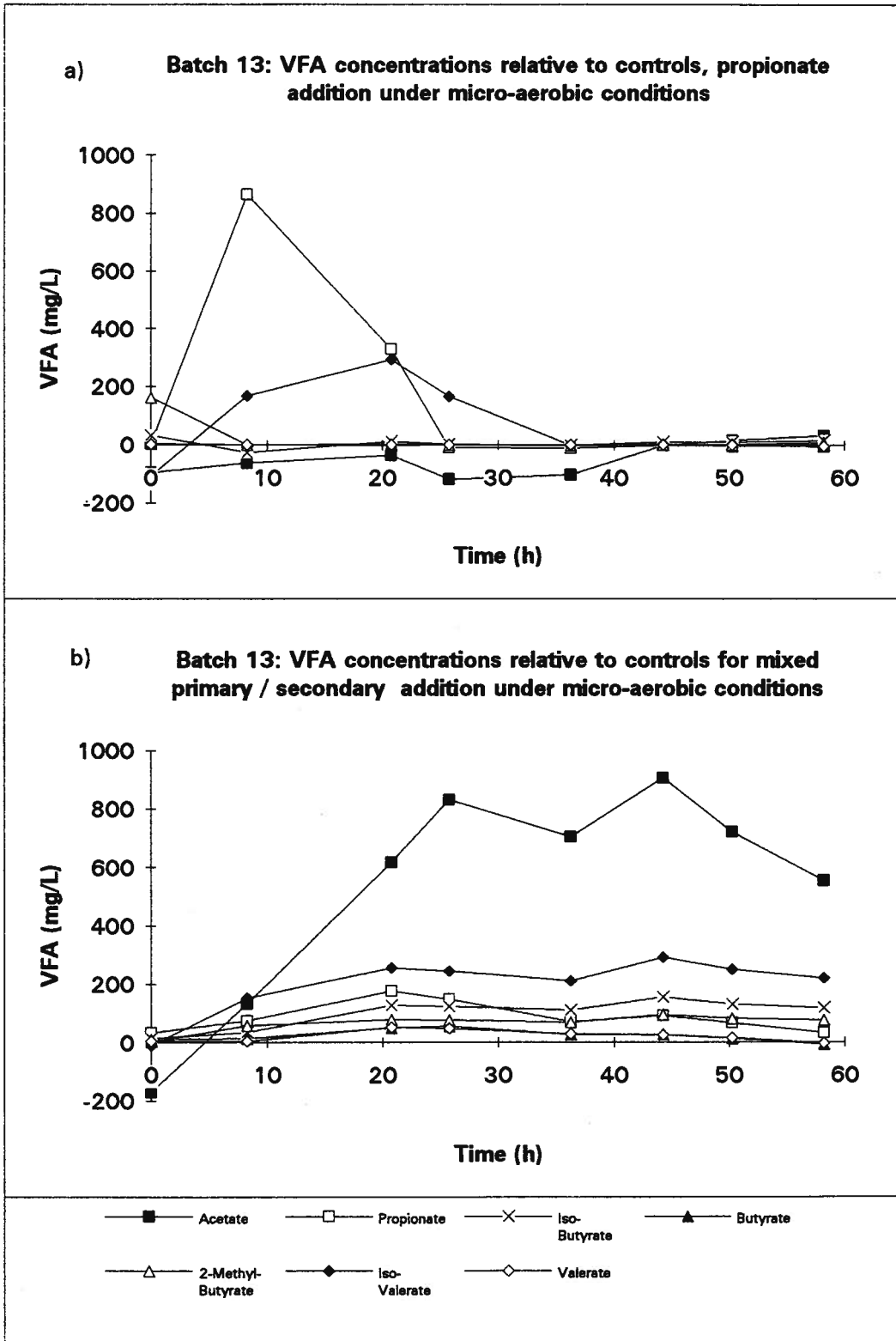


Figure 4.37 VFA difference plots of Salmon Arm ATAD sludge under microaerobic conditions to a) propionate and b) a mixture of primary and waste activated sludge additions.

4.2 Preliminary Pilot Scale TAD Experiments

Since there were no suitable guidelines as to the appropriate aeration rate that would stimulate maximum VFA production in TAD, an initial broad range of air flow rates were chosen. The tested air flow rates were 0 volume of air/volume of sludge-hour, which is defined as a microaerobic condition (ie. calculated flow rate of 0.126 V/V-h), an intermediate transition condition at 0.28 V/V-h and an aerobic condition at 0.6 V/V-h. Each run at the specified operating condition lasted for two solids retention times (SRTs) or 12 days (SRT equals HRT). The studies concentrated on the first stage of the two-stage TAD process, since preliminary results showed the highest production of VFA occurred in this stage.

Table 3. 1 is a comparison of operating conditions and solids destruction efficiencies in the pilot scale TAD and those recommended for full scale design (EPA, 1990; Kelly, 1990). The total measured solids destruction was roughly 3/4 of recommended destruction rates. The operating degree day product was below the recommended range of 400 to 500. The 29% total solids destruction was similar to the 30% observed by Koers and Mavinic (1977) for aerobically digested sludges operating at a similar degree-day product, but at lower temperatures.

Figure 4. 38 and Figure 4. 39 are examples of the daily ORP and temperature profiles in the first stage of the pilot scale TAD, representing the transition, microaerobic and aerobic conditions, respectively. In Figure 4. 38a, the air flow rate of 0.28 V/V-h consistently produced a period with a negative ORP signal of approximately -250 mV for about 5 h. At the end of this period, the TAD 'elbow' was observed. This elbow corresponded to the point at which a measurable concentration of dissolved oxygen was present. The elbow also corresponded to the

disappearance of measurable VFA. This graph also shows that acetate was the predominant VFA species produced.

Any measured VFA species is a function of both its anabolism and catabolism. In order for acetate to build up to 45 mg/L, its rate of synthesis has to exceed its rate of consumption. This excess anabolism occurred in the first 4.5 h of the cycle (Figure 4. 38b). Between 4.5 and 8 h, the catabolic rate exceeded the rate of synthesis. The result was a disappearance of acetate. These relative metabolic rates responded rapidly to changes of aeration. When the aeration rate was increased from 0 to 0.6 V/V-h, at approximately 70 h, measurable acetate concentrations rapidly dropped and by 80 h, approached 0 (Figure 4. 40a). Therefore, by increasing the air flow, the net observed concentration of acetate decreased. This figure also demonstrates the capacity of an equilibrated TAD, operating under highly reduced conditions and aerated far below its maximum oxygen demand, to immediately adjust its metabolic rates to meet the environmental pressures of the increased aerated condition. Figure 4. 40b shows the opposite trend. When the air flow rate was decreased from 0.6 to 0 V/V-h, at 97 h, accumulated acetate concentrations started to increase and reached an equilibrium by approximately 4 days (*i.e.* 1.3 SRTs).

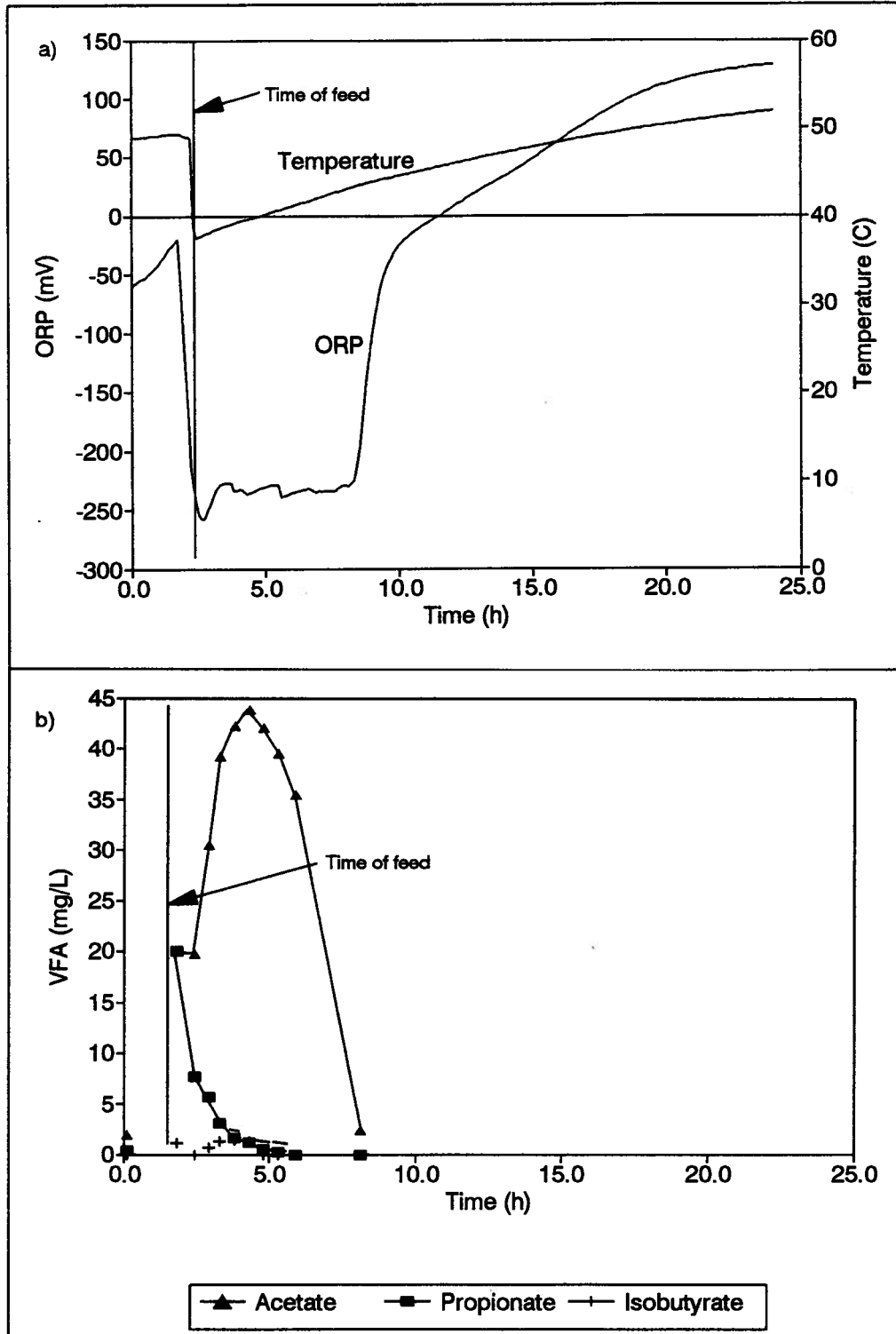


Figure 4.38 The transition condition in the first stage of the TAD process (air flow rate of 0.28 V/V-h). a) An example of one cycle of ORP and temperature profiles. b) VFA profiles of the same cycle.

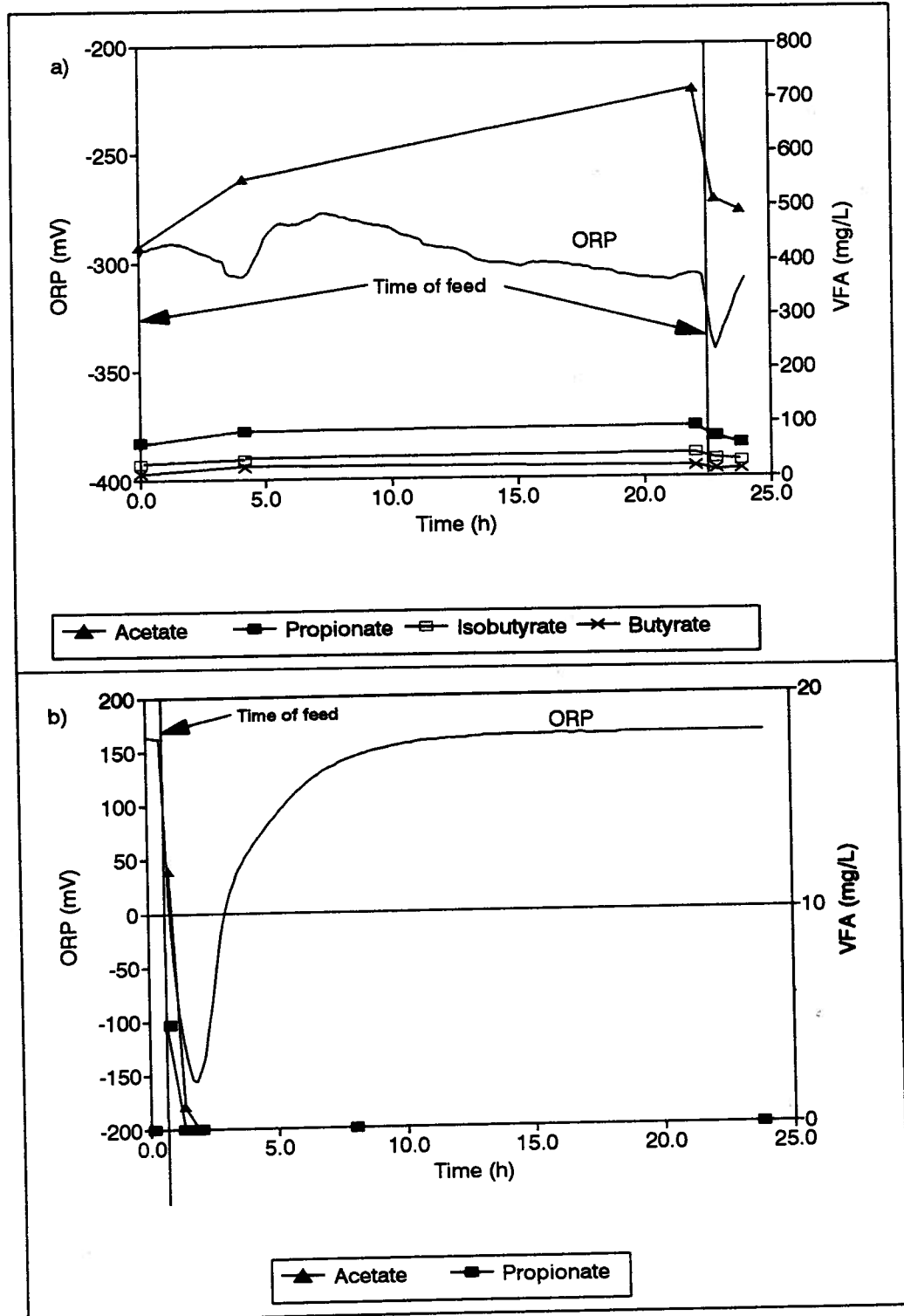


Figure 4.39 ORP and VFA profiles in the first stage of the TAD process under a) microaerobic (air flow rate of 0 V/V-h) and b) aerobic conditions (0.6 V/V-h).

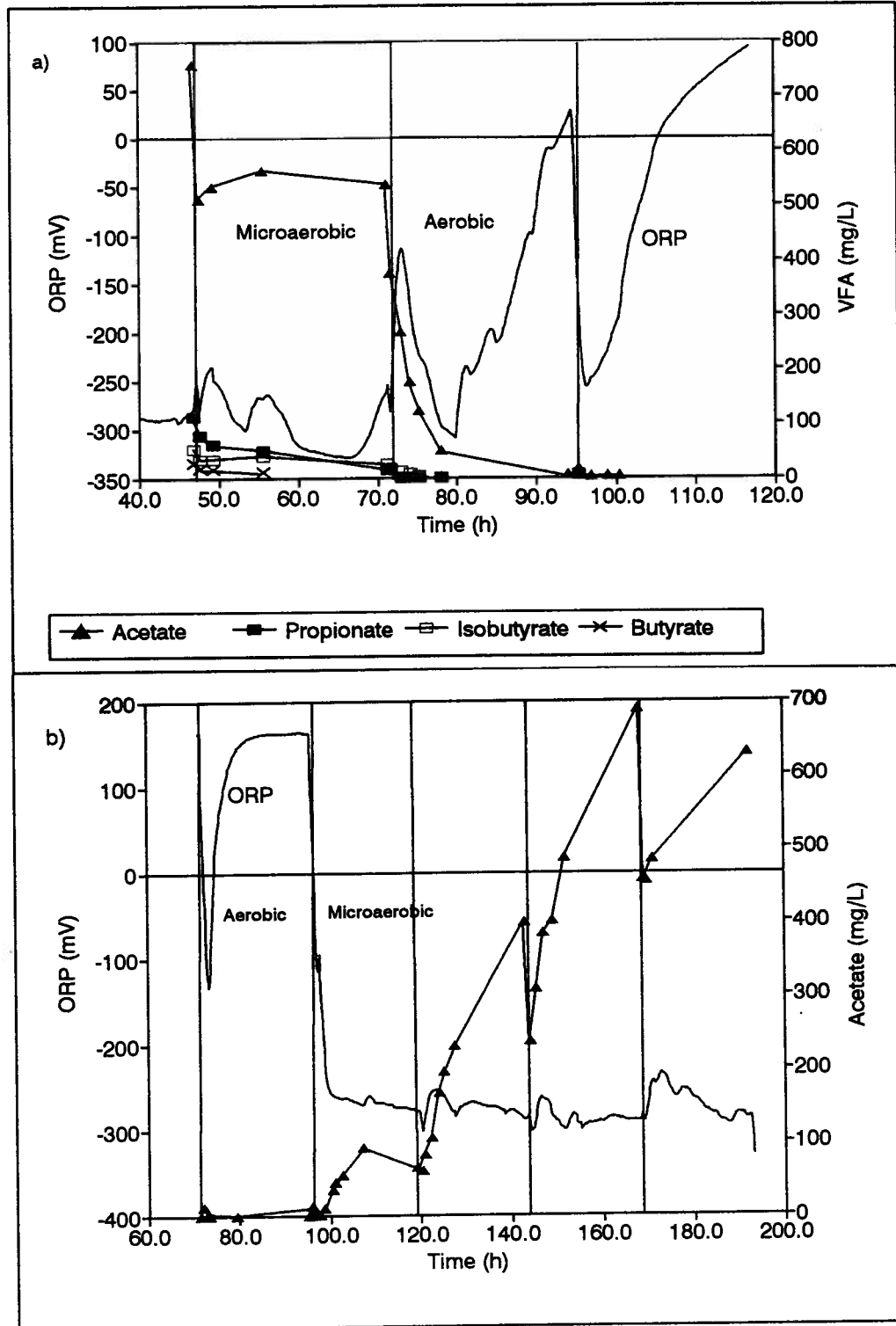


Figure 4. 40 ORP and VFA profiles in the first stage of the TAD process during a switch from a) microaerobic to aerobic conditions and from b) aerobic to microaerobic conditions. The vertical lines represent the points at which the TAD process had received feed sludge.

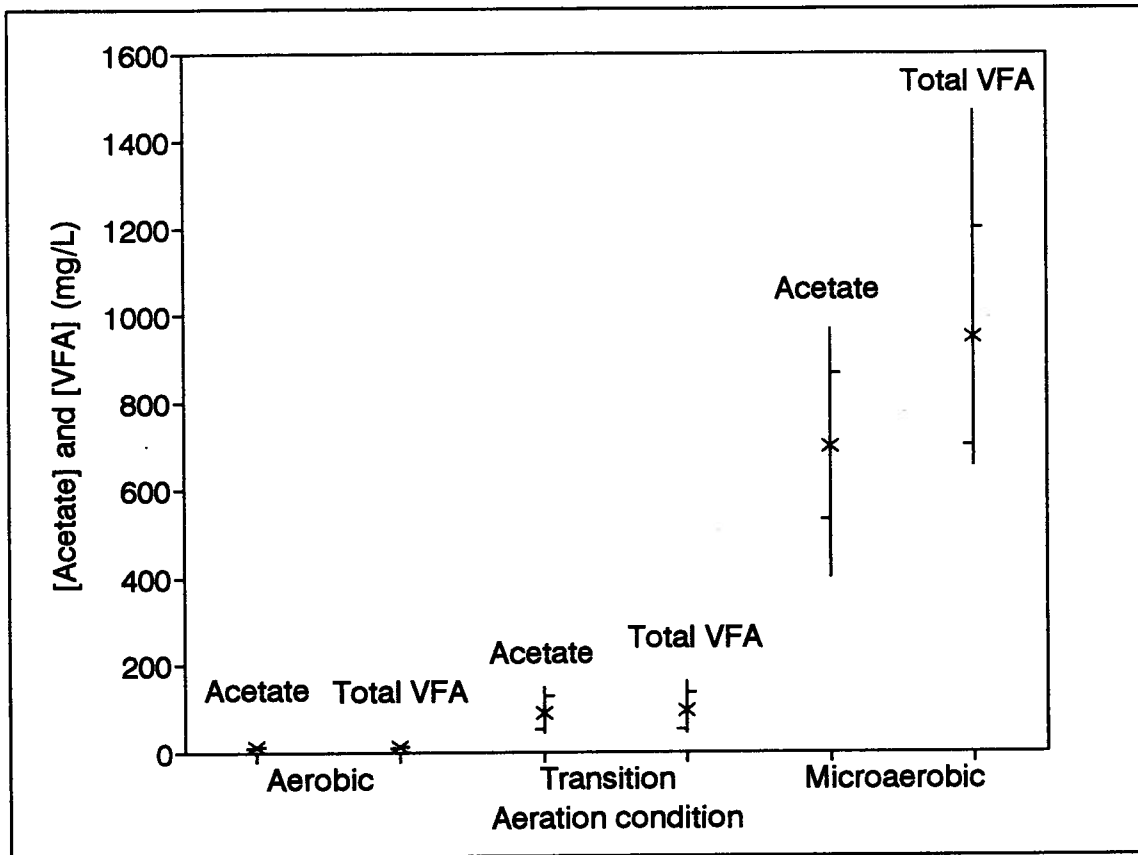


Figure 4. 41 Comparison of the net acetate and net total VFA production in the first stage of the TAD process under the three aeration conditions. Included are the mean, standard deviation and range.

The first 4.5 h of Figure 4. 38b shows some interesting results. As acetate concentrations increased, propionate concentrations decreased and after 5 h, propionate had disappeared completely. This result indicated that acetate and propionate, which are two fermentative end products, appear to behave in opposite trends under thermophilic sludge digesting conditions which was similar to the behavior of these VFA under batch test conditions in the microaerobic environment. Figure 4. 39a shows the optimal rate of aeration in terms of maximum net VFA production. With a negative ORP signal that lasted the entire 24 h cycle, acetate concentrations exceeded 700 mg/L. Figure 4. 39b shows the VFA profiles under the aerobic condition. It is clear from this graph that the rate of acetate catabolism had exceeded the rate of acetate synthesis. The result was no accumulation of VFA.

Table 4. 2 shows the duration of microaerobiosis observed under the three aeration conditions. The largest detectable range, of between 6 and 14 h of microaerobiosis (ORP values of below -250 mV), was under the transition condition (air flow rate: 0.28 V/V-h). This large range might be due to daily variability in sludge feed characteristics.

Table 4. 2 Duration of microaerobiosis during the three aeration conditions in the first stage of the TAD process. Each feeding cycle lasted for 24 h.

Variables	Microaerobic	Transition	Aerobic
Air flow (V/V-h)	0	0.28	0.60
Minimum duration (h)	24	6	0.5
Maximum duration (h)	24	14	3

Figure 4. 41 shows the capacity of the three aeration conditions to produce acetate and total VFA, respectively. This figure shows the mean, range and standard deviation of the net

production for each of the 3 conditions. It is clear that the lowest aeration rate of 0 V/V-h gave the highest acetate and total VFA concentrations.

Table 4. 3 compares the VFA distribution pattern between a TAD process, an ATAD process and two fermentative processes (Oldham *et al.*, 1992). When the TAD process is compared to a fermentative process, some striking differences appear. In fermentative processes, acetate contributes an average of 48% of the total VFA in the Penticton, B.C. treatment plant and 43% in the Kelowna, B.C. plant. However, the University of B.C. pilot plant and the Salmon Arm ATAD processes the contributions were 81% and 70%, respectively.

Table 4. 3 Comparison of VFA distribution between 2 thermophilic aerobic digestion processes and 2 fermentation processes.

Variables	Salmon Arm, B.C. ATAD	UBC pilot TAD	Penticton, B.C. Fermenter	Kelowna, B.C. Fermenter
Acetate (%)	70	81	48	43
Propionate (%)	14	11	42	43
Others (%)	16	8	10	14

Hamer (1987) conducted aerobic thermophilic experiments which measured the various VFA, as a function of time, in semicontinuous operating conditions in a laboratory scale bioreactor. The thermophilic organisms were from a full-scale operating ATAD process. The sludge feed source was a suspension of yeast cells. Their results were similar to the results of this study, in terms of overall trends and relative proportions of each VFA. Hamer (1987) explained those effects by suggesting that accumulation of carboxylic acids, predominantly acetic acid, is the result of the fermentative metabolism of the thermophilic process culture. This model suggests that near exhaustion of the preferred soluble substrate is followed by utilization

of the low molecular mass carboxylic acids produced earlier (eg. acetate, propionate). However, it does not explain why a readily usable substrate like acetate can accumulate to concentrations of 6 g/L, when the mixed microbial consortium mediating the biodegradation process would be expected to simultaneously use the produced fermentation products (Wilkinson and Hamer, 1979). This discrepancy was attributed to the possibility of some sort of inhibition of carboxylic acid biodegradation.

The results from this preliminary pilot scale study suggest that there was simultaneous utilization of VFA and that the measured concentration of VFA, at any given time, is a function of both the relative rates of its synthesis and biodegradation. Throughout the study, VFA concentrations increased when the catabolic rate of VFA consumption was expected to be lower than the anabolic rate of VFA production. In Figure 4. 38, the net acetate concentration built up to a maximum within 4.5 h and then had disappeared by 8 h. The ORP during this period remained at around -250 mV. It may be convenient to think that this environment represents a fermentative condition; however, it must be remembered that, throughout this cycle, the reactors were aerated at 0.28 V/V-h. Therefore, the oxygen demand between 0 and 8 h actually exceeded the oxygen supply. This range also happened to be the acetate detection range.

It is clear from the data that the measurable presence of easily oxidizable substrates contributed to the high oxygen demand (eg. acetate) and that the disappearance of these compounds correlated to the ORP elbow, which was the transition point between periods of high oxygen requirement and decreasing oxygen requirement. Figure 4. 40 shows the pattern of acetate behavior when the air flow rate is increased or decreased. When flow rates were

increased, the net acetate concentration fell rapidly. When flow rates decreased, the net acetate concentration increased. Since the response time of changes in measured acetate to increase or decrease in air flow was negligible, the inhibition of acetate degradation was in part a function of aeration. This correlation was expected, since the most important molecule required in acetate biodegradation, or its oxidation, is molecular oxygen. Therefore, it is clear that the measurable accumulation of acetate occurred despite aerobic respiration.

4.3 3 x 3 Pilot Scale TAD Experiments

From the preliminary study on TAD, it was discovered that microaerobic conditions produced the highest concentrations of VFA out of the three conditions examined (ie. microaerobic, transition and aerobic conditions). A 3x3 pilot TAD experiment narrowed the range of air flow rates such that all flow rates tested were encompassed within the microaerobic range. The mean flow rates were 0 mL/min, which was defined as a low flow microaerobic condition, 115 mL/min which was defined as a medium flow microaerobic condition and 165 mL/min which corresponded to a high flow microaerobic condition. SRT was the other independent variable tested. The SRT values examined were 3, 4.5, and 6 days.

To test main and interaction effects of these two variables, a total of 9 cells or runs would have to be done. A total of 9 runs were done with the high air flow and 4.5 d SRT combination repeated. This resulted in only 8 of the possible 9 combinations completed. As seen in Table 3. 2, due to an error in scheduling, the medium air flow and 6 d SRT combination was not done. In addition to these 9 runs, a tenth run was done in a true fermentative environment at a 4.5 d SRT to examine the metabolic behavior of substrates under anaerobic conditions. This anaerobiosis was achieved by purging the test reactor (B side) with an anaerobic gas mixture which contained 90% nitrogen, 5% carbon dioxide and 5% hydrogen. Since SRTs and air flow rates varied over the course of each run, Table 4. 4 shows the calculated SRTs and aeration rates. Included are the mean, standard deviation and range for these independently set variables. In all runs, the A side control independent variables were maintained at their respective medians (ie. 4.5 d SRT and medium aeration) while the B side experimental variables were adjusted to their appropriate

values. Since all control side (A side) runs had the same SRT and aeration rates, cumulative values for all runs were calculated for this reactor. This experimental design facilitated the comparison of the test condition (B side) to the corresponding control condition (A side) within the context of a single run.

Table 4. 4 Descriptive statistics of air flow rates and SRTs of pilot scale TAD experiments.

B side (expt.) Run #	SRT (d)			Aeration (mL/min)		
	Mean (target)	Standard deviation	Range	Mean (target)	Standard deviation	Range
1	4.6 (4.5)	0.3	4.1-5.1	0 (0)	0	0
2	3.3 (3.0)	0.4	2.6-4.0	0 (0)	0	0
3	5.6 (6.0)	0.6	4.5-6.7	0 (0)	0	0
4	4.6 (4.5)	0.2	4.3-4.9	110 (117)	22	65-145
5	3.4 (3.0)	0.1	3.2-3.6	123 (117)	7	114-132
6	6.4 (6.0)	0.2	6.1-6.7	160 (164)	3	156-164
7	4.5 (4.5)	0.7	3.1-5.2	165 (164)	0	165
8	5.5 (6.0)	0.3	5.0-6.0	165 (164)	1	164-166
9	4.6 (4.5)	0.4	3.9-5.3	164 (164)	3	160-168
10	4.4 (4.5)	0.2	4.1-4.7	n/a (n/a)	n/a	n/a
A side (cont.)	4.5 (4.5)	0.3	3.3-5.7	105 (117)	19	24-186

4.3.1 Temperature Variation of Pilot Scale TAD experiments

From the preliminary pilot scale study the first stage of the TAD process was shown to produce the highest measured concentrations of VFA. The temperature range of the first stage was 37° to 47° C. The second phase of operation attempted to reproduce similar temperature ranges under a different primary sludge feeding regime (once/hour instead of once/day). Figure

4. 42 shows examples of the on line temperature variations of both A and B sides during runs 1 and 8. As seen from these results, the temperature range was approximately 43 to 49° C. In addition, there seemed to be a daily cyclic temperature response. The temperatures inside the reactors seemed to be higher during the late morning and afternoon periods (eg. 10:00-13:00) relative to the night and early morning periods (22:00-03:00). This observation would be consistent with ambient temperature fluctuations over the course of a day. The ambient temperatures outside the reactor may have had enough of an effect to produce a temperature cycle within the reactors, since during the day, the ambient external temperature was invariably a few degrees warmer than at night.

One feature of these pilot scale units, which make them different from other pilot and bench scale processes, was that there was no need for any external heating device to maintain reactor temperatures. Reactor temperatures were maintained by biological heat production, mechanical mixing heat input and an adequately insulated reactor. Since there was no external heating controls, isothermal operation could not be maintained and some fluctuations did occur. However, there was an indirect way of controlling reactor temperatures. This was achieved by varying the only controllable heat input, which was the amount of mechanical mixing energy (ie. changing Turborator RPMs). When reactor temperatures were increasing, it could be reduced by slightly decreasing the RPM of the turborator, or vice versa. Figure 4. 43 illustrates this effect. When the A side temperature started to decrease (Figure 4. 43a), the RPM of the Turborator mixer/aerator was increased to 850 from 830 RPM at approximately 10:30 am. This increase in rotational speed resulted in an increase in reactor temperature. Therefore, a change of only 17

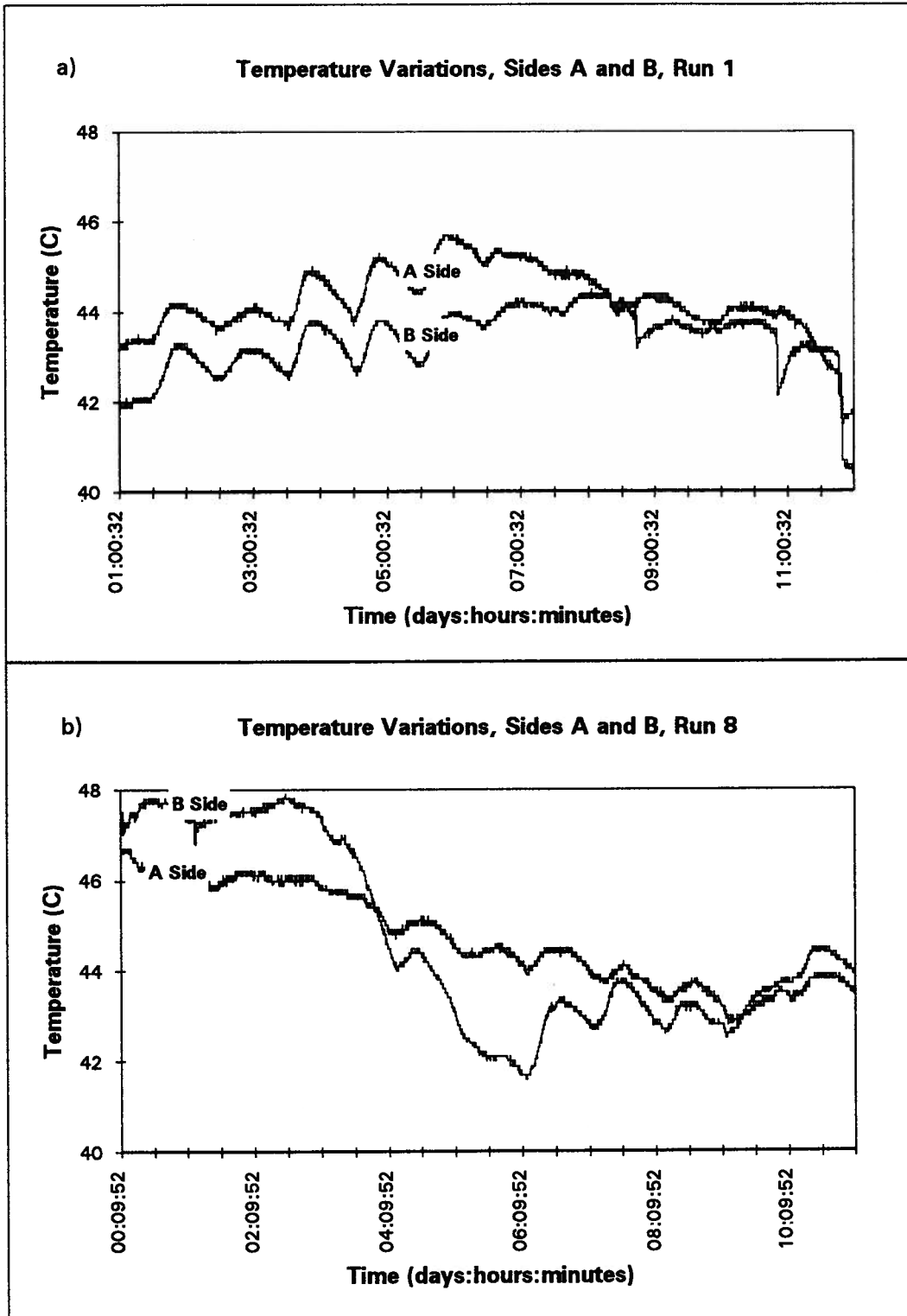


Figure 4.42 Examples of on line temperature measurements during pilot scale TAD experiments

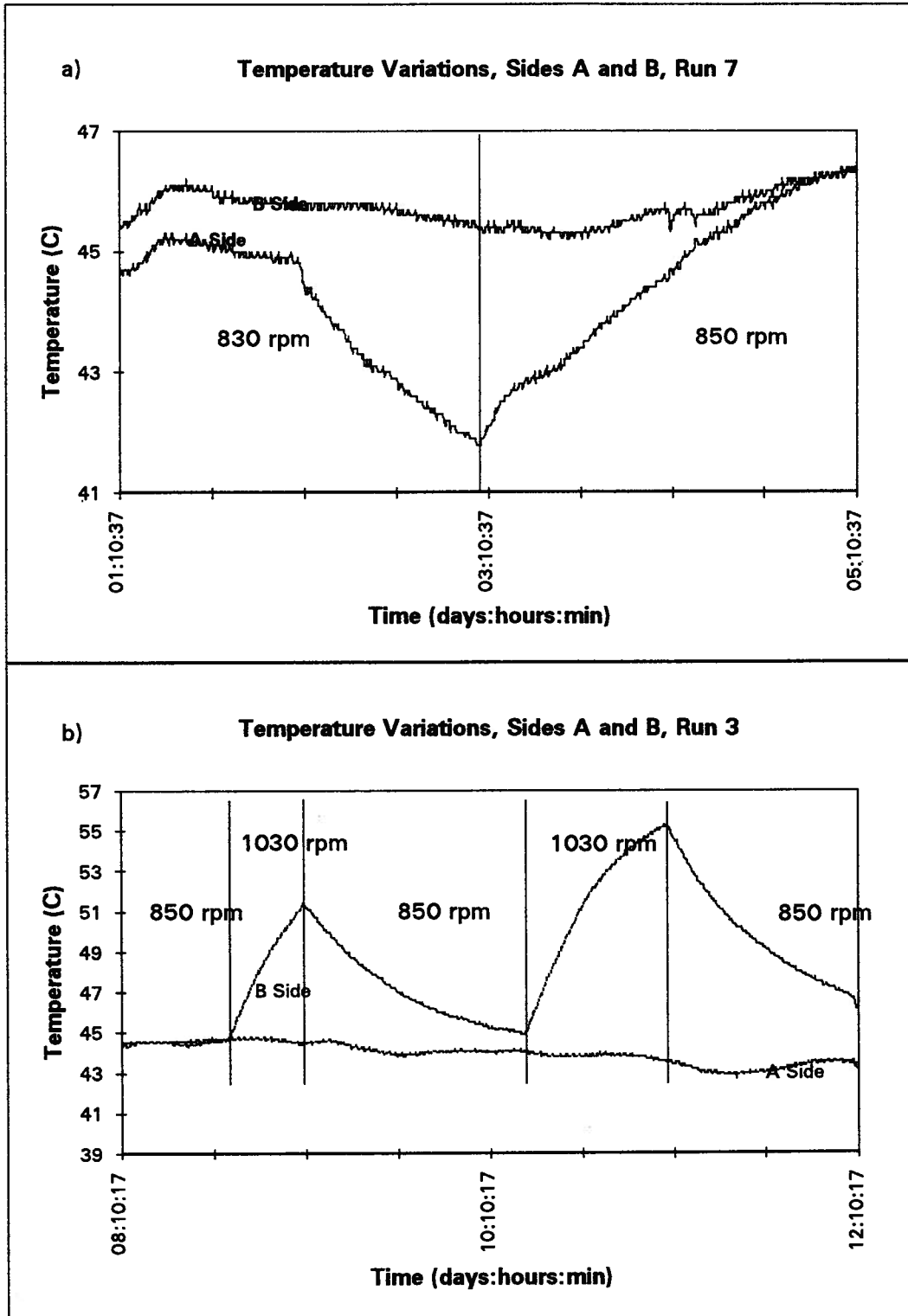


Figure 4.43 Temperature effects in TAD reactors from changing Turborator rotational speed.

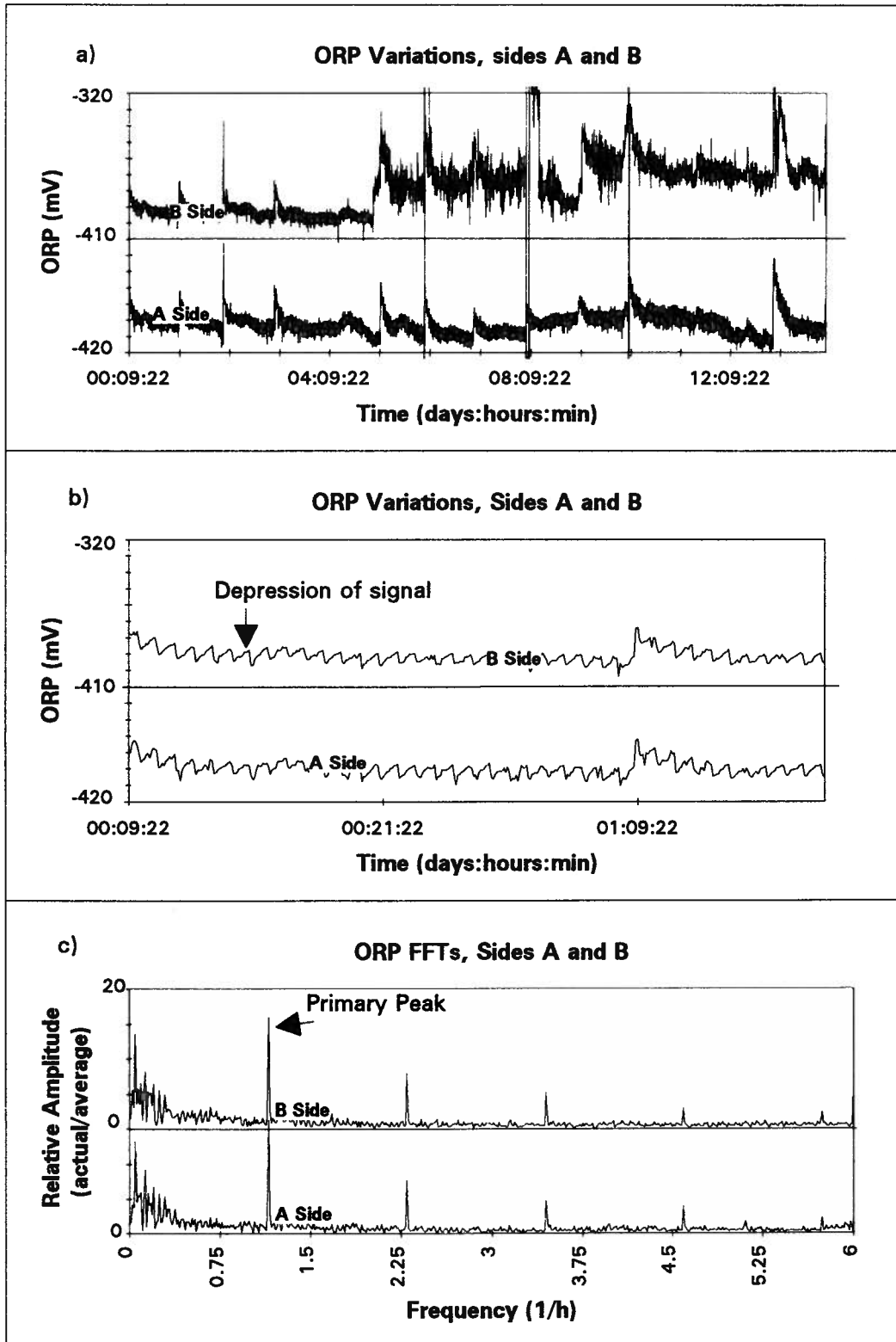


Figure 4.44 Examples of on line ORP measurements during pilot scale TAD experiments. a) ORP variation of both sides over a period of 12 days and b) an extract of the same period showing shark tooth pattern. c) Fast Fourier transform of this ORP

RPM resulted in a measurable temperature increase within the reactor. Figure 4. 43b shows the effect of a Turborator malfunction which resulted in an increase of rotational speed from 850 to 1030 RPM. The increase in reactor temperature was dramatic. Approximately 10 h after the malfunction, the rotational speed was decreased back to 850 RPM which resulted in a gradual decrease in temperature. Thirty six hours after the first malfunction had been rectified another identical malfunction occurred, which resulted in a similar temperature increase. Since isothermal temperatures could not be maintained, this could potentially have contributed to the variability in many of the measured parameters.

4.3.2 On Line ORP Measurements as State Variable

ORP has been used in the past to measure the state of different processes ranging from anaerobic digestion (Blanc and Molof, 1973; Dirasian *et al.*, 1963) to biological nutrient removal processes (Koch *et al.*, 1988). In an attempt to evaluate the suitability of ORP as a state variable in TAD, on line data acquisition of this variable was implemented. An example of the ORP trends of one of the runs is shown in Figure 4. 44. Since all runs were conducted under microaerobic aeration conditions, there was no obvious detectable difference in on line ORP profiles between the different aeration rates within this microaerobic range. The profiles of all 9 runs remained consistently negative at approximately -400 mV. This type of profile suggests that a highly reduced environment existed within each reactor. There seemed to be a daily transient ORP perturbation, which corresponded precisely to the time of wastage from each

bioreactor. This transient effect was short lived and the ORP signal returned quickly back to its basal response. This could have possibly been caused by forcing air into the headspace of the bioreactor by wasting a fixed volume of sludge from the contents of the reactor.

When the time scale is expanded, a cyclic nature becomes obvious (Figure 4. 44b) and as such was analyzed using Fourier analysis. The Fourier model decomposes a time series into a finite sum of trigonometric components (ie. sine and cosine waves of different frequencies). Fourier transforms are time consuming to compute because they involve numerous trigonometric functions. Cooley and Tukey (1965) developed a fast algorithm for computing the transform on a discrete series that makes the spectral analysis of lengthy series practical. A variant of this fast Fourier transform algorithm was used in Excel for Windows (Version 4.0). Figure 4. 44c shows the relative amplitude plotted against the inverse of frequency. This plot shows one primary peak at 52.6 minutes (frequency 1.12 h^{-1}), which is the exact period between reactor feedings. When the reactors were fed substrate (ie. primary sludge), this seemed to depress or decrease the ORP signal slightly in a more reduced direction (approximately 20 mV). Over the next 52.6 minutes the signals increased gradually until the next feed cycle was initiated. This approximate once/hour feeding regime created a 'Shark tooth' pattern response in the ORP profile. Kelly *et al.* (1993) also investigated the suitability of ORP measurements as a state variable at the District of Salmon arm ATAD facility, which has a similar feeding regime to the UBC pilot scale TAD process. Stable operation was found between -50 and -250 mV. They reported that the hourly sludge feedings were characterized, on the ORP charts, by abrupt negative depressions and a slow rise to a less negative norm (ie. 'shark tooth pattern').

It is somewhat strange that ORP, although insensitive to changes in aeration rates between runs, was extremely sensitive to the addition of substrate within each individual run. These results suggest that absolute ORP values are not a suitably stringent state variable for monitoring reactor conditions between runs, although relative ORP values are quite sensitive at detecting slight changes in reactor conditions within a narrow time window. The results from this section and those from the preliminary pilot scale experiments show that ORP can only discriminate between gross changes in aeration (ie. microaerobic, transition and aerobic conditions).

4.3.3 VFA Accumulation in TAD

The two independent variables examined for their effect on VFA accumulation in TAD were aeration and SRT. The following sections illustrate and discuss the effects of these variables on VFA accumulation and speciation. The first section introduces the variable nature of measuring individual VFA species over time and the factors that affect their variability. The second section discusses the variables in terms of their effect on the overall accumulation of VFA in TAD. The final section discusses the statistical significance of the effect of aeration and SRT on VFA accumulation.

4.3.3.1 Variability of VFA Measurements

Figures 4. 45 and 4. 46 show the effect of aeration and SRT on the variability of acetate

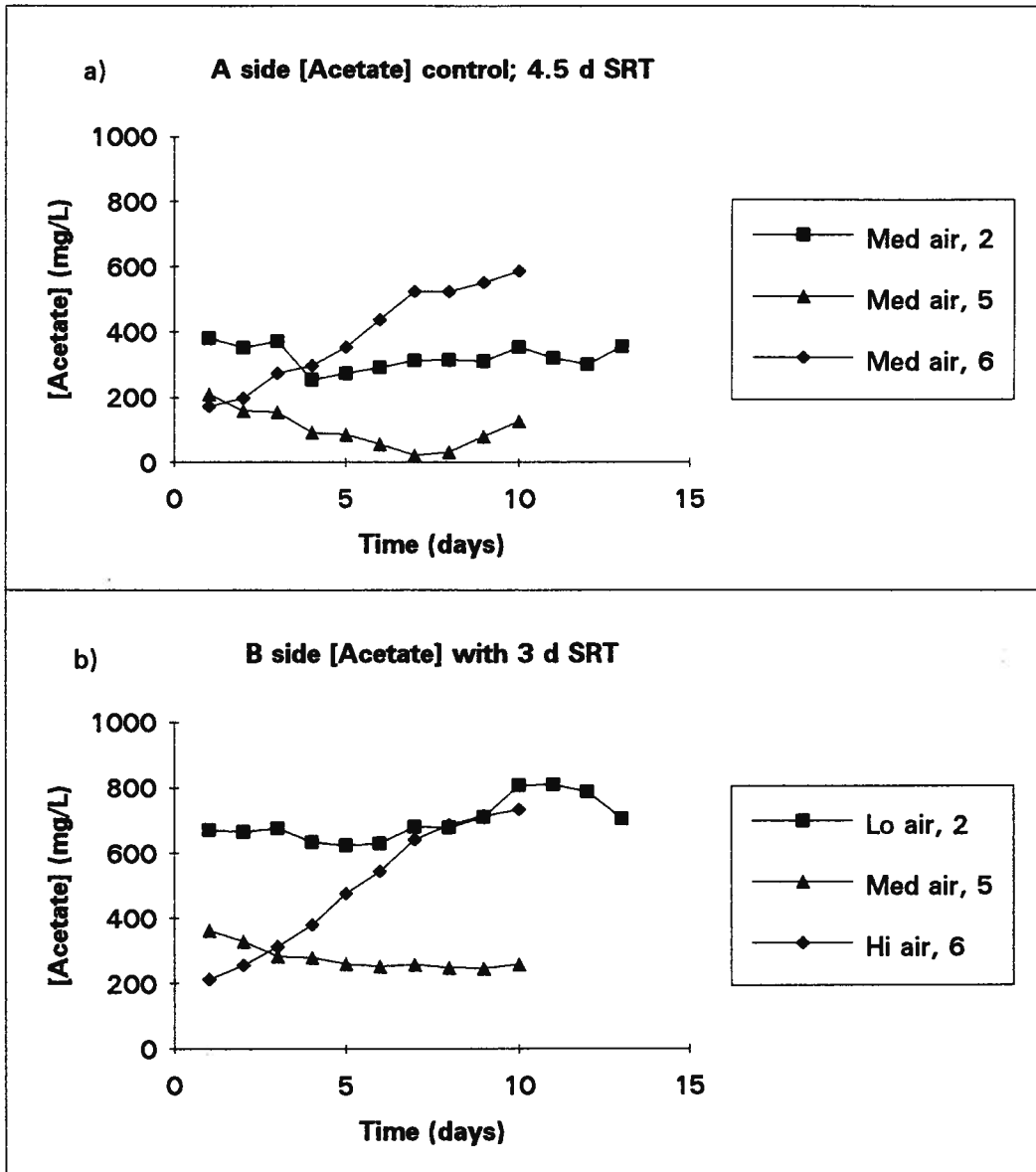


Figure 4.45 Variation of acetate concentrations over time in the pilot scale TAD experiments with a 3 d SRT. a) A side and b) B side (legend key: Symbol; aeration rate; run #).

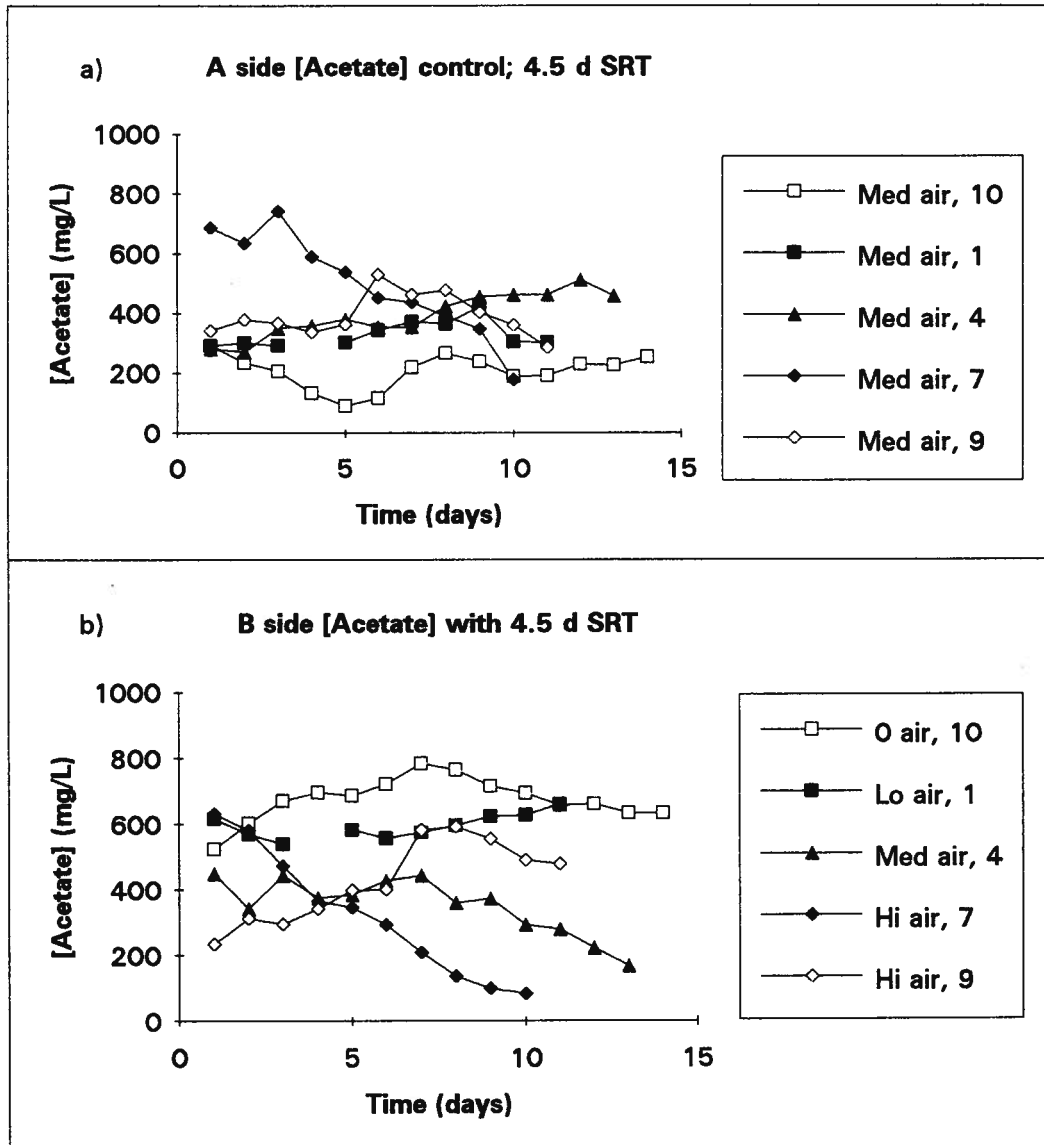


Figure 4.46 Variation of acetate concentrations over time in the pilot scale TAD experiments with a 4.5 d SRT. a) A side and b) B side (legend key: Symbol; aeration rate; run #).

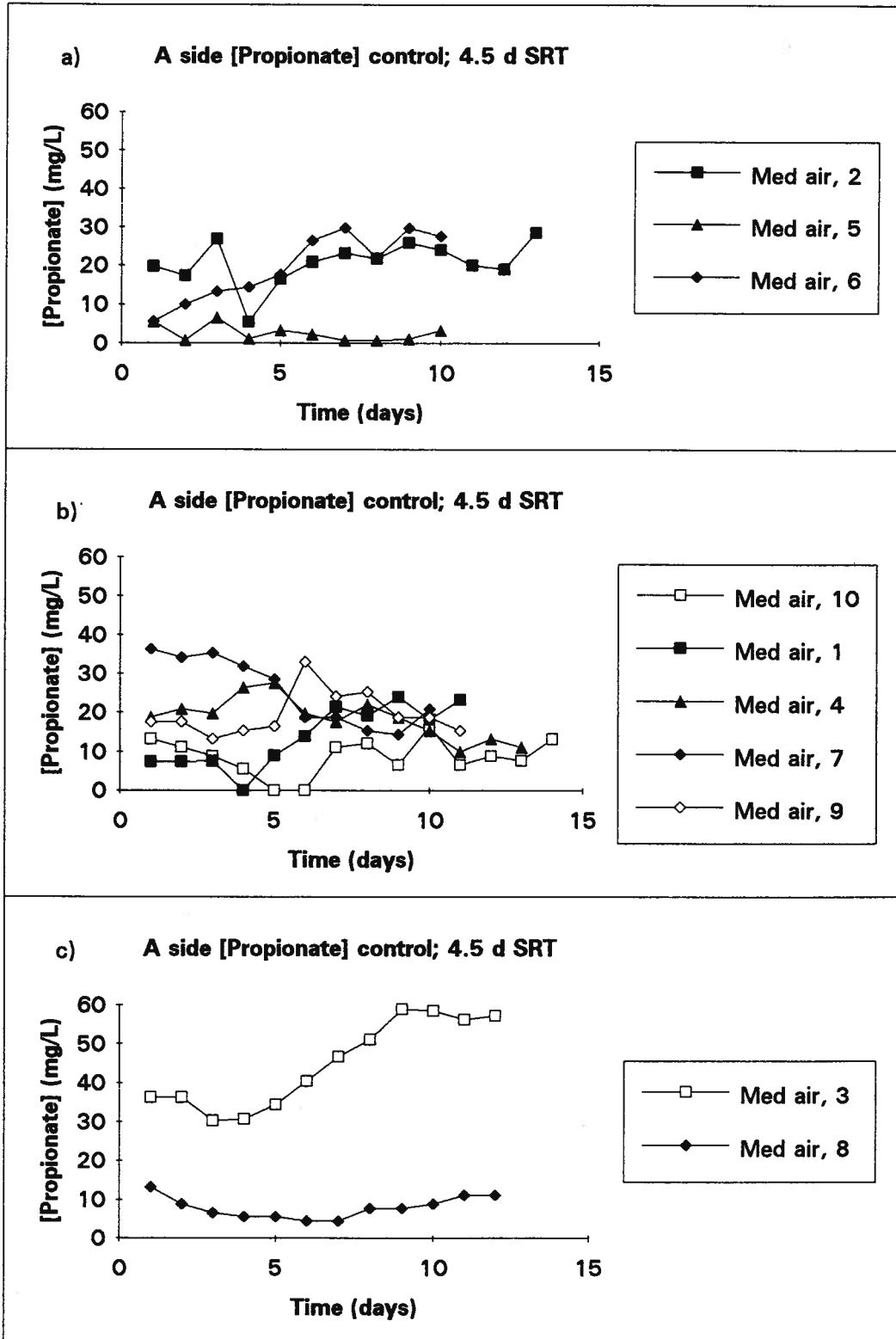


Figure 4.47 Variation of A side propionate concentrations over time for all 10 runs (legend key: Symbol; aeration rate; run #).

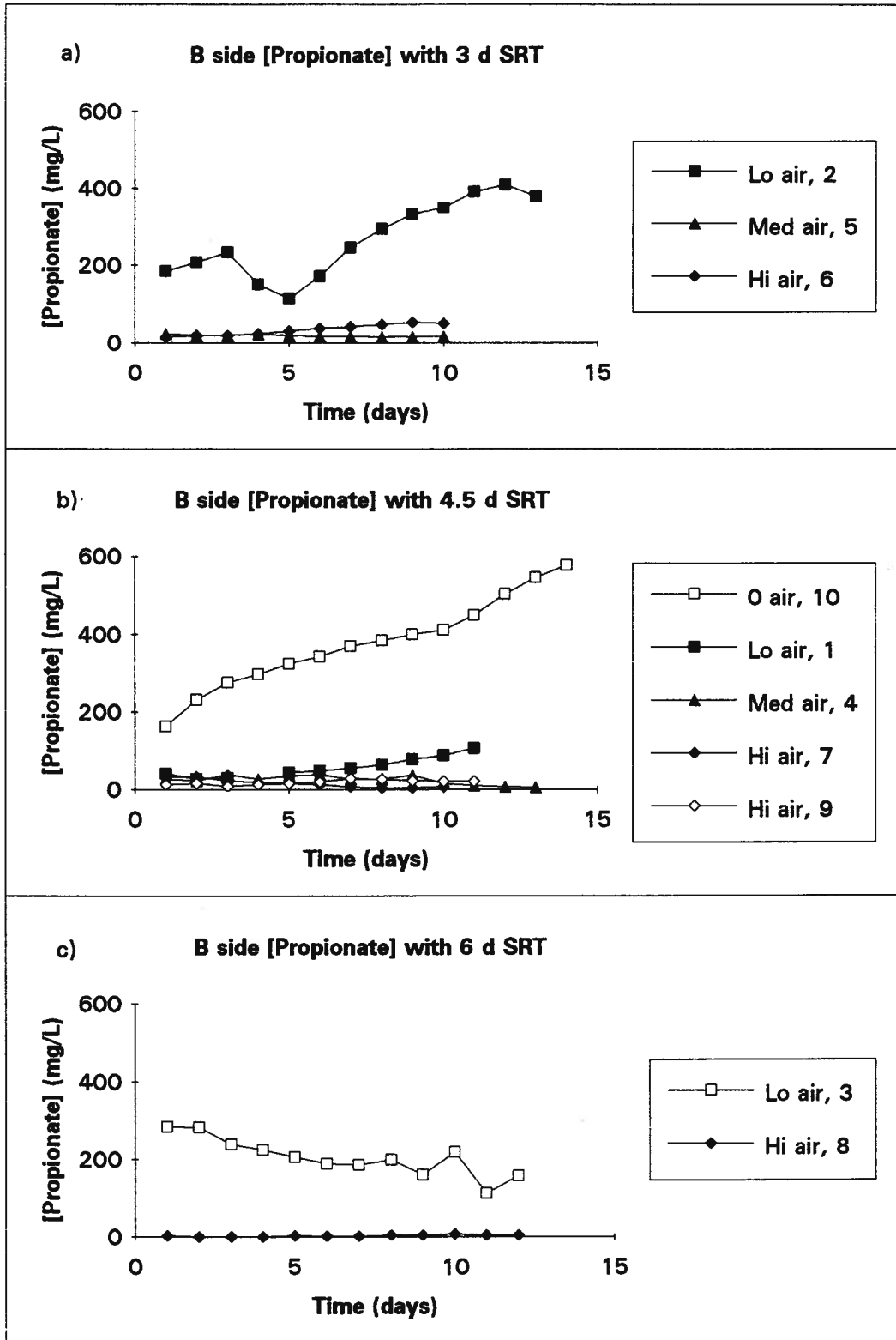


Figure 4.48 Variation of B side propionate concentrations over time for all 10 runs (legend key: Symbol; aeration rate; run #).

concentrations between the control (A) side and the experimental (B) side bioreactors. The variability over time of the A side acetate concentrations in the reactor was presumably due primarily to variations in uncontrollable environmental conditions (eg. sludge feed characteristics, external ambient temperatures). Even though the SRT and aeration rate in the A side reactor remained constant throughout the 10 runs (ie. 4.5 d SRT and medium air flow rate), the acetate concentrations measured in this reactor varied considerably. For example, in run 6, which corresponded to the high flow/3 d SRT combination, the control (A) side reactor began with an acetate concentration of 175 mg/L and steadily increased throughout the experiment to end at a concentration of 600 mg/L. Whatever effector that resulted in the increase in acetate concentrations in the control side reactor also affected the acetate concentrations on the experimental side in the same manner.

A similar but opposite observation can be made for run 7. The effector which caused a decrease in acetate concentrations in the A side reactor from a high of 700 mg/L, at the beginning, to 200 mg/L at the termination of the experiment, also caused a similar decrease on the B side reactor's acetate concentrations. Figures 4. 47 and 4. 48 show the propionate profiles for both the control and experimental sides of the TAD pilot scale reactors for all 10 runs. Under the control condition (ie. 4.5 d SRT and medium air flow rate) the propionate concentrations remained quite low (<60 mg/L). Under the test conditions (B side), the low flow/3 d SRT combination and true anaerobic aeration conditions stimulated propionate accumulation to well above 200 mg/L within the reactor. By the end of the experiment, under the true fermentative condition, propionate concentrations within the reactor had reached 577

mg/L, which was proportional to the concentration of acetate (635 mg/L, Figure 4. 46b) at that point. The results from these figures suggest that, as aeration rates decrease, propionate accumulation increase. By the time a true fermentative environment is established, propionate accumulation equals that of acetate. This is consistent with other fermentative studies dealing with the acid phase of anaerobic digestion processes. Of the total VFA produced, Elefsiniotis (1993) found that 46.3% was acetate and 31% was propionate.

4.3.3.2 VFA Accumulation in Pilot Scale TAD Experiments

Figures 4. 49 to 4. 52 show the effect of the two independent variables on VFA accumulation in the control (A side) and experimental reactors (B side). The accumulation of VFA was calculated using a mass balance approach, which is expressed by the following equation,

VFA accumulation = (Mass in effluent \pm Net change in mass within system)/Volume of effluent

Since the SRT changed from run to run, the mass of VFA accumulated necessitated normalization to a volume component to alleviate the effect of SRT and to facilitate comparison. This was done by dividing the mass accumulated by the volume of effluent. The net change in mass within the bioreactor must also be addressed due to the short SRTs used. The equation for calculating VFA accumulation is as follows,

$$\text{VFA accumulation} = \frac{\sum_{e=1}^n C_e V_e + \sum_{e=1}^n (C_e - C_{e-1}) V_r}{\sum_{e=1}^n V_e}$$

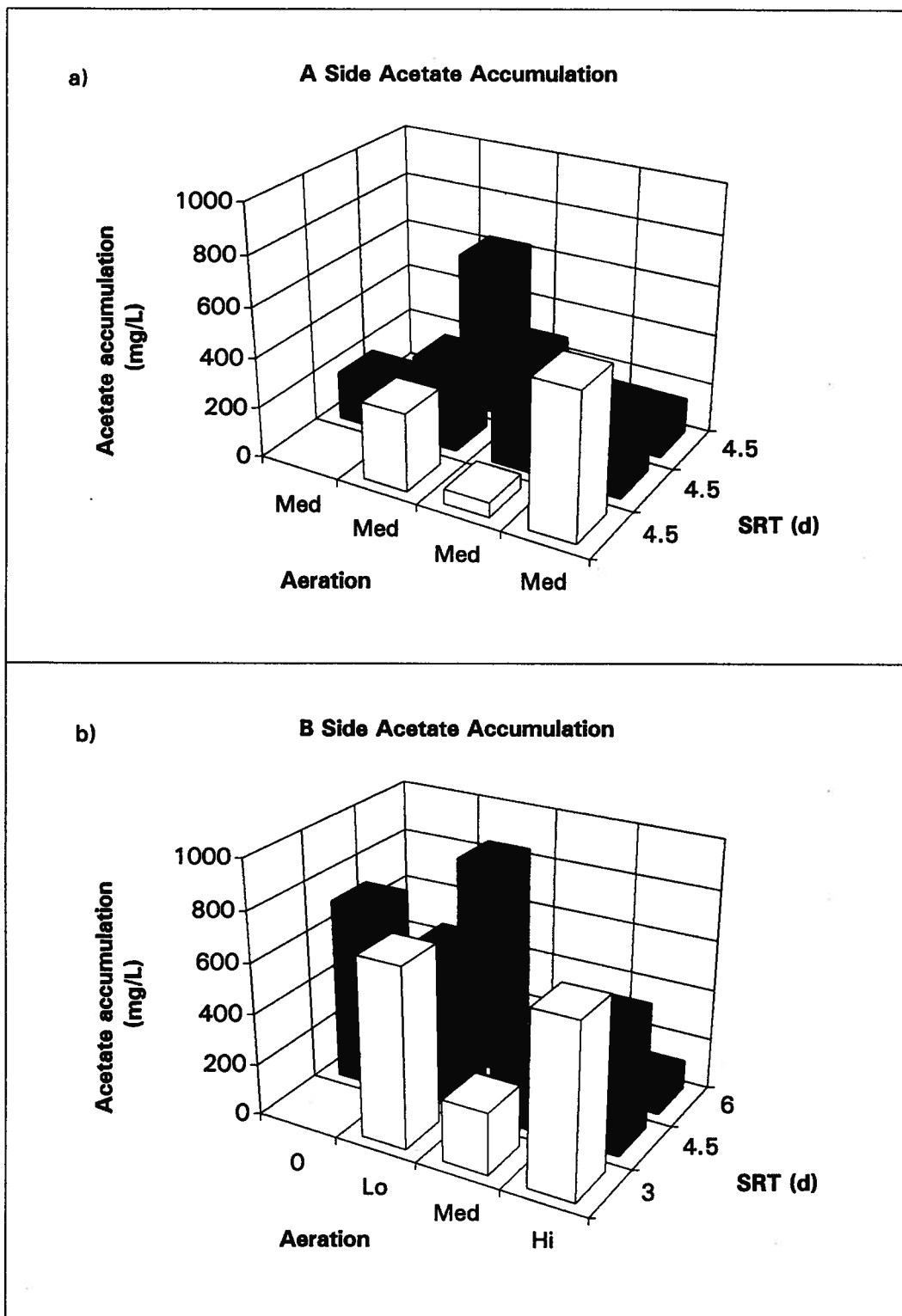


Figure 4.49 Acetate accumulation in pilot scale TAD experiments on the a) A and b) B sides.

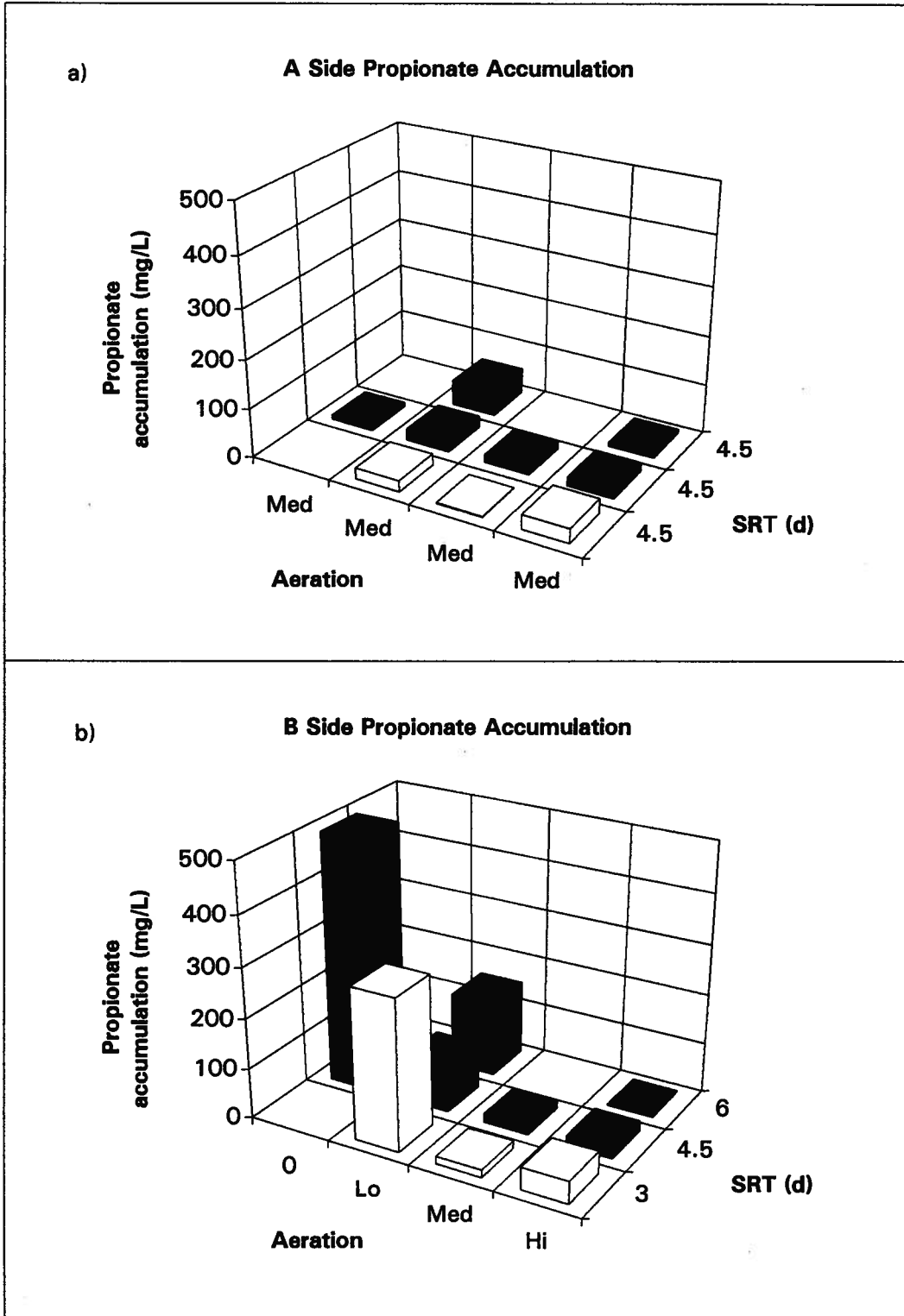


Figure 4.50 Propionate accumulation in pilot scale TAD experiments on the a) A and b) B sides.

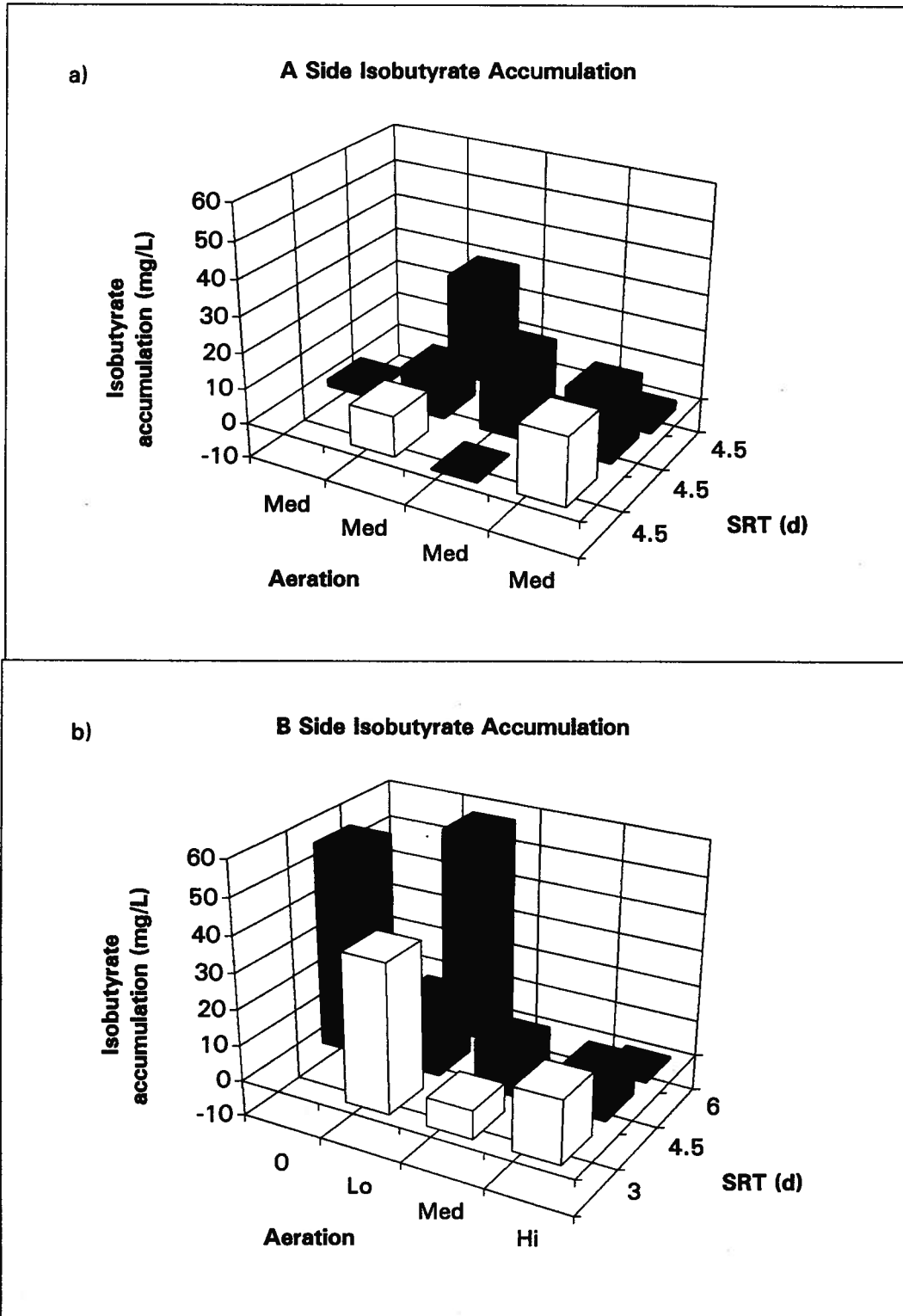


Figure 4.51 Isobutyrate accumulation rates in pilot scale TAD experiments on the a) A and b) B sides.

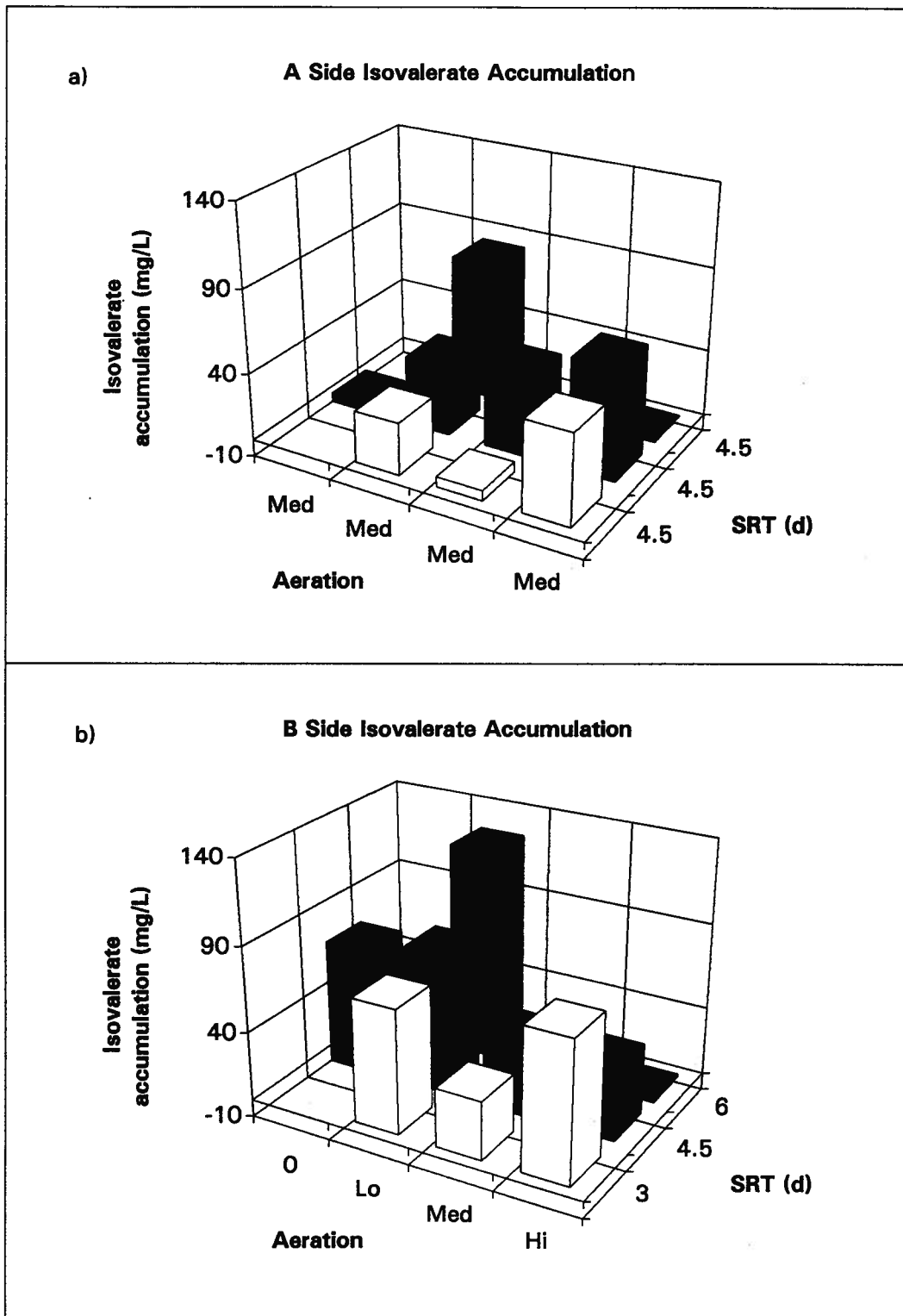


Figure 4.52 Isovalerate accumulation in pilot scale TAD experiments on the a) A and b) B sides.

where C_e = concentration of VFA in effluent (mg/L)

V_e = daily volume of effluent (L)

$(C_e - C_{e-1})$ = change in concentration of VFA in reactor (mg/L)

V_r = volume of reactor at time of wastage (L)

n = number of days in run (d)

The A side (control) VFA accumulation showed some interesting results (Figures 4. 49a, 4. 50a, 4. 51a, 4. 52a). Although the control side variables were kept constant, the variability of VFA accumulation between runs was large. This implies that there are, as yet, unknown effectors which can cause large deviations in terms of VFA accumulation from one run to the next. These runs also emphasized the need for a control condition, in order to normalize test results against.

Figures 4. 53 and 4. 54 show the experimental reactor (B side) VFA accumulation normalized to a control value (A side). This was done by subtracting the A side VFA accumulation value from that of the experimental (B) side. This would potentially alleviate the variability in response due to uncontrollable effectors, since the effect should be similar for both reactors. When this type of normalizing was applied, some main and interactive effects of SRT and aeration appeared. In terms of acetate accumulation, there was a general trend of increasing accumulation as SRT decreased from 6 to 3 d (with the exception of the high flow aeration condition) and as aeration decreased from high to low air flow. Increasing the amount of substrate (ie. decreasing SRT) seems to have a similar effect to that of decreasing the aeration rate. The maximum measured acetate accumulation rate was under the 4.5 d and true anaerobic

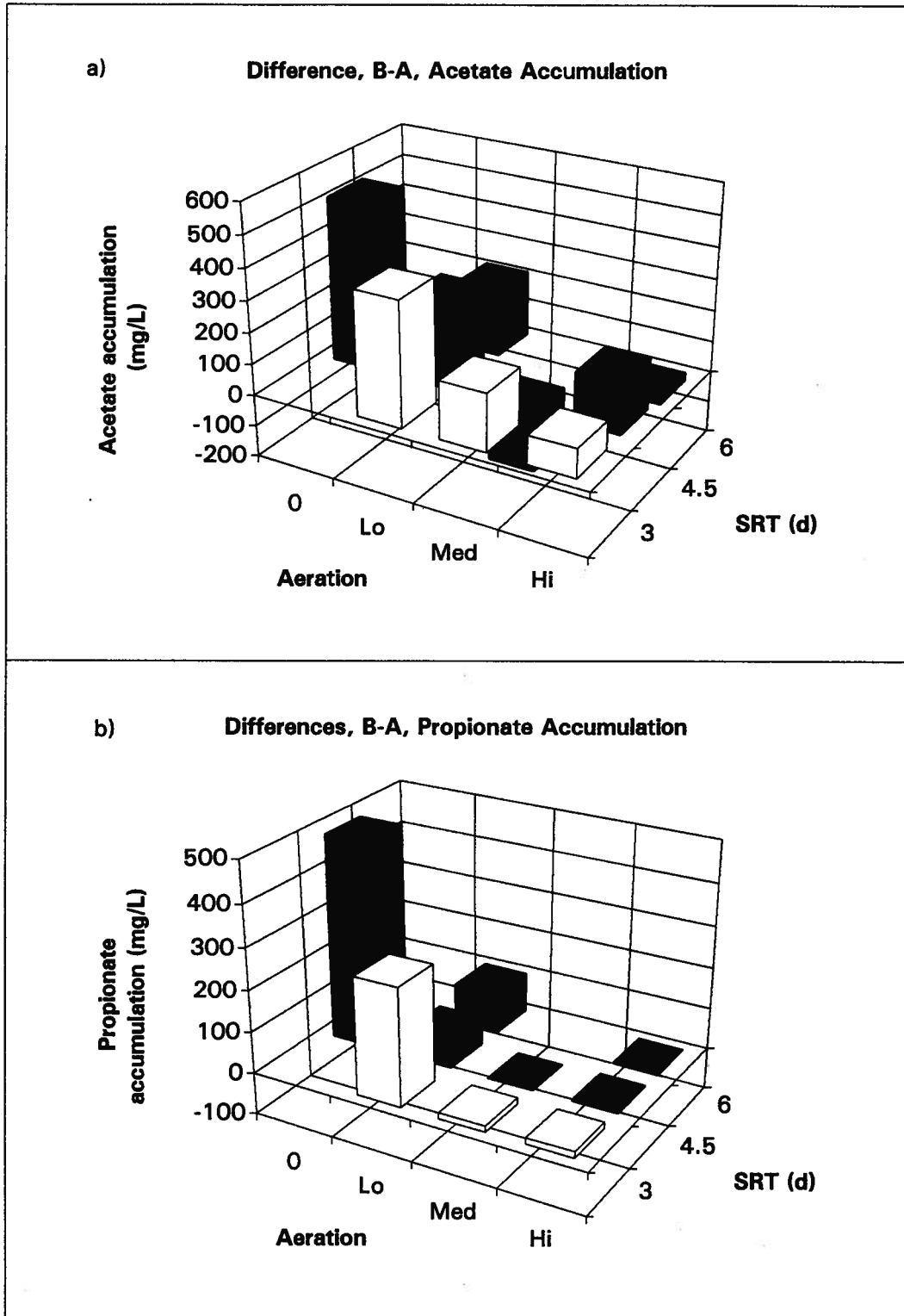


Figure 4.53 VFA accumulation normalized to their respective control values.
a) Acetate and b) propionate.

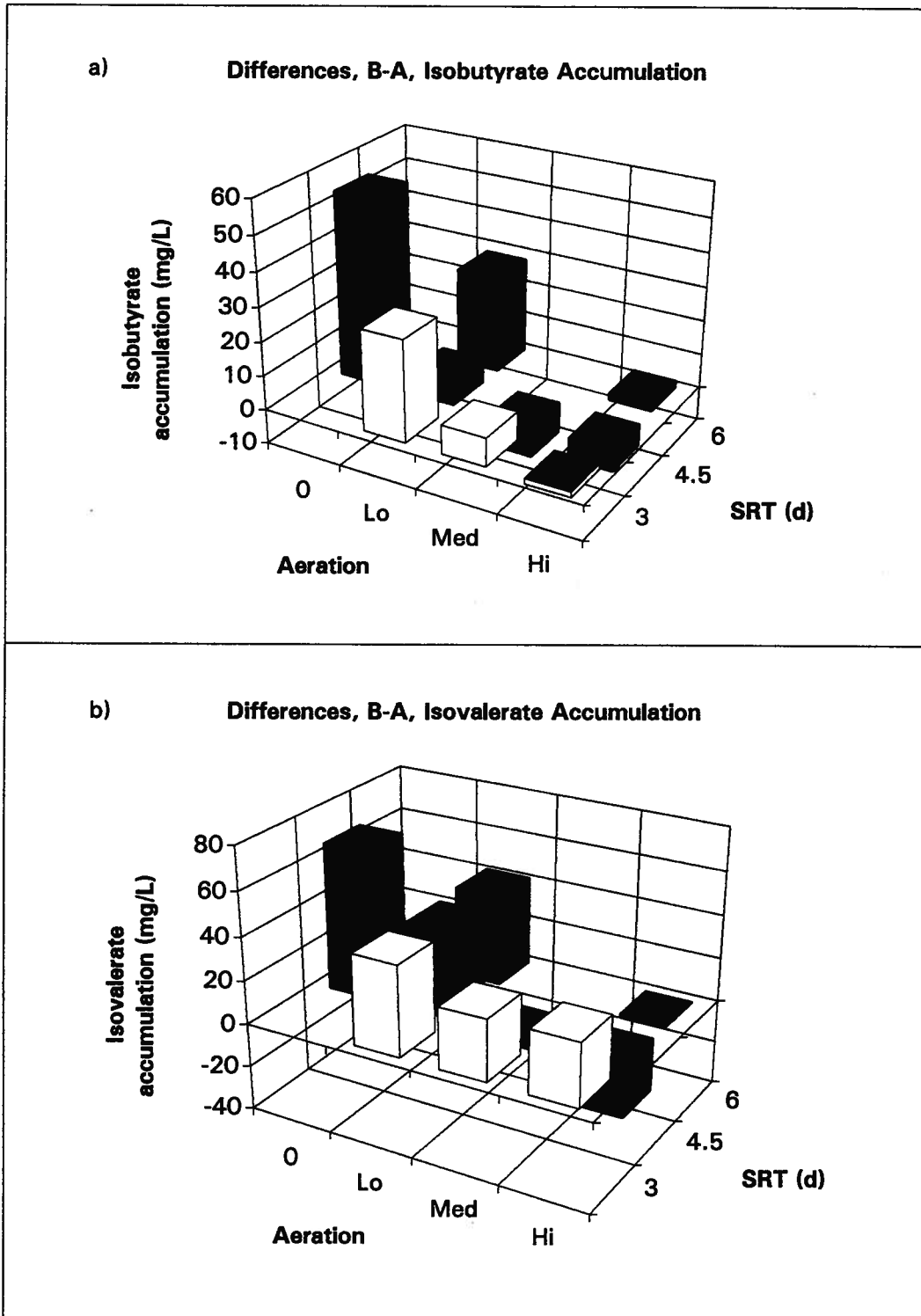


Figure 4.54 VFA accumulation normalized to their respective control values. a) Isobutyrate and b) isovalerate.

combination.

One important observation which must be considered from these graphs deals with duplication error. When both control and experimental bioreactors were operated under identical conditions (4.5d SRT, medium air flow) an interesting result appeared. With the exception of propionate, the experimental reactor produced less VFA than its corresponding control reactor (approximately 200 mg/L less acetate). This was unexpected, since both reactors were running under identical conditions. Presumably the effect was due to minor differences in temperature, aeration or steady state conditions within the bioreactor, but nothing more definitive can be stated at this time.

The propionate accumulation response was also different than that of acetate. Instead of a gradual increase in response, the propionate response was dramatic. The accumulation value of the majority of the experiments were low, until aeration had reached a reduced enough condition. Under these conditions (ie. low flow and true anaerobic) the propionate accumulation values were an order of magnitude higher when compared to the other combinations. These results suggested that a fermentative profile could be achieved and that a biochemical switch to propionate production was triggered when a sufficiently reduced environment was reached.

4.3.3.3 Kendall's Tau-b and Analysis of Variance of VFA Data

The appropriate application of a particular statistical procedure depends on how well a set of assumptions for that procedure are met. One important requirement of the data to be analyzed with an ANOVA model is that the data are independently distributed. The

independence assumption is often violated by data that are collected over a period of time. Each set of VFA data for any particular experimental run are composed of daily measurements taken over, typically, two SRTs. As can be seen from Figures 4. 45 and 4. 46, some of the acetate concentrations within the reactors never reached steady state (Runs 6,7 and 9), thus violating the assumption of independence. The method chosen to rectify this violation of independent distribution is to remove all data from experimental runs which violate this assumption and to perform a one-way ANOVA on the remaining data sets.

In order to assess dependence, correlation coefficients must be calculated. Correlation computes various measures of the strength of association between variables (ie. daily VFA production rates and days). The coefficient of correlation ranges from -1 to +1. Thus, the closer the coefficient is to +1 or -1, the stronger the linear relationship between the variables (eg. VFA

Table 4. 5 Matrix of Kendall's tau-b correlation coefficients for both acetate and propionate accumulation values versus time.

Run #	Kendall's tau-b		correlation coefficients		Operating conditions	
	Propionate Experimental (B) side	B side minus Control (A) side	Acetate Experimental (B) side	B side minus Control (A) side	Aeration	SRT (d)
1	0.778	0.833	0.833	0.556	Low	4.5
2	0.444	0.389	0.500	0.333	Low	3
3	0.111	0.056	0.500	-0.111	Low	6
4	-0.167	0.000	-0.111	-0.222	Medium	4.5
5	0.222	-0.111	-0.278	-0.389	Medium	3
6	0.661	0.333	0.667	0.167	High	3
7	-0.111	0.000	0.389	0.111	High	4.5
8	0.648	0.222	0.278	0.167	High	6
9	-0.056	0.056	0.000	0.056	High	4.5
10	0.167	-0.222	-0.444	-0.667	True anaerobic	4.5

production and time). On the other hand, as the coefficient approaches 0, the linear relationship between the variables becomes weaker, regardless of whether it is positive or negative.

Table 4. 5 shows the matrix of *Kendall's tau-b* correlation coefficients for all 10 experimental runs between both daily acetate and propionate accumulation values versus time. Included in this table are the calculated coefficients for the daily accumulation values of each run from the B side experimental reactor and the coefficients for the normalized data. This normalization was done by subtracting the control (A side) reactor's daily accumulation value from that of the experimental (B side) reactor. In the majority of runs, this form of transformation (ie. normalization) resulted in a weaker correlation coefficient (ie. coefficients closer to zero). All normalized experimental runs which had a calculated coefficient above 0.4 were removed (run 10 and 1 for the acetate and run 1 for the propionate data sets) and a one-way ANOVA was applied to the remaining data sets (Table 4. 6). For both acetate and propionate, the statistical decision is to reject the null hypothesis, concluding that there was a significant difference in the average daily accumulation values of these two VFA over the experimental runs analyzed. When runs 2 and 7 were removed from the acetate data set and runs 2, 3 and 10 were removed from the propionate data set and ANOVA was performed on the remaining runs, the statistical decision was to accept the null hypothesis, concluding that for acetate (runs 3, 4, 5, 6, 8, 9) and propionate (runs 4, 5, 6, 7, 8, 9) there was no difference among the average daily accumulation values of these two VFA. The conclusion, as tested by a one-way ANOVA model, was that VFA accumulation in runs 2 and 7 for acetate and runs 2, 3 and 10 for propionate were statistically different from the remaining runs.

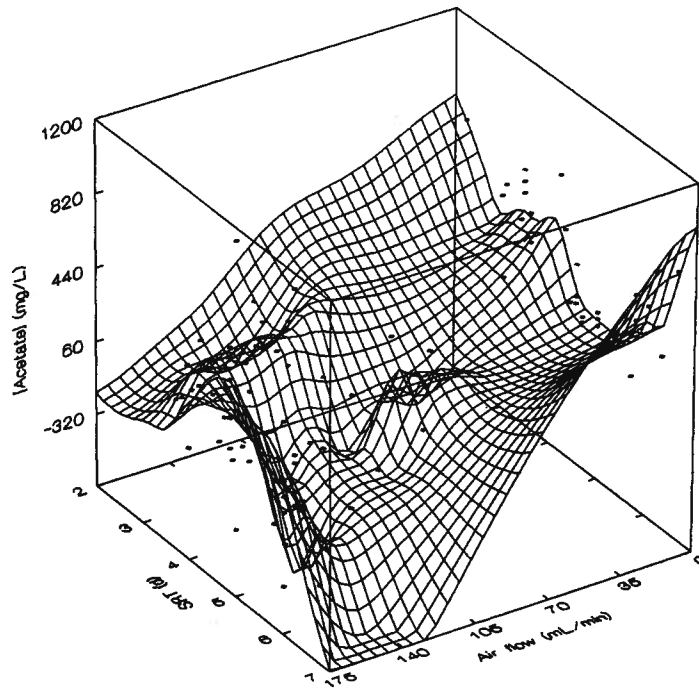
Table 4. 6 Analysis of variance table for acetate and propionate accumulation.

Compound tested	Runs deleted from data set	F _{statistic}	F _{critical}	P _{value}
		$\alpha = 0.05$		
Acetate	1,10	5.261	2.156	8.83×10^{-5}
	1,2,7,10	2.218	2.408	0.067
Propionate	1	41.188	2.069	6.95×10^{-24}
	1,2,3,10	1.303	2.408	0.278

4.3.3.4 Response Surface Plots of VFA Production in Pilot Scale TAD

The equation calculated in the previous section resulted in one accumulation value for each VFA per experiment. A useful method to display these data is to plot a 'response surface' for accumulation values for individual VFA, since SRT and aeration rates varied slightly over the course of each run. In this situation, every daily VFA accumulation value would have its own precise calculated SRT and aeration rate values. The response surface can then be based on more than 90 instead of only 9 discrete points. Figures 4. 55 and 4. 56 are response surface plots of individual daily VFA accumulation values versus SRT and aeration. Each point represents individual daily accumulation values from the B side normalized to the control condition (A side). This normalization was done by calculating an accumulation value for each day under the control condition and subtracting this from the accumulation value of each day calculated for the experimental condition. Distance weighted, least squares (DWLS) smoothing was used to fit the surface response to these data. DWLS smoothing fits a surface through a set of points by least squares. This method produces a locally weighted three dimensional surface using an algorithm developed by McLain (1974) and was used in Systat for Windows (Version 5.0). The discrete

a)



b)

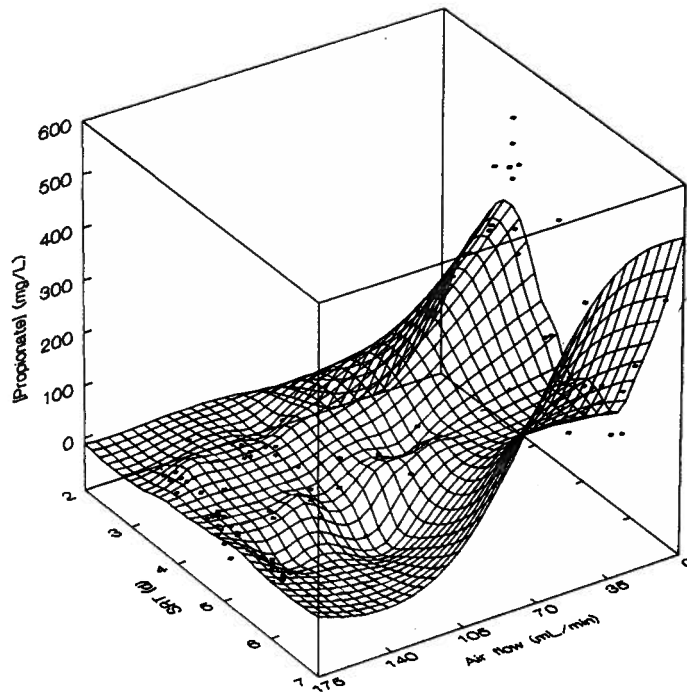
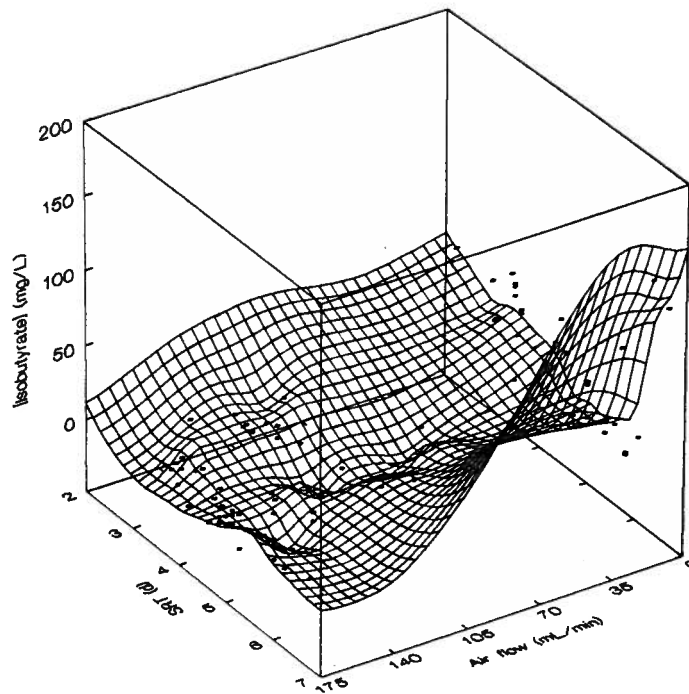


Figure 4.55 Response surface plots of daily VFA accumulation normalized to their respective control values for a) acetate and b) propionate.

a)



b)

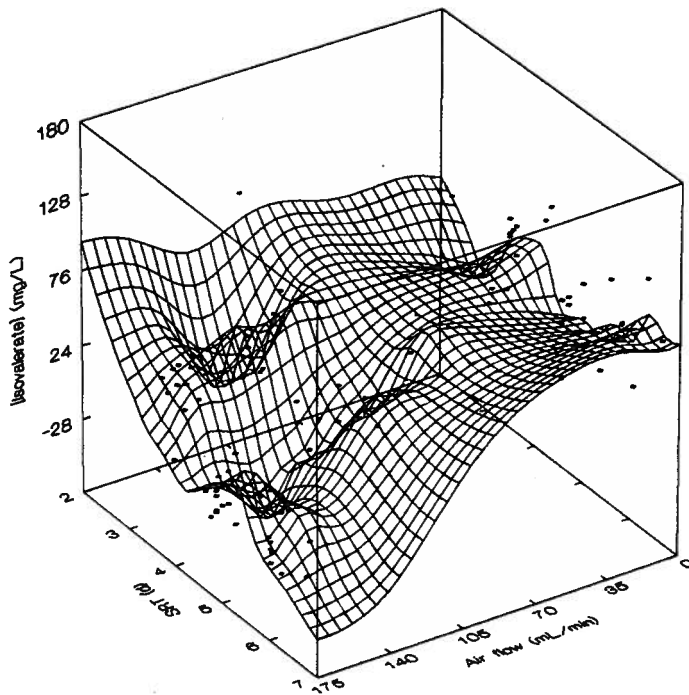


Figure 4.55 Response surface plots of daily VFA accumulation normalized to their respective control values for a) isobutyrate and b) isovalerate.

daily accumulation values for all runs as well as the fitted surface response are included in each graph.

It is clear from Figures 4. 55 and 4. 56 that, as SRT and aeration changed, there was no consistent response in VFA accumulation. The response of acetate and isovalerate seems to be more sensitive to SRT effects at higher aeration rates than propionate and isobutyrate (ie. Figure 4. 55b and 4. 56b). Unlike the acetate response at high air flows, propionate and isobutyrate seemed to be insensitive to changes in SRT. These two VFA are, however, sensitive to SRT at low air flow rates.

4.3.4 TAD Pilot Scale Process pH

In general, the process pH of a TAD system does not require control. The thermophilic operating temperatures suppress nitrification in the process (EPA, 1990). A typical TAD reactor with a feed sludge pH of 6.5 maintains a near neutral pH in the first reactor and often greater than a pH of 7.2. Figure 4. 57 shows pH profiles of the experimental side over all 10 runs. The control (A) side pH was relatively constant with an average pH of 7.2 (Figure 4. 58). However, the pH of the experimental (B) side seemed to decrease with decreasing aeration rates and SRTs. The average pH of the low flow and true anaerobic conditions was typically much lower than medium or high flow conditions. Under the low flow and 3 d SRT combination, the pH dropped

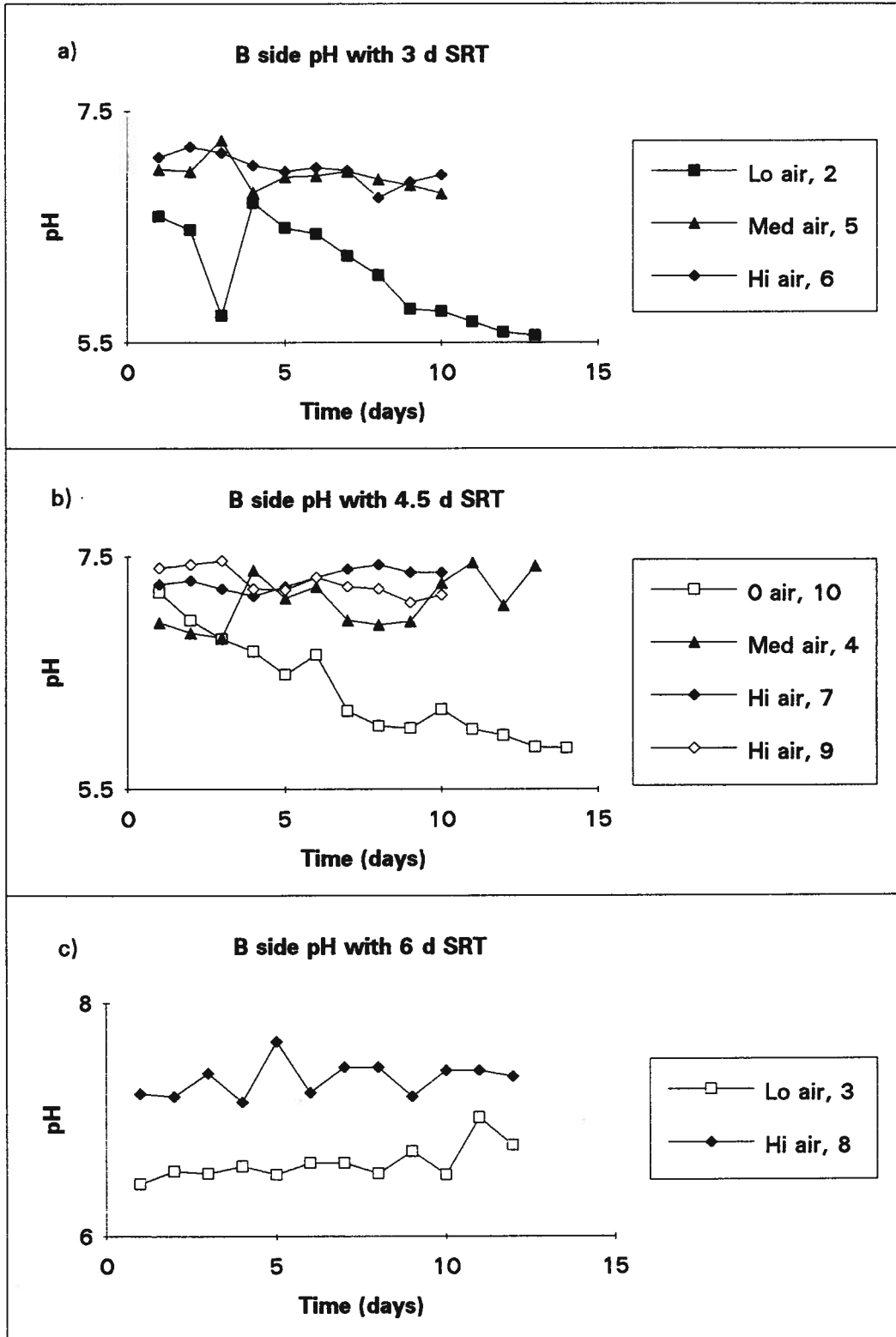


Figure 4.57 Experimental reactor (B side) pH values over time for all 10 runs (legend key: Symbol; aeration rate; run #).

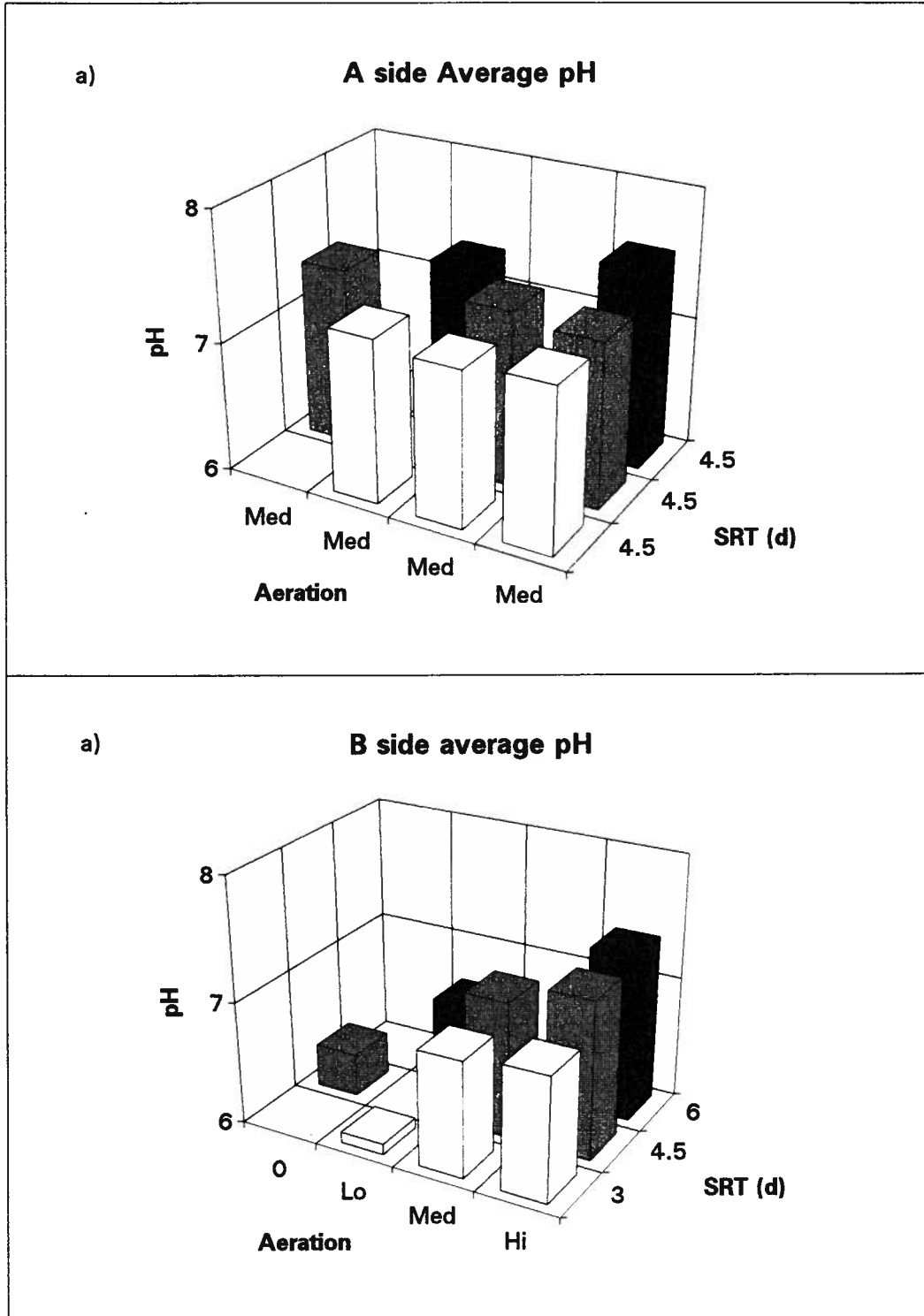


Figure 4.58 Average pH of a) A side and b) B side bioreactors

to as low as 5.5 by the end of the experiment (run 2). These results suggest that there is a point at which available oxygen becomes so limiting that production of acidic end products results in a substantial depression of the process pH.

4.3.5 Total and Volatile Solids Reduction of the Pilot Scale TAD Process

One important purpose of thermophilic aerobic digestion, like other sludge digestion processes, is the reduction of the total mass of sludge and the production of a stabilized final product suitable for disposal or reuse. Digestion processes reduce sludge mass mainly by converting carbonaceous substrates to gaseous end products that escape into the atmosphere. The percent solids reduction achievable by digestion varies, depending on the type of feed sludge and operating conditions employed in the treatment process. For example, volatile solids destruction can be influenced by process residence time, operating temperature, concentration of feed sludge and air flow rates. The two parameters investigated in this study were SRT and aeration. One of the most important directly measurable parameters in assessing digester performance or efficiency is the reduction in total and volatile sludge mass over a specified period of time. The process performance of the pilot scale TAD digesters was calculated utilizing a mass balance approach. This method can be expressed by the following equation, $\text{Change in mass} = \text{mass entering (primary sludge)} - \text{mass in effluent (TAD sludge)} \pm \text{net change within system}$

The determination of daily solids concentrations in both influent and effluent streams allowed the use of this mass balance technique. All solids added or removed from the system,

during any particular run, were used to calculate a single value for percent solids reduction for that run. The equation used for these calculations was as follows (Knezevic, 1993),

$$\% \text{ solids destroyed} = \frac{\sum_{i=1}^{n-1} C_i V_i - \sum_{e=2}^n C_e V_e - \Delta C_r V_r}{\sum_{i=1}^{n-1} C_i V_i} \cdot 100$$

where C_i = concentration of solids in influent (mg/L)

V_i = daily volume of influent sludge (L)

C_e = concentration of solids in effluent (mg/L)

V_e = daily volume of effluent (L)

C_r = concentration of solids in reactor (mg/L)

V_r = volume of reactor (L)

n = number of days in run (d)

Figures 4. 59 and 4. 60 summarize the total and volatile solids destruction rates in both the control (A side) and experimental (B side) reactors under all combinations of SRT and aeration tested. The control side destruction rates were relatively constant with the exception of the considerably higher rate for run number 2. The average A side volatile solids destruction was 20.8%, which was similar to that observed by Boulanger (1994) in the first stage of a TAD operating at a 3 d SRT under both an oxygen deprived and oxygen excess environment. In the experimental reactor (B side), the solids destruction seemed to change as aeration and SRT increased.

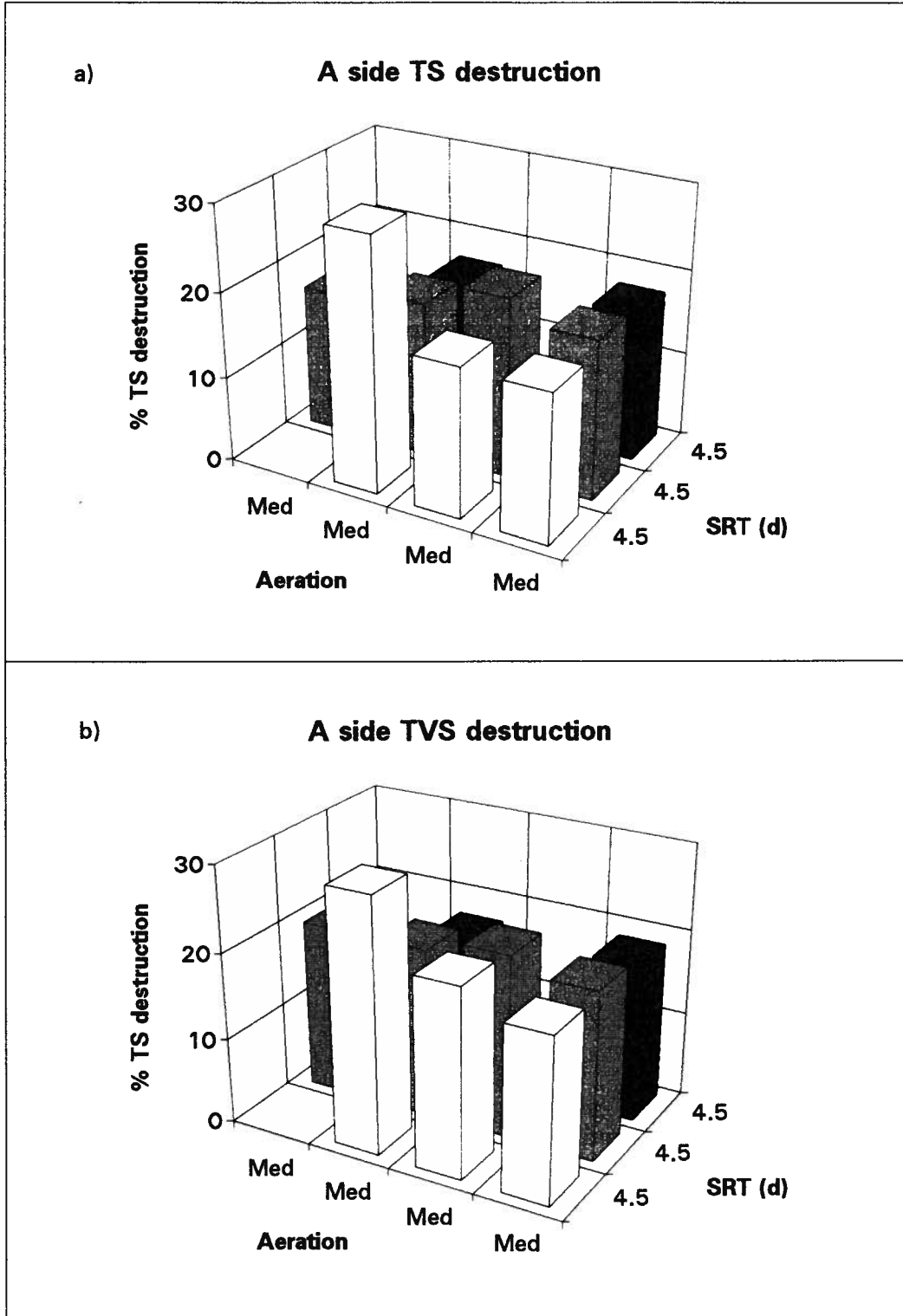


Figure 4.59 Total solids destruction capacity in pilot scale TAD experiments: A side (control) a) TS and b) TVS.

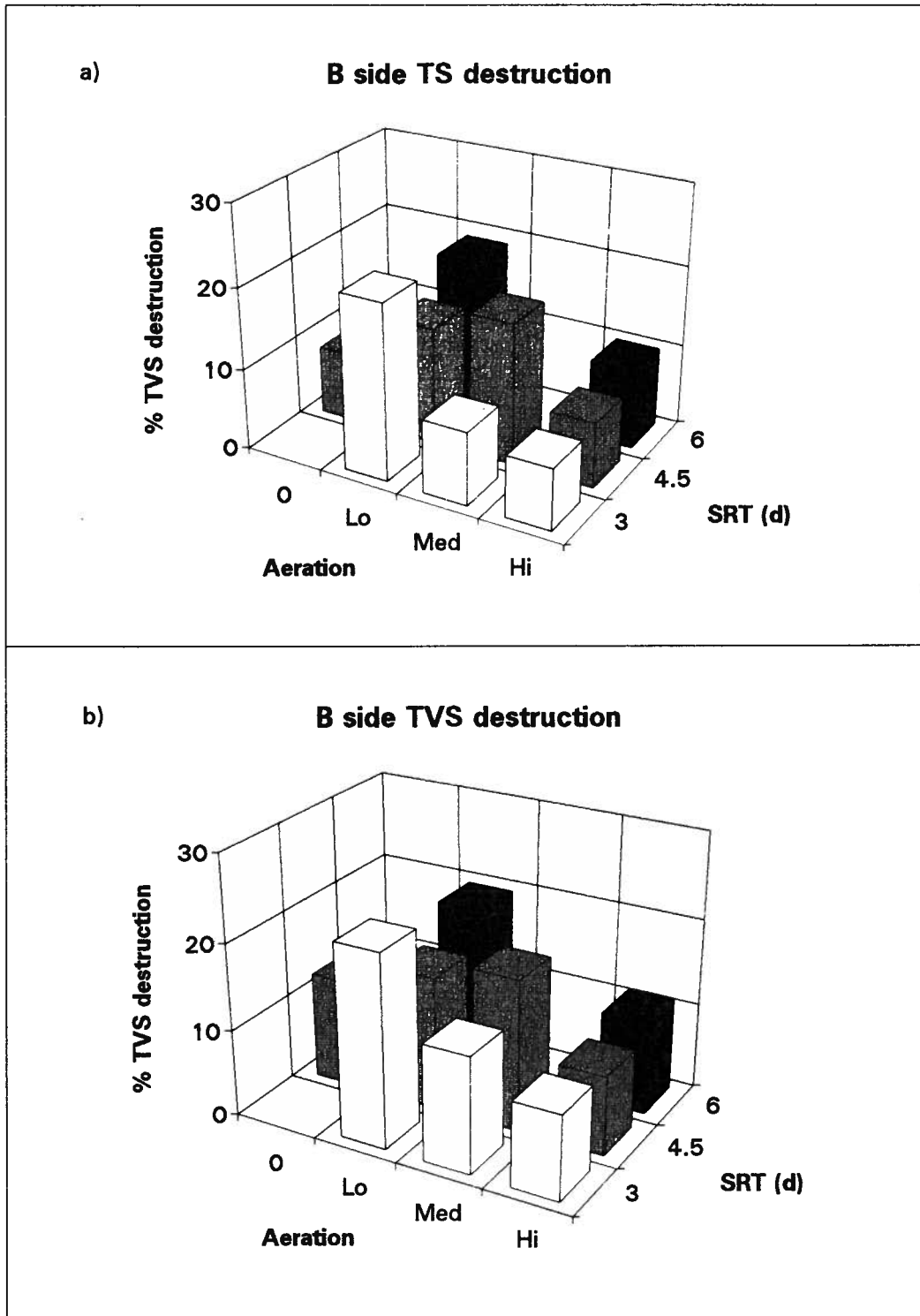
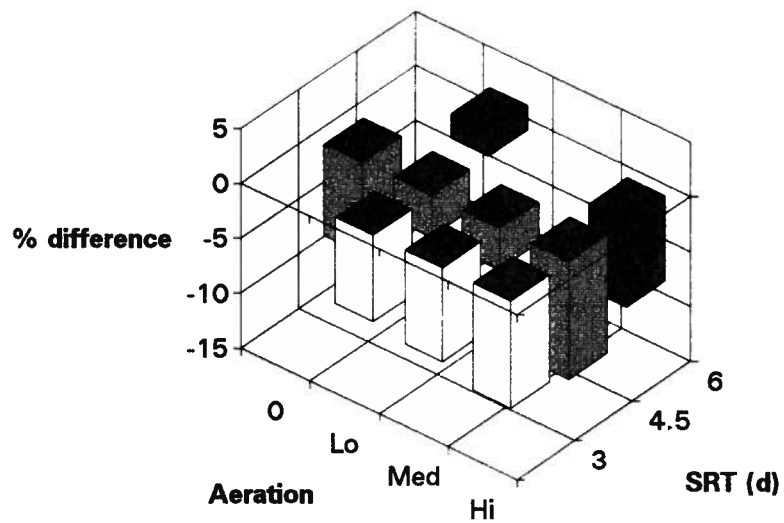


Figure 4.60 Total solids destruction capacity in pilot scale TAD experiments: B side (experimental) a) TS and b) TVS.

a) **Difference plot of TS destruction, B-A**



b) **Difference plot of TVS destruction, B-A**

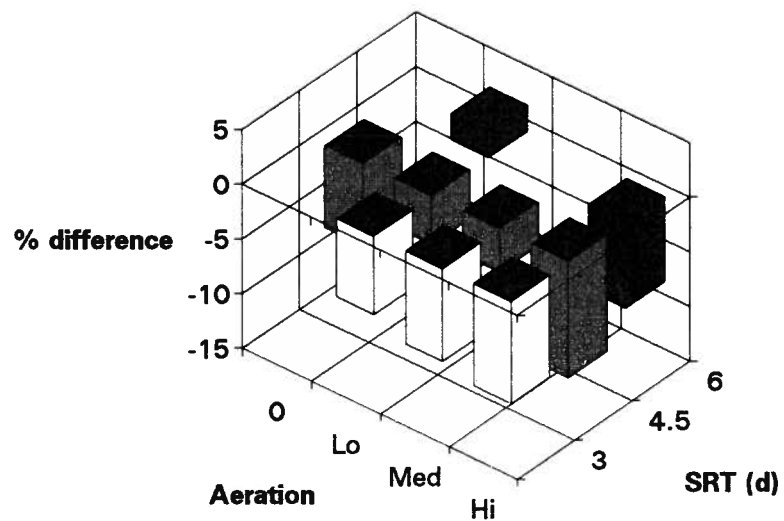


Figure 4.61 Total and volatile solids destruction capacities relative to their control values (ie, B-A): a) TS and b) TVS.

In order to properly compare the data between the runs conducted on the B side experimental reactor, the destruction results were normalized to the A side control values. This was done by subtracting the A side destruction rates from the B side destruction rates for each run combination. This normalization resulted in difference plots for both total and volatile solids destruction rates (Figure 4. 61). As can be seen from these plots, the 3 d SRT under all aeration rates resulted in a lower percent destruction than its corresponding control condition. Similarly, under high flow rates and all SRTs, the percent destruction was considerably lower than the corresponding controls. The only combination that resulted in a better solids destruction than the control condition was the low flow/6 d SRT combination.

One interesting observation is that the destruction rate resulting from a true fermentative condition (0 flow/4.5 d SRT) was similar to the destruction rate resulting from high air flows. Mason (1986) observed similar results under oxygen limited and oxygen sufficient conditions. Laboratory scale bioreactors fed with a suspension of yeast cells were used in that study. Aerobic thermophilic bacteria were obtained from an operating municipal thermophilic aerobic sludge digester. Comparison between the extent of solubilization/biodegradation under oxygen sufficient conditions showed that, for most residence times studies, considerably greater solids removal was possible under the oxygen limited set of conditions. There was no definite trend in the variation of solubilization/biodegradation with residence time.

4.3.5.1 Role of Enzymes in Solids Destruction

In all digestion processes, to achieve solids destruction, one group of organisms utilize other organisms as substrate (Mason, 1986). In order for this process to occur, the substrate bacteria first have to lose viability and subsequently lyse. In TAD processes, the substrate organisms are first subjected to a temperature shock and then to the effects of autolysis or to the action of lytic enzymes produced by the thermophilic organisms. Only after lysis has occurred, is it possible for the process culture to utilize the lytic products as substrate. In a study of bacteria isolated from a thermophilic aerobic sludge treatment process, Sonnleitner and Fiechter (1983) characterized a thermophilic population of bacteria of which over 90% were able to degrade starch. Extracellular enzyme production, particularly proteases and polysaccharases are well known features of species of *Bacillus* (Norris *et al.*, 1981).

Given the role of extracellular enzyme production in the solubilization and biodegradation process, which is the first step in the destruction of solids, the factors regulating their production must be considered. The results from this study indicate that the highest solids destructions occurred within a range of aeration; operation below or above this range resulted in a decrease in destruction capacity. These results suggest that optimal extracellular enzyme production may occur within this range of air flow rates. This belief is supported by the observation that amylase production is induced by oxygen limited conditions in a shake flask culture of thermophilic Bacilli derived from a TAD process (Grueninger *et al.*, 1984).

4.3.5.2 Solids Destruction Variability Discussion

There are two major sources of variability which must be considered when drawing conclusions from the solids data. The first source of variability was in the changing sludge feed source characteristics and composition. The A side bioreactor solids destruction (Figures 4. 59a and 4. 60a) varied considerably from a low of 17 to a high of 29%, even though the independent variables were maintained at their respective means (eg. 4.5 d SRT and medium air flow). Although there was a large variability in the A side bioreactor from one run to the next, the variability from one reactor to the other (A and B sides) was much smaller. When both reactors were operated under the same conditions of SRT and aeration, the A side bioreactor's total solids destruction was 21%, compared to a rate of 17.4% in the B side reactor.

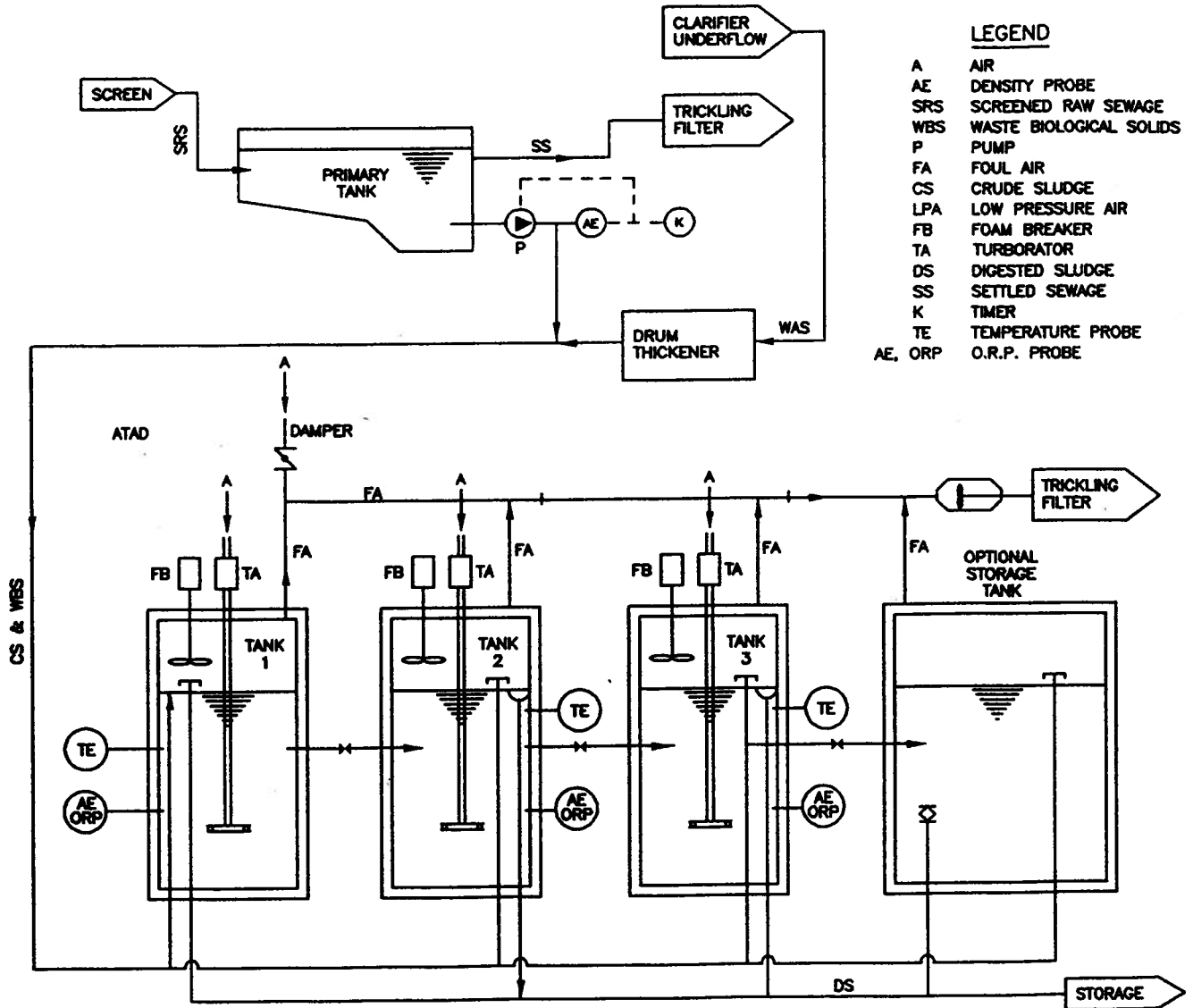
The second major source of variability only becomes evident when one of the experimental runs was replicated. Runs 7 and 9 are replicates of the high air flow rate and 4.5 d SRT combination. Although solids destruction in both the A and B side bioreactors were lower in run 7 when compared to run 9 (eg. 3-5% lower), the difference between the reactors for either runs 7 or 9 remained fairly constant. This suggests that although the measured values are different between runs, the overall effect is similar. These results indicate that comparison of data sets between runs are inappropriate under these pilot scale experiments. In order to decipher the effect of SRT and aeration on solids destruction capacity, the comparison must be made within each individual run.

4.3.6 Salmon Arm ATAD

In 1985, the District of Salmon Arm chose for their plant expansion a biological phosphorus removal facility and a high temperature aerobic digestion process. As part of the solids train, the original aerobic digester was retrofitted for autothermal thermophilic aerobic digestion. This was done by sectioning the existing rectangular digester into 3 unequally sized compartments, which operate in series and are fed a mixture of primary and waste activated sludges semicontinuously throughout the day by sludge pumps operated on timers. The aeration device chosen was a British Columbia developed aerator/mixer (Turborator). The schematic of the Salmon Arm ATAD process is shown in Figure 4. 62. Since this process utilized the same aeration device as the UBC pilot scale TAD process, valuable full scale VFA information could be obtained.

Obtaining VFA data from an operating full scale ATAD process was thought necessary to augment the existing data from the pilot scale process. Samples were taken over two visits to the sewage treatment plant (ie. once in March, 1993 and a second visit in May, 1994). Figure 4. 63 shows the daily operating temperature profiles of all three cells during each of the visits. The range of temperatures, of the first and second cells, were invariably much greater than the temperature range of the third cell, during both periods. Figure 4. 64 shows the VFA profile of the Salmon Arm ATAD process across the 3 cells.

During the 1994 visit, the propionate concentration in the first cell was almost as high as that of acetate. This somewhat unexpected result was probably due to the uncharacteristically



DISTRICT OF SALMON ARM – PROCESS SCHEMATIC

Figure 4. 62 District of Salmon Arm ATAD process schematic.

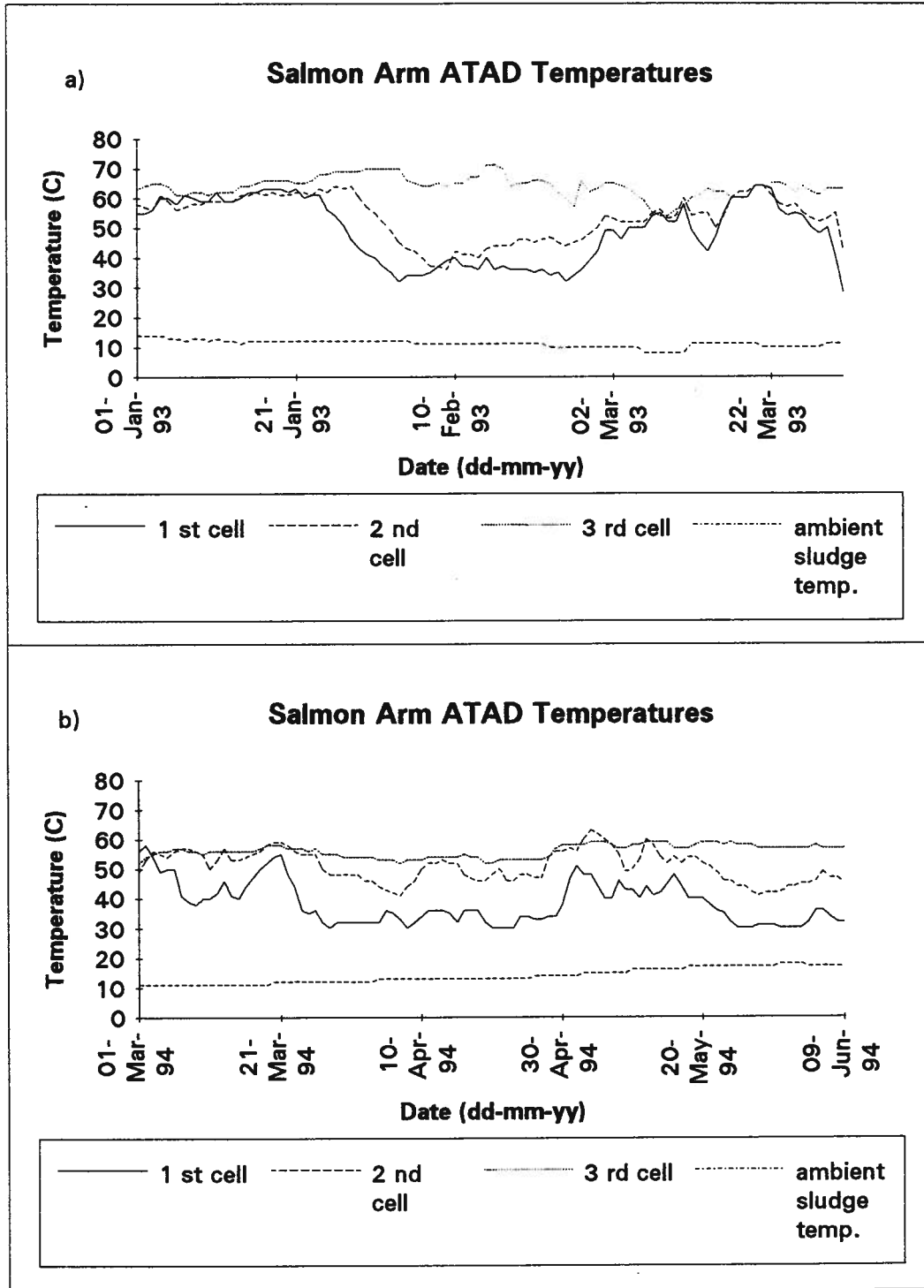


Figure 4.63 District of Salmon Arm ATAD reactor temperatures during the a) March, 1993 visit and b) May, 1994 visit.

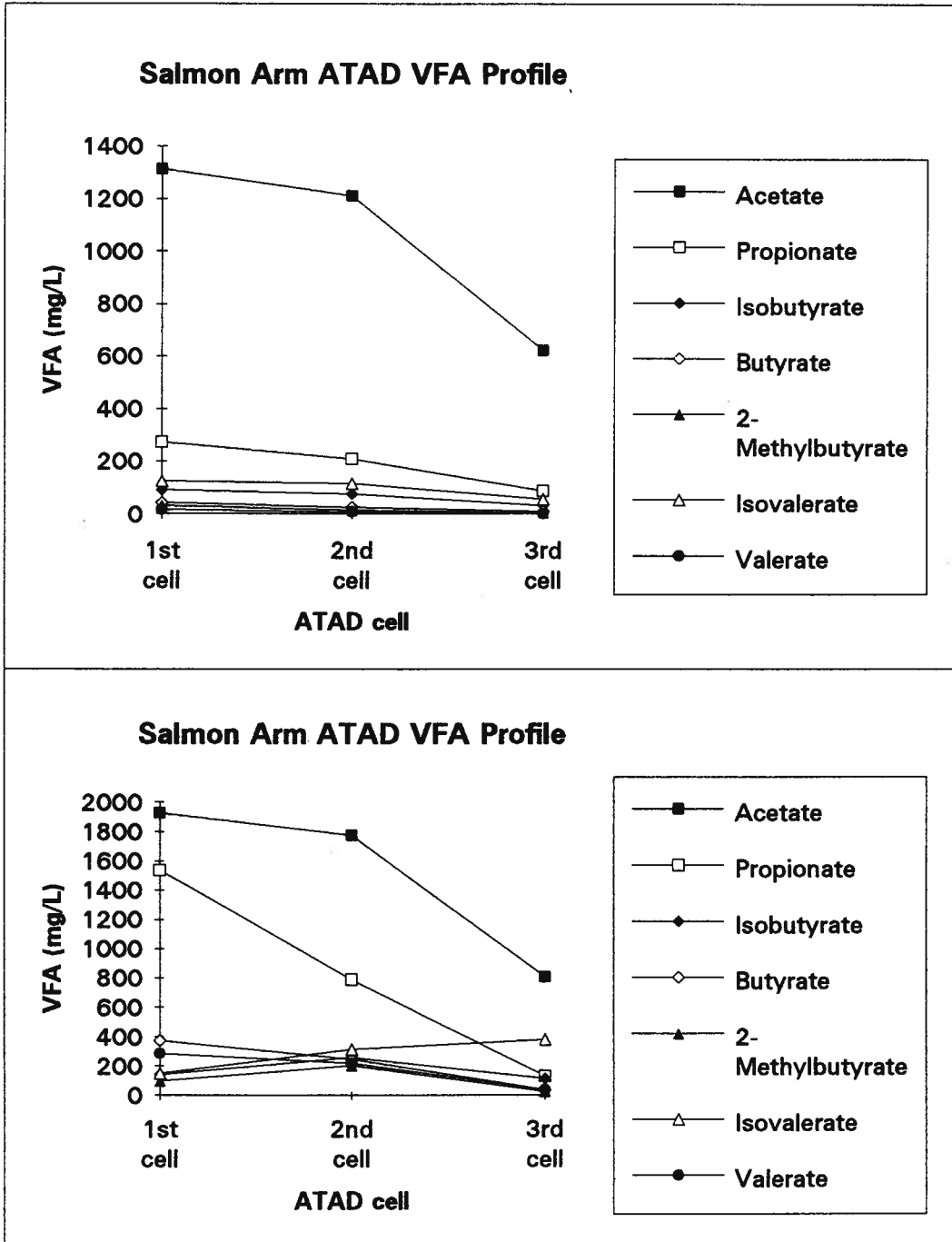


Figure 4.64 Salmon Arm ATAD VFA profile in all three cells during the a) March, 1993 visit and b) May, 1994 visit.

high solids concentration in the first cell of 9.4 %. During this time period, the sewage treatment plant operators were attempting to decrease the sludge blanket in their primary clarifiers by increasing the pumping rate of primary sludge into the first cell. This effectively increased the solid content in the first cell beyond the capacity of the Turborator aerator/mixer to maintain adequately mixed conditions. Visual inspection of the first cell confirmed that the contents, even though the Turborator was operating normally, were static. The inability of the Turborator to completely mix sludge at these concentrations would result in the majority of the bioreactor becoming anaerobic. Consequently, this fermentative environment would result in the VFA profile seen. Another indication that anaerobic conditions existed in the first cell was the lower pH of this cell, when compared to the others. A pH of 5.62 would be consistent with the accumulation of large amounts of fermentative acidic end products. The VFA profiles in the second and third cells were more in line with typical VFA profiles of TAD processes, since the concentration of the sludge had decreased sufficiently that the aerator could maintain completely mixed conditions. These profiles show that acetate was the predominant VFA produced in all 3 stages of the Salmon Arm ATAD facility and that higher VFA concentrations under full scale operation (up to 2,000 mg/L) could be achieved when compared to the pilot scale experiments.

5. Overview and Summary

5.1 Biochemical Model of Substrate Metabolism in TAD

To understand the biochemistry involved in substrate metabolism in TAD, one first must understand some basic fundamentals of bacterial energetics. An example of *E. coli* utilizing glucose is considered. This organism is a facultative anaerobe and as such can grow both aerobically and anaerobically by utilizing sugars, such as glucose, as a sole carbon and energy source (Gottschalk, 1986). The first step in glucose energy metabolism, irrespective of the presence or absence of oxygen, is the transport into the cell and its catabolism into pyruvate. It is in the further metabolism of pyruvate that differences between aerobic and anaerobic conditions occur.

In an aerobic environment, NADH generated during glycolysis, the TCA cycle and other associated reactions, is reoxidized by the operation of the respiratory chain (Ingeldew and Poole, 1984)(Figure 5. 1a). In the absence of oxygen, the respiratory chain is nonfunctional. The TCA cycle and pyruvate dehydrogenase reactions that generate large amounts of NADH are inoperative. However, NADH produced by glycolysis must be reoxidized to NAD^+ so that the glycolytic sequence can proceed (Figure 5. 1b). Therefore, the key issue in fermentation is the recycling of NADH by conversion of pyruvate to different fermentation products which can generate the oxidized form of NADH. Since the ratio of NADH to NAD^+ varies with the nature of the substrate, so must the composition of the mixture of fermentative end products. Thus, to achieve a proper fermentation balance, it is necessary to match the NADH produced with

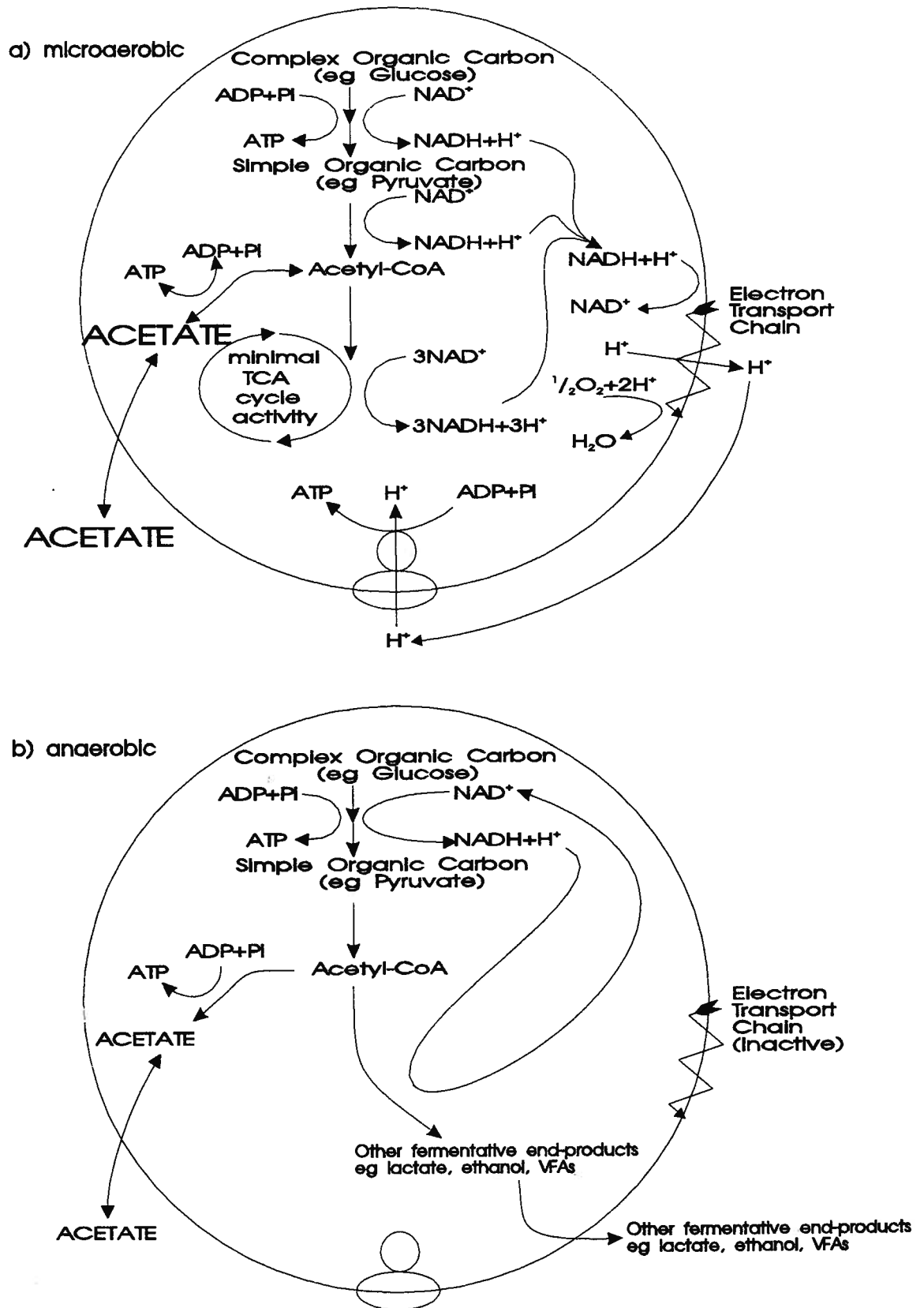


Figure 5.1 Biochemical model of acetate production in TAD under
 a) microaerobic and
 b) anaerobic conditions

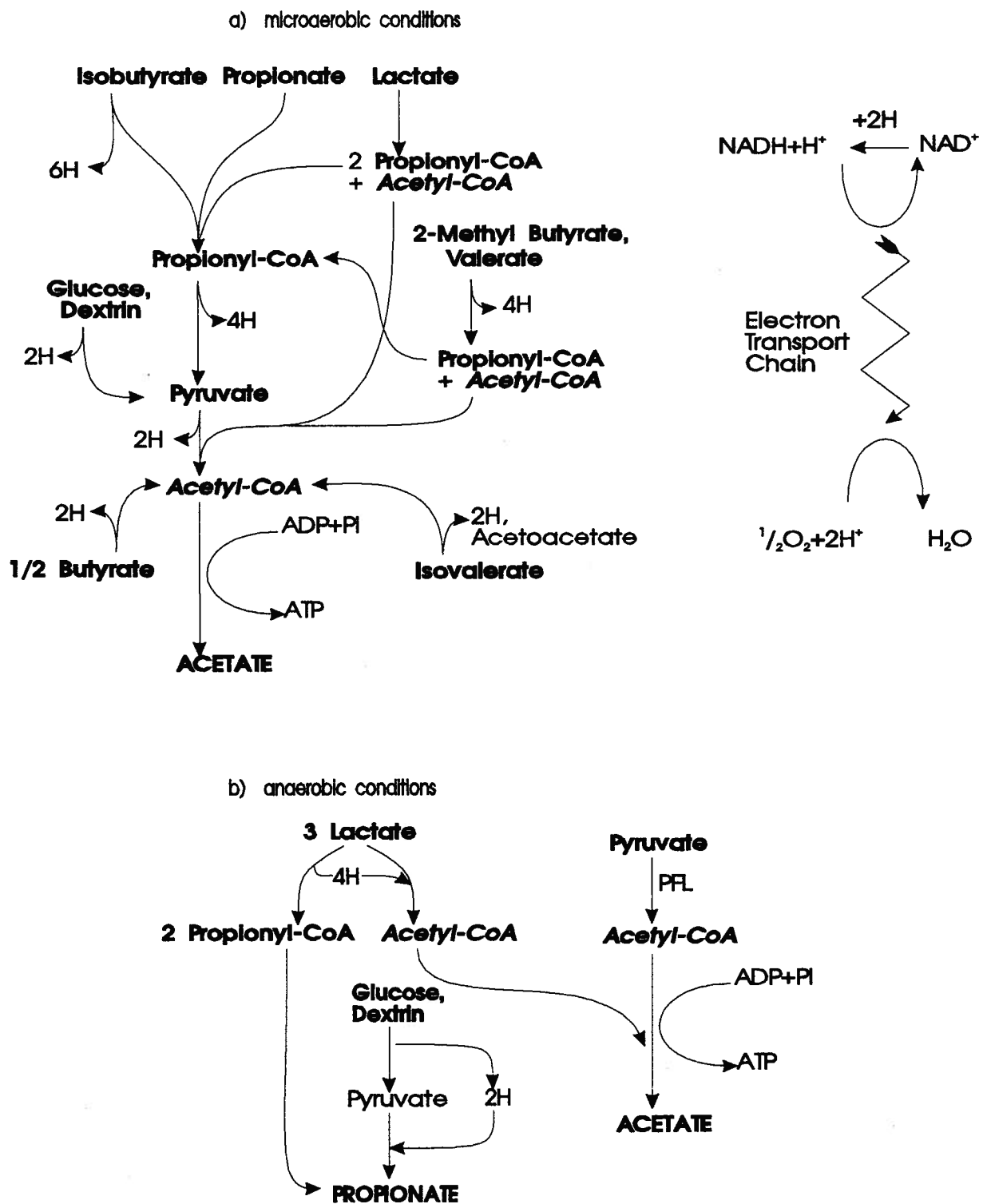


Figure 5.2 Summary of carbon flow from substrate addition experiments under a) microaerobic and b) anaerobic conditions

the NADH consumed by excretion of specific products. By varying the proportions of these products, it is possible to match the NADH produced from the oxidation of various substrates, thus achieving redox balance.

In the TAD batch studies, under fermentative conditions, the process bacteria must similarly achieve redox balance by diverting the catabolic flow of carbon to fermentative end products that will consume NADH (Clarke, 1989). Figure 5. 2b shows the flux of carbon as well as the redox balance for most of the substrates tested. The oxidation of substrates that result in the net accumulation of NAD^+ cannot proceed under fermentative conditions. Consequently, the substrates added remained in their unoxidized form and persisted in the medium (eg. 2-methylbutyrate, propionate, valerate, butyrate isovalerte, isobutyrate). The oxidation of substrates which can maintain redox balance can and did proceed under anaerobic conditions. Using the acrylate pathway (Gottschalk, 1986), lactate can be converted to propionate and acetate by the following equation,



The hydrogen evolved during oxidation of lactate to propionate was consumed by the production of acetate from lactate, thus recycling the reduced NADH to regenerate the oxidized form in order to maintain the net redox balance. The oxidation of glucose and dextrin could operate via a similar principal to lactate oxidation. NADH produced during glycolysis could be reoxidized by coupling this oxidation reaction to the reductive conversion of pyruvate to propionate.

In the TAD batch studies, under microaerobic conditions, the NADH produced during oxidation of substrates could be reoxidized by operation of the respiratory chain (Figure 5. 2a). Therefore, the flow of carbon may be uncoupled from the necessity to maintain redox balance via fermentative means. This uncoupling would presumably allow the organisms in a TAD process to achieve the global objective of maximizing ATP generation by increasing the flux of substrates to acetate (Majewski and Domach, 1990). Figure 5. 2a illustrates the net flow of carbon from most of the substrates examined. This figure shows that the majority of the oxidized substrates evolved hydrogen, in the form of reduced electron carrier, and acetate. These reduced electron carriers can then be reoxidized by operation of the electron transport chain, allowing the catabolism of the substrates added to proceed in an oxidative direction. Since the terminal electron acceptor, oxygen, was limited in a microaerobic environment, there would be a limited rate of transport of electrons down the respiratory chain, which would, in turn, limit the rate of oxidation of NADH to NAD^+ . This limitation would result in the accumulation of NADH.

The model suggests that the organisms can meet part of the NADH required for oxidative phosphorylation by operation of substrate level redox reactions and the remainder by operation of the TCA cycle to generate NADH. In response to this condition, the bacteria in a TAD process could preferentially shuttle acetyl-CoA through an acetyl-phosphate intermediate to acetate, transferring the high energy phosphate bond to ADP generating ATP. These reactions generate energy without the reduction of NAD^+ as would be the situation if acetyl-CoA is fed directly into the TCA cycle. Thus, by employing substrate level redox reactions and a limited

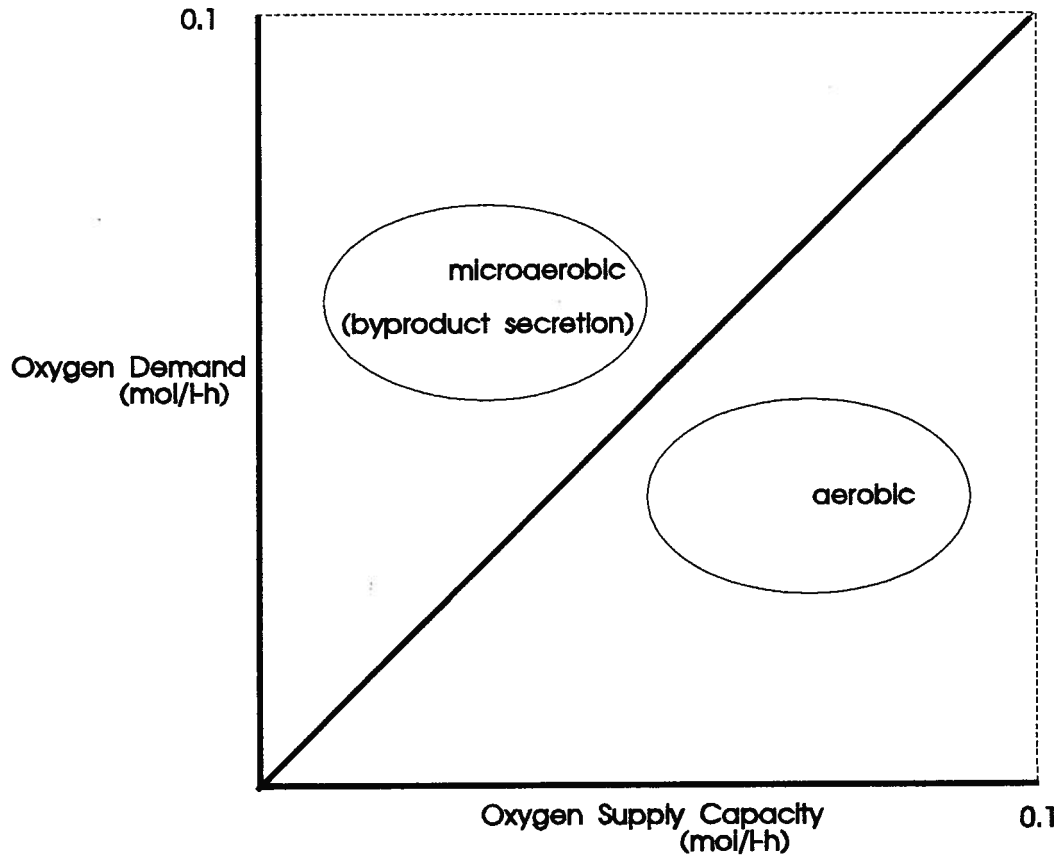


Figure 5.3 Comparison between oxygen demand and oxygen supply of any aerobically metabolizing culture

flow of carbon through the TCA cycle, bacteria in a TAD process could match the NADH produced to meet the limited capacity of the respiratory chain to transport electrons, while at the same time, maximizing ATP production by channeling excess acetyl-CoA to acetate. By incorporating this strategy these organisms can maximize ATP production in the O₂ limiting environment of a TAD process.

5.2 Acetate Accumulation Phenomenon in TAD

Microbial cultures are often oxygen limited. Oxygen limitations can occur because of limits in the capacity of the respiratory systems of the process microbes or because of the oxygenation limits of the external aeration devices. When oxygen becomes limiting, the substrate is only partially oxidized, which leads to byproduct evolution. This secretion of metabolic byproducts is coupled to the generation of energy while maintaining cellular redox balance.

Figure 5. 3 graphically shows the balance between oxygen demand and oxygen supply of an aerobically metabolizing biological system. If the aeration equipment can transfer more O₂ into solution than the biomass can utilize, as is the case for typical activated sludge systems which operate in a dissolved oxygen concentration range of 1-3 mg/L, aerobic conditions will prevail. However, if the oxygen demand of the system is higher than the aeration capacity to meet this requirement, microaerobic conditions will prevail (Figure 5. 3), which will be accompanied by byproduct secretion.

Mason (1986) investigated some effects of dissolved oxygen concentrations on VFA production in a laboratory scale bioreactor operated in a continuous flow mode. Aerobic thermophilic organisms were obtained from an operating waste sludge aerobic thermophilic digester. Bakers yeast was used as the sole biodegradable particulate carbon source. No carboxylic acid was detected under oxygen sufficient conditions. The amount of each VFA produced under oxygen limiting conditions varied with residence time, although, clearly, acetate was produced in the highest concentrations; at 2500 mg/L, it was 5 to 10 times higher than the next highest VFA measured (eg. propionate). In a batch study using the same process microbes and feed yeast cells, considerable amounts of VFA were produced and subsequently utilized (Hamer, 1987). These results showed an accumulation of up to 6000 mg/L acetate and 800 mg/L propionate (Figure 2. 3). Boulanger (1994) and Chu *et al.* (1994) also reported similar effects. The production of high concentrations of VFA was evident only when the O₂ demand was higher than the ability of the aeration equipment to meet this demand, resulting in a microaerobic environment. Similarly, when Kelly (1990) conducted experiments on VFA production in an autothermal thermophilic aerobic digester at Salmon Arm, B. C., Canada, the first stage digester produced up to 10,000 mg/L (personal communication).

VFA production has also been demonstrated in a number of aerobic thermophilic pretreatment processes. These pretreatment systems also provide thermophilic digestion and are normally incorporated in the process ahead of conventional anaerobic digestion. Baier and Zwiefelhofer (1991) reported VFA concentrations as high as 6081 mg/L after aerobic thermophilic pretreatment; 3315 mg/L was acetate. Zwiefelhofer (1985) reported much lower

VFA concentrations from a four year full scale demonstration project in Switzerland. Average VFA concentrations in the effluent of the AEROTHERM plant were 658 mg/L acetate, 75 mg/L propionate and 26 mg/L butyrate. As can be seen from the majority of these studies, acetate was cited as the most predominant VFA produced in ATAD. The results from this thesis are similar to those from the references that implicate acetate as the predominant VFA produced.

5.3 ¹⁴C-Acetate Label Experiment

Häner *et al.* (1994) examined the nature and fate of the organic fraction released during aerobic thermophilic biodegradation of microbial cells in a laboratory scale treatment system. The process culture was obtained from a full scale, aerobic thermophilic, sludge pretreatment plant in Switzerland. To simulate feed sludge, a culture of *Klebsiella pneumoniae* was used as the feed stock. In order to assess the dynamic pattern of the production and utilization of biodegradable intermediates, cultures were spiked with ¹⁴C-radiolabelled acetate. By 50 h into the experiment, the relative radioactivity associated with the acetate fraction was approaching zero, while the VFA concentration was approximately 500 mg/L. Since bacteria cannot distinguish between labeled and unlabelled acetate, the authors suggested that the production of acetate must have occurred concomitant with its utilization, which was a departure from previous models of acetate metabolism that suggested oxidative metabolism was somehow inhibited in the ATAD process (Hamer, 1987). This most recent model contained the first piece of direct evidence that recognizes acetate production can be concomitant with its oxidation, which is an important assertion made in this thesis. Although a major fraction of the added radiolabel was

converted to carbon dioxide, some was also incorporated into biomass and a significant fraction was either released or excreted into the culture supernatant in the form of unidentified, radiolabelled, dissolved organic carbon.

5.4 Acetate Production in Microorganisms

Aerobic production of acetic acid in *Escherichia coli* has been reported by a number of investigators. (Brown *et al.*, 1985; Curless *et al.*, 1989; Ishikawa and Shado, 1983; Pan *et al.*, 1987; Meyer *et al.*, 1984). The production of acetate by *E. coli* typically occurs at rapid growth rates and commences after a critical growth rate has been exceeded. Acetate production is a symptom of a change in cellular physiological state. The accumulation of acetate arises from an overflow phenomenon where acetyl-CoA is diverted from the TCA cycle to first acetyl-phosphate and then to acetate, which results in the production of one substrate level ATP per molecule of acetate.

Han *et al.* (1991) studied acetic acid formation in *E. coli* fermentation in a continuous culture system. They believed that the limited TCA cycle was responsible for the limited energy metabolism which resulted in acetic acid formation. Reichelt and Doelle (1971) looked at the influence of dissolved oxygen concentrations, on the enzyme phosphofructokinase, in *E. coli* K12 (ie. Pasteur effect). Acetic acid production did not occur above an oxygen partial pressure of 25.6 mm Hg, which was referred to as an excess oxygen state. Below this partial pressure,

acetate production increased progressively with an additional sharp increase below a partial pressure of 5.9 mm Hg.

MacDonald and Neway (1990) looked at the effects of media quality on the expression of human Interleukin-2 (IL-2) at high cell densities of fermenter cultures of *E. coli* K12. The dissolved oxygen concentrations were maintained at 40% of air saturation and cell densities at an OD₆₈₀ of 60 (ie. 2.5% solids) throughout the experiments. Induction of IL-2 accumulation at high culture optical densities was also accompanied by increased acetate accumulation in the culture medium of up to 300 mM (ie. 18 g/L). Their results suggested that the accumulation of diffusible inhibitors, such as acetate, during induction may be a significant factor limiting IL-2 expression in high density cultures.

Recently, stoichiometrically based methods have been developed for the study of optimal metabolic behavior (Fell and Small, 1986; Savinell and Palsson, 1992). In an attempt to develop a rationale for acetate secretion, Majewski and Domach (1990) examined acetate overflow metabolism in *E. coli* from the capacitated flow network viewpoint. This viewpoint focuses on the routing of metabolic flows (ie. fluxes) through a connected network where loads exist. Capacitation refers to the existence of constraints such that each reaction process within the network has a finite capacity. In other words, the total flow through the network has an upper limit defined by the limiting reaction process. The term load suggests that some metabolites are drained from the cycle at a rate dependent on growth rate. It was found that, when flux constraints are imposed at either the level of NADH turnover or the activity of a key TCA cycle enzyme (eg. α -ketoglutarate dehydrogenase), switching to acetate overflow was predicted. In

their analysis, maximization of ATP and GTP production was considered to be a global objective of *E. coli* metabolism.

In a study by Varma *et al.* (1993), a flux balance approach was used to determine optimal metabolic performance of *E. coli* under variable oxygen limitations. This method uses linear optimization to find optimal metabolic flux patterns with respect to cell growth. From computations, increased oxygen limitations were found to result in the secretion of acetate, formate and ethanol. The computed optimal growth under increasing O₂ limitation revealed 4 critical growth rates at which changes in the byproduct secretion patterns were concomitant with changes in metabolic pathway utilization. The redox potential was identified as a likely trigger that led to shifts in metabolic flows. Doelle *et al.* (1982) suggested that the accumulation of NADH switches carbon flow towards acetic acid. Their model suggested that a high glucose feed concentration represses enzymes in the TCA cycle and electron transport system. This condition resulted in a high accumulated intracellular NADH concentration, which ultimately switched carbon flow in the direction of acetate production. This model is consistent with the biochemical model of substrate metabolism in TAD. Under batch test conditions, in the microaerobic environment, the limited flow through the electron transport system, would result in a high concentration of accumulated intracellular NADH. The results from the batch experiments show that under this condition, carbon flow was predominantly in the production of acetate.

Harrison and Pirt (1967) investigated the influence of different dissolved oxygen concentrations on the metabolism and respiration of *Klebsiella aerogenes* by means of a

continuous flow culture technique. Different dissolved oxygen tensions were obtained by varying the partial pressure of oxygen in the gas phase. In the excess oxygen state, acetic acid was formed. The transition from excess oxygen to limiting oxygen concentrations was consistently marked by a large increase in volatile acid production. Within the limited oxygen state, which encompasses a range of oxygen tensions, the highest percentage of volatile acids as acetic acid occurred at higher oxygen supplies. With decreasing oxygen supply, formic acid production increased until it equaled the concentration of acetic acid. Thus, to maximize acetic acid production and to minimize other fermentative end products, there existed an optimal aeration rate.

Britten (1954) observed that acetate accumulated in the medium of well aerated cultures of *E. coli* growing on glucose. Hadjipetrow *et al.* (1964) observed similar results for *Aerobacter aerogenes*. The latter group showed that, following glucose exhaustion, oxidation of the accumulated acetate occurred. Coultate and Sundaram (1975) were the first to confirm similar observations with a thermophilic system (*Bacillus stearothermophilus*). They observed that a greater proportion of glucose carbon was left as acetate, at growth temperatures a few degrees higher than the optimal growth temperature. Their suggested reasoning was that the oxidative (eg. Tricarboxylic acid [TCA] cycle and the electron transport chain) and non-oxidative (eg. glycolysis) phases of glucose metabolism are less coordinated at these temperatures.

It is possible that the accumulation of acetate in a TAD process is at least partially due to an inefficient coordination or uncoupling between the oxidative and non-oxidative biochemical systems (ie. acetate overflow phenomenon), rather than simply due to pure fermentation. The

anomalies in the TAD results, that do not correlate to a fermentative model, may be explained within the context of the biochemical model presented in this thesis. This alternative process would account for the relatively high levels of acetate in the VFA samples. In general, the fermentation of sludge generates an acetate to total VFA ratio of 40% (Rabinowitz and Oldham, 1985; Fongsatitkul, 1991). In both TAD publications by Hamer (1987) and Mason *et al.* (1987), the acetate constituted 80 -90% of the total VFA. This raises the possibility that, in addition to fermentation, there are other processes that could contribute to the production of VFA (eg. acetate overflow phenomenon). This effect could also account for the sequential utilization of VFA and is consistent with known biochemical properties of pure cultures of bacteria.

Acetyl-CoA is converted to acetate via an acetyl phosphate intermediate. The successive reactions are catalyzed by 2 enzymes (Rose *et al.*, 1954; Fox and Rosemann, 1986). This pathway produces acetic acid and generates an ATP for every acetyl-CoA. Although only a single ATP is obtained, this level is significant when compared with a net gain of 2 ATP/glucose realized from the glycolytic pathway. When aerated cultures of *E. coli* grow on glucose, the majority of the acetyl-CoA is converted to acetate via this pathway, and only a minority is metabolized via the TCA cycle to give NADH (nicotinamide adenine dinucleotide) and CO₂. Thus, acetate accumulates in the medium in large amounts, even when oxygen is present, although aerobic cells growing on glucose produce negligible amounts of other fermentation end products. When the glucose supply is exhausted, there is a brief lag period, after which the accumulated acetate is taken back into the cells and respired (Kornberg, 1966; Maloy and Nunn, 1982). These observations are consistent with the results obtained from the batch experiments

conducted with TAD sludge. Specifically, that acetate accumulation was a transient phenomenon, and could be subsequently oxidized when the more complex substrates were exhausted.

Jenson and Michelson (1992) investigated carbon and energy metabolism of *atp* mutants of *Escherichia coli*. The membrane bound H⁺-ATPase plays a key role in free energy transduction of biological systems. The authors report how the carbon and energy metabolism changes in response to deletion of the ATP operon that encodes this enzyme. Compared with the wild type strain, the *atp* mutant strain produced twice as much acetate as a by-product and exhibited increased flow through the glycolytic pathway and TCA cycle. This leads to an increase in substrate level phosphorylation. They suggested that the *atp* mutants use uncoupled respiration in order to profit from increased substrate level phosphorylation.

It is possible that the mixed consortium of organisms in the TAD process behaves in a similar manner to *atp* mutants. These TAD organisms may support a similar process, to profit from increased substrate level phosphorylation. This would undoubtedly be advantageous (in terms of a competitive edge) under the oxygen limiting environment of many TAD processes.

The results of this thesis suggest that there may be a number of processes involved in the production of VFA. A degree of fermentation is probably occurring due to the highly reduced nature of part of the TAD process (eg. ORP values of below -250 mV). In addition, there is probably simultaneous aerobic oxidation of VFA, which is most likely limited by the aeration rate, even under the most reduced of conditions.

6. Conclusions and Recommendations

6.1 Conclusions

During the course of this research, a detailed examination of VFA metabolism in TAD was undertaken at both bench and pilot scale. A biochemical model was developed in an attempt to explain this phenomenon. Based on results of the research program, the following conclusions can be drawn:

1. A pilot scale TAD process was studied under a range of aeration rates and SRTs. VFA accumulation was found to be a function of both SRT and aeration. In general, as SRT and air flow rates decreased, VFA accumulation increased (specifically acetate and propionate). The maximum accumulation of acetate occurred under the 4.5d/true anaerobic combination.
2. Under microaerobic conditions, the major byproduct of TAD was acetate, which accounted for between 70 to 80% of the total VFA produced. This characteristic VFA pattern is different than the typical profiles of fermentation processes.
3. Under strict anaerobic conditions, the VFA profiles in the pilot scale TAD process were similar to fermentation type processes (ie. an even distribution of VFA between acetate and propionate). This anaerobic condition also stimulated the highest production of propionate.
4. ORP profiles were able to delineate between gross changes in aeration (eg. between microaerobic, transition and aerobic conditions).
5. Fourier analysis performed on the ORP data, of the pilot scale TAD process, indicated a cyclic nature with a period of 52.6 minutes. The approximate once/hour feeding regime created a 'shark tooth' pattern response in the ORP profile. Although insensitive to changes in aeration

rates between runs, the ORP signals were extremely sensitive to the addition of substrates (ie. primary sludge) within each run. These results suggest that absolute ORP values are not a suitably stringent state variable for monitoring and comparing reactor conditions between runs, under microaerobic conditions, although relative ORP values are quite sensitive at detecting slight changes in reactor conditions within a narrow time window.

6. In the TAD batch studies, the oxidation of substrates that require the net reduction of NAD^+ cannot proceed under anaerobic conditions. Consequently, the substrates added, under batch test conditions, remained in their unoxidized form and persisted in the medium (eg. 2-methylbutyrate, propionate, valerate, butyrate, isovalerate, isobutyrate). The pathways for oxidation of substrates to end products, which can maintain redox balance, under anaerobic conditions, can and does proceed (eg. lactate, pyruvate, glucose, dextrin).

7. In the TAD batch studies, under microaerobic conditions, the majority of the substrates examined were oxidized to an acetate intermediate. These results suggest that the NADH produced during oxidation of substrates can be reoxidized by operation of the respiratory chain. Therefore, the flow of carbon may be uncoupled from the necessity of maintaining redox balance via fermentative means.

8. In terms of fermenter sludge the highest production rate of total VFA occurred under anaerobic batch test conditions, at ambient room temperatures, when no primary sludge feed was added. However, by slightly aerating fermenter biomass it was possible to improve acetate production under high substrate addition rates (ie. primary sludge), when compared to strict fermentative conditions.

6.2 Recommendations

1) Traditional microbiological methodology has focused on monospecies cultures growing on defined media under stringently controlled conditions. Bull and Quale (1982) have argued that such approaches have resulted in a restricted perspective of microbial behavior in complex mixed culture environments. TAD, which is a process comprised of mixed cultures, is obviously more complex in many respects, than are monoculture systems. It is for this reason that the generation of definitive evidence for the existence and operation of specific biochemical pathways is an unrealistic goal when working with such a complex system. Alternatively, monospecies of representative isolates from TAD processes should be studied under stringently controlled conditions, in order to investigate the biochemistry involved in the phenomenon of acetate overflow.

2) Throughout the batch experiments, there was no direct evidence that the added substrates were metabolized to an acetate intermediate. In order to prove the carbon that originated from the added substrate accumulates in the acetate fraction, radiolabelled ^{14}C experiments should be conducted. In addition to the random labeling of substrates, radiolabel of specific carbons within a substrate should be done. These experiments should give insight into the biochemical pathways possibly involved in the conversion of substrate to acetate. For example, the labeling of the first, second or third carbons in propionate and the distribution pattern of label in the byproducts (eg. acetate, CO_2) should elucidate the specific pathways utilized by the organisms in the catabolism of propionate.

3) From an operational perspective, enhancing anaerobic digestion by phase separation is accomplished by providing more optimal environments for each major group of bacteria and their associated biochemical reactions. The two steps commonly cited as rate limiting in the process of anaerobic digestion are: 1) the hydrolysis of complex substrates and 2) methanogenesis (Kaspar and Wuhrman, 1978). In the second phase of two phase digestion, VFA and hydrogen are converted to methane and carbon dioxide by two coupled reactions mediated by acetogenic and methanogenic bacteria. Acetogenic bacteria convert the products of fermentation into acetate, formate and hydrogen, which act as substrates for methanogenic conversion to methane and carbon dioxide. The syntrophic coupling of many acetogenic reactions to methanogenic reactions is often critical, since the conversion of VFA to acetate and hydrogen is only thermodynamically favorable in the presence of methanogens; these organisms then utilize these products as substrate and can therefore maintain them at low concentrations. Consequently, the second phase reactor must provide a balance of optimal environments for both groups of organisms.

The methane derived from methanogenesis comes from two main sources. Approximately 70% is produced from acetate and the remaining 30% from CO_2 and H_2 (Metcalf and Eddy, 1991). Since methanogenic organisms can only utilize a very narrow range of substrates, a process that could potentially pretreat the sludge and provide a substrate (eg. acetate) amenable for methanogenesis would be invaluable. Such a process is referred to, in the literature, as a thermophilic prestage or dual digestion system (EPA, 1991). Zwiefelhofer (1985) claims that pretreatment of sludge, using thermophilic aerobic digestion prior to mesophilic

anaerobic digestion, through solubilization of particulate organic matter, allows short sludge ages in the anaerobic stage (10 d); insoluble, complex compounds are thus transformed into soluble byproducts of bacterial metabolism (eg. VFA) or readily degradable intermediate products of less complex structure, that serve as substrates that are more amenable to anaerobic digestion than untreated raw sludge.

According to the biochemical model proposed for acetate metabolism in TAD, the predominant byproduct is acetate. The acetate rich effluent from a thermophilic prestage process has the potential of uncoupling the syntrophic relationship that exists between methanogenic and acetogenic organisms by providing methanogens with a readily utilizable substrate, thus relieving the necessity to optimize the environmental conditions within the reactor for both of these groups of organisms. The feasibility of a thermophilic prestage process to provide acetate, in order to uncouple the syntrophic relationship between acetogenic and methanogenic reactions in the second phase of anaerobic digestion, requires more study. Specifically, if this syntrophic relation can be uncoupled, can methanogenic reactions be further optimized?

4) The effect of 2,4-dinitrophenol on VFA metabolism in TAD fed with primary sludge has been examined. These experiments have shown some interesting results. In addition to primary sludge, other substrates should be tested in terms of 2,4-dinitrophenol effects on metabolism (eg. propionate, butyrate, glucose, etc.).

5) The biochemical model of acetate production, under microaerobic conditions, in TAD sludge is not restricted to thermophilic temperatures or organisms. The majority of evidence that deals with this acetate 'overflow' anomaly comes from research done on mesophilic organisms. The

batch experiments conducted, as part of this thesis, with pilot scale fermenter sludge at mesophilic temperatures, under both anaerobic and microaerobic conditions, indicate that under high primary sludge addition rates, VFA production rates were improved under the latter condition. It would be a valuable follow up to this thesis to study the effect of slightly aerating pilot scale fermenter sludge on VFA production rates and composition, and their subsequent effects on the biological phosphorus removal process. This could be done at the UBC Bio-P pilot plant facility, which contains both control (traditional fermentation) and experimental (aerated fermentation) sides.

7. References

- Andrews J.F. and Kambhu K. (1973) Thermophilic aerobic digestion of organic solid wastes. EPA/670-2-73-061. August. NTIS PB 73-222396.
- A.P.H.A. (1989) *Standard Methods for the Examination of water and Wastewater*. 17 th. Edition. American Public Health Association, Washington, D.C.
- Appleton A.R. and Venosa A.D. (1986) Technology evaluation of the dual digestion process. *Journal of the Water Pollution Control Federation* 58, 764-773.
- Arvin E. and Kristensen G.H. (1985) Exchange of organics, phosphate and cations between sludge and water in biological phosphorus and nitrogen removal processes. *Water Science and Technology* 17, 147-162.
- Baier U., and Zwiefelhofer H.D. (1991) Sludge stabilization, effects of aerobic thermophilic pretreatment. *Water Environment and Technology* 3:1, 56-61.
- Barker H.A. (1981) Amino acid degradation by anaerobic bacteria. *Annual Review of Biochemistry* 99, 593-603.
- Barnard G.F. and Makhtar A. (1979) Mechanistic and stereochemical studies on the glycine reductase of *Clostridium sticklandii*. *European Journal of Biochemistry* 99, 593-603.
- Barnard J.L. (1984) Activated primary tanks for phosphorus removal. *Water SA*, 10, 121-126.
- Blanc F.C. and Molof A.H. (1973) Electrode potentials and electrolytic control in the anaerobic digestion process. *Journal of the Water Pollution Control Federation* 45, 655-666.
- Bomio M., Sonnleitner B. and Fiechter A. (1989) Growth and biocatalytic activities of aerobic thermophilic populations in sewage sludge. *Applied Microbiology and Biotechnology* 32, 356-362.
- Boulanger, M (1994) *The effect of air supply on solids destruction and nutrient balances for thermophilic aerobic digesters*. MA Sc thesis, Civil Engineering, UBC
- Boyd R.F. (1984) *General Microbiology*. Times Mirror/Mosby College Publishing, Toronto.
- Britten R.J. (1954) Extracellular metabolic products of *Escherichia coli* during rapid growth. *Science* 119, 578.

Brock, T.D. 1986. *Thermophiles, General, Molecular and Applied Microbiology*. Ed. T.D. Brock Wiley Interscience Publication, New York.

Brown S.W., Meyer H. and Fiecher A. (1985) Continuous production of human interferon with *Escherichia coli* and continuous cell lysis in a two stage chemostat. *Applied Microbiology and Biotechnology* 23, 5-9.

Chu A., Mavinic D.S., Kelly H.G. and Ramey W.D. (1994) Volatile fatty acid production in thermophilic aerobic digestion of sludge. *Water Research* 28, 1513-1522.

Clark D.P. (1989) The fermentation pathways of *Escherichia coli*. *FEMS Microbiology Reviews* 63, 223-234.

Cohen-Bazaire G., Cohen G.N. and Prevot A.R. (1948) Nature et Mode de Formation des acides Volatiles dans les Cultures de Quelques Bacteries Anaerobies Proteolitiques du group de *Clostridium sporogenes*. Formation par la reaction Stickland les Acides Isobutyrique, Isovalerianique et Valerianique Optiquement Actif. *Annales de l'Institut Pasteur* 75, 291-309.

Comeau Y., Hall K.J., Hancock R.E.W., Oldham W.K. (1986) Biochemical model for biological enhanced phosphorus removal. *Water Research* 20, 1511-1521.

Comeau Y., Hall K.J., Rabinowitz B. and Oldham W.K. (1987) Phosphorus release and uptake in enhanced biological phosphorus removal from wastewater. *Journal of the Water Pollution Control Federation* 59, 707-715.

Conrad R.S., Massey L.K. and Sokatch J.R. (1974) D- and L-isoleucine metabolism and regulation of their pathways in *Pseudomonas putida*. *Journal of Bacteriology* 118, 103-111.

Conradt H, Hohmann-Berger M., Hohmann H.P., Blanschowski H.P. and Knappe J. (1984) Pyruvate formate lyase (inactive form) and pyruvate formate lyase activating enzyme of *Escherichia coli*. Isolation and structural properties. *Archives of Biochemistry and Biophysics* 288, 133-142.

Cooley, J.W. and Tukey J.W. (1965) An algorithm for the machine computation of complex Fourier series. *Mathematical Computation* 19, 297-301.

Cooney, C.L., Wang D.I.C. and Mateles R.I. (1968) Measurement of heat evolution and correction with oxygen consumption during microbial growth. *Biotechnology Engineering* 11, 269.

Coultate T.P. and Sundaram T.K. (1975) Energetics of *Bacillus stearothermophilus* growth: Molar growth yield and temperature growth effects on growth efficiencies. *Journal of Bacteriology* 121, 55-64.

Curless C.E., Forrer P.P., Mann M.B., Fenton D.M. and Tsai L.B. (1989) Chemostat study of kinetics of human lymphokine synthesis in recombinant *Escherichia coli*. *Biotechnology and Bioengineering* 34, 415-421.

DeLaval Separation Company. (1978) The Licom System. In *Manufacturers bulletin*, Poughkeepsie, NY.

Dirasian H.A., Molof A.H. and Borchardt J.A. (1963) Electrode potentials developed during sludge digestion. *Journal of the Water Pollution Control Federation* 55, 424.

Doelle H.W., Ewing K.N. and Hollywood N.W. (1982) Regulation of glucose metabolism in bacterial systems. *Advances in Biochemical Engineering* 23, 1-35.

Duysens, L.M.N. and Amesz J. (1957) Fluorescence spectrophotometry of reduced phosphopyridine nucleotide in intact cells in the near ultraviolet and visible region. *Biochimica Biophysica Acta* 24, 19-26.

Elefsioniotis P. (1992) *The effect of operational and environmental parameters on the acid phase anaerobic digestion of primary sludge*. PhD thesis, University of British Columbia, Department of Civil Engineering, Vancouver, Canada.

Elsden S.R. and Hilton M.G. (1978) Volatile acid production from threonine, valine, leucine and isoleucine. *Archives of Microbiology* 117, 165-172.

Environmental Protection Agency. (1990) *Autothermal Thermophilic Aerobic Digestion of Municipal Wastewater Sludges*. EPA/625/10-90/007 September, Cincinnati, OH.

Fell D.A., and Small J.A. (1986) Fat synthesis in adipose tissue. An examination of stoichiometric constraints. *Biochemistry Journal* 238, 781-786.

Fongsatitkul P. (1991) *A modified two-phase anaerobic digestion process (UASB-UASB) for sewage sludge*. PhD thesis, University of British Columbia

Fox P. and Pohland F.G. (1994) Anaerobic treatment fundamentals: Substrate specificity during phase separation. *Water Environment Research* 66, 716-724.

Fox D.K. and Rosemann S. (1986) Isolation and characterization of homogenous acetate kinase from *Salmonella typhimurium* and *Escherichia coli*. *Journal of Biological Chemistry* 261, 13487-13497.

Fuchs, H. and Fuchs L. (1980) Exotherme, Aerob-thermophile Stabilization Verfahrenstechnik, Energiehaushalt, Hygiene Korrespondenz Abwasser 27, Jahrgang4, 241.

- Frese H., Robinson L. and Kelly H.G. (1993) Biological Sludge Thickening Using a Rotating Drum Thickener. *Proceedings, BCW&W Annual Conference*, Vernon, April.
- Ghosh S., Conrad J.R. and Klass D.L. (1975) Anaerobic acidogenesis of wastewater sludge. *Journal of the Water Pollution Control Federation* 47, 30-44.
- Ghosh S. and Pohland F.G. (1974) Kinetics of substrate assimilation and product formation in anaerobic digestion. *Journal of the Water Pollution Control Federation* 46, 748-759.
- Gibb A.J., Kelly H.G., Koch F.A. and Oldham W.K. (1989) A full scale evaluation of biological phosphorus removal using a fixed and suspended growth combination. *Proceedings from the 12th International Symposium on Wastewater Treatment*, Montreal, Canada, November 20,21.
- Gottschalk G. (1986) *Bacterial Metabolism*. 2nd edition. Springer-Verlag, New York.
- Gray C.T., Wimpenny J.W.T., Hughes D.E. and Mossman M.R. (1966) Regulation of metabolism in bacteria. I. Structural and functional changes in *Escherichia coli* associated with shifts between the aerobic and anaerobic states. *Biochemistry and Biophysics Acta* 117, 22-32.
- Gruenginger H., Sonnleitner B., and Fiechter A. (1984) Bacterial diversity in thermophilic aerobic sewage sludge III. A source of organisms producing heat stable industrially useful enzymes, eg. α -amylase. *Applied Microbiology and Biotechnology* 19, 414-421.
- Guarnaschelli C. and Elstone K.G. (1987) *A New Turbine Aerator for Treating Wastewaters*. 12th. Annual Seminar of the Alberta Water and Wastewater Operators Association, Banff, March.
- Hadjipetrow L.P., Gerritis J.P., Teulings F.A.G. and Stouthamer A.H. (1964) Relation between energy production and growth of *Aerobacter aerogenes*. *Journal of General Microbiology* 65, 57-68.
- Hamer G. (1987) Fundamental aspects of aerobic thermophilic biodegradation. In *Treatment of Sewage: Thermophilic aerobic digestion and processing requirements for land filling*. (ed. A.M. Bruce, F. Colin and P.J. Newman). Elsevier Applied Science, pp. 2-19.
- Han K., Lim H.C. and Hong J. (1992) Acetic acid formation in *Escherichia coli* fermentation. *Biotechnology and Bioengineering* 39, 663-671.
- Häner A., Mason C.A. and Hamer G. (1994) Death and lysis during aerobic thermophilic sludge treatment: Characterization of recalcitrant products. *Water Research* 28, 863-869.
- Harper S.R. and Pohland F.G. (1986) Recent developments in hydrogen management during anaerobic biological wastewater treatment. *Biotechnology and Bioengineering* 28, 585-602.

- Harrison D.E.F. and Pirt S.J. (1967) The influence of dissolved oxygen concentration on the respiration and glucose metabolism of *Klebsiella aerogenes* during growth. *Journal of General Microbiology* 46, 193-211.
- Harrison, D.E.F. and Chance B. (1970) Fluorometric technique for monitoring changes in the level of reduced nicotinamide nucleotides in continuous cultures of microorganisms. *Applied Microbiology* 19, 446-450.
- Hoffman, B. and L.S. Crauer (1979) Liquid composting of dairy cow waste. National Dairy Housing Conference press ASAIE SP-01-73:429.
- Ingeldew W.J. and Poole R.K. (1984) The respiratory pathways of *Escherichia coli*. *Microbiological Reviews* 48, 222-271.
- Ishikawa Y., Shado M. (1983) Calorimetric analysis of *Escherichia coli* in continuous culture. *Biotechnology and Bioengineering* 25, 1817-1827.
- Jensen P.R. and Michelson O. (1992) Carbon and energy metabolism of *atp* mutants of *Escherichia coli*. *Journal of Bacteriology* 174, 7635-7641.
- Jewell, W.J. *et al.* (1982) Autoheated aerobic thermophilic digestion with air aeration. EPA project No. R804636, MERL Report, NTIS PB-82-196908.
- Kambhu, K. and Andrews J.F. (1969) Aerobic thermophilic process for the biological treatment of waste simulated studies. *Journal of the Water Pollution Control Federation* 41, R127-R141.
- Kaspar H.F. and Wuhrmann K. (1978) Kinetic parameters and relative turnover of some important catabolic reactions in digesting sludge. *Applied and Environmental Microbiology* 36, 1-7.
- Keller, U., Berninger I. (1984) Aerob-thermophile Schlammfermentation mit anschließender Faulung. Vergleichende Pilotversuche in der ARA Altenrhein. Dokumentationsdienst Bundesamt für Umweltschutz, Bern, 1-65.
- Kelly, H.G. (1987) *Bio-P Treatment Using a Fixed and Suspended Growth Combination: A Demonstration Project. Proceedings Annual Conference, Environmental Engineering Division/ASCE, Orlando, Fl., July, pp. 79-91.*
- Kelly H.G. (1990) *Demonstration of an Improved Digestion Process for Municipal Sludges: Supply and Services Contract KE405-8-6575/01-SE, Ottawa, Canada.*

- Kelly, H.G., Melcer H. and Mavinic D.S. (1993) Autothermal thermophilic aerobic digestion of municipal sludges: A one year, full scale demonstration project. *Water Environment Research* 65, 849-861.
- Knappe J. and Schmitt T. (1976) A novel reaction of S-adenosyl-L-methionine correlated with the activation of pyruvate formate lyase. *Biochemistry and Biophysics Research Communication* 71, 1110-1117.
- Knezevic, Z. (1993) *Enhanced Anaerobic Digestion of Combined Wastewater Sludges Through Solubilization of Waste Activated Sludge*. MSc. Thesis, University of British Columbia.
- Koch F.A., Oldham W.K. and Wang N.Z. (1988) ORP as a tool for monitoring and control of bionutrient removal systems. Proceedings from CSCE-ASCE, National Conference on Environmental Engineering, Vancouver, B.C., Canada, July 13-15, 162-170.
- Koers D.A. and Mavinic D.S. (1977) Aerobic digestion of waste activated sludge at low temperatures. *Journal of the Water Pollution Control Federation* 49, 460-468.
- Kornberg H.L. (1966) Anaplerotic sequences and their role in metabolism. *Essays in Biochemistry* 2, 1-31.
- Kelly, H.G., 1989. Aerobic thermophilic digestion or liquid composting of municipal sludges. In Proc. Conference of Am. Soc. Civil Eng., Austin, Texas, p. 650.
- Lehninger A.L. (1982) *Principles of Biochemistry*. Ed. S. Anderson, J. Fox. Worth Publishing, New York, N.Y.
- Majewski R.A. and Domach M.M. (1990) Simple constrained optimization. View of acetate overflow in *Escherichia coli*. *Biotechnology and Bioengineering* 35, 732-738.
- Maloy S.R. and Nunn W.D. (1982) Genetic regulation of the glyoxylate shunt in *Escherichia coli*. K12. *Journal of Bacteriology* 149, 173-180.
- Mason C.A. (1986) *Microbial Death, Lysis and 'Cryptic' Growth: Fundamental and Applied Aspects*. Diss. ETH No. 8150 Swiss Federal Institute of Technology, Zurich.
- Mason C.A., Hamer G., Fleishman T. and Lang C. (1987) Aerobic thermophilic biodegradation of microbial cells. *Applied Microbiology and Biotechnology* 25, 568-576.
- Massey L.K., Sokatch J.R. and Conrad R.S. (1976) Branched chain amino acid catabolism in bacteria. *Bacteriological Reviews* 40, 42-54.

- Mastch, L.C. and R.F. Drnevich. 1977. Autothermal aerobic digestion. *Journal of the Water Pollution Control Federation* 49, 196-301.
- Mayer H., Leist C. and Fiechter A. (1984) Acetate formation on continuous culture of *Escherichia coli K12DI* on defined and complex media. *Journal of Biotechnology* 1, 335-358.
- Mclain, D.H. (1974) Drawing contours from arbitrary data points. *The Computer Journal* 17, 318-324.
- MacDonald H.L. and Neway J.O. (1990) Effects of medium quality on the expression of human interleukin-2 at high cell density in fermenter cultures of *Escherichia coli K12*. *Applied and Environmental Microbiology* 56, 640-645.
- Metcalf and Eddy Inc. (1991) *Wastewater Engineering: Treatment, Disposal and Reuse*. 3rd Edition. McGraw-Hill, New York, N.Y.
- Messenger J.R. (1990) *An evaluation of the autothermal thermophilic aerobic digester in dual digestion*. PhD thesis, Department of Civil Engineering, University of Cape Town, South Africa.
- Morrison K. (1988) *An assessment of the feasibility of biological phosphorus removal in Canadian wastewater treatment plants*. M.A. Sc. thesis, University of British Columbia, Vancouver, Canada.
- Nesbit J.B. (1969) Phosphorus removal, the state of the art. *Journal of the Water Pollution Control Federation* 41, 701-713.
- Norris J.G., Berkely, R.C.N., Logan, N.A. and O'Donnell, A.G. (1981) The genera *Bacillus* and *Sporolactobacillus*. In *The Prokaryotes- a Handbook on Habitats, Isolation and Identification of Bacteria*. Ed. Starr M.P., Stolp H., Trüper H.G., Balonus A., Schegel H.G. Springer, Berlin, Heidelberg, New York, 1711.
- Novak, J.T. and Carlson D.A. (1970) The Kinetics of long chain fatty acid degradation. *Journal of the Water Pollution Control Federation* 42, 1932-1943.
- Oldham W.K., Abraham K., Dawson R.N. and McGeachie G. (1992) Primary sludge fermentation design and optimization for biological nutrient removal plants. In *European Conference on Nutrient Removal from Wastewater*, 1-4, September. University of Leeds, U.K.
- Pan J.G., Rhee J.S. and Lebeault J.M. (1987) Physiological constraints in increasing biomass concentration of *Escherichia coli B* in fed batch culture. *Biotechnology letters* 9, 89-94.

Pascal M.C., Chippaux M., Abou-Jaoude A., Blaschkowski H.P. and Knappe J. (1981) Mutants of *Escherichia coli* K-12 with defects in anaerobic pyruvate metabolism. *Journal of General Microbiology* 124, 35-42.

Pecher A., Blaschkowski H.P., Knappe K and Bock A. (1982) Expression of pyruvate formate lyase of *Escherichia coli* from the cloned structural gene. *Archives of Microbiology* 132, 365-371.

Popel, F. and Ohnmacht C. (1972) Thermophilic bacterial oxidation of highly concentrated substrates. *Water Research* 6, 807-815.

Potgeiter D.J.J. and Evans B.W. (1983) Biochemical changes associated with luxury phosphorus uptake in a modified phoredox activated sludge system. *Water Science and Technology* 15, 105-115.

Rabinowitz, B. and W.K. Oldham. 1985. The use of primary sludge fermentation in the enhanced biological phosphorus removal process. From *New Directions and Research in Waste Treatment and Residuals Management*. June 23-28, UBC, 347-363.

Reichelt J.L. and Doelle H.W. (1971) The influence of dissolved oxygen concentration on phosphofructokinase and the glucose metabolism of *Escherichia coli* K12. *Antoine van Leeuwenhoek* 37, 497-506.

Rose I.A., Grunberg-Manago M., Korey S.R. and Ochoa S. (1954) Enzymatic phosphorylation of acetate. *Journal of Biological Chemistry* 211, 737-756.

Savinell J.M. and Palsson B.O. (1992) Network analysis of intermediary metabolism using linear optimization. I. Development of mathematical formalism. *Journal of Theoretical Biology* 154, 421-454.

Schaak K.P., Boschet A.F., Chevalier D., Kerlain F. and Senelier Y. (1985) Efficiency of existing biological treatment plants against phosphorus pollution. *Tech. Sci. Municip.* 80, 73-181.

Shimadzu (1987) *TOC-500 Brief Instruction Manual*. Publication number CM 393-066B, Shimadzu Corporation, Tokyo, Japan.

Siebritz F.P., Ekama G.A. and Marais G.v.R. (1983) A parametric model for biological excess phosphorus removal. *Water Science and Technology* 15, 127-152.

Smith M.W. and Neidhardt F.C. (1983) Proteins induced by anaerobiosis in *Escherichia coli*. *Journal of Bacteriology* 154, 336-343.

Sokatch J.R. (1969) *Bacterial Physiology and Metabolism*. Academic press, London and New York.

Sokatch J.R., Sanders L.E. and Marshall V.P. (1968) Oxidation of methylmalonate semialdehyde to propionyl-Coenzyme A in *Pseudomonas aeruginosa* grown on valine. *Journal of Biological Chemistry* 243, 2500-2506.

Sonnleitner B. and Fiechter A. (1983) Bacterial diversity in thermophilic aerobic sewage sludge II. Types of organisms and their capacities. *European Journal of Applied Microbiology and Biotechnology* 18, 174-180.

Spencer M.E. and Guest J.R. (1985) Transcription analysis of the *sucAB*, *aceEF* and *ipd* genes in *Escherichia coli*. *Mol. Gen. Genet.* 200, 145-154.

Supelco. (1989) *Separating Aqueous Carboxylic Acids (C₂ to C₆) at ppm Concentrations*. Bulletin 751-E, Supelco Inc., Bellefonte, PA.

Stryer L. (1975) *Biochemistry*. W.H. Freeman and Company, San Francisco.

Terwilleger, A.R. and Craver L.S. (1975) Liquid composting applied to agricultural wastes. In *Managing Livestock Wastes: Proceedings of the Third International Symposium on Livestock Wastes*, 501.

Thiele J.H. and Zeikus J.G. (1988) Substrate shuttle process for high rate biomethanation. From *Anaerobic Digestion*, Pergamon press, Oxford.

Toerien D.F., Gerber A., Lotter L.H. and Cloete T.E. (1990) Enhanced biological phosphorus removal in the activated sludge systems. In *Advances in Microbial Ecology*. (ed. K.C. Marshall) Vol. II Plenum press, N.Y., pp. 173-229.

Varma A., Boesch B.W., Palsson B.O. (1993) Stoichiometric interpretation of *Escherichia coli* glucose catabolism under various oxygenation rates. *Applied and Environmental Microbiology* 59/8, 2465-2473.

Weichers H.N.S. (1983) Phosphate removal in biological treatment processes. *Water Science and Technology* 15, 1-382.

Wentzell M.C., Loewenthal R.E., Ekama G.A. and Marais G.v.R. (1988) Enhanced phosphate organism cultures in activated sludge systems- Part 1: Enhanced culture development. *Water SA* 14, 81-92.

Wilkinson T.G. and Hamer G. (1979) The microbial oxidation of mixtures of methanol, phenol, acetone and isopropanol with reference to effluent purification. *Journal of Chemical Technology and Biotechnology* 29, 56-67.

Wolin M.J. (1976) Interactions hydrogen producing bacteria and methane producing species. In *Microbial Production and Utilization of Gasses*. H.G. Schlegel, G. Gottschalk and N. Pfenny (ed.), Germany, 141-150.

Windholz, M. (1983) *The Merck Index, an Encyclopedia of Chemicals, Drugs and Biologicals*. Merck and Company Inc., Rahway, New Jersey.

Woodley, R.A. (1961) A study of aerobic biochemical oxidation of primary sewage sludge at mesophilic and thermophilic temperatures. Masters Thesis, Purdue University.

Zabrisky, D.W. and Humphrey A E. (1978) Estimation of biomass concentration by measuring culture fluorescence. *Applied and Environmental Microbiology* 35, 336-363.

Zwifelhofer H.D. (1985) Aerobic thermophilic/ anaerobic mesophilic two stage sewage sludge treatment: Practical experiences in Switzerland. *Conservation and Recycling* 8/1, 2, 285-301.

Appendix A: Batch Test Results

Figure A1.1	Batch Test 1: [VFA] v time (0% primary feed)	198
Figure A1.2	Batch Test 1: [VFA] v time (10% primary feed)	198
Figure A1.3	Batch Test 1: [VFA] v time (20% primary feed)	198
Figure A1.4	Batch Test 1: [VFA] v time (30% primary feed)	199
Figure A2.1	Batch Test 2: [VFA], TOC, pH v time (micro-aerobic control w 300 mL A sludge)	199
Figure A2.2	Batch Test 2: [VFA], TOC, pH v time (micro-aerobic w lactic acid and 300 mL A side sludge)	199
Figure A3.1	Batch Test 2: [VFA], TOC, pH v time (anaerobic w lactic acid and 1 L A side sludge)	200
Figure A3.2	Batch Test 2: [VFA], TOC, pH v time (anaerobic control w 1 L A side sludge)	200
Figure A4.1	Batch Test 4: [VFA], TOC v time (micro-aerobic control w 300 mL A side sludge)	200
Figure A4.2	Batch Test 4: [VFA], TOC v time (micro-aerobic w propionate and 300 mL A side sludge)	201
Figure A4.3	Batch Test 4: [VFA], TOC v time (anaerobic w propionate and 1 L A side sludge)	201
Figure A4.4	Batch Test 4: [VFA], TOC v time (anaerobic control w 1 L A side sludge)	201
Figure A5.1	Batch Test 5: [VFA], TOC, pH v time (micro-aerobic w/o cyanide, 300 mL A side and 30 mL primary sludge)	202
Figure A5.2	Batch Test 5: [VFA], TOC, pH v time (micro-aerobic w cyanide, 300 mL A side and 30 mL primary sludge)	202
Figure A5.3	Batch Test 5: [VFA], TOC, pH v time (anaerobic w/o cyanide, 1 L A side and 100 mL primary sludge)	202

Figure A5.4	Batch Test 5: [VFA], TOC, pH v time (anaerobic w cyanide, 1 L A side and 100 mL primary sludge)	203
Figure A6.1	Batch Test 6: [VFA], TOC, pH, ORP v time (anaerobic control w 1 L A side sludge)	204
Figure A6.2	Batch Test 6: [VFA], TOC, pH, ORP v time (anaerobic w valerate add'n + 1 L A side sludge)	204
Figure A6.3	Batch Test 6: [VFA], TOC, pH, ORP v time (anaerobic w iso-valerate add'n + 1 L A side sludge)	205
Figure A6.4	Batch Test 6: [VFA], TOC, pH, ORP v time (anaerobic w butyrate add'n + 1 L A side sludge)	205
Figure A6.5	Batch Test 6: [VFA], TOC, pH, ORP v time (anaerobic w methylbutyrate add'n + 1 L A side sludge)	206
Figure A6.6	Batch Test 6: [VFA], TOC, pH, ORP v time (micro-aerobic control w 300 mL A side sludge)	206
Figure A6.7	Batch Test 6: [VFA], TOC, pH, ORP v time (micro-aerobic w valerate add'n + 300 mL A side sludge)	207
Figure A6.8	Batch Test 6: [VFA], TOC, pH, ORP v time (micro-aerobic w iso-valerate add'n + 300 mL A side sludge)	207
Figure A6.9	Batch Test 6: [VFA], TOC, pH, ORP v time (micro-aerobic w butyrate add'n + 300 mL A side sludge)	208
Figure A6.10	Batch Test 6: [VFA], TOC, pH, ORP v time (micro-aerobic w methylbutyrate add'n + 300 mL A side sludge)	208
Figure A7.1	Batch Test 7: [VFA], TOC, pH, ORP v time (anaerobic control w 1 L A side sludge)	209
Figure A7.2	Batch Test 7: [VFA], TOC, pH, ORP v time (anaerobic w linoleic acid add'n + 1 L A side sludge)	209
Figure A7.3	Batch Test 7: [VFA], TOC, pH, ORP v time (anaerobic w glucose add'n + 1 L A side sludge)	210
Figure A7.4	Batch Test 7: [VFA], TOC, pH, ORP v time (anaerobic w dextrin add'n + 1 L A side sludge)	210

Figure A7.5	Batch Test 7: [VFA], TOC, pH, ORP v time (anaerobic w peptone add'n + 1 L A side sludge)	211
Figure A7.6	Batch Test 7: [VFA], TOC, pH, ORP v time (micro-aerobic control w 300 mL A side sludge)	211
Figure A7.7	Batch Test 7: [VFA], TOC, pH, ORP v time (micro-aerobic w linoleic acid add'n + 300 mL A side sludge)	212
Figure A7.8	Batch Test 7: [VFA], TOC, pH, ORP v time (micro-aerobic w glucose add'n + 300 mL A side sludge)	212
Figure A7.9	Batch Test 7: [VFA], TOC, pH, ORP v time (micro-aerobic w dextrin add'n + 300 mL A side sludge)	213
Figure A7.10	Batch Test 7: [VFA], TOC, pH, ORP v time (micro-aerobic w peptone add'n + 300 mL A side sludge)	213
Figure A8.1	Batch Test 8: [VFA], TOC, pH, ORP v time (anaerobic control w 1 L A side sludge)	214
Figure A8.2	Batch Test 8: [VFA], TOC, pH, ORP v time (anaerobic w ethanol add'n + 1 L A side sludge)	214
Figure A8.3	Batch Test 8: [VFA], TOC, pH, ORP v time (anaerobic w propanol add'n + 1 L A side sludge)	215
Figure A8.4	Batch Test 8: [VFA], TOC, pH, ORP v time (anaerobic w isobutyrate add'n + 1 L A side sludge)	215
Figure A8.5	Batch Test 8: [VFA], TOC, pH, ORP v time (anaerobic w pyruvate add'n + 1 L A side sludge)	216
Figure A8.6	Batch Test 8: [VFA], TOC, pH, ORP v time (micro-aerobic control w 300 mL A side sludge)	216
Figure A8.7	Batch Test 8: [VFA], TOC, pH, ORP v time (micro-aerobic w ethanol add'n + 300 mL A side sludge)	217
Figure A8.8	Batch Test 8: [VFA], TOC, pH, ORP v time (micro-aerobic w propanol add'n + 300 mL A side sludge)	217
Figure A8.9	Batch Test 8: [VFA], TOC, pH, ORP v time (micro-aerobic w isobutyrate add'n + 300 mL A side sludge)	218

Figure A8.10	Batch Test 8: [VFA], TOC, pH, ORP v time (micro-aerobic w pyruvate add'n + 300 mL A side sludge)	218
Figure A9.1	Batch Test 9: [VFA], TOC, pH, ORP v time (anaerobic control w 700 mL A side and 300 mL primary sludge)	219
Figure A9.2	Batch Test 9: [VFA], TOC, pH, ORP v time (anaerobic w 2,4-dinitrophenol add'n + 700 mL A side + 300 mL primary sludge)	219
Figure A9.3	Batch Test 9: [VFA], TOC, pH, ORP v time (anaerobic w NaF add'n + 700 mL A side + 300 mL primary sludge)	220
Figure A9.4	Batch Test 9: [VFA], TOC, pH, ORP v time (anaerobic w pellet add'n + 700 mL A side + 300 mL primary sludge)	220
Figure A9.5	Batch Test 9: [VFA], TOC, pH, ORP v time (anaerobic w supernatant add'n + 700 mL A side + 300 mL primary sludge)	221
Figure A9.6	Batch Test 9: [VFA], TOC, pH, ORP v time (micro-aerobic control w 270 mL A side and 30 mL primary sludge)	221
Figure A9.7	Batch Test 9: [VFA], TOC, pH, ORP v time (micro-aerobic w 2,4-dinitrophenol add'n + 270 mL A side + 30 mL primary sludge)	222
Figure A9.8	Batch Test 9: [VFA], TOC, pH, ORP v time (micro-aerobic w NaF add'n + 270 mL A side + 30 mL primary sludge)	222
Figure A9.9	Batch Test 9: [VFA], TOC, pH, ORP v time (micro-aerobic w pellet add'n + 270 mL A side + 30 mL primary sludge)	223
Figure A9.10	Batch Test 9: [VFA], TOC, pH, ORP v time (micro-aerobic w supernatant add'n + 270 mL A side + 30 mL primary sludge)	223
Figure A10.1	Batch Test 10: [VFA], TOC, pH, ORP v time (anaerobic control w 1 L A side + 0 mL primary sludge)	224
Figure A10.2	Batch Test 10: [VFA], TOC, pH, ORP v time (anaerobic w 800 mL A side + 200 mL primary sludge)	224
Figure A10.3	Batch Test 10: [VFA], TOC, pH, ORP v time (anaerobic w 600 mL A side + 400 mL primary sludge)	225
Figure A10.4	Batch Test 10: [VFA], TOC, pH, ORP v time (anaerobic w 400 mL A side + 600 mL primary sludge)	225

Figure A10.5	Batch Test 10: [VFA], TOC, pH, ORP v time (anaerobic w 200 mL A side + 800 mL primary sludge)	226
Figure A10.6	Batch Test 10: [VFA], TOC, pH, ORP v time (micro-aerobic w 300 mL A side + 0 mL primary sludge)	226
Figure A10.7	Batch Test 10: [VFA], TOC, pH, ORP v time (micro-aerobic w 240 mL fermenter + 60 mL primary sludge)	227
Figure A10.8	Batch Test 10: [VFA], TOC, pH, ORP v time (micro-aerobic w 180 mL fermenter + 120 mL primary sludge)	227
Figure A10.9	Batch Test 10: [VFA], TOC, pH, ORP v time (micro-aerobic w 120 mL fermenter + 180 mL primary sludge)	228
Figure A10.10	Batch Test 10: [VFA], TOC, pH, ORP v time (micro-aerobic w 60 mL fermenter + 240 mL primary sludge)	228
Figure A10.11	Batch Test 10: [VFA], TOC, pH, ORP v time (anaerobic control w 1 L fermenter + 0 mL primary sludge)	229
Figure A10.12	Batch Test 10: [VFA], TOC, pH, ORP v time (anaerobic w 800 mL fermenter + 200 mL primary sludge)	229
Figure A10.13	Batch Test 10: [VFA], TOC, pH, ORP v time (anaerobic w 600 mL fermenter + 400 mL primary sludge)	230
Figure A10.14	Batch Test 10: [VFA], TOC, pH, ORP v time (anaerobic w 400 mL fermenter + 600 mL primary sludge)	230
Figure A10.15	Batch Test 10: [VFA], TOC, pH, ORP v time (anaerobic w 200 mL fermenter + 800 mL primary sludge)	231
Figure A10.16	Batch Test 10: [VFA], TOC, pH, ORP v time (micro-aerobic control w 300 mL fermenter + 0 mL primary sludge)	231
Figure A10.17	Batch Test 10: [VFA], TOC, pH, ORP v time (micro-aerobic w 240 mL fermenter + 60 mL primary sludge)	232
Figure A10.18	Batch Test 10: [VFA], TOC, pH, ORP v time (micro-aerobic w 180 mL fermenter + 120 mL primary sludge)	232
Figure 10.19	Batch Test 10: [VFA], TOC, pH, ORP v time (micro-aerobic w 120 mL fermenter + 180 mL primary sludge)	233

Figure 10.20	Batch Test 10: [VFA], TOC, pH, ORP v time (micro-aerobic w 60 mL fermenter + 240 mL primary sludge)	233
Figure A11.1	Batch Test 11: [VFA], TOC, pH, ORP v time (anaerobic control w 1 L A)	234
Figure A11.2	Batch Test 11: [VFA], TOC, pH, ORP v time (anaerobic A side w 25% primary sludge)	234
Figure A11.3	Batch Test 11: [VFA], TOC, pH, ORP v time (anaerobic control w 1 L B side)	235
Figure A11.4	Batch Test 11: [VFA], TOC, pH, ORP v time (anaerobic B side w 25% primary sludge)	235
Figure A11.5	Batch Test 11: [VFA], TOC, pH, ORP v time (Microaerobic A side w 25% primary sludge)	236
Figure A11.6	Batch Test 11: [VFA], TOC, pH, ORP v time (micro-aerobic control w 1 L A side sludge)	236
Figure A11.7	Batch Test 11: [VFA], TOC, pH, ORP v time (micro-aerobic A side w 50% primary sludge)	237
Figure A11.8	Batch Test 11: [VFA], TOC, pH, ORP v time (micro-aerobic control with 1 L B side sludge)	237
Figure A11.9	Batch Test 11: [VFA], TOC, pH, ORP v time (micro-aerobic B side w 50% primary sludge)	238
Figure A11.10	Batch Test 11: [VFA], TOC, pH, ORP v time (micro-aerobic B side w 25% primary sludge)	238
Figure A12.1	Salmon Arm 1st stage ATAD: [VFA], TOC, pH, ORP v time (anaerobic control)	239
Figure A12.2	Salmon Arm 1st stage ATAD: [VFA], TOC, pH, ORP v time (anaerobic w 50% primary sludge)	239
Figure A12.3	Salmon Arm 1st stage ATAD: [VFA], TOC, pH, ORP v time (anaerobic w 50% secondary sludge)	240
Figure A12.4	Salmon Arm 1st stage ATAD: [VFA], TOC, pH, ORP v time (anaerobic w propionate add'n)	240

Figure A12.5	Salmon Arm 1st stage ATAD: [VFA], TOC, pH, ORP v time (anaerobic w mixed secondary and primary sludge)	241
Figure A12.6	Salmon Arm 1st stage ATAD: [VFA], TOC, pH, ORP v time (micro-aerobic control)	241
Figure A12.7	Salmon Arm 1st stage ATAD: [VFA], TOC, pH, ORP v time (micro-aerobic w 50% primary sludge)	242
Figure A12.8	Salmon Arm 1st stage ATAD: [VFA], TOC, pH, ORP v time (micro-aerobic w 50% secondary sludge)	242
Figure A12.9	Salmon Arm 1st stage ATAD: [VFA], TOC, pH, ORP v time (micro-aerobic w propionate add'n)	243
Figure A12.10	Salmon Arm 1st stage ATAD: [VFA], TOC, pH, ORP v time (micro-aerobic w mixed secondary and primary sludge)	243
Figure A13.1	Salmon Arm 3rd stage ATAD: [VFA], TOC, pH, ORP v time (anaerobic control)	244
Figure A13.2	Salmon Arm 3rd stage ATAD: [VFA], TOC, pH, ORP v time (anaerobic w 50% primary sludge)	244
Figure A13.3	Salmon Arm 3rd stage ATAD: [VFA], TOC, pH, ORP v time (anaerobic w 50% secondary sludge)	245
Figure A13.4	Salmon Arm 3rd stage ATAD: [VFA], TOC, pH, ORP v time (anaerobic w propionate add'n)	245
Figure A13.5	Salmon Arm 3rd stage ATAD: [VFA], TOC, pH, ORP v time (anaerobic w mixed secondary and primary sludge)	246
Figure A13.6	Salmon Arm 3rd stage ATAD: [VFA], TOC, pH, ORP v time (micro-aerobic control)	246
Figure A13.7	Salmon Arm 3rd stage ATAD: [VFA], TOC, pH, ORP v time (micro-aerobic w 50% primary sludge)	247
Figure A13.8	Salmon Arm 3rd stage ATAD: [VFA], TOC, pH, ORP v time (micro-aerobic w 50% secondary sludge)	247
Figure A13.9	Salmon Arm 3rd stage ATAD: [VFA], TOC, pH, ORP v time (micro-aerobic w propionate add'n)	248

Figure A13.10 Salmon Arm 3rd stage ATAD: [VFA], TOC, pH, ORP v time (micro-aerobic w mixed secondary and primary sludge)	248
Table A1 Concentration of sludges for all batch experiments	249

Figure A1.1: Batch Test 1: [VFA] v time (0% primary feed)

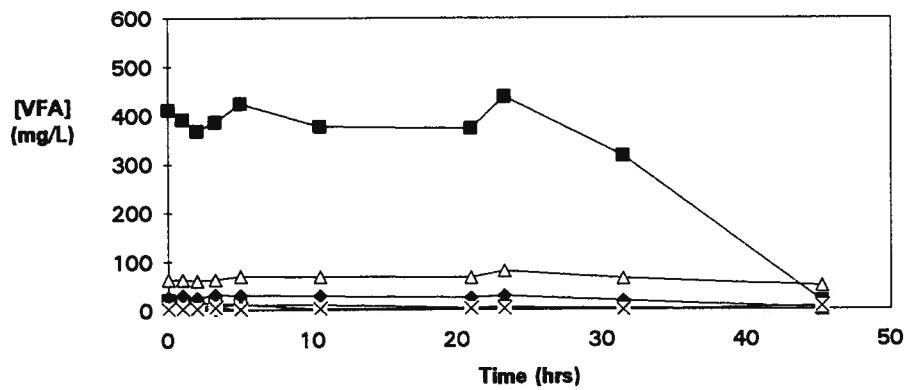


Figure A1.2: Batch Test 1: [VFA] v time (10% primary feed)

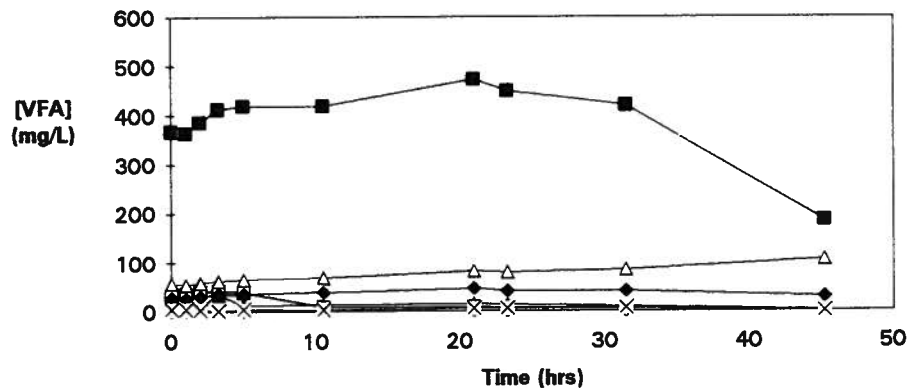
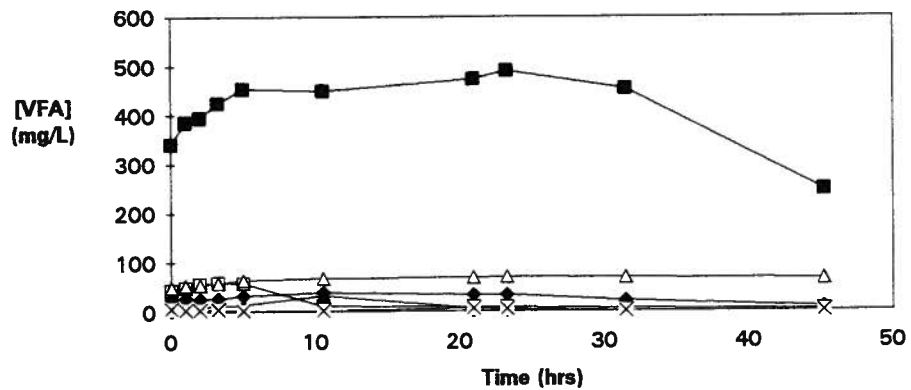


Figure A1.3: Batch Test 1: [VFA] v time (20% primary feed)



■ acetate □ propionate ◆ isobutyrate ◇ butyrate
 ▲ 2-methyl-butyrate △ isovalerate × valerate

Figure A1.4: Batch Test 1: [VFA] v time (30% primary feed)

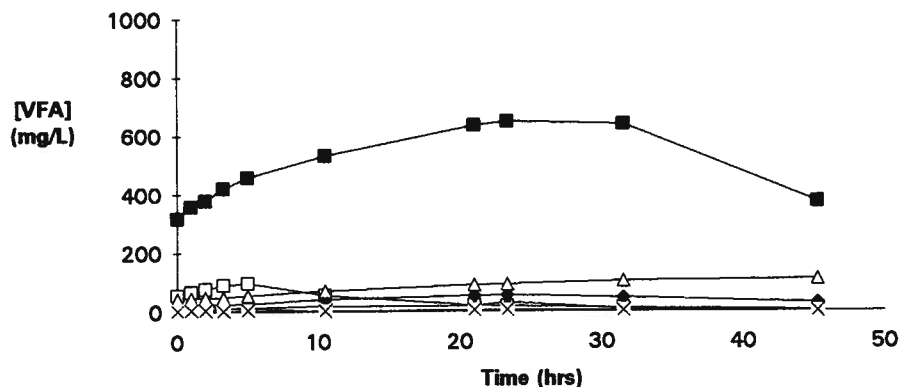


Figure A2.1: Batch Test 2: [VFA], TOC, pH v time (micro-aerobic control w 300 mL A side sludge)

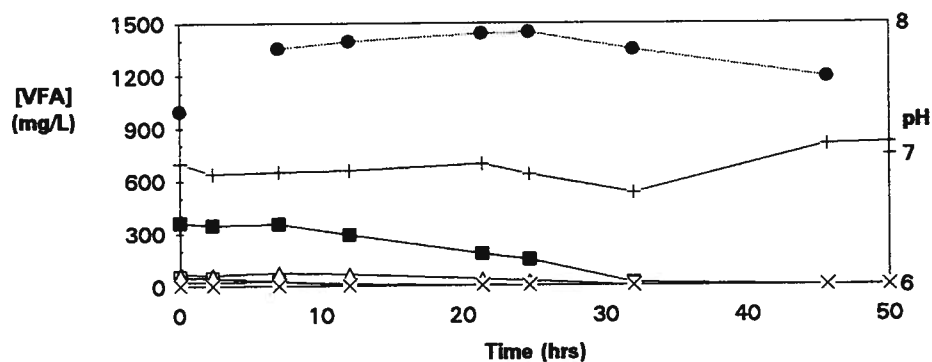
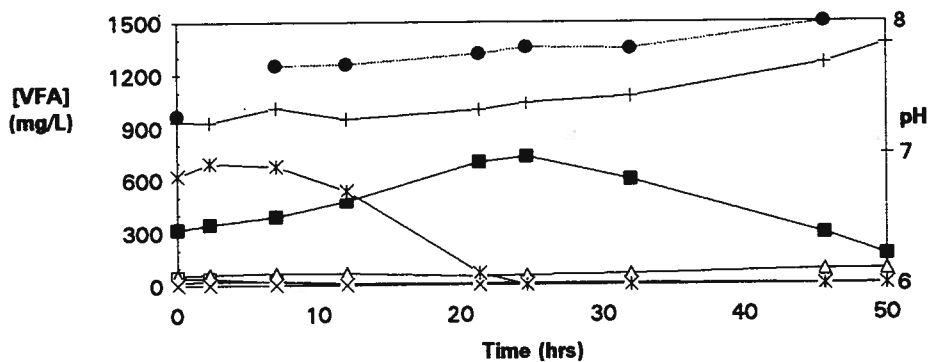


Figure A2.2: Batch Test 2: [VFA], TOC, pH v time (micro-aerobic w lactic acid and 300 mL A side sludge)



- acetate □ propionate ◆ isobutyrate
- ◇ butyrate ▲ 2-methylbutyrate △ isovalerate
- × valerate * lactate + TOC ● pH

Figure A3.1: Batch Test 2: [VFA], TOC, pH v time (anaerobic w lactic acid and 1 L A side sludge)

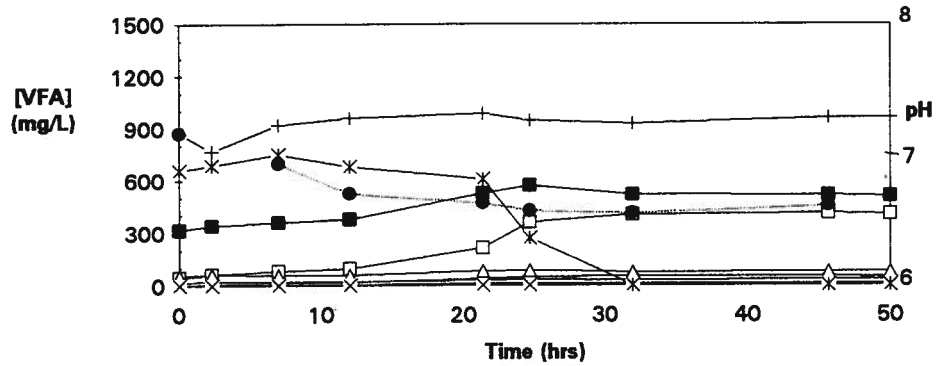


Figure A3.2: Batch Test 2: [VFA], TOC, pH v time (anaerobic control w 1 L A side sludge)

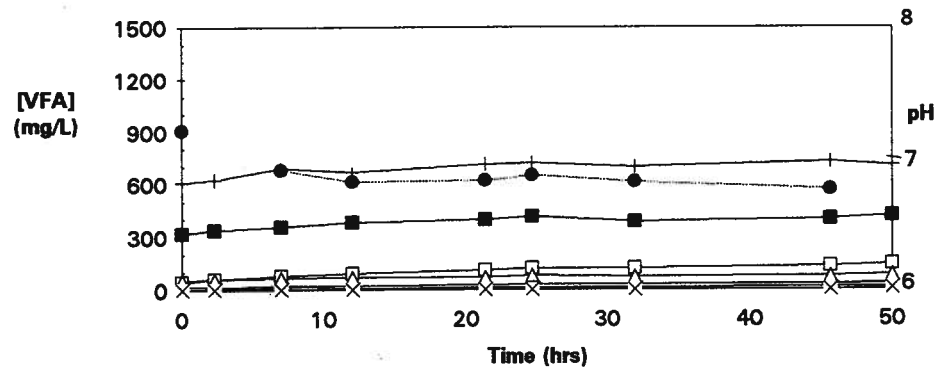
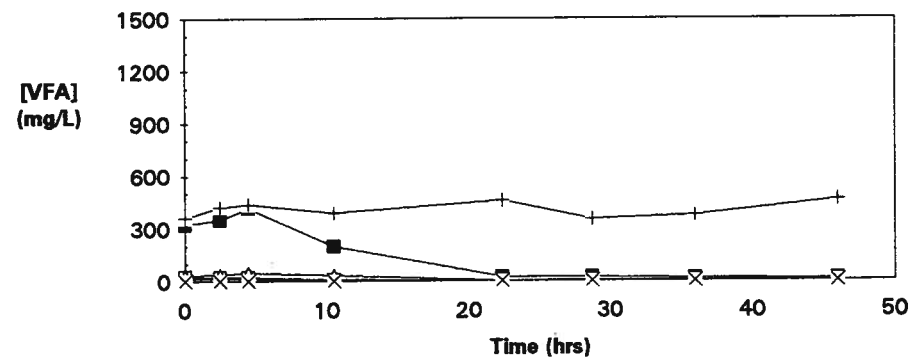


Figure A4.1: Batch Test 4: [VFA], TOC v time (micro-aerobic control 300 ml A side sludge)



- acetate □ propionate ◆ isobutyrate
- ◇ butyrate ▲ 2-methylbutyrate △ isovalerate
- × valerate * lactate + TOC ● pH

Figure A4.2: Batch Test 4: [VFA], TOC v time (micro-aerobic w propionate and 300 mL A sludge)

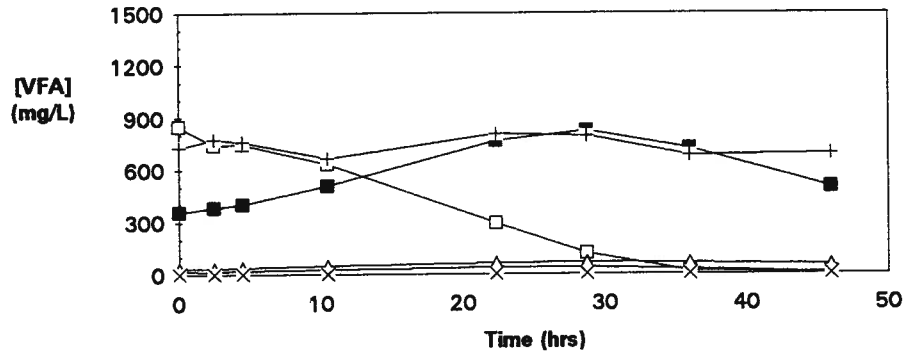


Figure A4.3: Batch Test 4: [VFA], TOC v time (anaerobic w propionate and 1 L A side sludge)

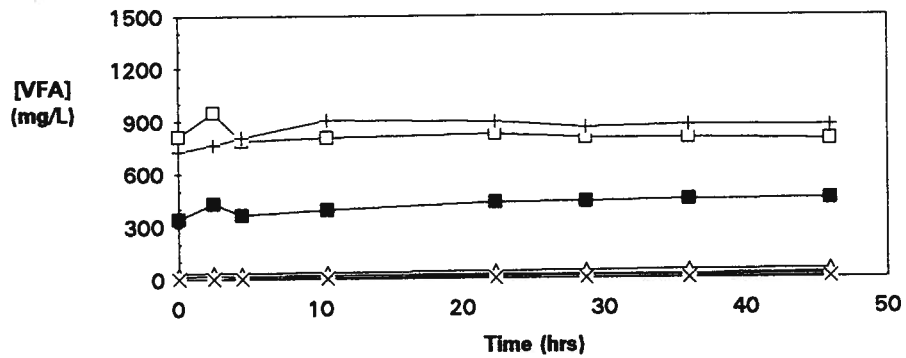
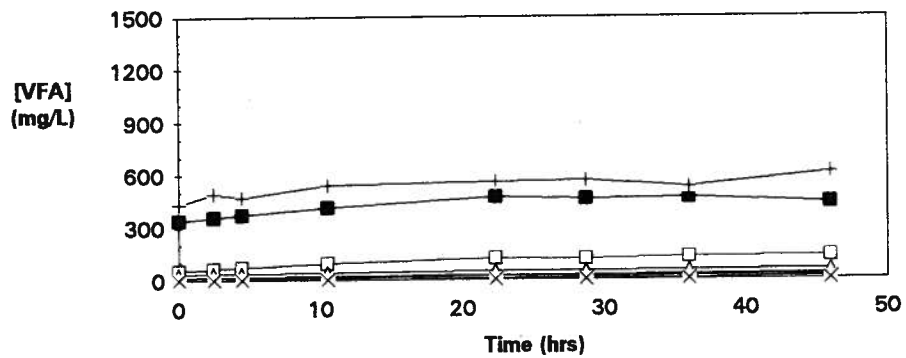


Figure A4.4: Batch Test 4: [VFA], TOC v time (anaerobic control w 1 L A side sludge)



- acetate □ propionate ◆ isobutyrate
- ◇ butyrate ▲ 2-methylbutyrate △ isovalerate
- × valerate ✕ lactate + TOC ● pH

Figure A5.1: Batch Test 5: [VFA], TOC, pH v time (micro-aerobic w/o cyanide, w 300 mL A side and 30 mL primary sludge)

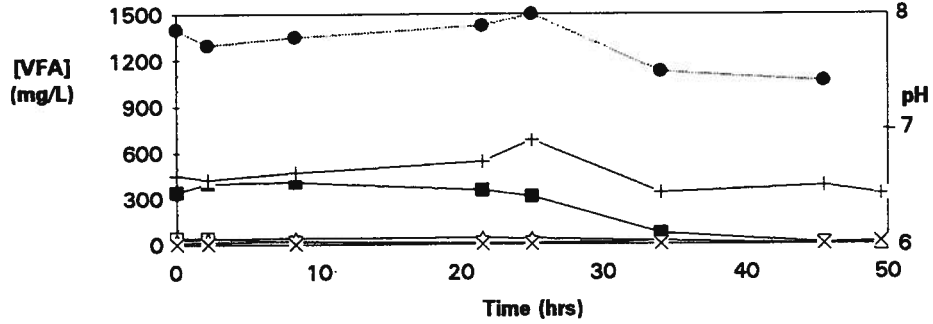


Figure A5.2: Batch Test 5: [VFA], TOC, pH v time (micro-aerobic w cyanide, 300 mL A side and 30 mL primary sludge)

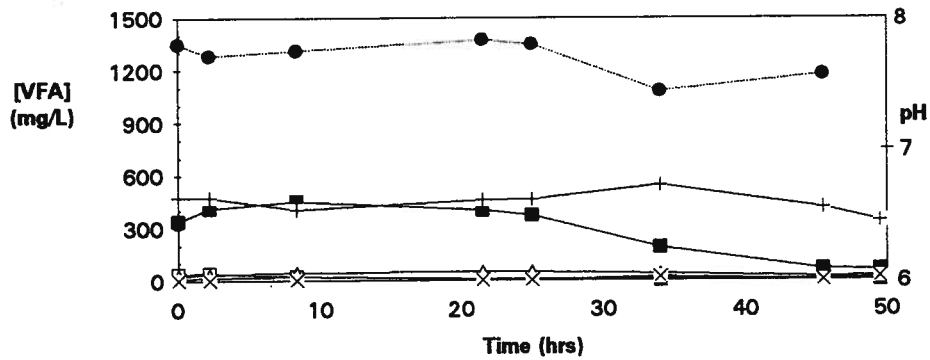
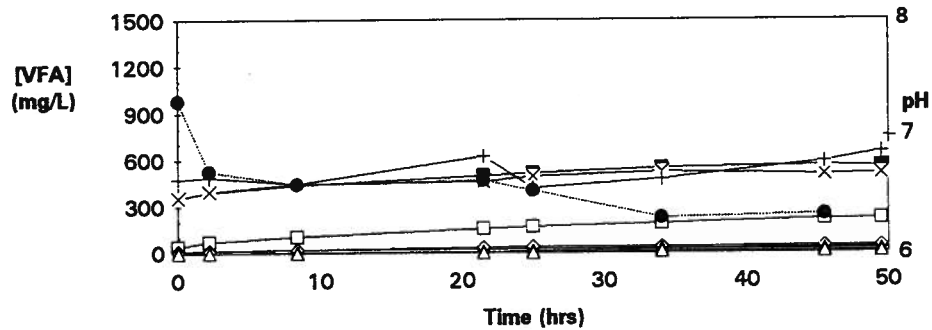
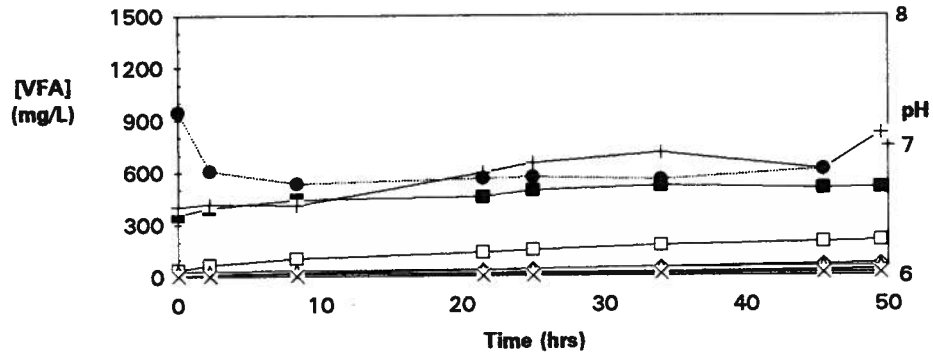


Figure A5.3: Batch Test 5: [VFA], TOC, pH v time (anaerobic w/o cyanide, 1 L A side and 100 mL primary sludge)



- acetate □ propionate ◆ isobutyrate
- ◇ butyrate ▲ 2-methylbutyrate △ isovalerate
- × valerate * lactate + TOC ● pH

**Figure A5.4: Batch Test 5: [VFA], TOC, pH v time
(anaerobic w cyanide, 1 L A side and 100 mL primary sludge)**



- acetate □ propionate ◆ isobutyrate
- ◇ butyrate ▲ 2-methylbutyrate △ isovalerate
- × valerate × lactate + TOC ● pH

Figure A6.1: Batch Test 6: [VFA], TOC, pH, ORP v time (anaerobic control w 1 L A side sludge)

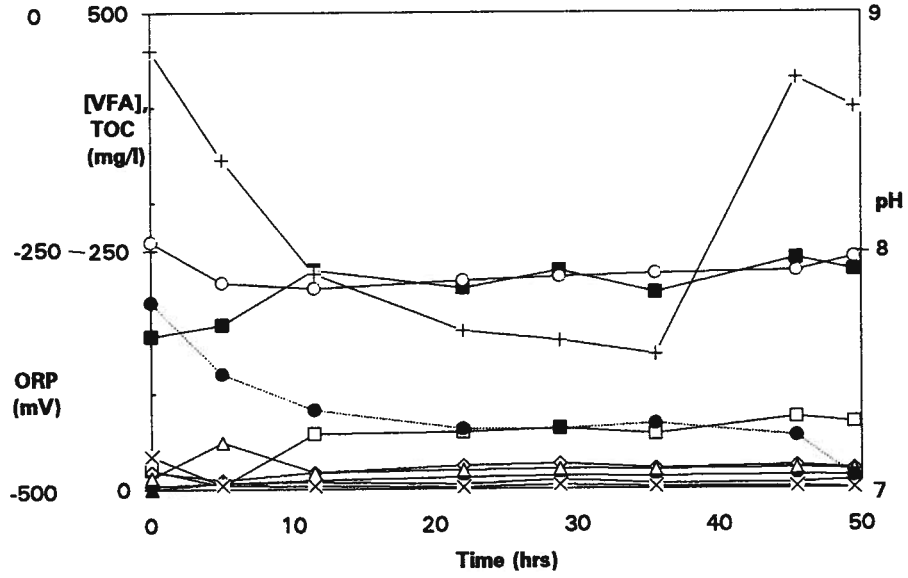
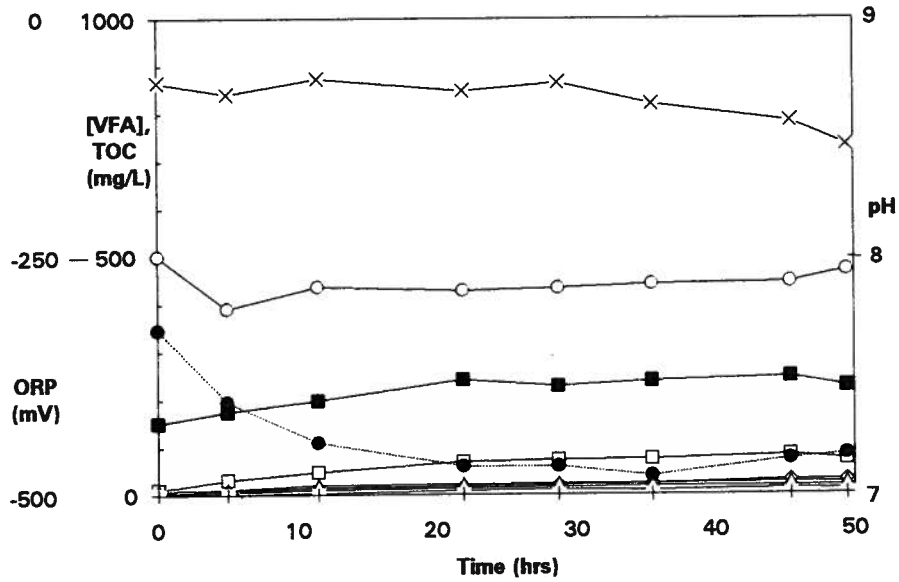


Figure A6.2: Batch Test 6: [VFA], TOC, pH, ORP v time (anaerobic w valerate add'n + 1 L A side sludge)



- acetate □ propionate ◆ isobutyrate
- ◇ butyrate ▲ 2-methylbutyrate △ isovalerate
- × valerate * lactate + TOC ● pH ○ ORP

Figure A6.3: Batch Test 6: [VFA], TOC, pH, ORP v time (anaerobic w iso-valerate add'n + 1 L A side sludge)

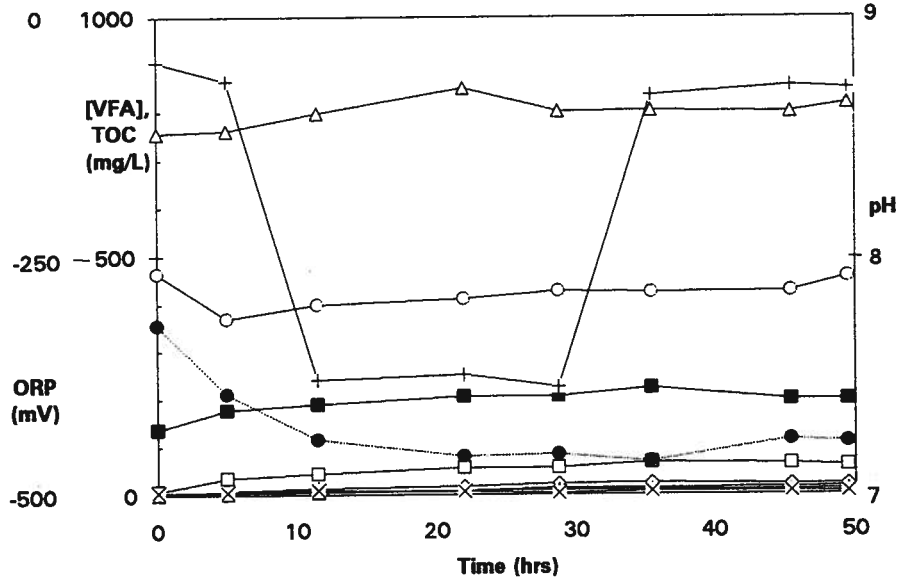
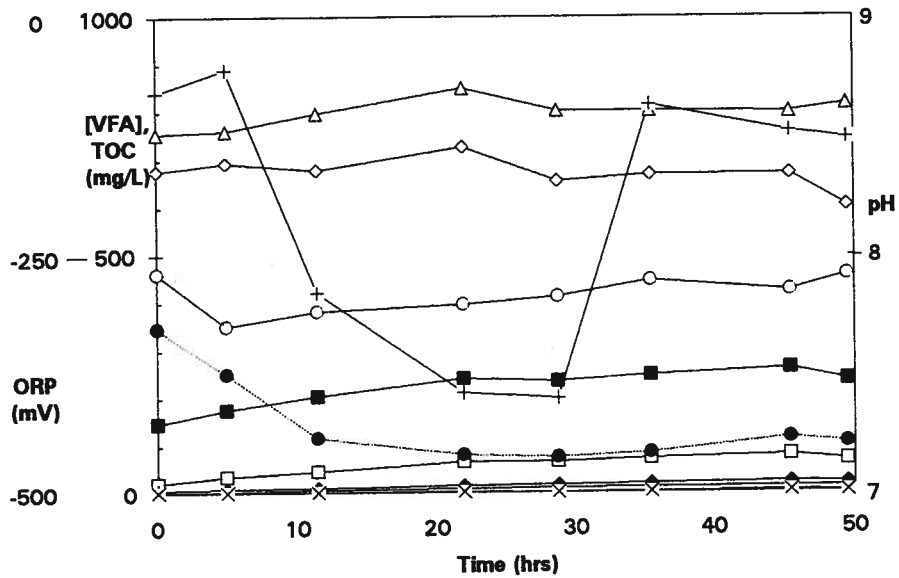
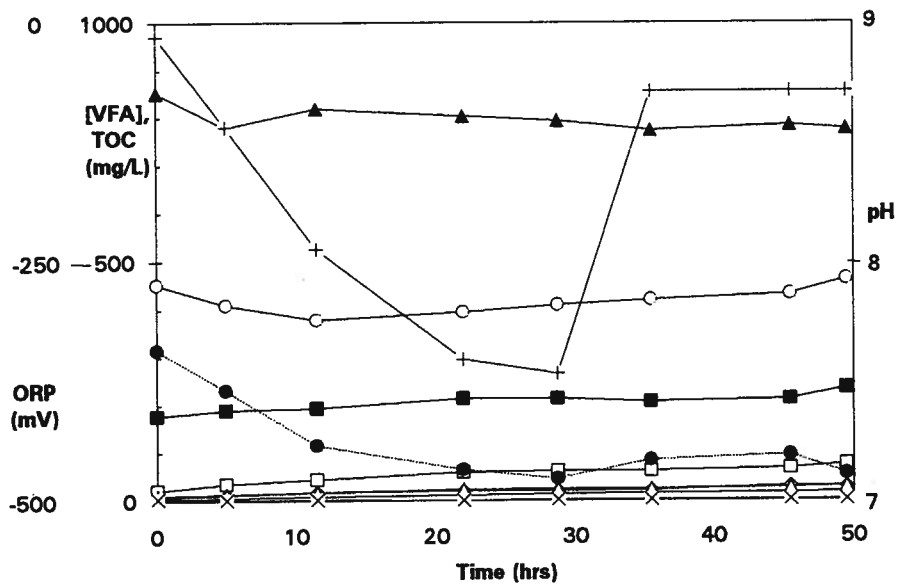


Figure A6.4: Batch Test 6: [VFA], TOC, pH, ORP v time (anaerobic w butyrate add'n + 1 L A side sludge)

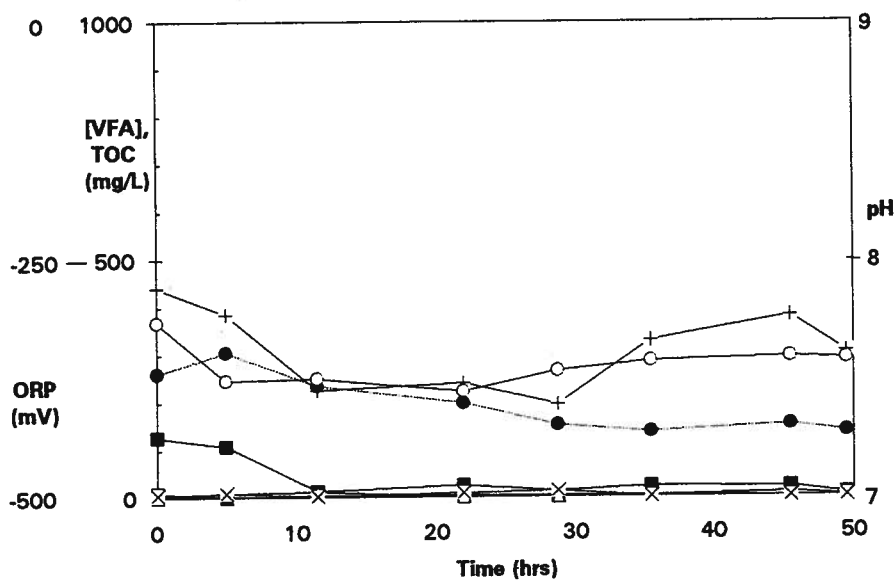


■ acetate □ propionate ◆ isobutyrate
 ◇ butyrate ▲ 2-methylbutyrate △ isovalerate
 × valerate * lactate + TOC ● pH ○ ORP

**Figure A6.5: Batch Test 6: [VFA], TOC, pH, ORP v time
(anaerobic w methylbutyrate add'n + 1 L A side sludge)**



**Figure A6.6: Batch Test 6: [VFA], TOC, pH, ORP v time
(micro-aerobic control w 300 ml A side sludge)**



■ acetate □ propionate ◆ isobutyrate
 ◇ butyrate ▲ 2-methylbutyrate △ isovalerate
 × valerate * lactate + TOC ● pH ○ ORP

Figure A6.7: Batch Test 6: [VFA], TOC, pH, ORP v time (micro-aerobic w valerate add'n + 300 mL A side sludge)

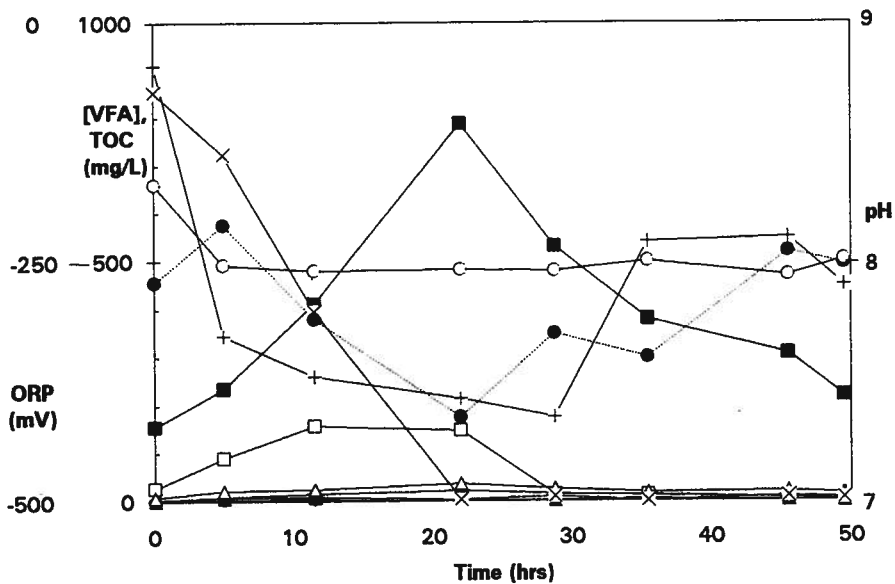
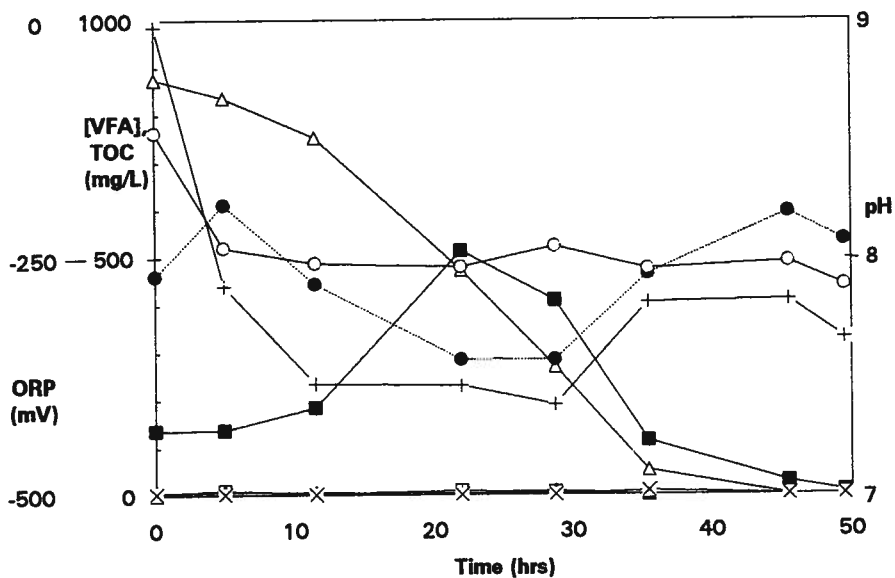


Figure A6.8: Batch Test 6: [VFA], TOC, pH, ORP v time (micro-aerobic w iso-valerate add'n + 300 mL A side sludge)



- acetate □ propionate ◆ isobutyrate
- ◇ butyrate ▲ 2-methylbutyrate △ isovalerate
- × valerate * lactate + TOC ● pH ○ ORP

Figure A6.9: Batch Test 6: [VFA], TOC, pH, ORP v time (micro-aerobic w butyrate add'n + 300 mL A side sludge)

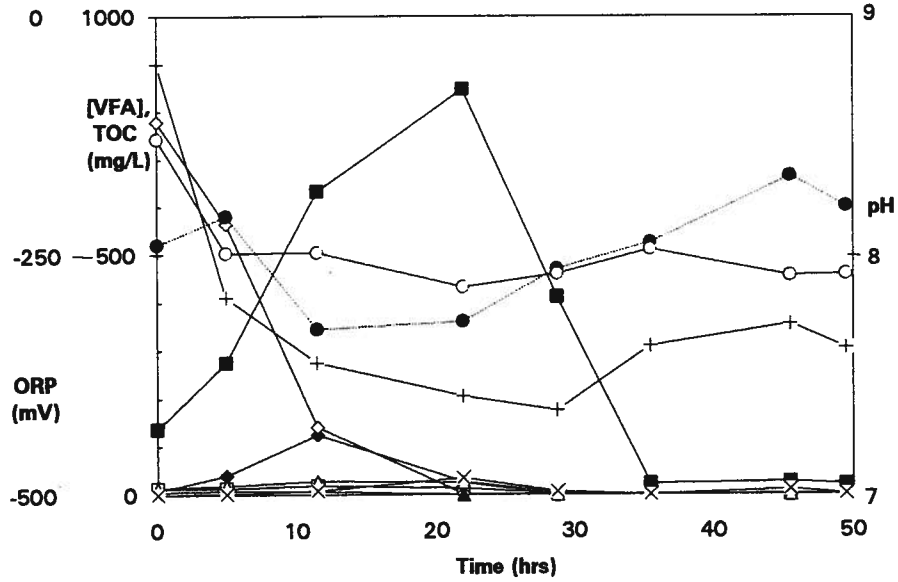
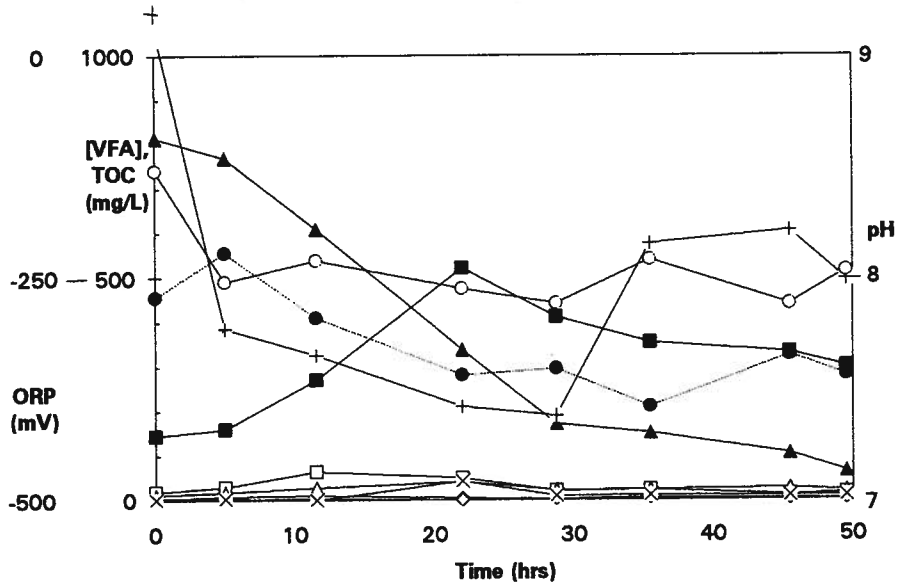


Figure A6.10: Batch Test 6: [VFA], TOC, pH, ORP v time (micro-aerobic w methylbutyrate add'n + 300 mL A side sludge)



- acetate □ propionate ◆ isobutyrate
- ◇ butyrate ▲ 2-methylbutyrate △ isovalerate
- × valerate * lactate + TOC ● pH ○ ORP

Figure A7.1: Batch Test 7: [VFA], TOC, pH, ORP v time (anaerobic control w 1 L A side sludge)

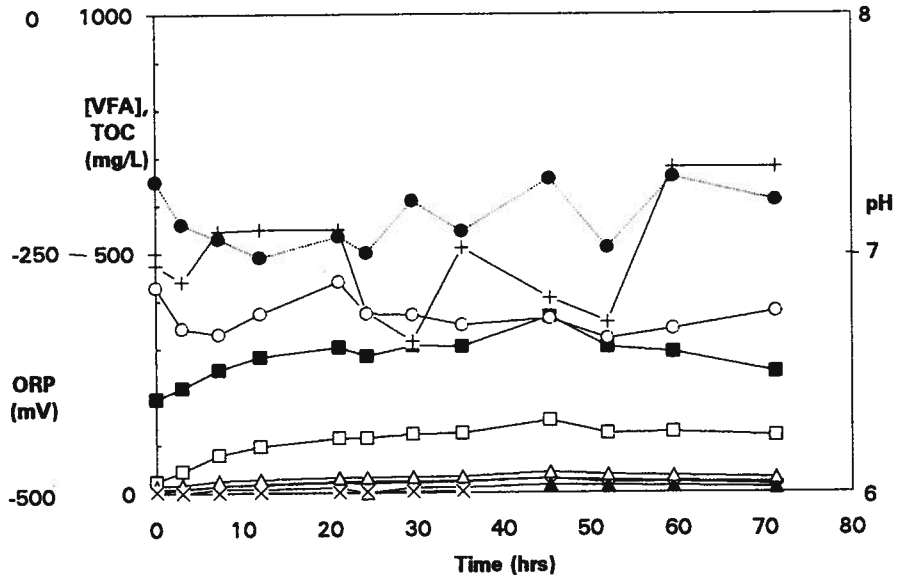
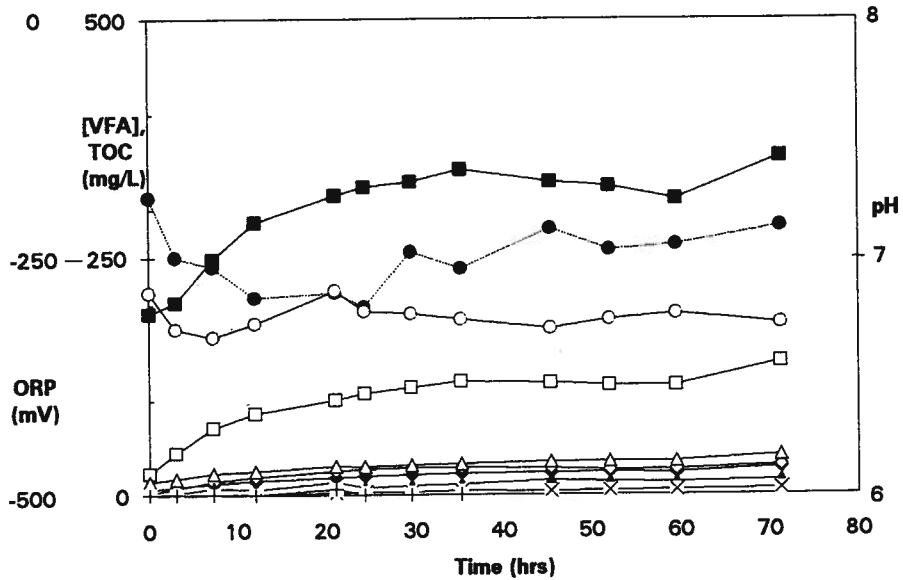


Figure A7.2: Batch Test 7: [VFA], TOC, pH, ORP v time (anaerobic w linoleic acid add'n + 1 L A side sludge)



- acetate □ propionate ◆ isobutyrate
- ◇ butyrate ▲ 2-methylbutyrate △ isovalerate
- × valerate ✕ lactate + TOC ● pH ○ ORP

Figure A7.3: Batch Test 7: [VFA], TOC, pH, ORP v time (anaerobic w glucose add'n + 1 L A side sludge)

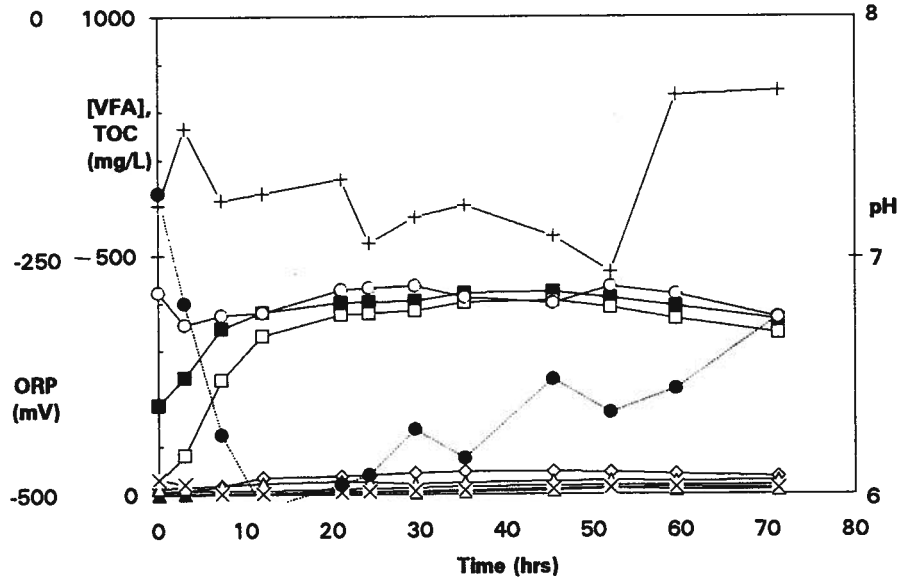
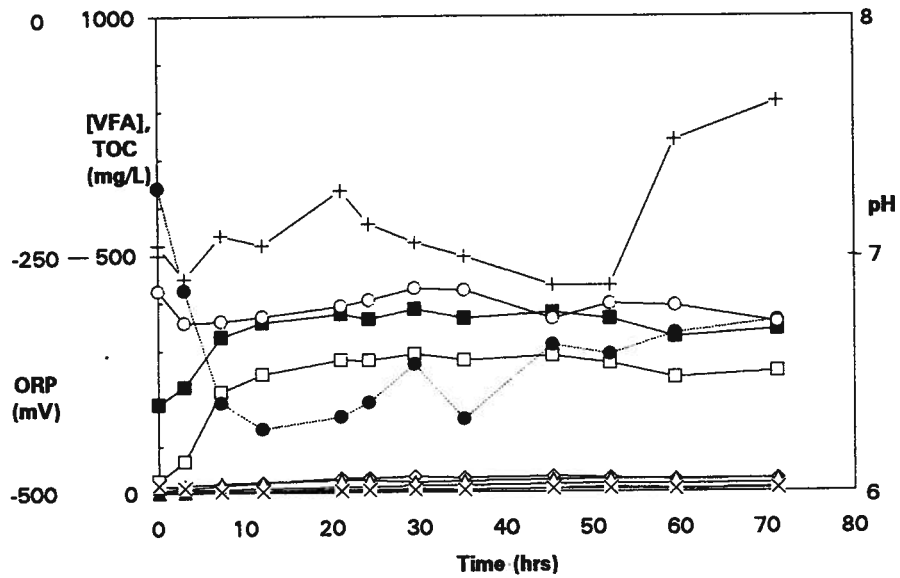


Figure A7.4: Batch Test 7: [VFA], TOC, pH, ORP v time (anaerobic w dextrin add'n + 1 L A side sludge)



- acetate □ propionate ◆ isobutyrate
- ◇ butyrate ▲ 2-methylbutyrate △ isovalerate
- × valerate * lactate + TOC ● pH ○ ORP

Figure A7.5: Batch Test 7: [VFA], TOC, pH, ORP v time (anaerobic w peptone add'n + 1 L A side sludge)

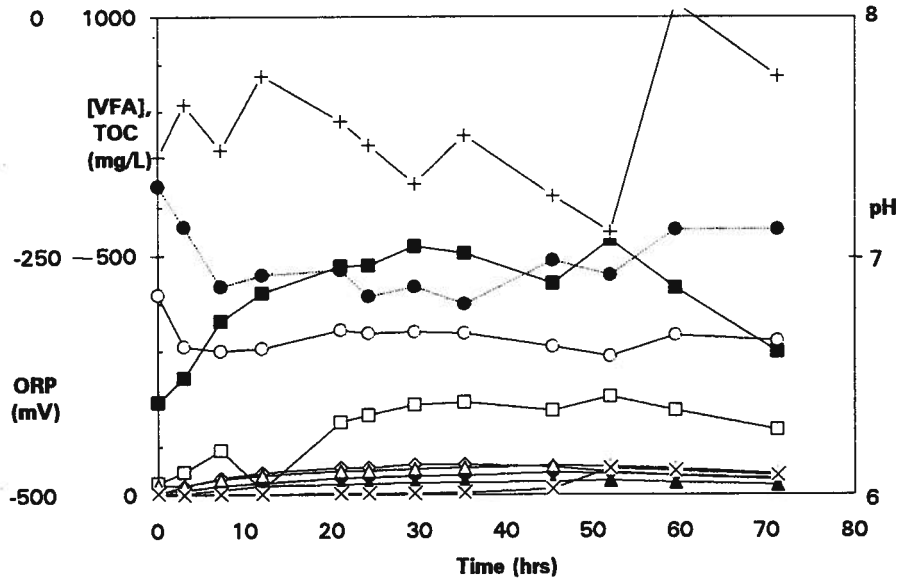
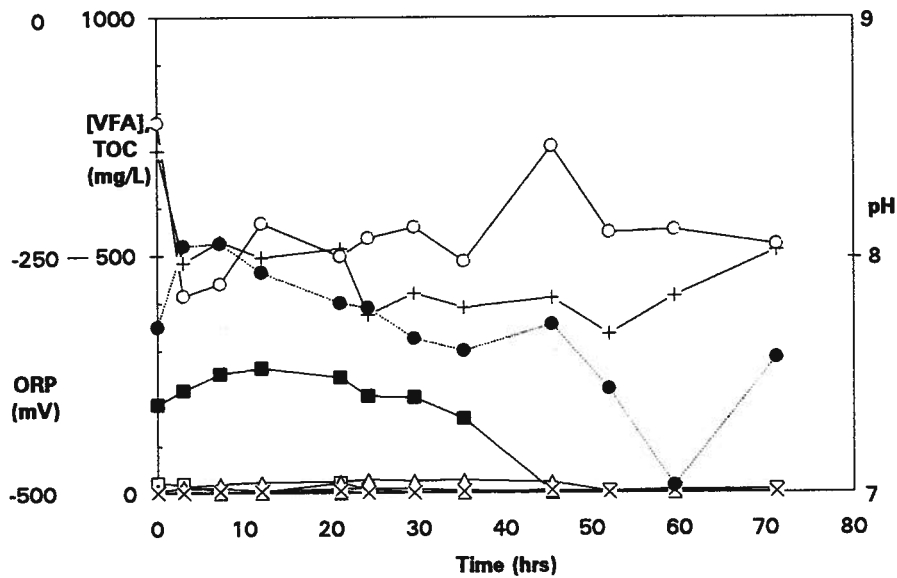


Figure A7.6: Batch Test 7: [VFA], TOC, pH, ORP v time (micro-aerobic control w 300 mL A side sludge)



- acetate □ propionate ◆ isobutyrate
- ◇ butyrate ▲ 2-methylbutyrate △ isovalerate
- × valerate * lactate + TOC ● pH ○ ORP

Figure A7.7: Batch Test 7: [VFA], TOC, pH, ORP v time (micro-aerobic w linoleic acid add'n + 300 mL A side sludge)

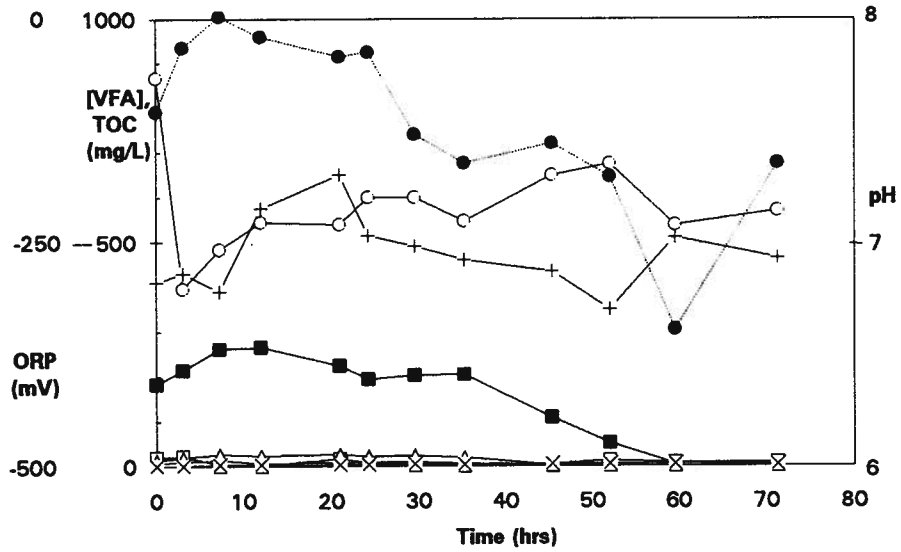
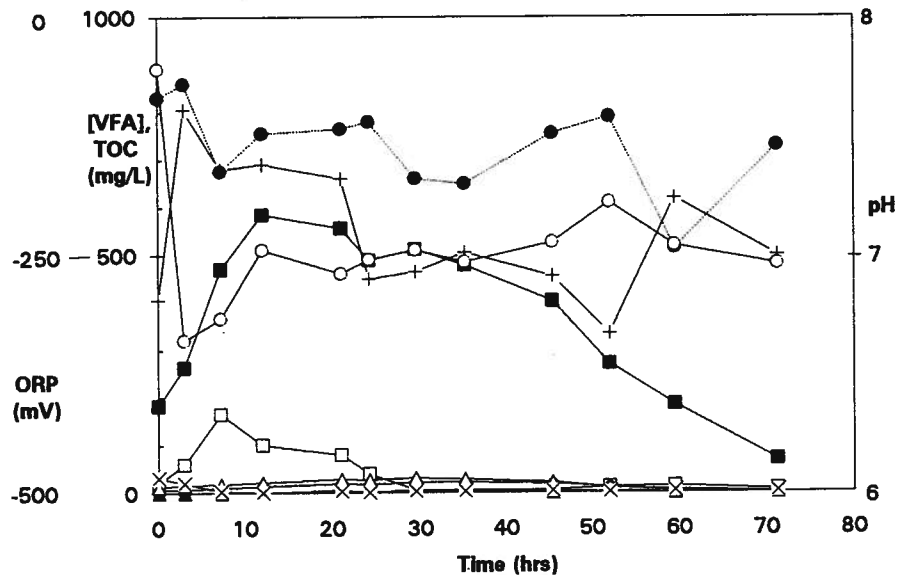


Figure A7.8: Batch Test 7: [VFA], TOC, pH, ORP v time (micro-aerobic w glucose add'n + 300 mL A side sludge)



- acetate □ propionate ◆ isobutyrate
- ◇ butyrate ▲ 2-methylbutyrate △ isovalerate
- × valerate * lactate + TOC ● pH ○ ORP

Figure A7.9: Batch Test 7: [VFA], TOC, pH, ORP v time (micro-aerobic w dextrin add'n + 300 mL A side sludge)

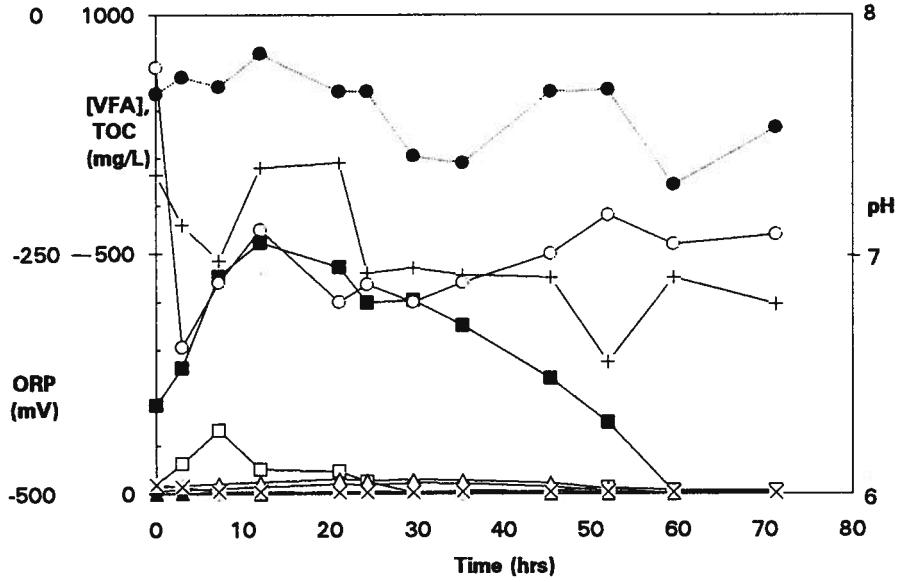
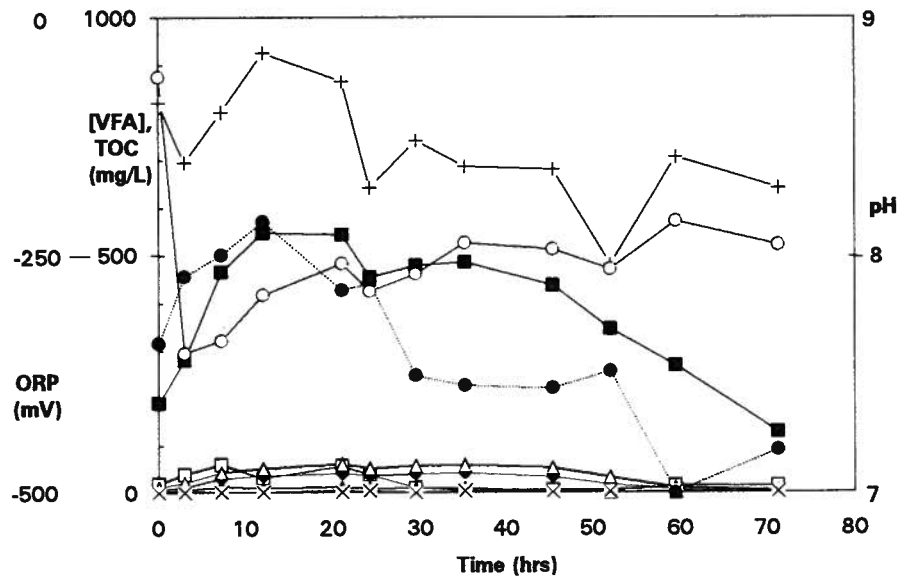


Figure A7.10: Batch Test 7: [VFA], TOC, pH, ORP v time (micro-aerobic w peptone add'n + 300 mL A side sludge)



- acetate □ propionate ◆ isobutyrate
- ◇ butyrate ▲ 2-methylbutyrate △ isovalerate
- × valerate * lactate + TOC ● pH ○ ORP

Figure A8.1: Batch Test 8: [VFA], TOC, pH, ORP v time (anaerobic control w 1 L A side sludge)

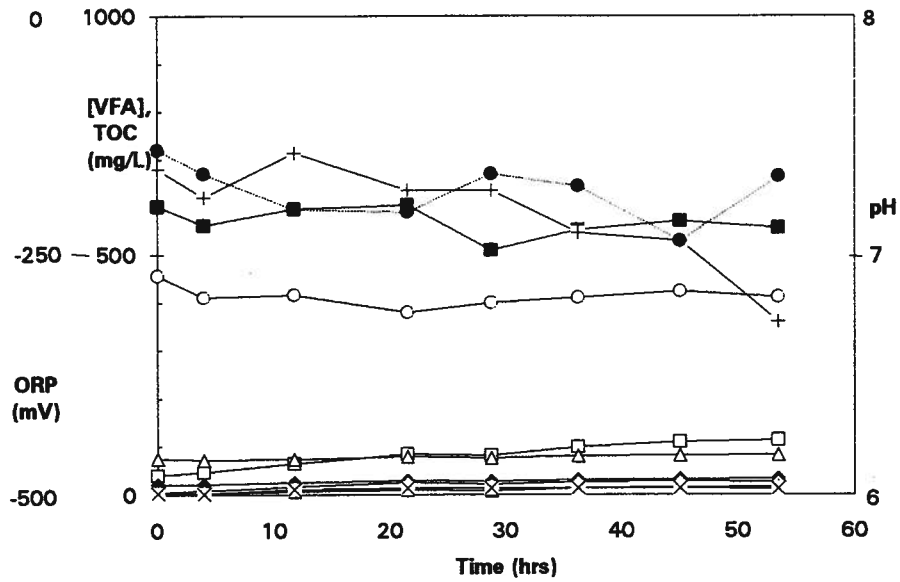
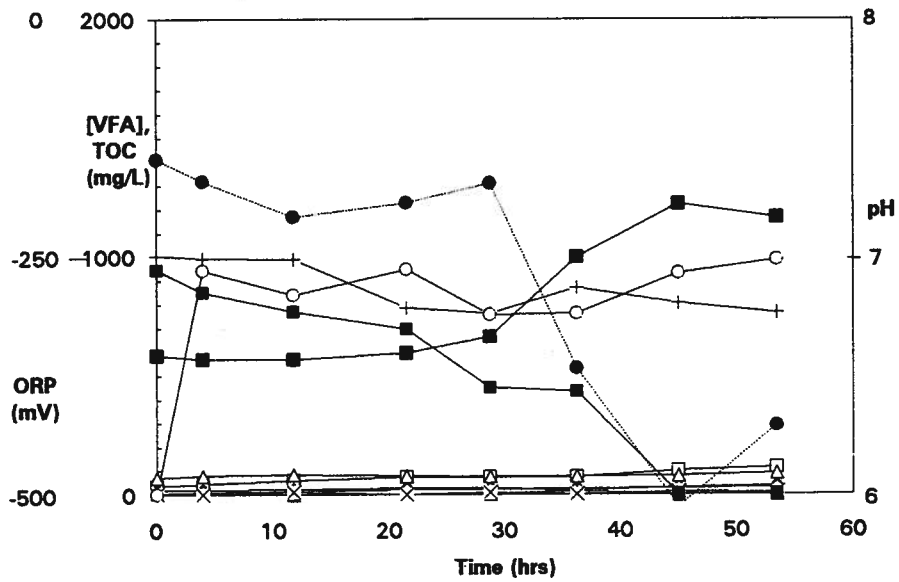


Figure A8.2: Batch Test 8: [VFA], TOC, pH, ORP v time (anaerobic w ethanol add'n + 1 L A side sludge)



- acetate □ propionate ◆ isobutyrate ■ ethanol
- ◇ butyrate ▲ 2-methylbutyrate △ isovalerate
- × valerate × lactate + TOC ● pH ○ ORP

Figure A8.3: Batch Test 8: [VFA], TOC, pH, ORP v time (anaerobic w propanol add'n + 1 L A side sludge)

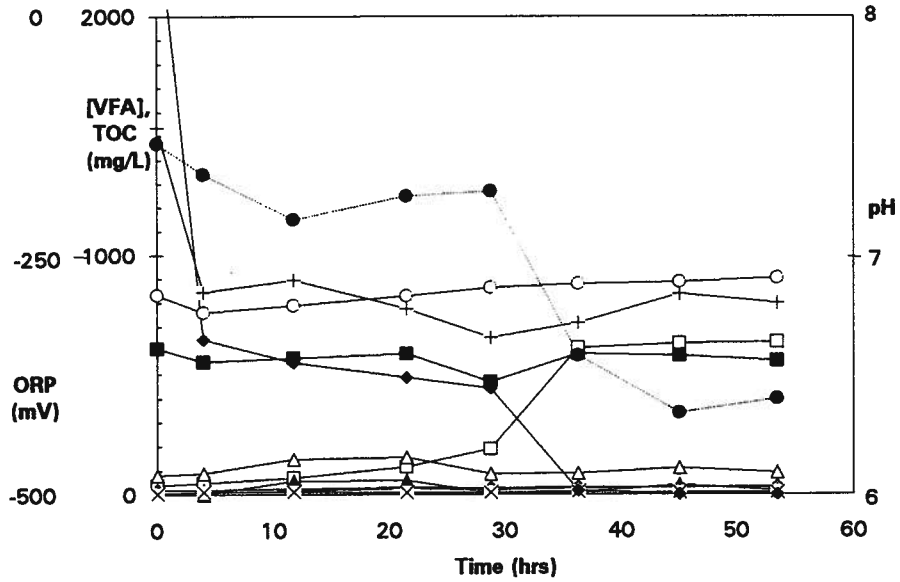
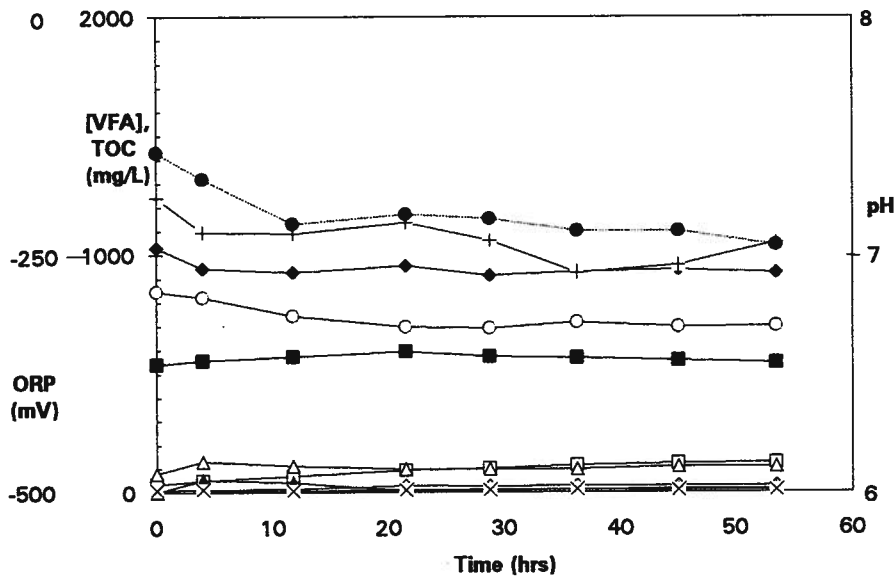


Figure A8.4: Batch Test 8: [VFA], TOC, pH, ORP v time (anaerobic w isobutyrate add'n + 1 L A side sludge)



- acetate □ propionate ◆ isobutyrate ◇ propanol
- ◇ butyrate ▲ 2-methylbutyrate △ isovalerate
- × valerate × lactate + TOC ● pH ○ ORP

Figure A8.5: Batch Test 8: [VFA], TOC, pH, ORP v time (anaerobic w pyruvate add'n + 1 L A side sludge)

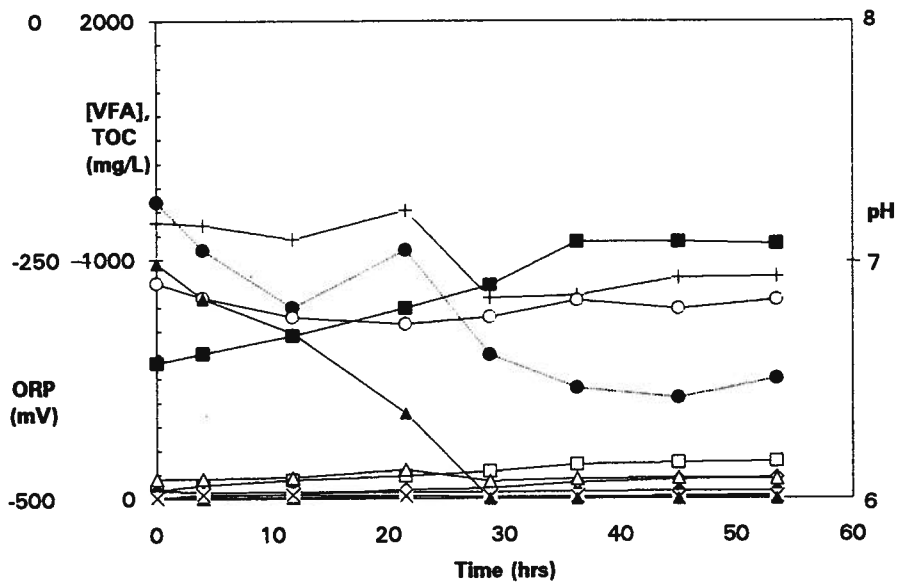
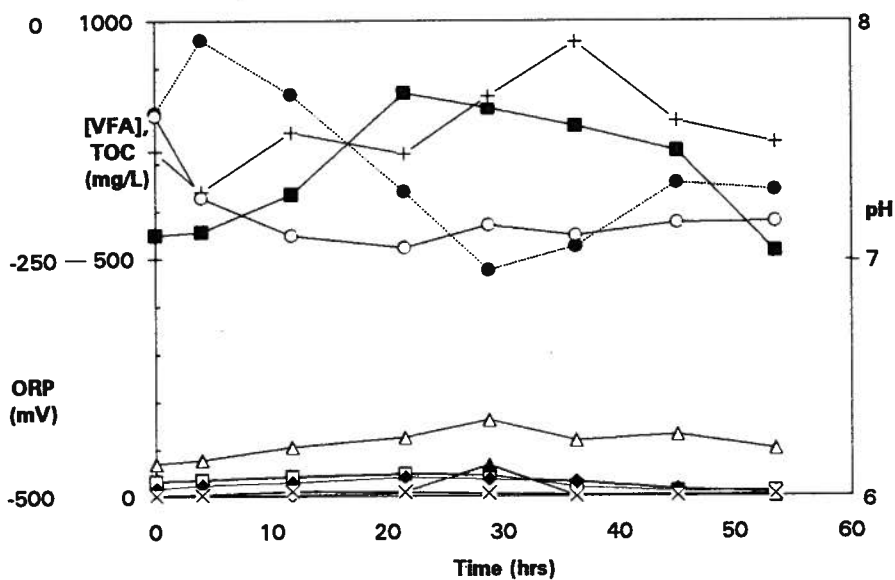


Figure A8.6: Batch Test 8: [VFA], TOC, pH, ORP v time (micro-aerobic control w 300 mL A side sludge)



- acetate □ propionate ◆ isobutyrate ■ pyruvate
- ◇ butyrate ▲ 2-methylbutyrate △ isovalerate
- × valerate × lactate + TOC ● pH ○ ORP

Figure A8.7: Batch Test 8: [VFA], TOC, pH, ORP v time (micro-aerobic w ethanol add'n + 300 mL A side sludge)

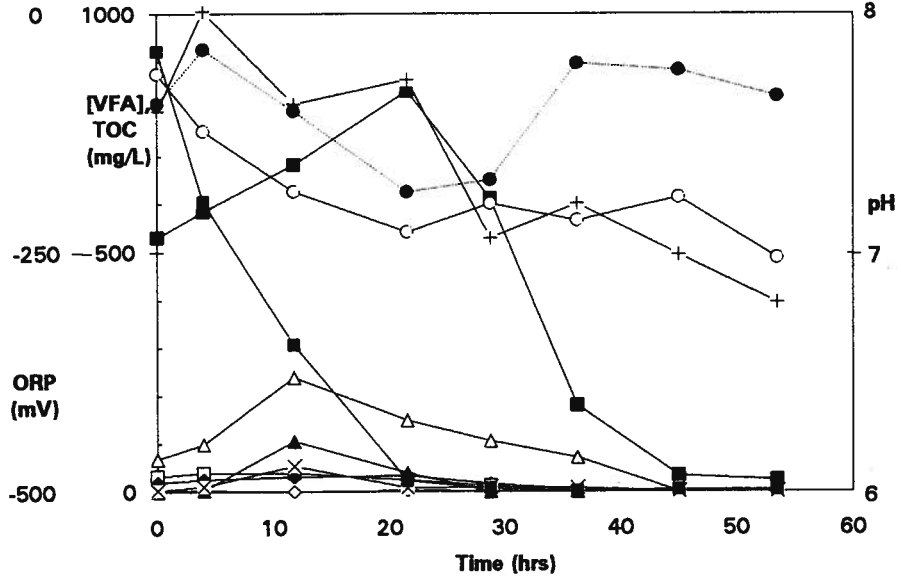
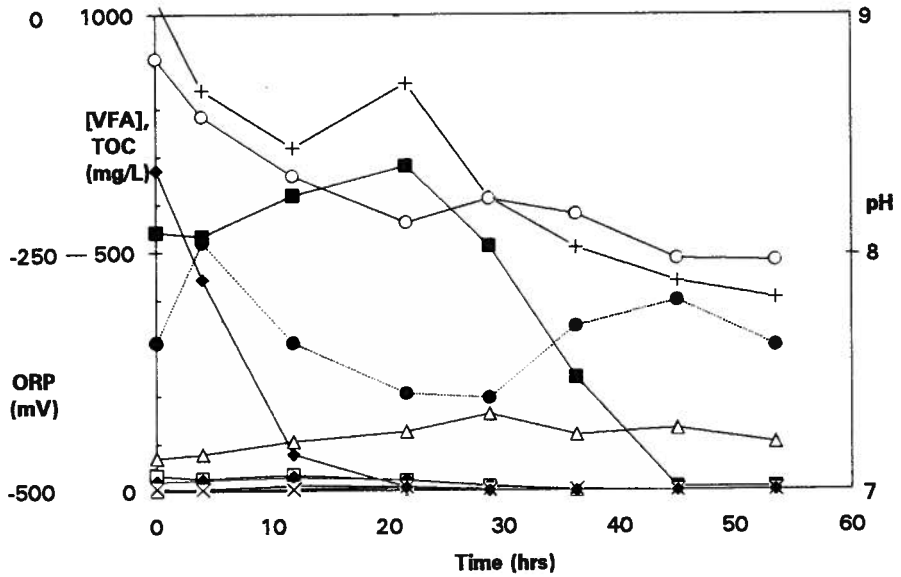


Figure A8.8: Batch Test 8: [VFA], TOC, pH, ORP v time (micro-aerobic w propanol add'n + 300 mL A side sludge)



- acetate □ propionate ◆ isobutyrate ■ ethanol ◆ propanol
- ◇ butyrate ▲ 2-methylbutyrate △ isovalerate
- × valerate × lactate + TOC ● pH ○ ORP

Figure A8.9: Batch Test 8: [VFA], TOC, pH, ORP v time (micro-aerobic w isobutyrate add'n + 300 mL A side sludge)

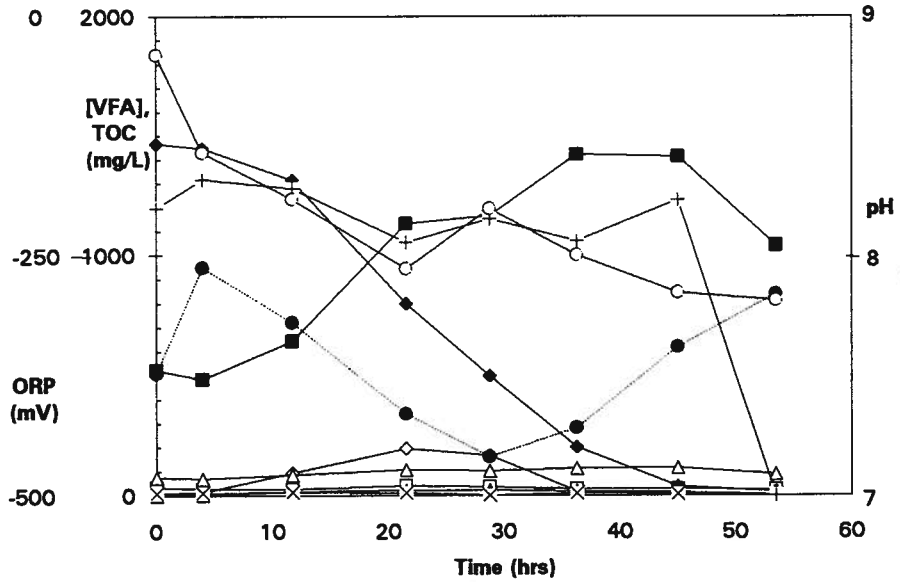
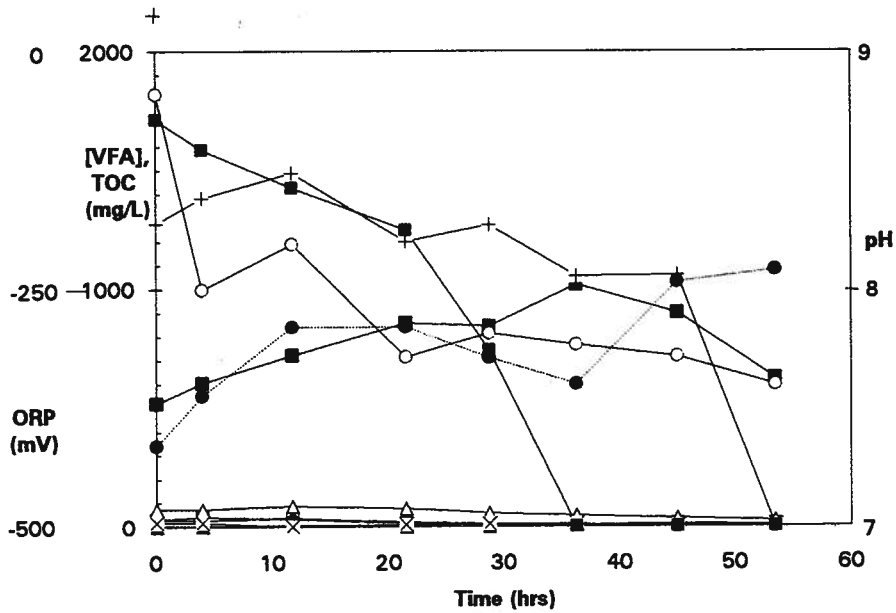


Figure A8.10: Batch Test 8: [VFA], TOC, pH, ORP v time (micro-aerobic w pyruvate add'n + 300 mL A side sludge)



- acetate □ propionate ◆ isobutyrate ■ pyruvate
- ◇ butyrate ▲ 2-methylbutyrate △ isovalerate
- × valerate * lactate + TOC ● pH ○ ORP

Figure A9.1: Batch Test 9: [VFA], TOC, pH, ORP v time (anaerobic control w 700 mL A side and 300 mL primary sludge)

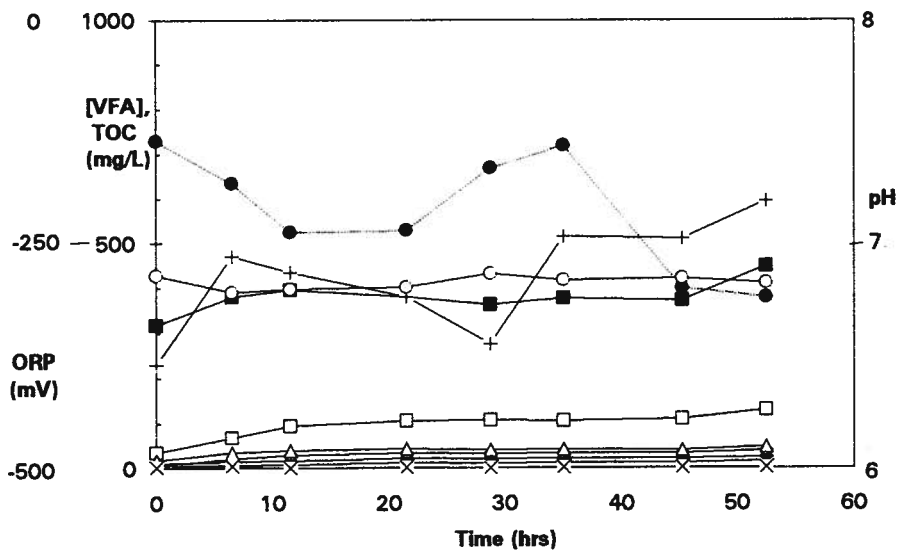
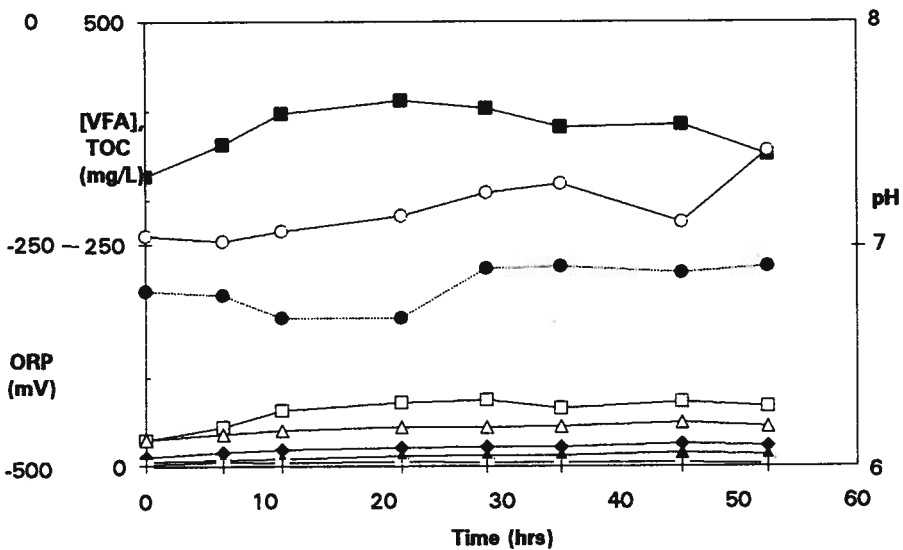


Figure A9.2: Batch Test 9: [VFA], TOC, pH, ORP v time (anaerobic w 2,4-dinitrophenol add'n + 700 mL A side + 300 mL primary sludge)



- acetate □ propionate ◆ isobutyrate
- ◇ butyrate ▲ 2-methylbutyrate △ isovalerate
- × valerate * lactate + TOC ● pH ○ ORP

Figure A9.3: Batch Test 9: [VFA], TOC, pH, ORP v time (anaerobic w NaF add'n + 700 mL A side + 300 mL primary sludge)

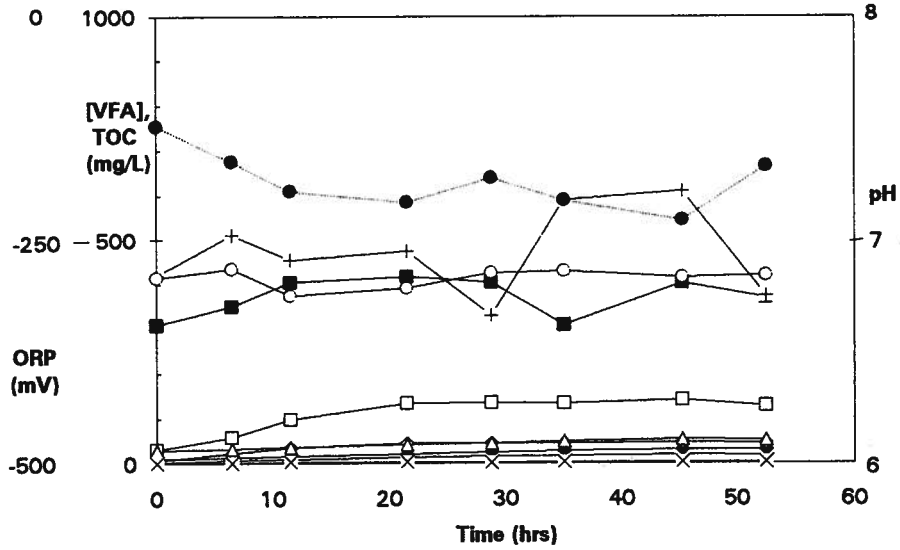
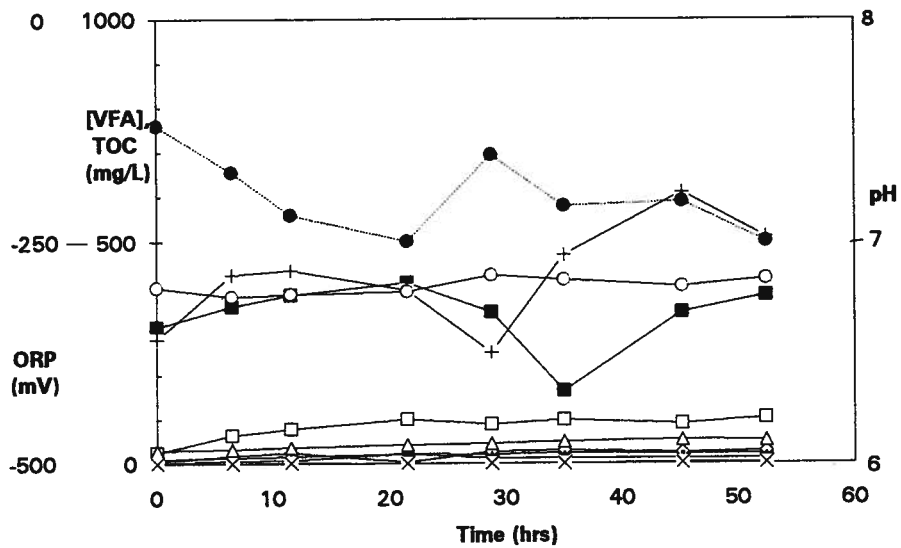


Figure A9.4: Batch Test 9: [VFA], TOC, pH, ORP v time (anaerobic w pellet add'n + 700 mL A side + 300 mL primary sludge)



- acetate □ propionate ◆ isobutyrate
- ◇ butyrate ▲ 2-methylbutyrate △ isovalerate
- × valerate * lactate + TOC ● pH ○ ORP

Figure A9.5: Batch Test 9: [VFA], TOC, pH, ORP v time (anaerobic w supernatant add'n + 700 mL A side + 300 mL primary sludge)

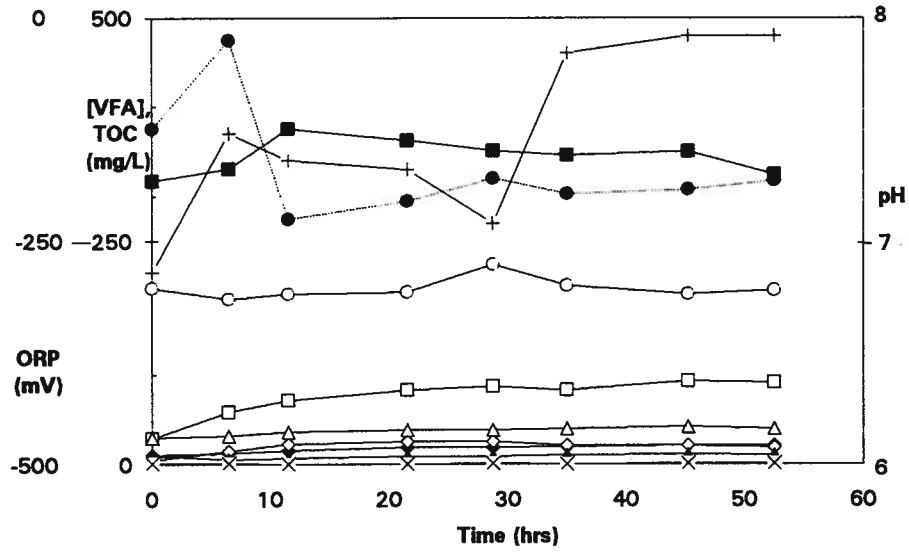
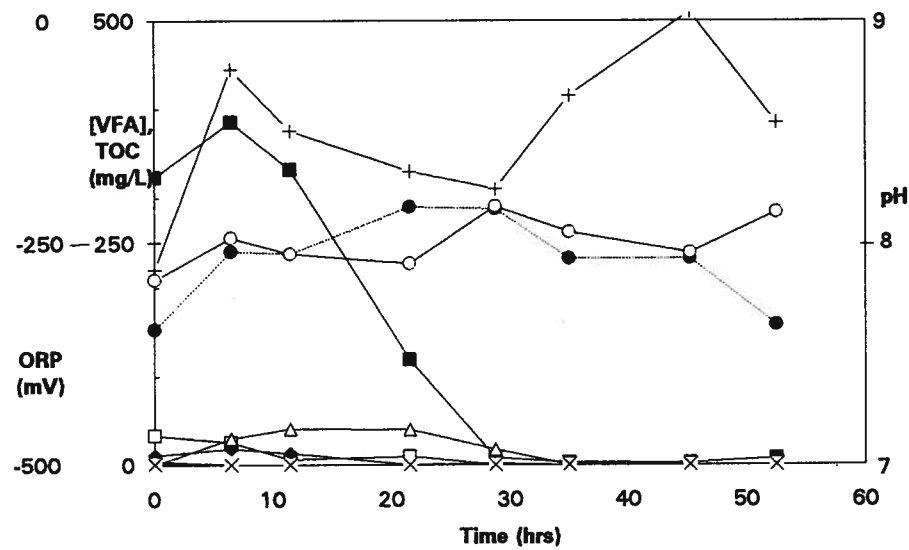


Figure A9.6: Batch Test 9: [VFA], TOC, pH, ORP v time (micro-aerobic control w 270 mL A side + 30 mL primary sludge)



- acetate □ propionate ◆ isobutyrate
- ◇ butyrate ▲ 2-methylbutyrate △ isovalerate
- × valerate * lactate + TOC ● pH ○ ORP

Figure A9.7: Batch Test 9: [VFA], TOC, pH, ORP v time (micro-aerobic w 2,4-dinitrophenol add'n + 270 mL A side + 30 mL primary sludge)

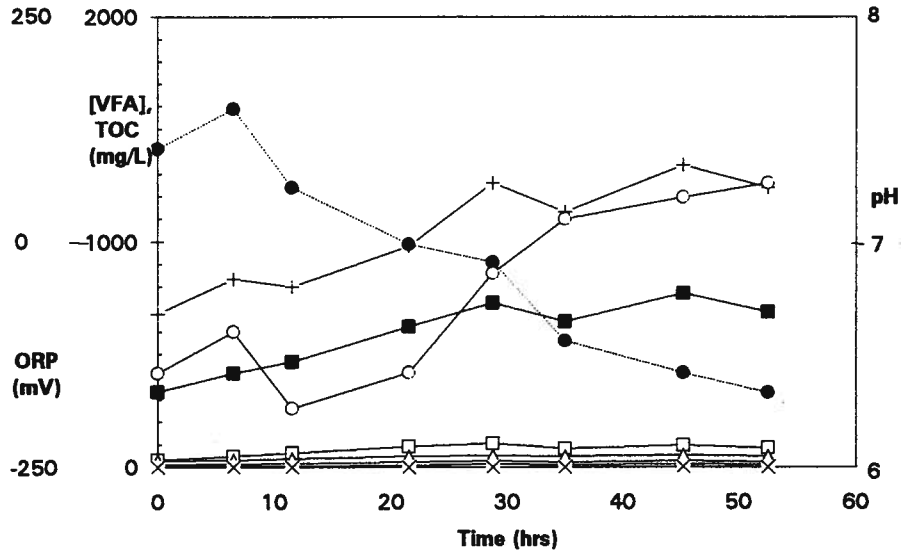
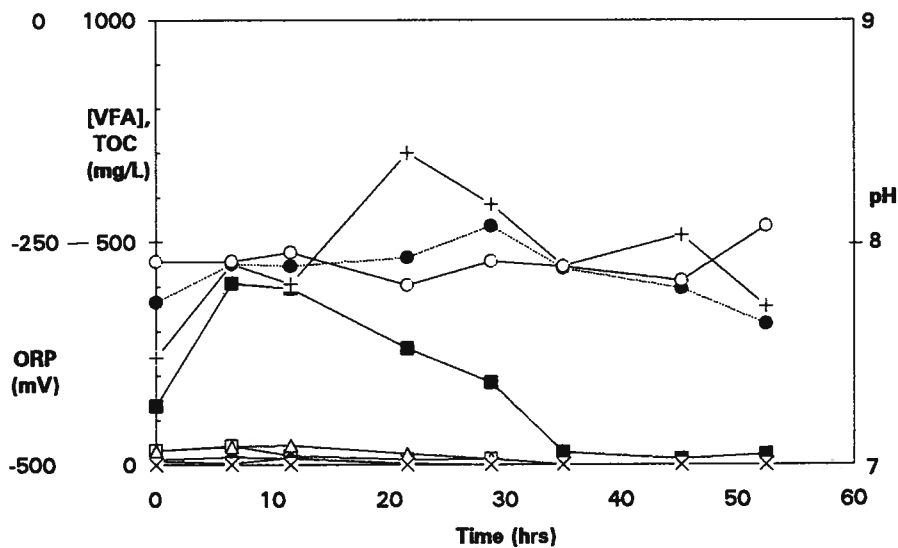


Figure A9.8: Batch Test 9: [VFA], TOC, pH, ORP v time (micro-aerobic w NaF add'n + 270 mL A side + 30 mL primary sludge)



- acetate □ propionate ◆ isobutyrate
- ◇ butyrate ▲ 2-methylbutyrate △ isovalerate
- × valerate * lactate + TOC ● pH ○ ORP

Figure A9.9: Batch Test 9: [VFA], TOC, pH, ORP v time (micro-aerobic w pellet add'n + 270 mL A side + 30 mL primary sludge)

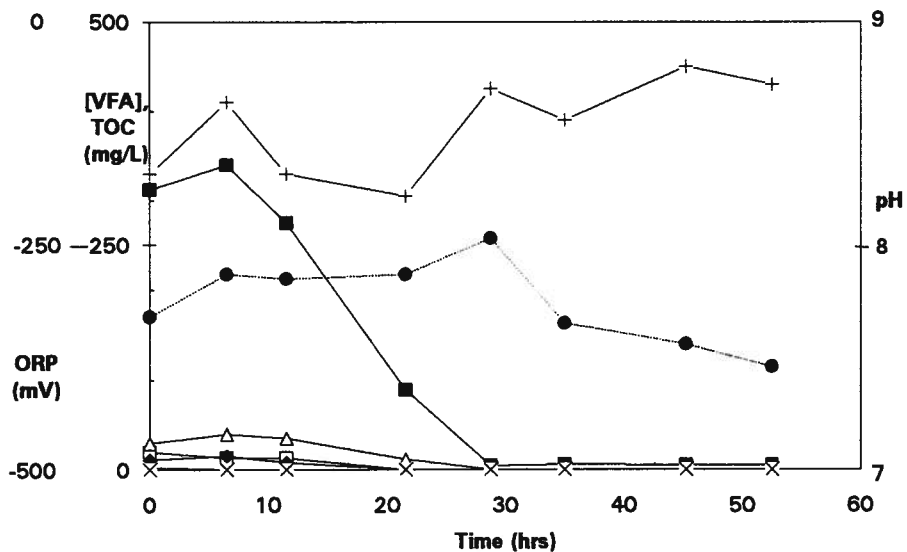
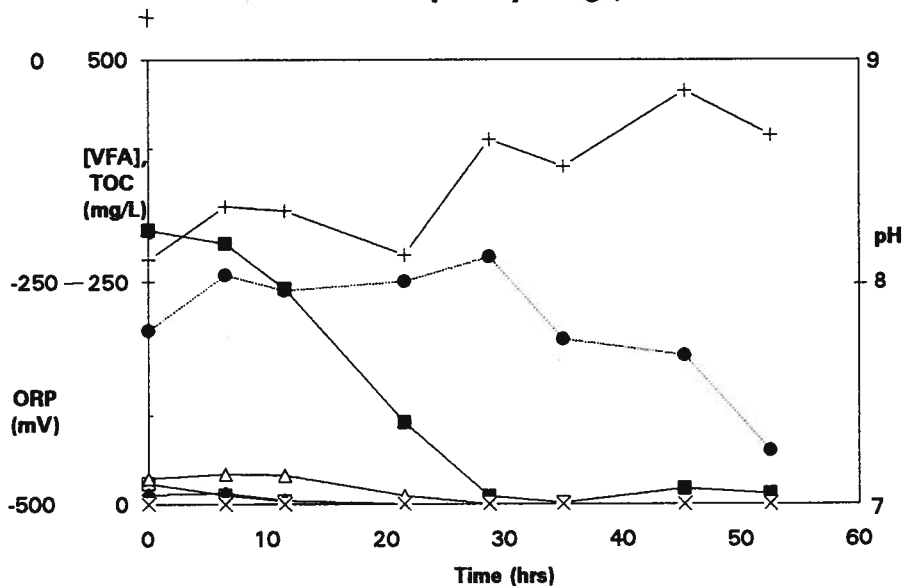


Figure A9.10: Batch Test 9: [VFA], TOC, pH, ORP v time (micro-aerobic w supernatant add'n + 270 mL A side + 30 mL primary sludge)



- acetate □ propionate ◆ isobutyrate
- ◇ butyrate ▲ 2-methylbutyrate △ isovalerate
- × valerate * lactate + TOC ● pH ○ ORP

Figure A10.1: Batch Test 10: [VFA], TOC, pH, ORP v time (anaerobic control w 1L A side and 0 mL primary sludge)

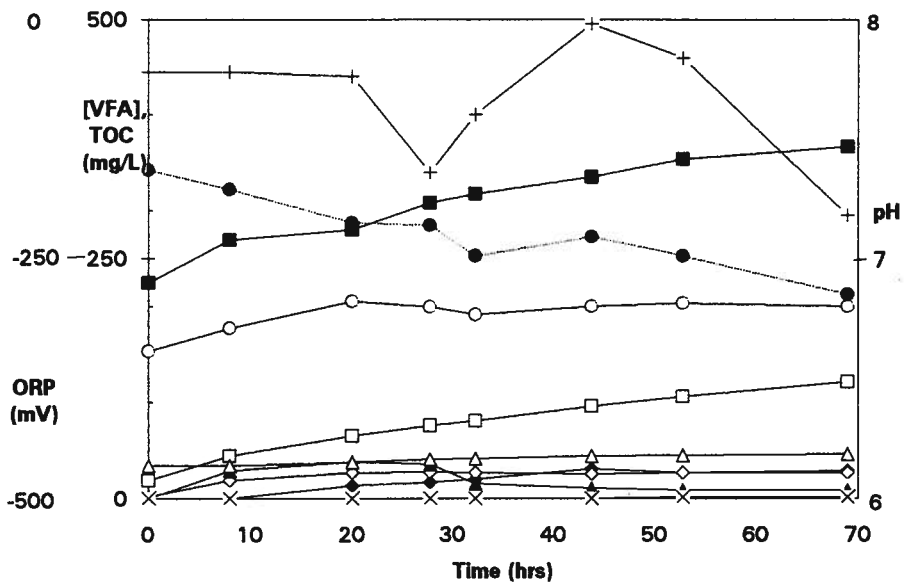
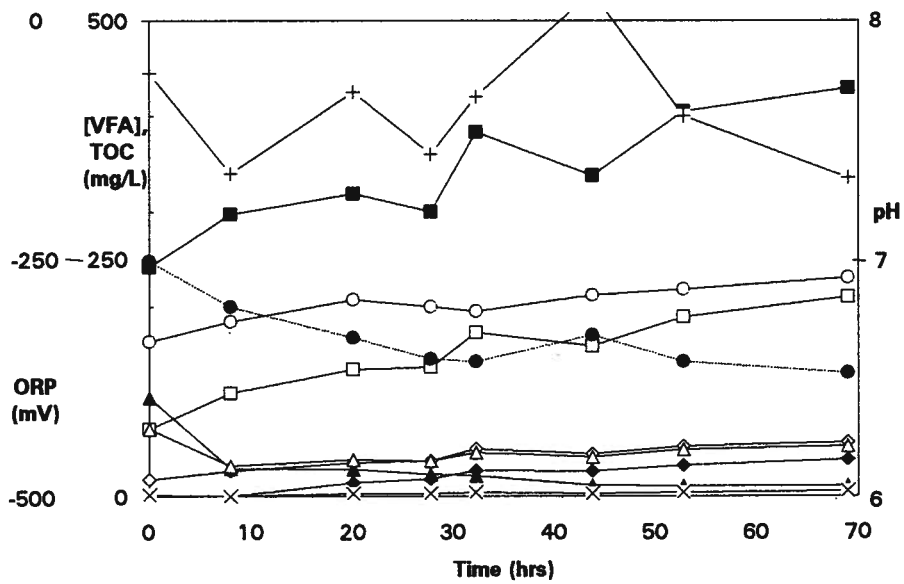


Figure A10.2: Batch Test 10: [VFA], TOC, pH, ORP v time (anaerobic w 800 mL A side + 200 mL primary sludge)



- acetate □ propionate ◆ isobutyrate
- ◇ butyrate ▲ 2-methylbutyrate △ isovalerate
- × valerate * lactate + TOC ● pH ○ ORP

Figure A10.3: Batch Test 10: [VFA], TOC, pH, ORP v time (anaerobic w 600 mL A side + 400 mL primary sludge)

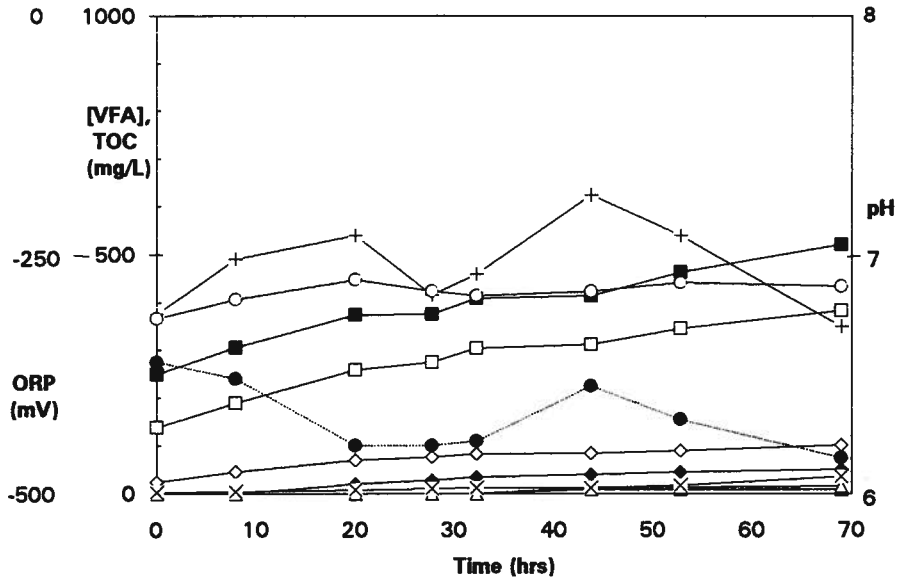
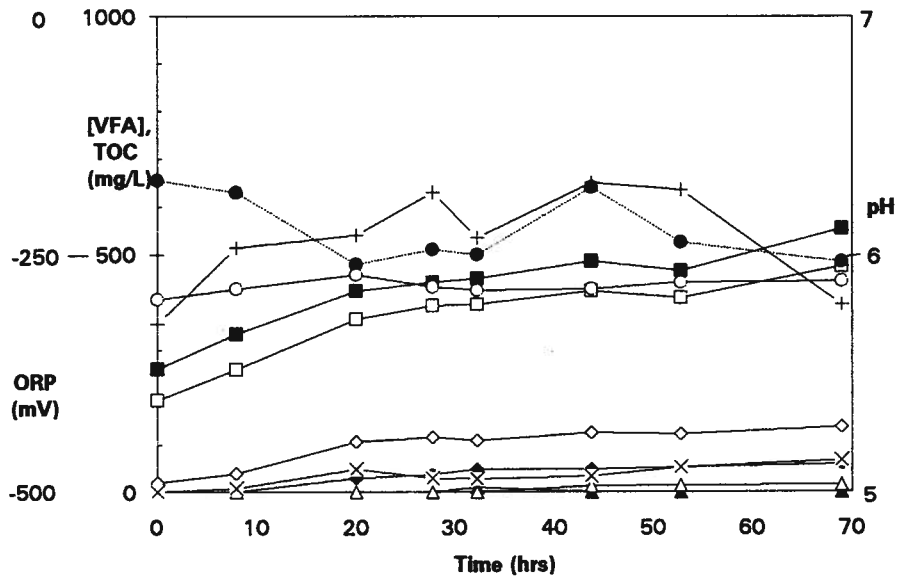


Figure A10.4: Batch Test 10: [VFA], TOC, pH, ORP v time (anaerobic w 400 mL A side + 600 mL primary sludge)



- acetate □ propionate ◆ isobutyrate
- ◇ butyrate ▲ 2-methylbutyrate △ isovalerate
- × valerate * lactate + TOC ● pH ○ ORP

Figure A10.5: Batch Test 10: [VFA], TOC, pH, ORP v time (anaerobic w 200 mL A side + 800 mL primary sludge)

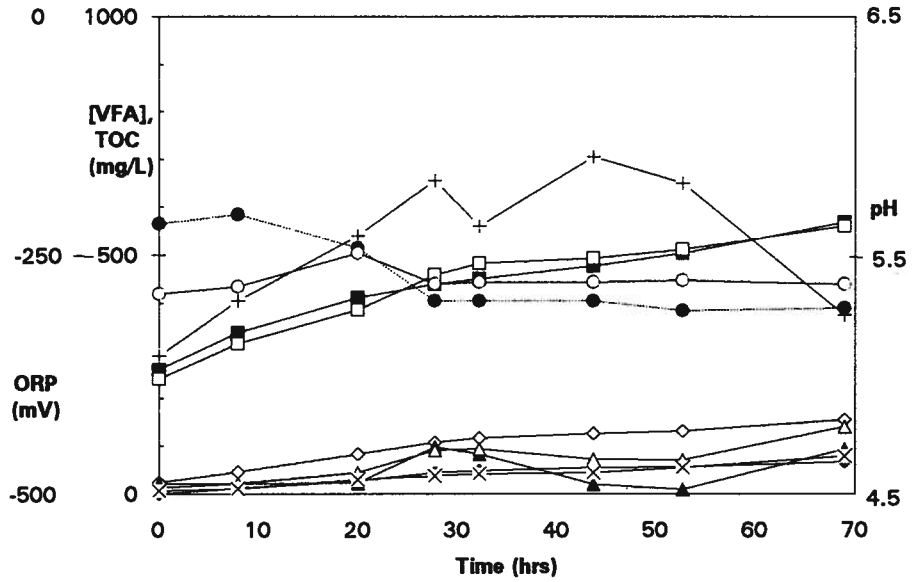
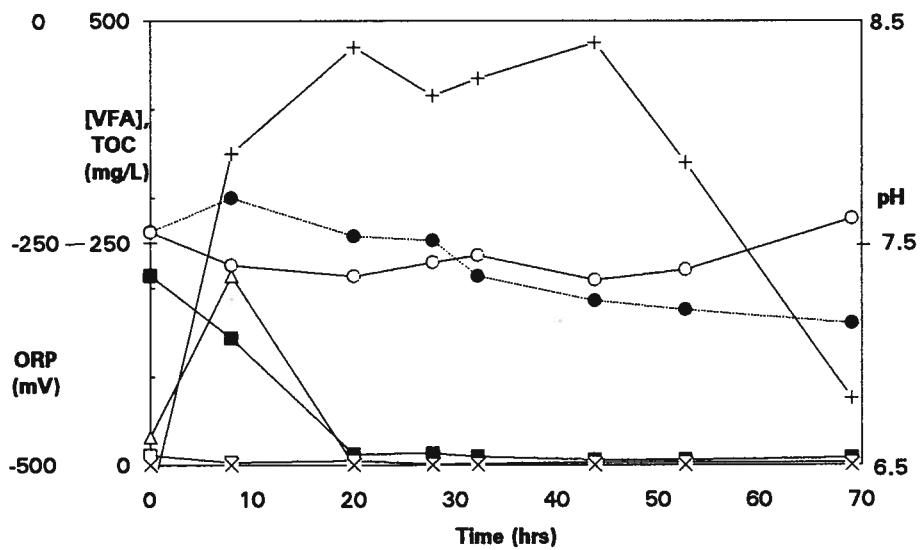


Figure A10.6: Batch Test 10: [VFA], TOC, pH, ORP v time (micro-aerobic control w 300 mL A side + 0 mL primary sludge)



- acetate □ propionate ◆ isobutyrate
- ◇ butyrate ▲ 2-methylbutyrate △ isovalerate
- × valerate × lactate + TOC ● pH ○ ORP

Figure A10.7: Batch Test 10: [VFA], TOC, pH, ORP v time
(micro-aerobic w 240 mL A side + 60 mL primary sludge)

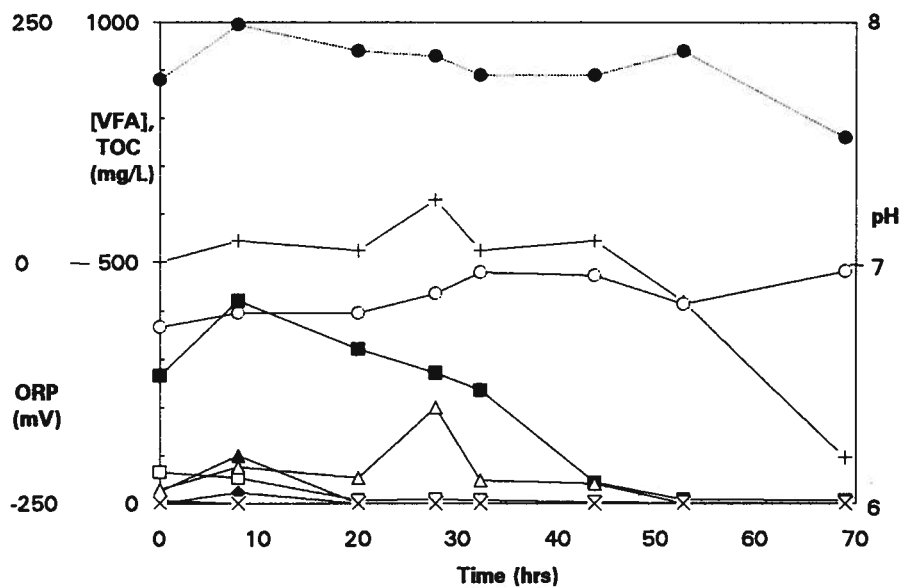
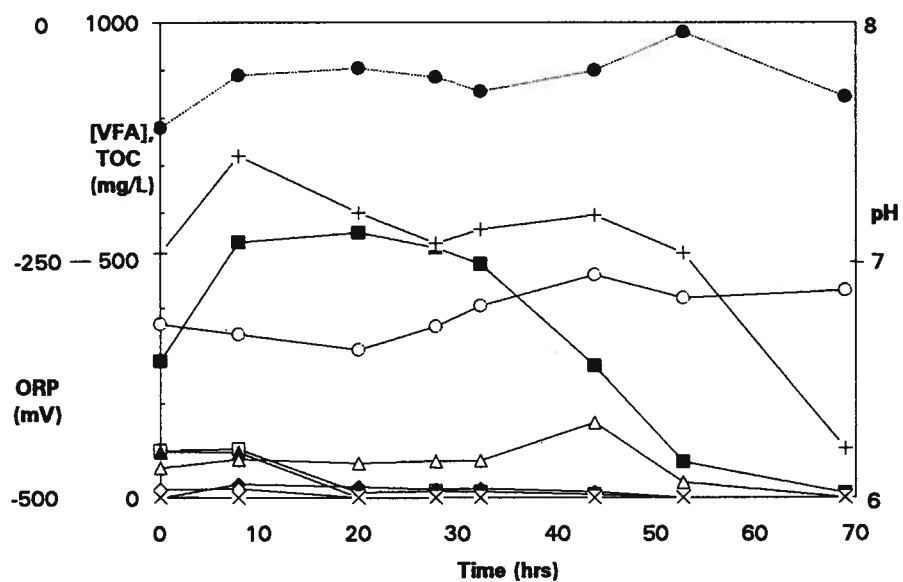


Figure A10.8: Batch Test 10: [VFA], TOC, pH, ORP v time
(micro-aerobic w 180 mL A side + 120 mL primary sludge)



■ acetate □ propionate ◆ isobutyrate
 ◇ butyrate ▲ 2-methylbutyrate △ isovalerate
 × valerate * lactate + TOC ● pH ○ ORP

Figure A10.9: Batch Test 10: [VFA], TOC, pH, ORP v time (micro-aerobic w 120 mL A side + 180 mL primary sludge)

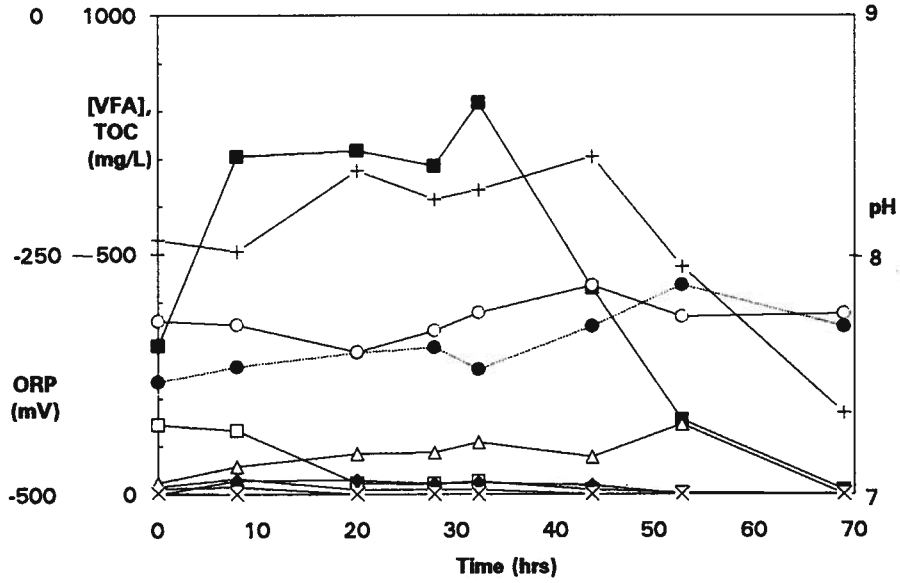
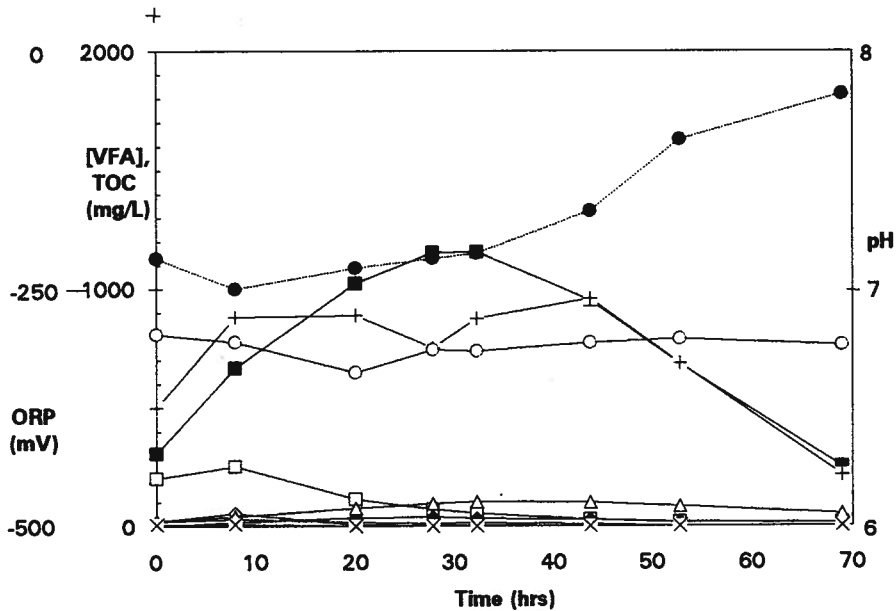


Figure A10.10: Batch Test 10: [VFA], TOC, pH, ORP v time (micro-aerobic w 60 mL A side + 240 mL primary sludge)



- acetate □ propionate ◆ isobutyrate
- ◇ butyrate ▲ 2-methylbutyrate △ isovalerate
- × valerate * lactate + TOC ● pH ○ ORP

Figure A10.11: Batch Test 10: [VFA], TOC, pH, ORP v time (anaerobic control w 1L fermenter and 0 mL primary sludge)

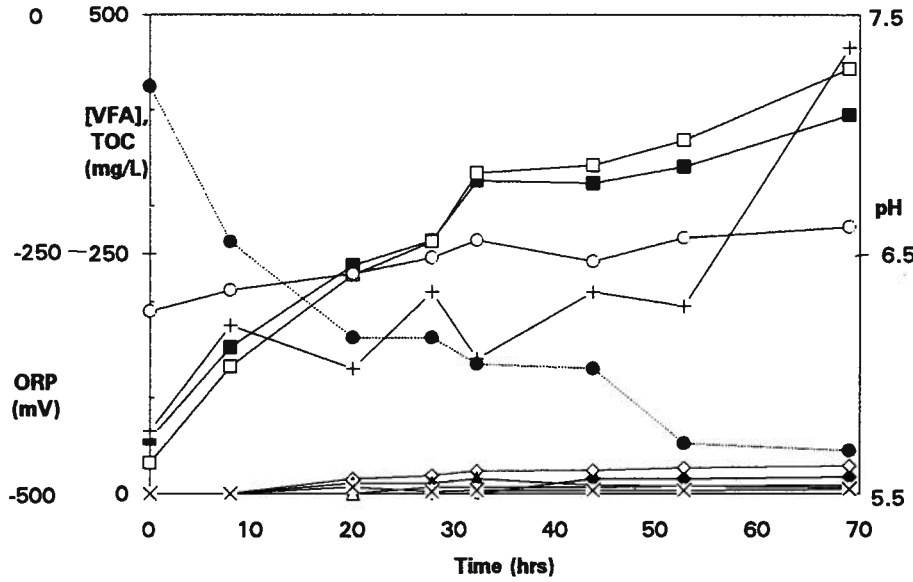
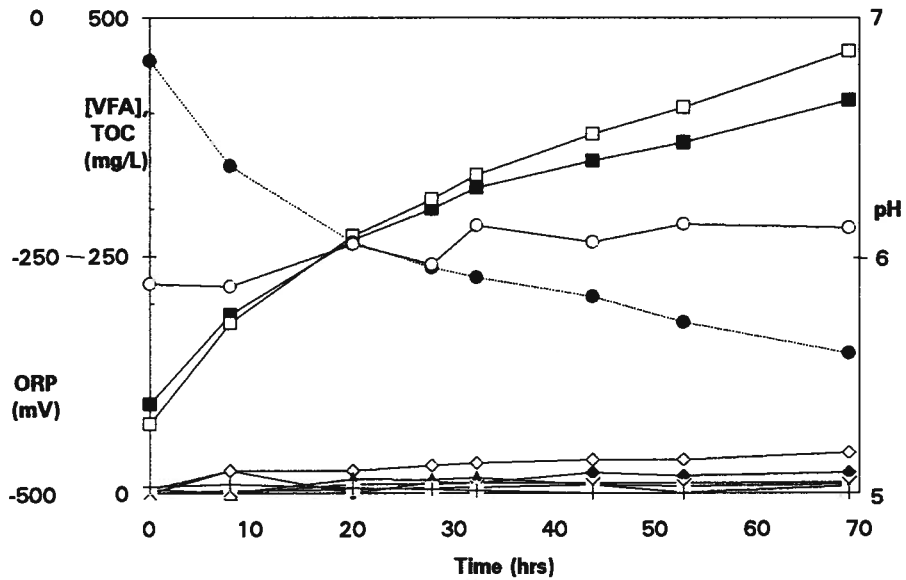


Figure A10.12: Batch Test 10: [VFA], TOC, pH, ORP v time (anaerobic w 800 mL fermenter + 200 mL primary sludge)



- acetate □ propionate ◆ isobutyrate
- ◇ butyrate ▲ 2-methylbutyrate △ isovalerate
- × valerate * lactate + TOC ● pH ○ ORP

Figure A10.13: Batch Test 10: [VFA], TOC, pH, ORP v time (anaerobic w 600 mL fermenter + 400 mL primary sludge)

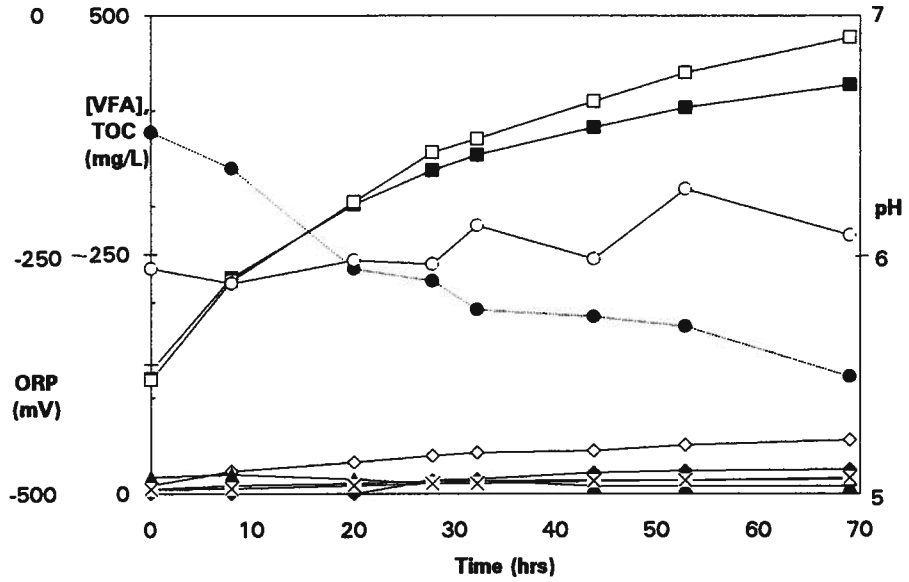
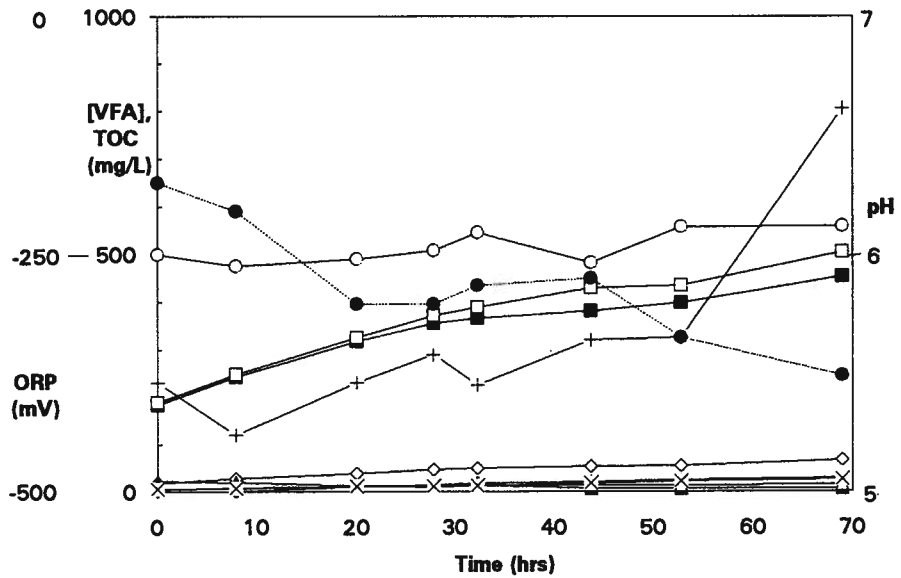


Figure A10.14: Batch Test 10: [VFA], TOC, pH, ORP v time (anaerobic w 400 mL fermenter + 600 mL primary sludge)



- acetate □ propionate ◆ isobutyrate
- ◇ butyrate ▲ 2-methylbutyrate △ isovalerate
- × valerate * lactate + TOC ● pH ○ ORP

Figure A10.15: Batch Test 10: [VFA], TOC, pH, ORP v time (anaerobic w 200 mL fermenter + 800 mL primary sludge)

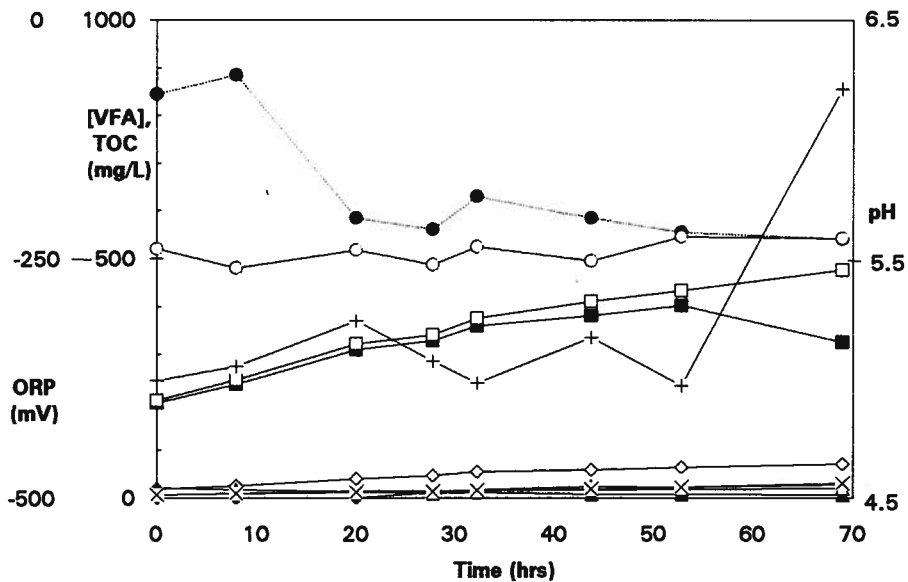
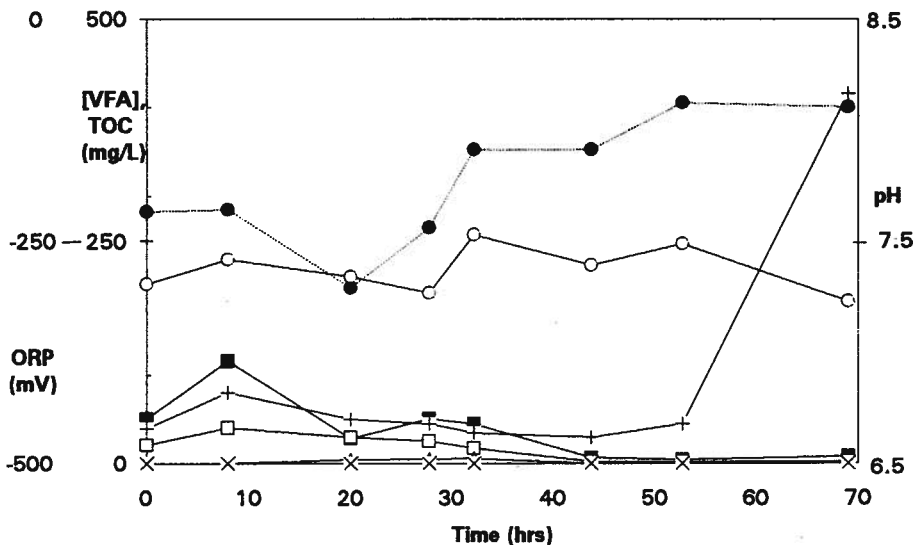


Figure A10.16: Batch Test 10: [VFA], TOC, pH, ORP v time (micro-aerobic control w 300 mL fermenter + 0 mL primary sludge)



- acetate □ propionate ◆ isobutyrate
- ◇ butyrate ▲ 2-methylbutyrate △ isovalerate
- × valerate * lactate + TOC ● pH ○ ORP

Figure A10.17: Batch Test 10: [VFA], TOC, pH, ORP v time
(micro-aerobic w 240 mL fermenter + 60 mL primary sludge)

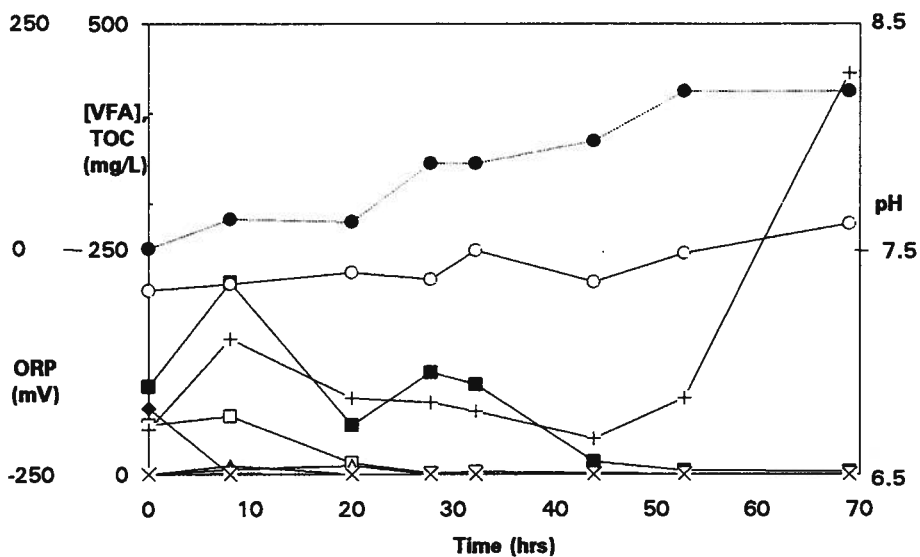
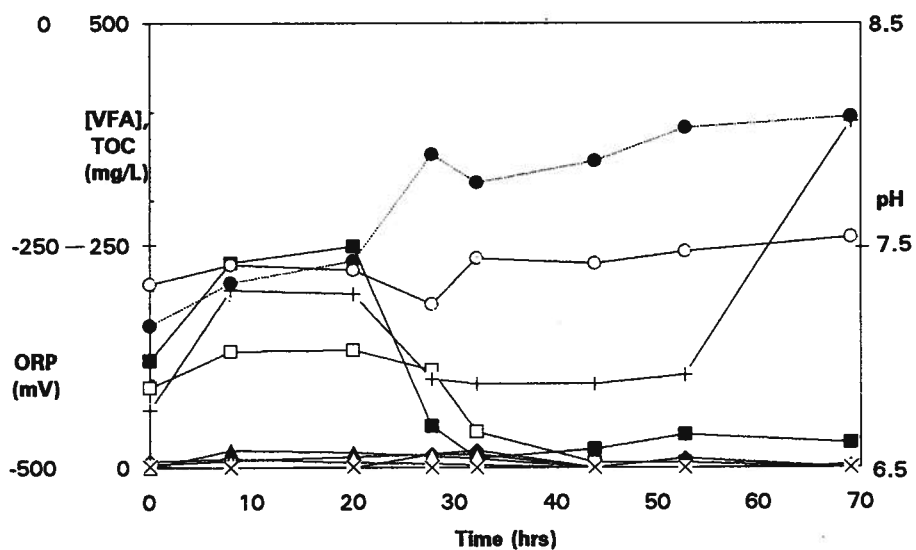


Figure A10.18: Batch Test 10: [VFA], TOC, pH, ORP v time
(micro-aerobic w 180 mL fermenter + 120 mL primary sludge)



■ acetate □ propionate ◆ isobutyrate
 ◇ butyrate ▲ 2-methylbutyrate △ isovalerate
 × valerate * lactate + TOC ● pH ○ ORP

Figure A10.19: Batch Test 10: [VFA], TOC, pH, ORP v time (micro-aerobic w 120 mL fermenter + 180 mL primary sludge)

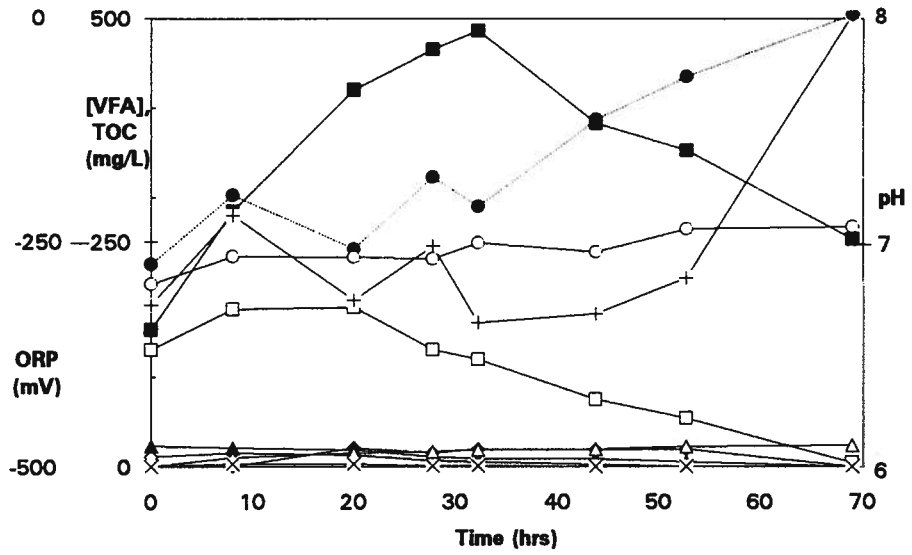
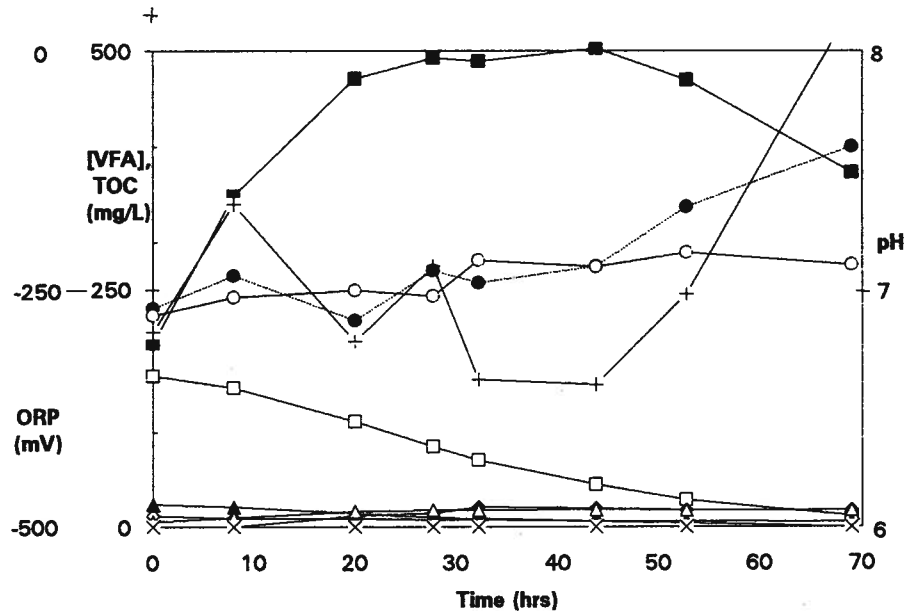


Figure A10.20: Batch Test 10: [VFA], TOC, pH, ORP v time (micro-aerobic w 60 mL fermenter + 240 mL primary sludge)



- acetate □ propionate ◆ isobutyrate
- ◇ butyrate ▲ 2-methylbutyrate △ isovalerate
- × valerate * lactate + TOC ● pH ○ ORP

Figure A11.1: Batch Test 11: [VFA], TOC, pH, ORP v time (anaerobic control w 1L A side sludge)

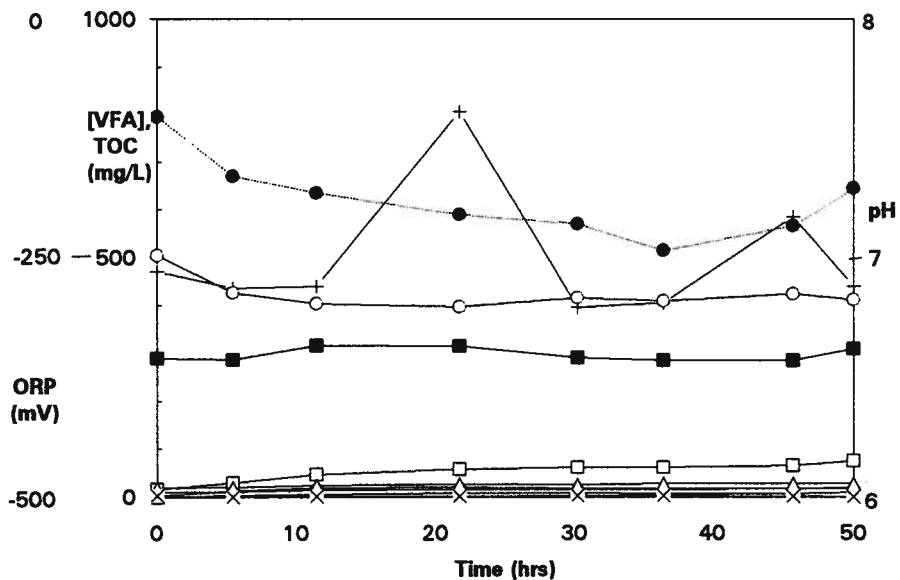
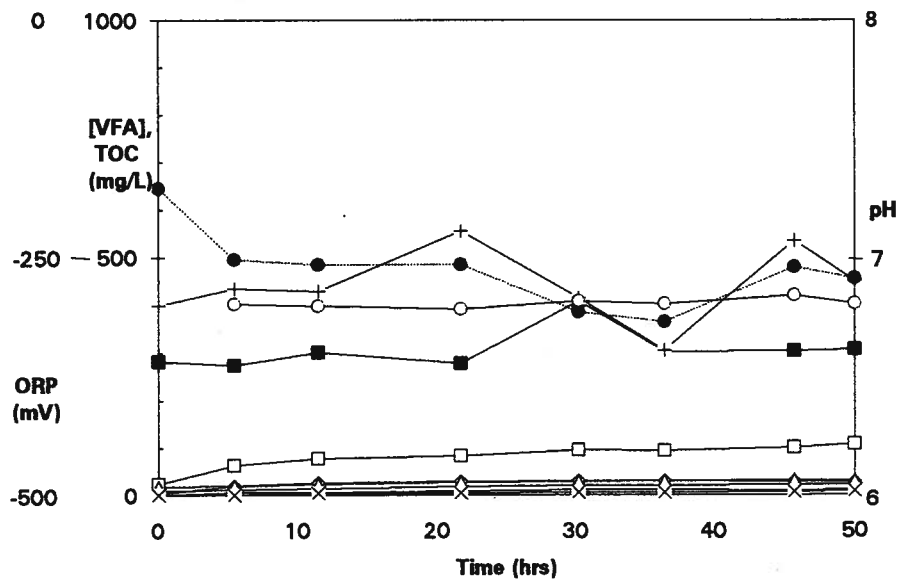


Figure A11.2: Batch Test 11: [VFA], TOC, pH, ORP v time (anaerobic A side w 25% primary sludge)



■ acetate □ propionate ◆ isobutyrate
 ◇ butyrate ▲ 2-methylbutyrate △ isovalerate
 × valerate * lactate + TOC ● pH ○ ORP

Figure A11.3: Batch Test 11: [VFA], TOC, pH, ORP v time (anaerobic control w 1 L B side sludge)

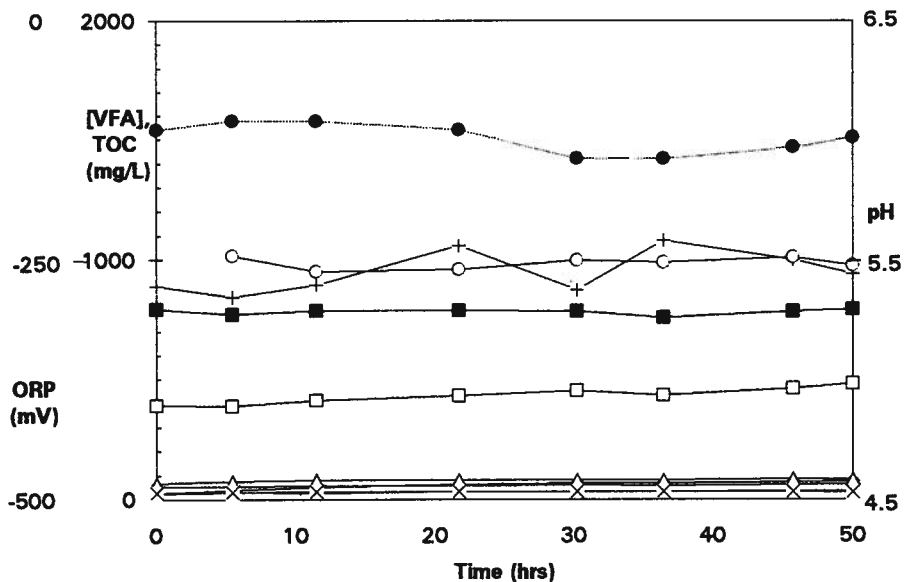
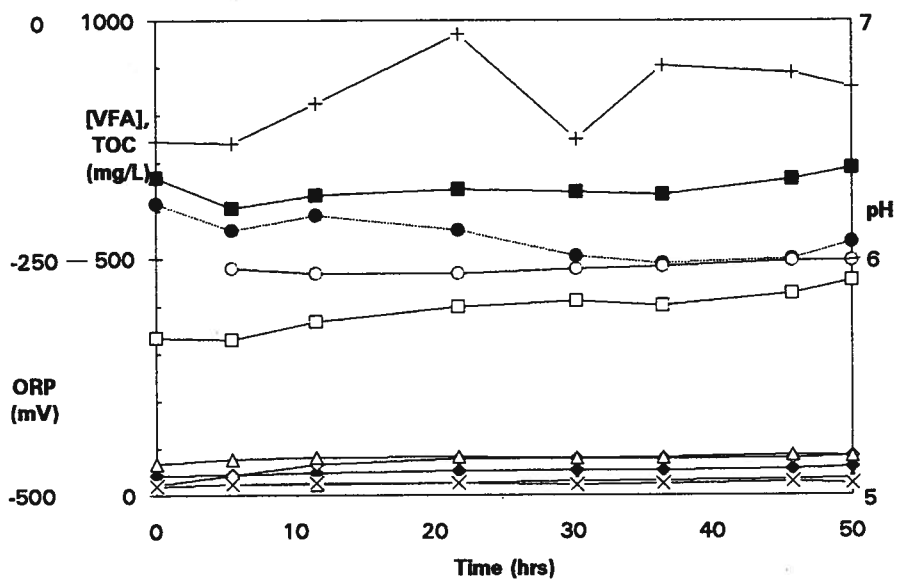


Figure A11.4: Batch Test 11: [VFA], TOC, pH, ORP v time (anaerobic B side w 25% primary sludge)



- acetate □ propionate ◆ isobutyrate
- ◇ butyrate ▲ 2-methylbutyrate △ isovalerate
- × valerate * lactate + TOC ● pH ○ ORP

Figure A11.5: Batch Test 11: [VFA], TOC, pH, ORP v time (micro-aerobic A side w 25% primary sludge)

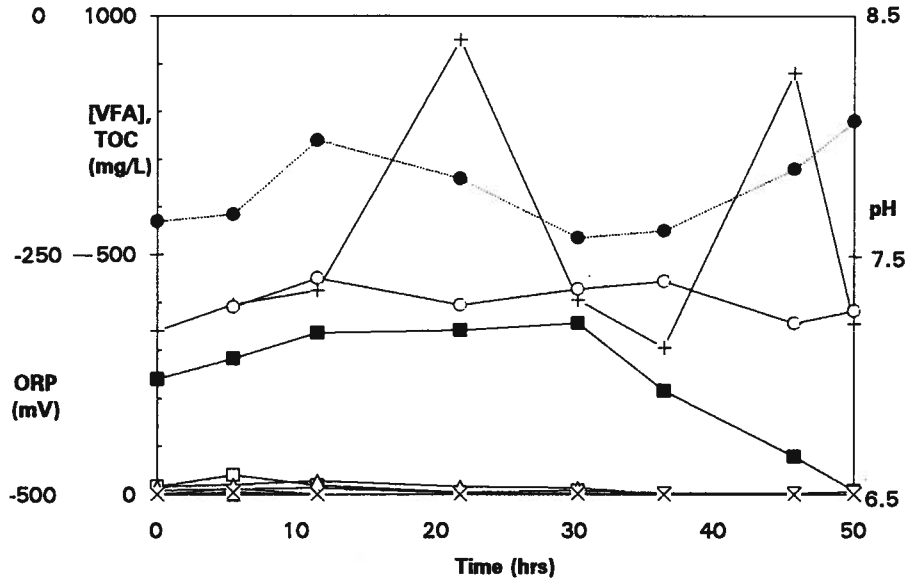
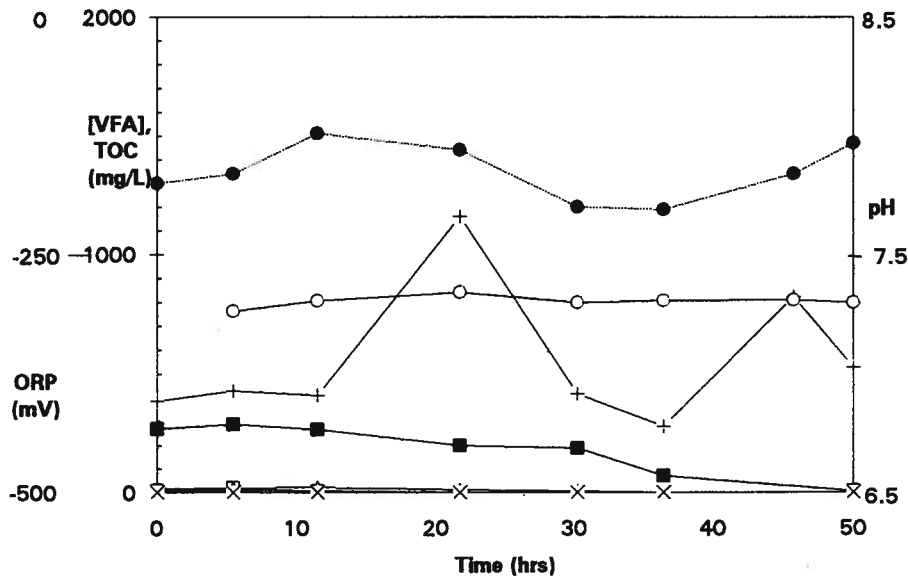


Figure A11.6: Batch Test 11: [VFA], TOC, pH, ORP v time (micro-aerobic control w 1L A side sludge)



- acetate □ propionate ◆ isobutyrate
- ◇ butyrate ▲ 2-methylbutyrate △ isovalerate
- × valerate * lactate + TOC ● pH ○ ORP

Figure A11.7: Batch Test 11: [VFA], TOC, pH, ORP v time (micro-aerobic A side w 50% primary sludge)

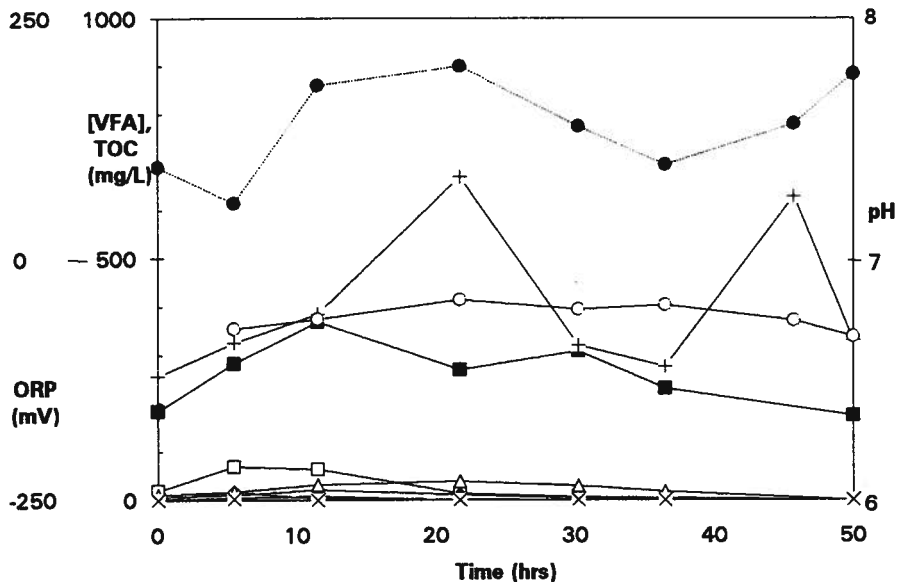
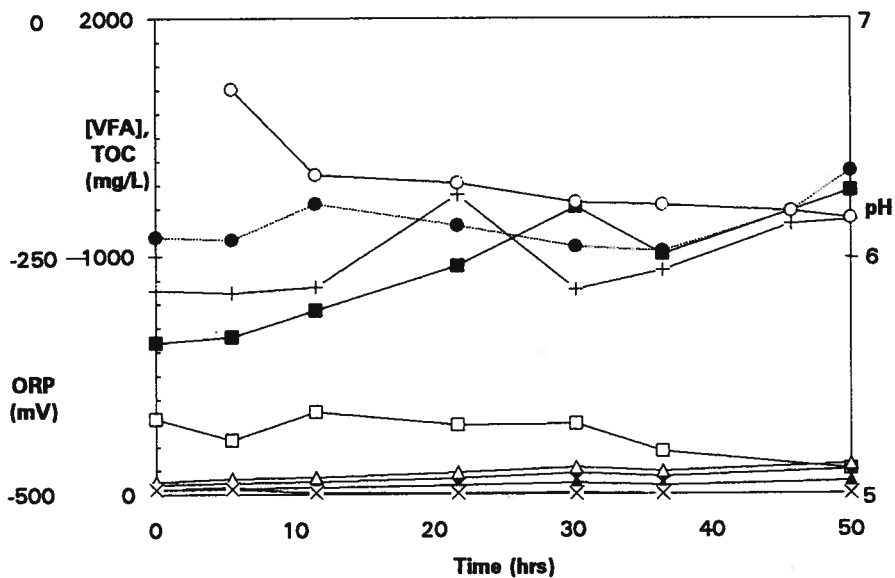


Figure A11.8: Batch Test 11: [VFA], TOC, pH, ORP v time (micro-aerobic control w 1 L B side sludge)



- acetate □ propionate ◆ isobutyrate
- ◇ butyrate ▲ 2-methylbutyrate △ isovalerate
- × valerate * lactate + TOC ● pH ○ ORP

Figure A11.9: Batch Test 11: [VFA], TOC, pH, ORP v time (micro-aerobic B side w 50% primary sludge)

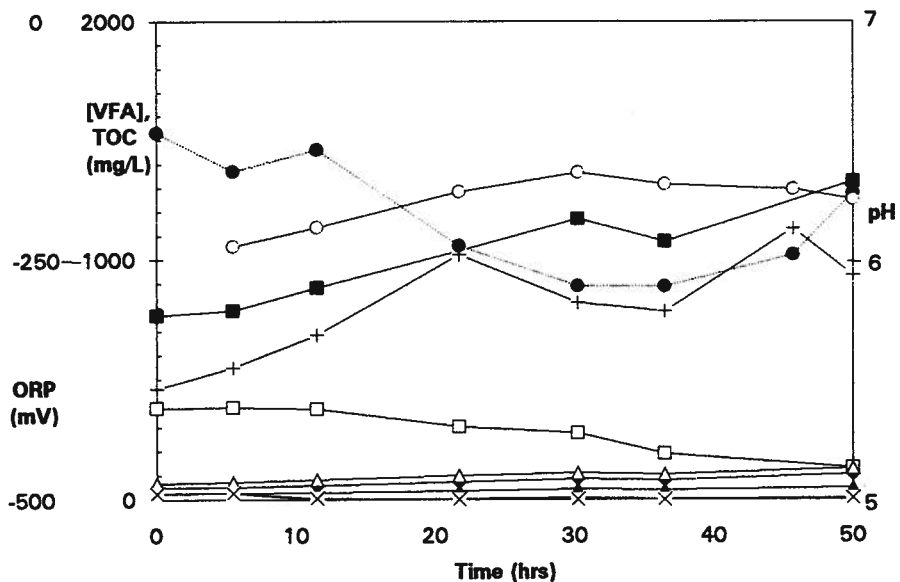
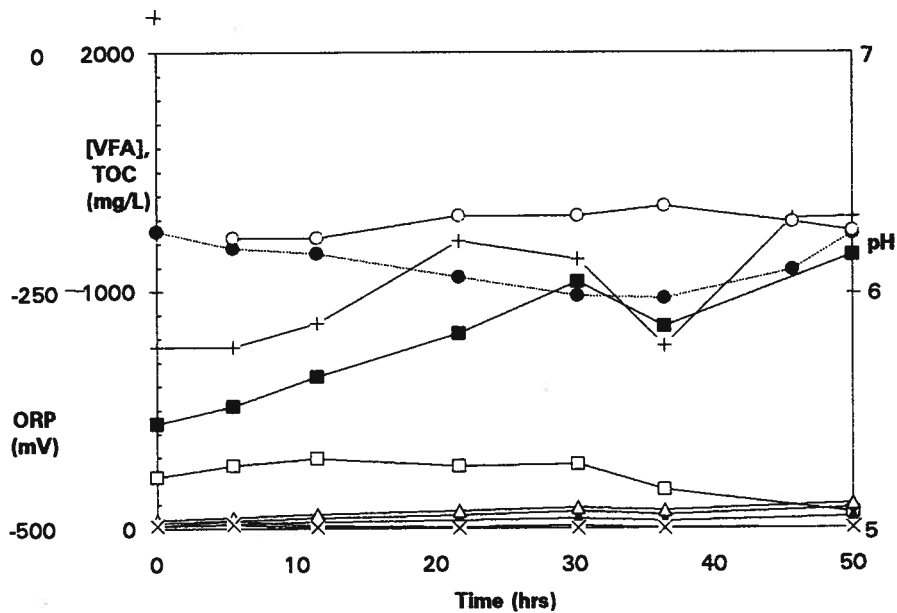


Figure A11.10: Batch Test 11: [VFA], TOC, pH, ORP v time (micro-aerobic B side w 25% primary sludge)



- acetate □ propionate ◆ isobutyrate
- ◇ butyrate ▲ 2-methylbutyrate △ isovalerate
- × valerate * lactate + TOC ● pH ○ ORP

Figure A12.1: Salmon Arm 1st stage ATAD: [VFA], TOC, pH, ORP v time (anaerobic control)

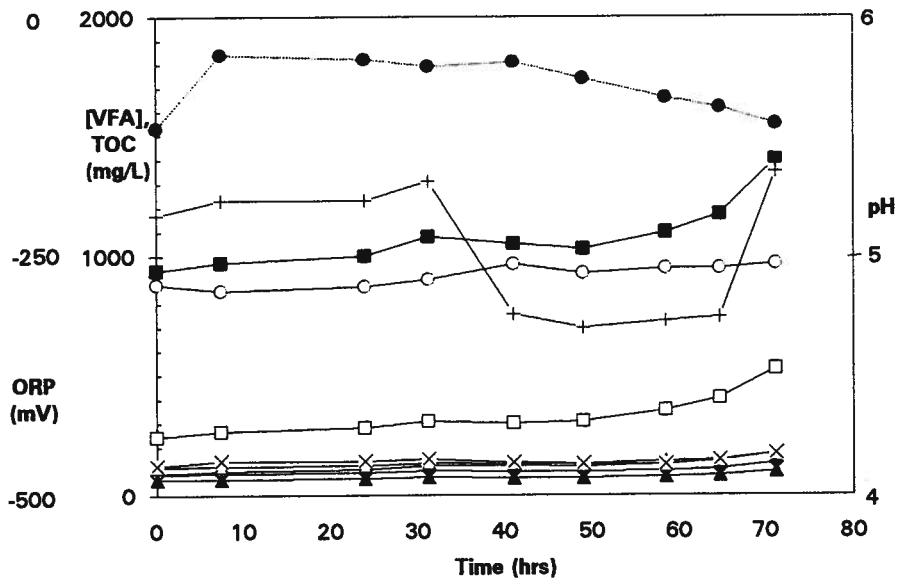
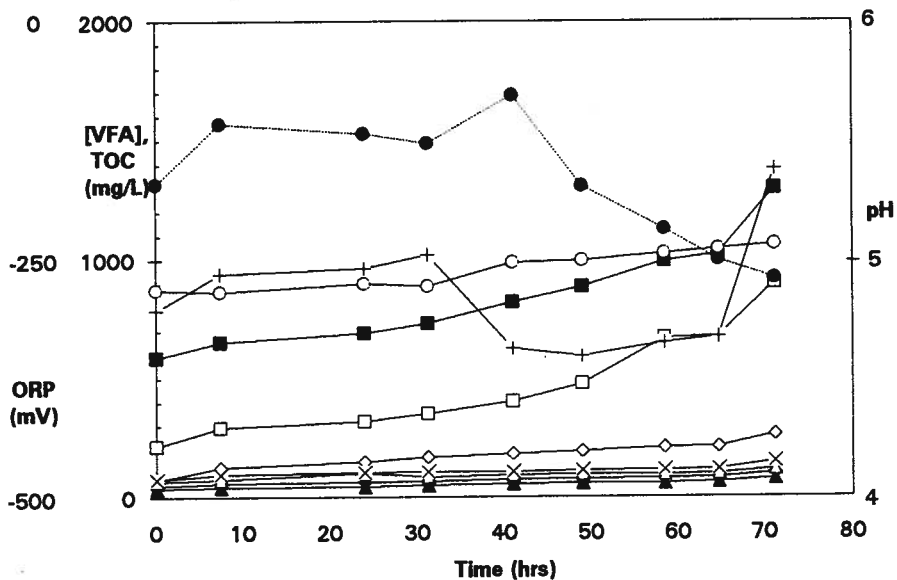


Figure A12.2: Salmon Arm 1st stage ATAD: [VFA], TOC, pH, ORP v time (anaerobic w 50% primary sludge)



- acetate □ propionate ◆ isobutyrate
- ◇ butyrate ▲ 2-methylbutyrate △ isovalerate
- × valerate * lactate + TOC ● pH ○ ORP

Figure A12.3: Salmon Arm 1st stage ATAD: [VFA], TOC, pH, ORP v time (anaerobic w 50% secondary sludge)

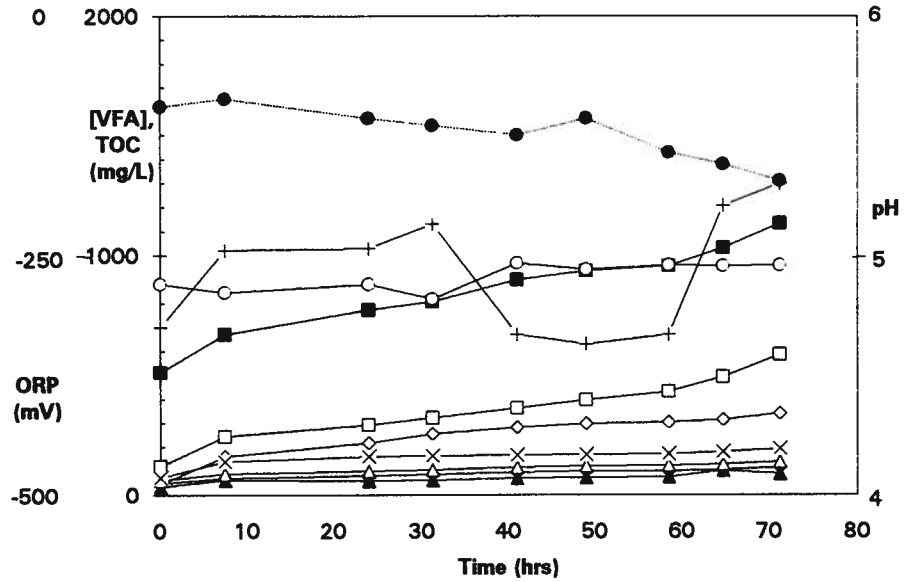
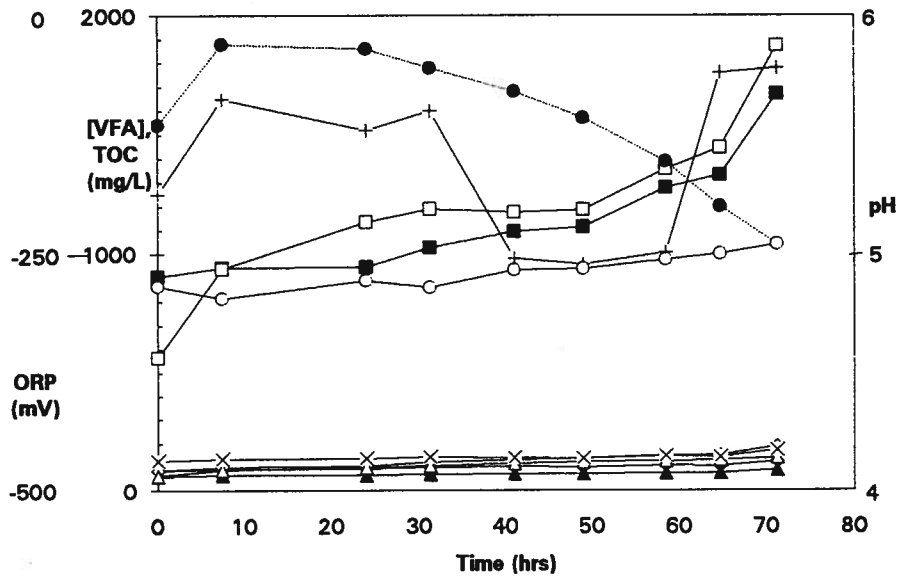


Figure A12.4: Salmon Arm 1st stage ATAD: [VFA], TOC, pH, ORP v time (anaerobic w propionate add'n)



- acetate □ propionate ◆ isobutyrate
- ◇ butyrate ▲ 2-methylbutyrate △ isovalerate
- × valerate * lactate + TOC ● pH ○ ORP

Figure A12.5: Salmon Arm 1st stage ATAD: [VFA], TOC, pH, ORP v time (anaerobic w mixed secondary and primary sludge)

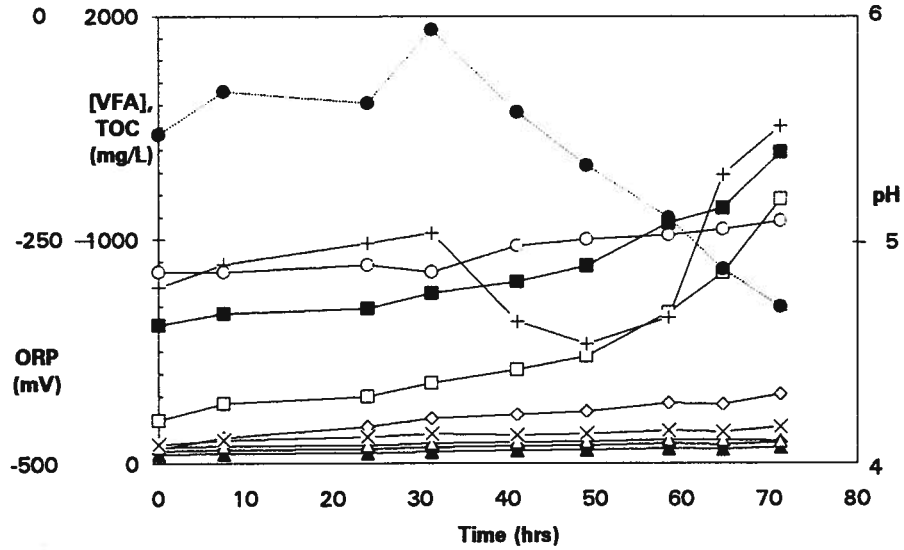
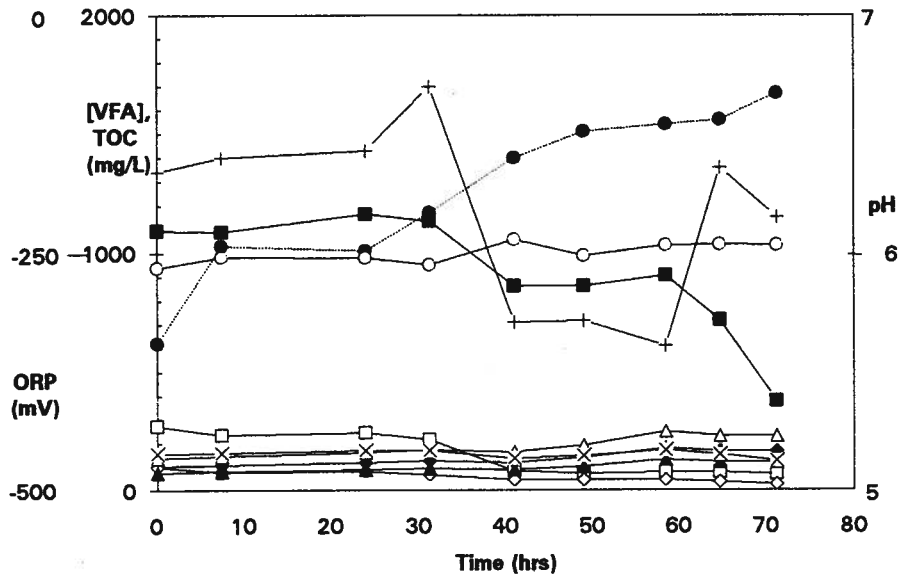


Figure A12.6: Salmon Arm 1st stage ATAD: [VFA], TOC, pH, ORP v time (micro-aerobic control)



- acetate □ propionate ◆ isobutyrate
- ◇ butyrate ▲ 2-methylbutyrate △ isovalerate
- × valerate * lactate + TOC ● pH ○ ORP

Figure A12.7: Salmon Arm 1st stage ATAD: [VFA], TOC, pH, ORP v time (micro-aerobic w 50% primary sludge)

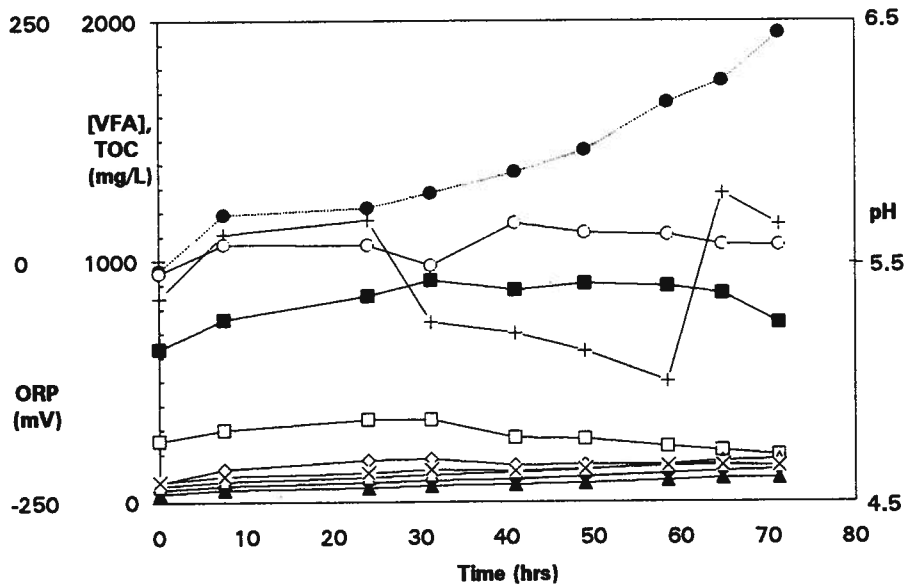
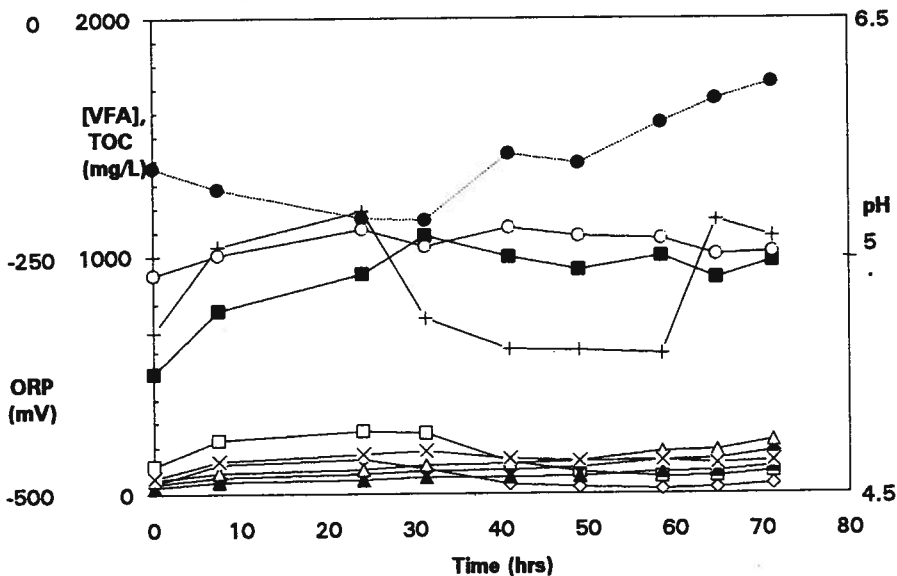


Figure A12.8: Salmon Arm 1st stage ATAD: [VFA], TOC, pH, ORP v time (micro-aerobic w 50% secondary sludge)



- acetate □ propionate ◆ isobutyrate
- ◇ butyrate ▲ 2-methylbutyrate △ isovalerate
- × valerate * lactate + TOC ● pH ○ ORP

Figure A12.9: Salmon Arm 1st stage ATAD: [VFA], TOC, pH, ORP v time (micro-aerobic w propionate add'n)

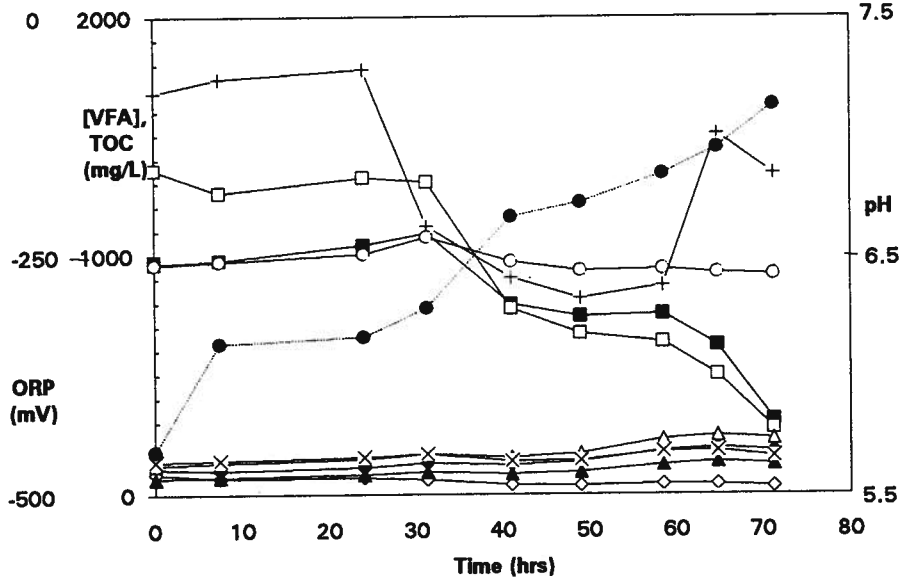
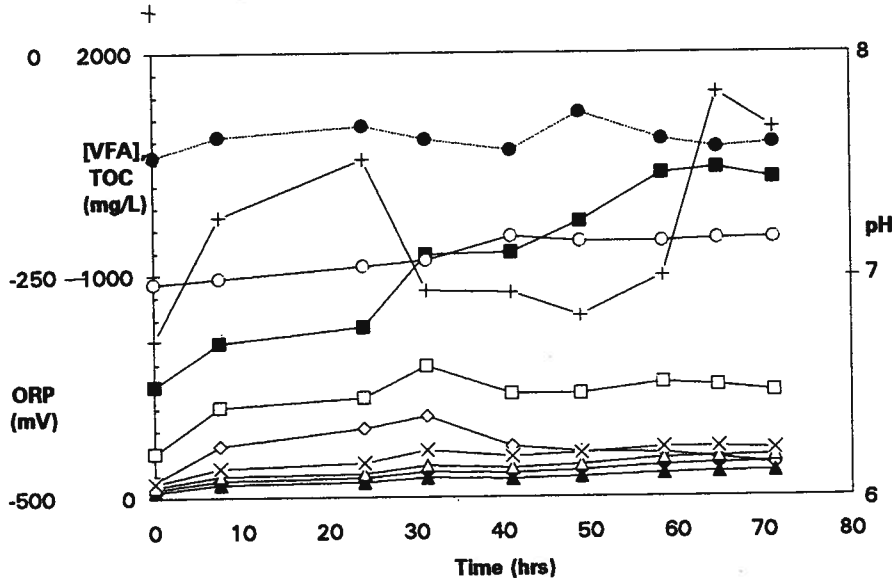


Figure A12.10: Salmon Arm 1st stage ATAD: [VFA], TOC, pH, ORP v time (micro-aerobic w mixed secondary and primary sludge)



- acetate □ propionate ◆ isobutyrate
- ◇ butyrate ▲ 2-methylbutyrate △ isovalerate
- × valerate * lactate + TOC ● pH ○ ORP

Figure A13.1: Salmon Arm 3rd stage ATAD: [VFA], TOC, pH, ORP v time (anaerobic control)

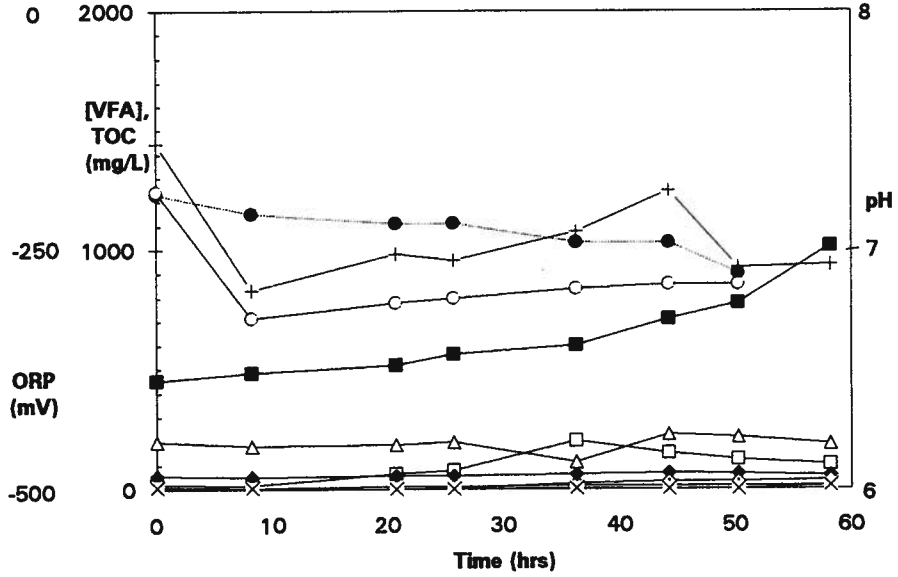
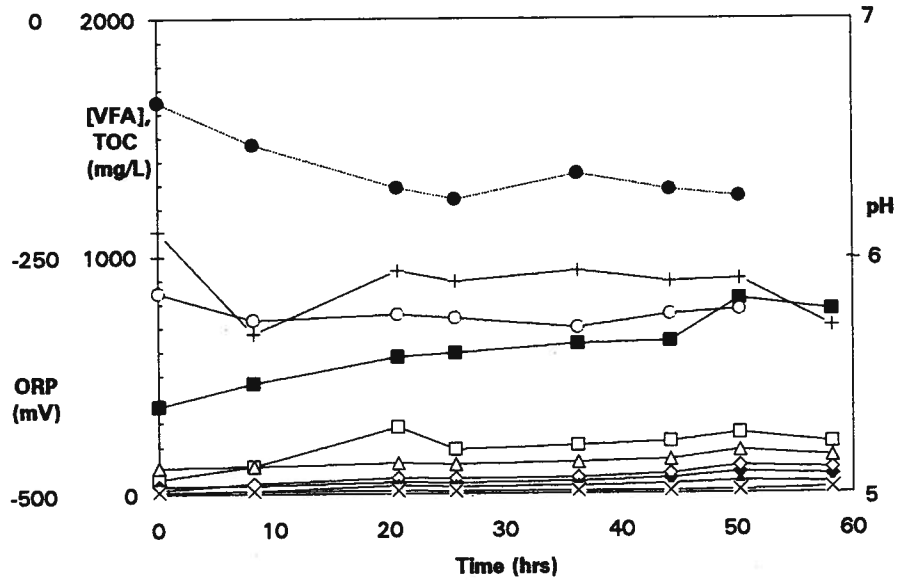


Figure A13.2: Salmon Arm 3rd stage ATAD: [VFA], TOC, pH, ORP v time (anaerobic w 50% primary sludge)



- acetate □ propionate ◆ isobutyrate
- ◇ butyrate ▲ 2-methylbutyrate △ isovalerate
- × valerate * lactate + TOC ● pH ○ ORP

Figure A13.3: Salmon Arm 3rd stage ATAD: [VFA], TOC, pH, ORP v time (anaerobic w 50% secondary sludge)

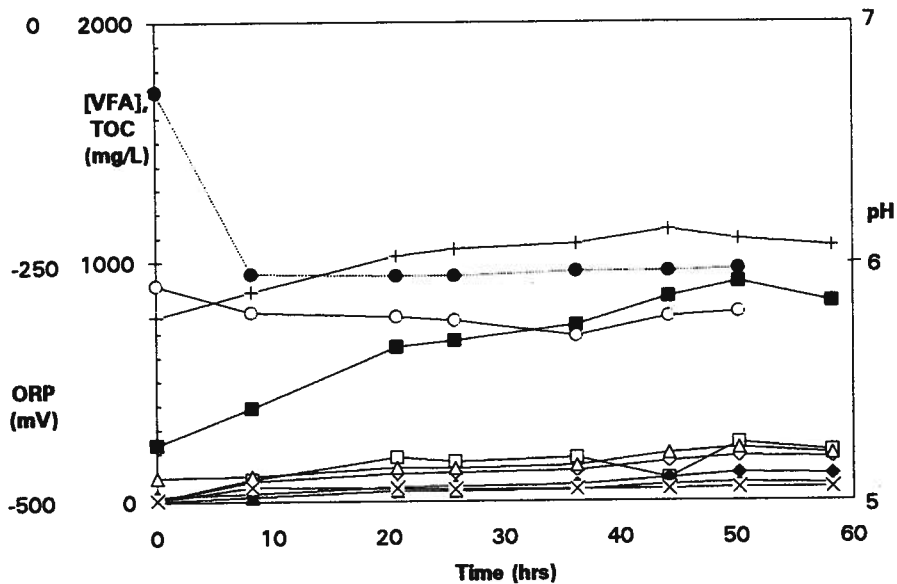
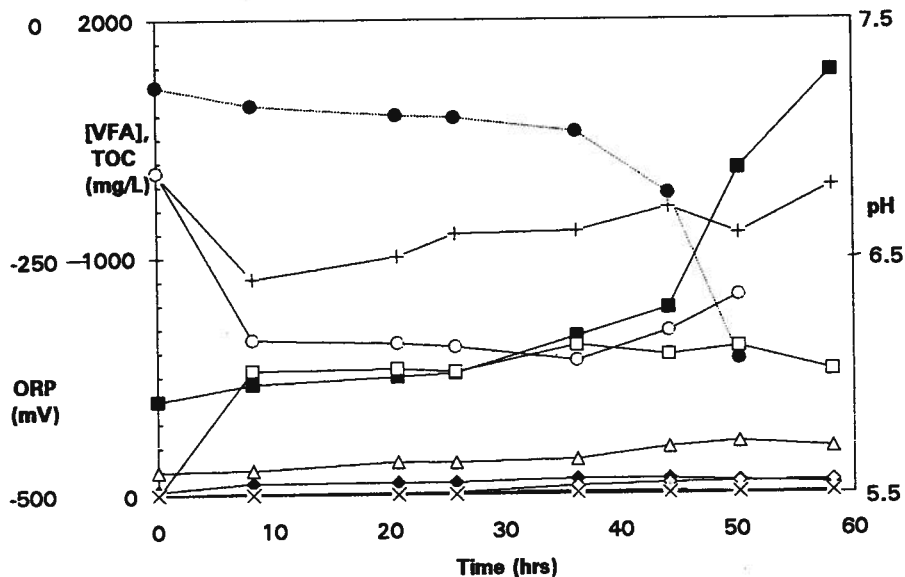


Figure A13.4: Salmon Arm 3rd stage ATAD: [VFA], TOC, pH, ORP v time (anaerobic w propionate add'n)



- acetate □ propionate ◆ isobutyrate
- ◇ butyrate ▲ 2-methylbutyrate △ isovalerate
- × valerate × lactate + TOC ● pH ○ ORP

Figure A13.5: Salmon Arm 3rd stage ATAD: [VFA], TOC, pH, ORP v time (anaerobic w mixed secondary and primary sludge)

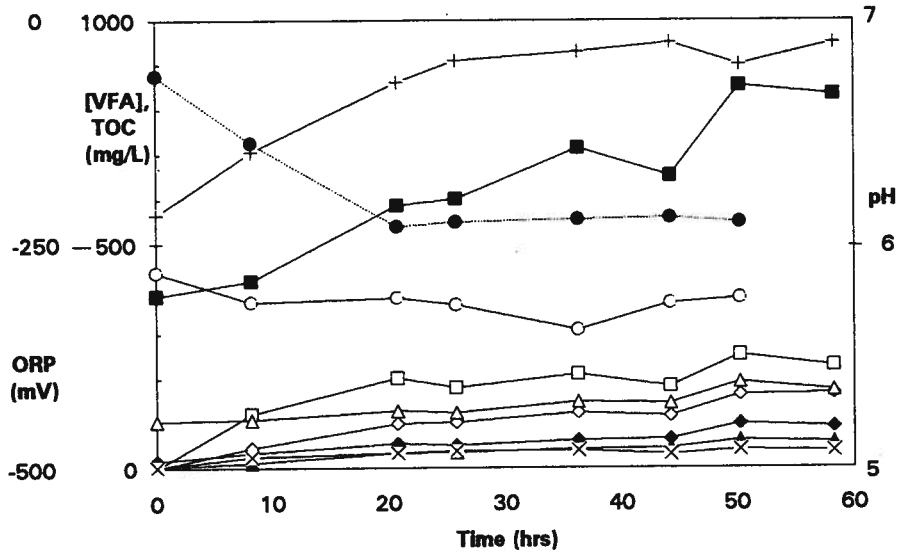
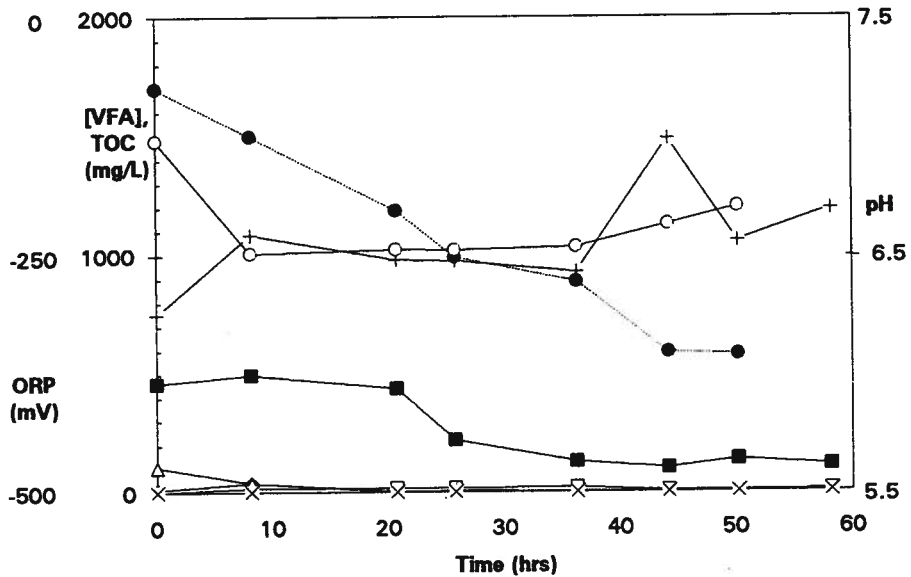


Figure A13.6: Salmon Arm 3rd stage ATAD: [VFA], TOC, pH, ORP v time (micro-aerobic control)



- acetate □ propionate ◆ isobutyrate
- ◇ butyrate ▲ 2-methylbutyrate △ isovalerate
- × valerate × lactate + TOC ● pH ○ ORP

Figure A13.7: Salmon Arm 3rd stage ATAD: [VFA], TOC, pH, ORP v time (micro-aerobic w 50% primary sludge)

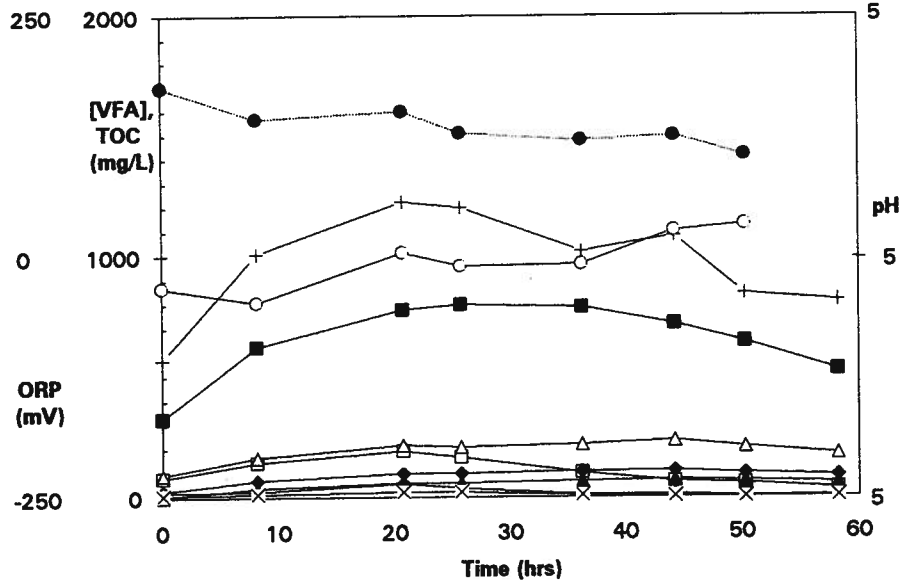
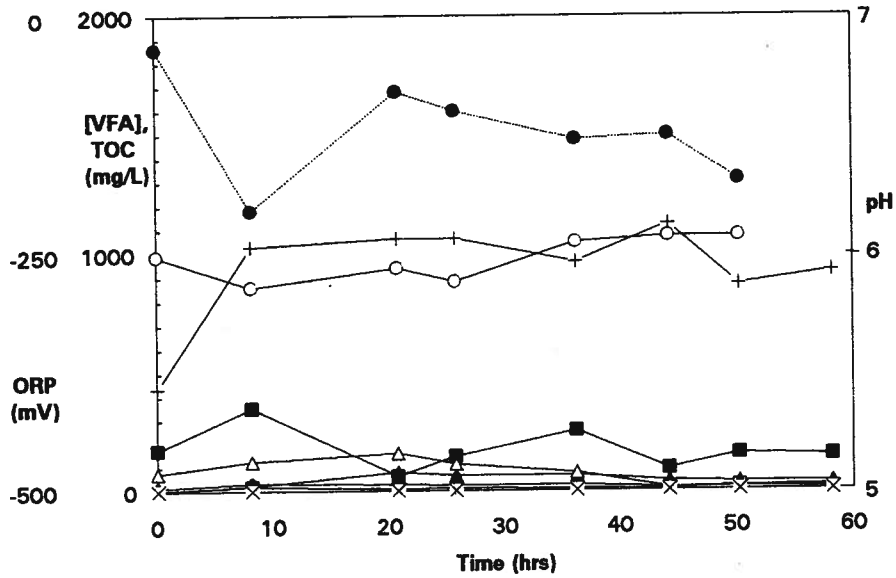


Figure A13.8: Salmon Arm 3rd stage ATAD: [VFA], TOC, pH, ORP v time (micro-aerobic w 50% secondary sludge)



- acetate □ propionate ◆ isobutyrate
- ◇ butyrate ▲ 2-methylbutyrate △ isovalerate
- × valerate * lactate + TOC ● pH ○ ORP

Figure A13.9: Salmon Arm 3rd stage ATAD: [VFA], TOC, pH, ORP v time (micro-aerobic w propionate add'n)

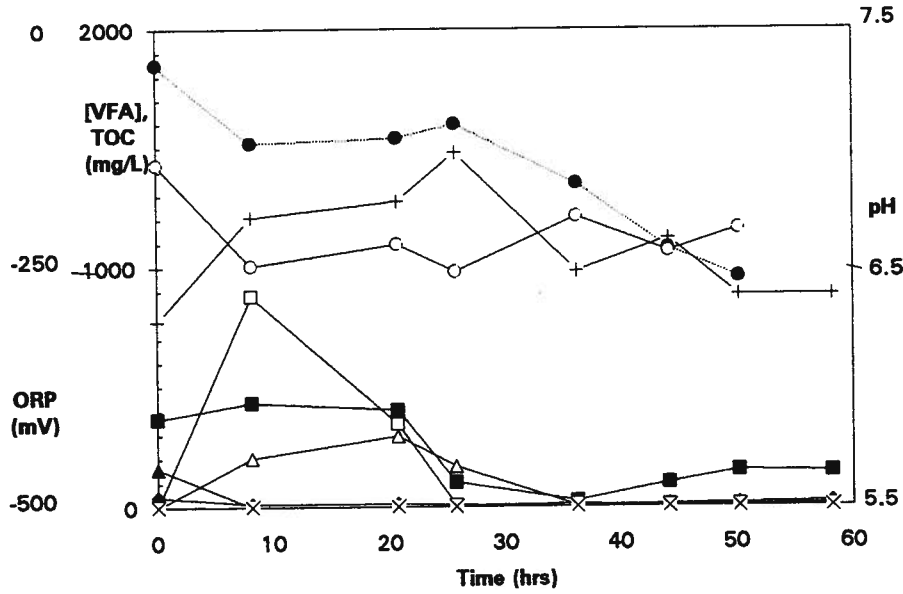
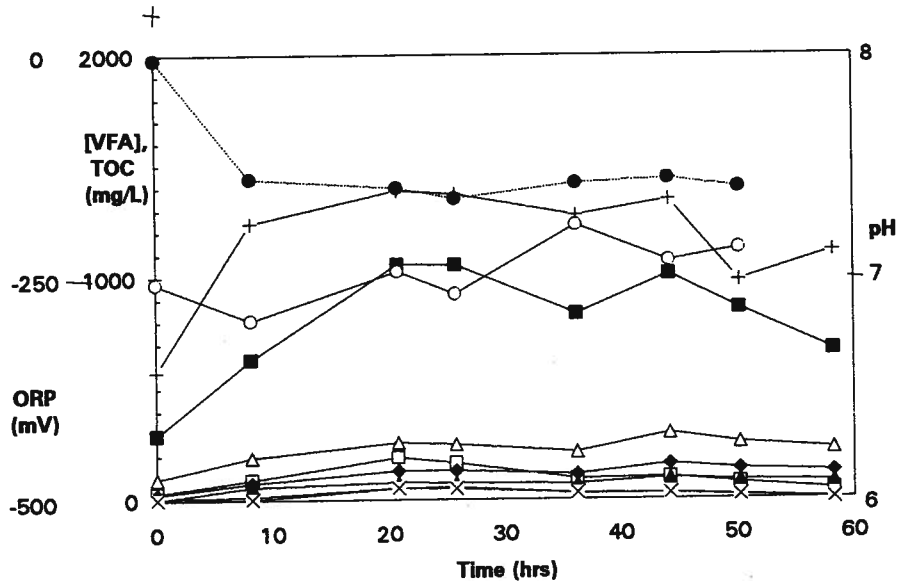


Figure A13.10: Salmon Arm 3rd stage ATAD: [VFA], TOC, pH, ORP v time (micro-aerobic w mixed secondary and primary sludge)



- acetate □ propionate ◆ isobutyrate
- ◇ butyrate ▲ 2-methylbutyrate △ isovalerate
- × valerate * lactate + TOC ● pH ○ ORP

Table A1: Concentration of sludges for all batch experiments

Batch #	Process sludge source	Concentration (%)	Feed sludge source	Concentration (%)	Incubation temperature (°C)
3	A side TAD	1.51	Primary	2.37	45
4	A side TAD	1.63	n/a	n/a	45
6	A side TAD	1.97	n/a	n/a	45
8	A side TAD	1.95	n/a	n/a	45
2	A side TAD	1.71	n/a	n/a	45
7	A side TAD	1.89	n/a	n/a	45
9	A side TAD	1.86	Primary	1.81	45
10 _{Fermenter}	Side stream fermenter	1.82	Primary	2.16	20
10 _{TAD}	A side TAD	1.96	Primary	2.16	45
11 _(A side)	A side TAD	1.63	Primary	1.12	45
11 _(B side)	B side TAD	1.66	Primary	1.12	45
13	Salmon Arm 3rd cell ATAD	2.1	Salmon Arm primary and secondary	5.07 (prim.) 3.85 (sec.)	59

Appendix B: 3x3 Pilot Scale TAD Results

Figure B1.1	A side [Acetate] with 4.5 d SRT	256
Figure B1.2	A side [Acetate] with 4.5 d SRT	256
Figure B1.3	A side [Acetate] with 4.5 d SRT	256
Figure B1.4	A side [Propionate] with 4.5 d SRT	257
Figure B1.5	A side [Propionate] with 4.5 d SRT	257
Figure B1.6	A side [Propionate] with 4.5 d SRT	257
Figure B1.7	A side [Isobutyrate] with 4.5 d SRT	258
Figure B1.8	A side [Isobutyrate] with 4.5 d SRT	258
Figure B1.9	A side [Isobutyrate] with 4.5 d SRT	258
Figure B1.10	A side [Isovalerate] with 4.5 d SRT	259
Figure B1.11	A side [Isovalerate] with 4.5 d SRT	259
Figure B1.12	A side [Isovalerate] with 4.5 d SRT	259
Figure B2.1	B side [Acetate] with 3 d SRT	260
Figure B2.2	B side [Acetate] with 4.5 d SRT	260
Figure B2.3	B side [Acetate] with 6 d SRT	260
Figure B2.4	B side [Propionate] with 3 d SRT	261
Figure B2.5	B side [Propionate] with 4.5 d SRT	261
Figure B2.6	B side [Propionate] with 6 d SRT	261
Figure B2.7	B side [Isobutyrate] with 3 d SRT	262
Figure B2.8	B side [Isobutyrate] with 4.5 d SRT	262

Figure B2.9	B side [Isobutyrate] with 6 d SRT	262
Figure B2.10	B side [Isovalerate] with 3 d SRT	263
Figure B2.11	B side [Isovalerate] with 4.5 d SRT	263
Figure B2.12	B side [Isovalerate] with 6 d SRT	263
Figure B2.13	B side [Butyrate] with 3 d SRT	264
Figure B2.14	B side [Butyrate] with 4.5 d SRT	264
Figure B2.15	B side [Butyrate] with 6 d SRT	264
Figure B3.1	Primary [Acetate] with B side 3 d SRT	265
Figure B3.2	Primary [Acetate] with B side 4.5 d SRT	265
Figure B3.3	Primary [Acetate] with B side 6 d SRT	265
Figure B3.4	Primary [Propionate] with B side 3 d SRT	266
Figure B3.5	Primary [Propionate] with B side 4.5 d SRT	266
Figure B3.6	Primary [Propionate] with B side 6 d SRT	266
Figure B3.7	Primary [Isobutyrate] with B side 3 d SRT	267
Figure B3.8	Primary [Isobutyrate] with B side 4.5 d SRT	267
Figure B3.9	Primary [Isobutyrate] with B side 6 d SRT	267
Figure B3.10	Primary [Butyrate] with B side 3 d SRT	268
Figure B3.11	Primary [Butyrate] with B side 4.5 d SRT	268
Figure B3.12	Primary [Butyrate] with B side 6 d SRT	268
Figure B4.1	A side TOC with 4.5 d SRT	269
Figure B4.2	A side TOC with 4.5 d SRT	269
Figure B4.3	A side TOC with 4.5 d SRT	269

Figure B5.1	B side TOC with 3 d SRT	270
Figure B5.2	B side TOC with 4.5 d SRT	270
Figure B5.3	B side TOC with 6 d SRT	270
Figure B6.1	Primary TOC with B side 3 d SRT	271
Figure B6.2	Primary TOC with B side 4.5 d SRT	271
Figure B6.3	Primary TOC with B side 6 d SRT	271
Figure B7.1	A side pH with 4.5 d SRT	272
Figure B7.2	A side pH with 4.5 d SRT	272
Figure B7.3	A side pH with 4.5 d SRT	272
Figure B8.1	B side pH with 3 d SRT	273
Figure B8.2	B side pH with 4.5 d SRT	273
Figure B8.3	B side pH with 6 d SRT	273
Figure B9.1	A side solids levels with B side 3 d SRT	274
Figure B9.2	A side solids levels with B side 4.5 d SRT	274
Figure B9.3	A side solids levels with B side 6 d SRT	274
Figure B10.1	B side solids levels with 3 d SRT	275
Figure B10.2	B side solids levels with 4.5 d SRT	275
Figure B10.3	B side solids levels with 6 d SRT	275
Figure B11.1	Primary solids levels with B side 3 d SRT	276
Figure B11.2	Primary solids levels with B side 4.5 d SRT	276
Figure B11.3	Primary solids levels with B side 6 d SRT	276
Figure B12.1	A side air flow with 4.5 d SRT	277

Figure B12.2	A side air flow with 4.5 d SRT	277
Figure B12.3	A side air flow with 4.5 d SRT	277
Figure B13.1	B side air flow with 3 d SRT	278
Figure B13.2	B side air flow with 4.5 d SRT	278
Figure B13.3	B side air flow with 6 d SRT	278
Figure B14.1	A side mixer RPM with 4.5 d SRT	279
Figure B14.2	A side mixer RPM with 4.5 d SRT	279
Figure B14.3	A side mixer RPM with 4.5 d SRT	279
Figure B15.1	B side mixer RPM with 3 d SRT	280
Figure B15.2	B side mixer RPM with 4.5 d SRT	280
Figure B15.3	B side mixer RPM with 6 d SRT	280
Figure B16.1	A side actual SRT for nominal B side 3 d SRT	281
Figure B16.2	A side actual SRT for nominal B side 4.5 d SRT	281
Figure B16.3	A side actual SRT for nominal B side 6 d SRT	281
Figure B17.1	B side actual SRT for nominal B side 3 d SRT	282
Figure B17.2	B side actual SRT for nominal B side 4.5 d SRT	282
Figure B17.3	B side actual SRT for nominal B side 6 d SRT	282
Figure B18.1	Temperature Variations, Sides A and B, run 1	283
Figure B18.2	ORP Variations, Sides A and B, run 1	283
Figure B18.3	ORP FFTs, Sides A and B, run 1	283
Figure B19.1	Temperature Variations, Sides A and B, run 2	284
Figure B19.2	ORP Variations, Sides A and B, run 2	284

Figure B19.3	ORP FFTs, Sides A and B, run 2	284
Figure B20.1	Temperature Variations, Sides A and B, run 3	285
Figure B20.2	ORP Variations, Sides A and B, run 3	285
Figure B20.3	ORP FFTs, Sides A and B, run 3	285
Figure B21.1	Temperature Variations, Sides A and B, run 4	286
Figure B21.2	ORP Variations, Sides A and B, run 4	286
Figure B21.3	ORP FFTs, Sides A and B, run 4	286
Figure B22.1	Temperature Variations, Sides A and B, run 5	287
Figure B22.2	ORP Variations, Sides A and B, run 5	287
Figure B22.3	ORP FFTs, Sides A and B, run 5	287
Figure B23.1	Temperature Variations, Sides A and B, run 6	288
Figure B23.2	ORP Variations, Sides A and B, run 6	288
Figure B23.3	ORP FFTs, Sides A and B, run 6	288
Figure B24.1	Temperature Variations, Sides A and B, run 7	289
Figure B24.2	ORP Variations, Sides A and B, run 7	289
Figure B24.3	ORP FFTs, Sides A and B, run 7	289
Figure B25.1	Temperature Variations, Sides A and B, run 8	290
Figure B25.2	ORP Variations, Sides A and B, run 8	290
Figure B25.3	ORP FFTs, Sides A and B, run 8	290
Figure B26.1	Temperature Variations, Sides A and B, run 9	291
Figure B26.2	ORP Variations, Sides A and B, run 9	291
Figure B26.3	ORP FFTs, Sides A and B, run 9	291

Figure B27.1	Temperature Variations, Sides A and B, run 10	292
Figure B27.2	ORP Variations, Sides A and B, run 10	292
Figure B27.3	ORP FFTs, Sides A and B, run 10	292

Figure B1.1: A side [Acetate] with 4.5 d SRT

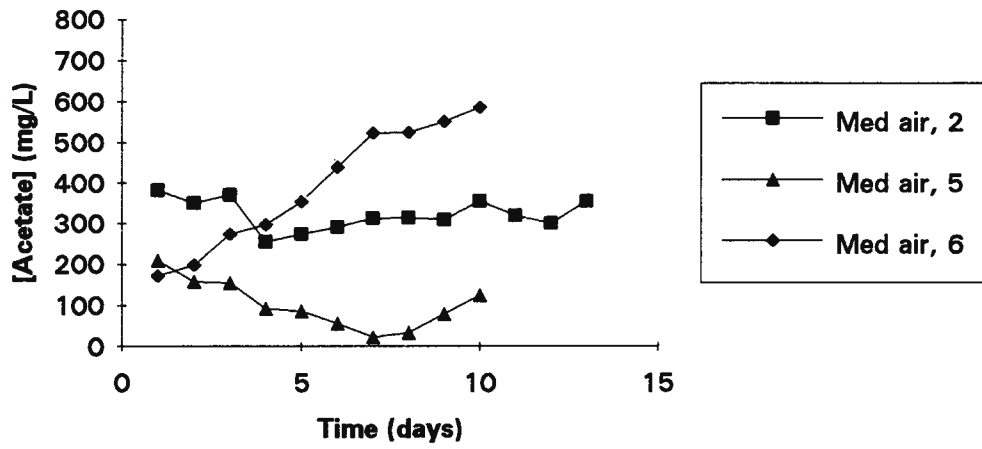


Figure B1.2: A side [Acetate] with 4.5 d SRT

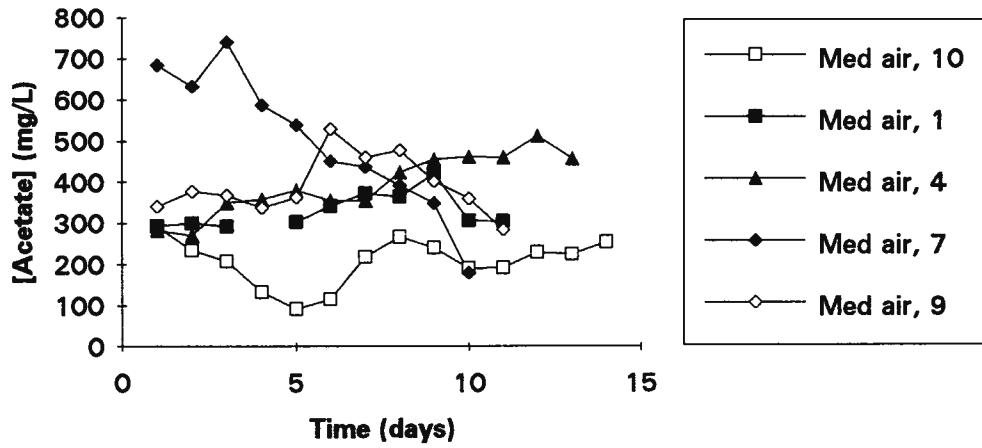


Figure B1.3: A side [Acetate] with 4.5 d SRT

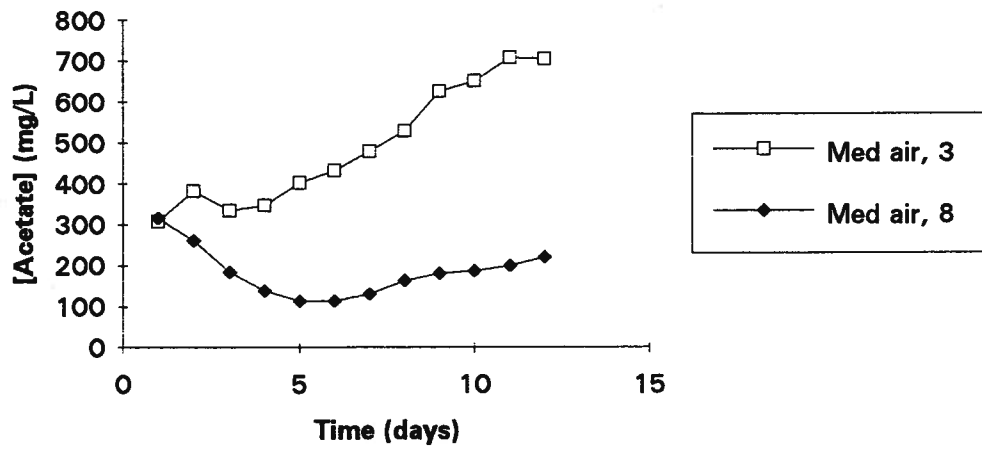


Figure B1.4: A side [Propionate] with 4.5 d SRT

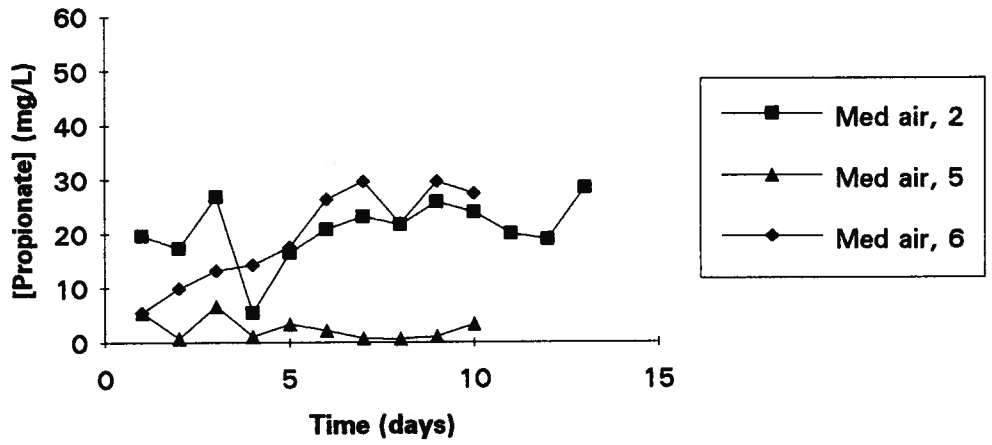


Figure B1.5: A side [Propionate] with 4.5 d SRT

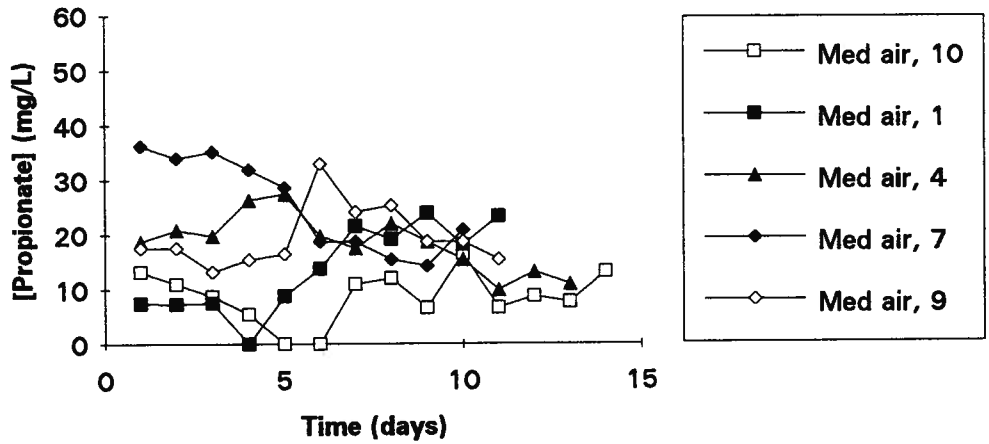


Figure B1.6: A side [Propionate] with 4.5 d SRT

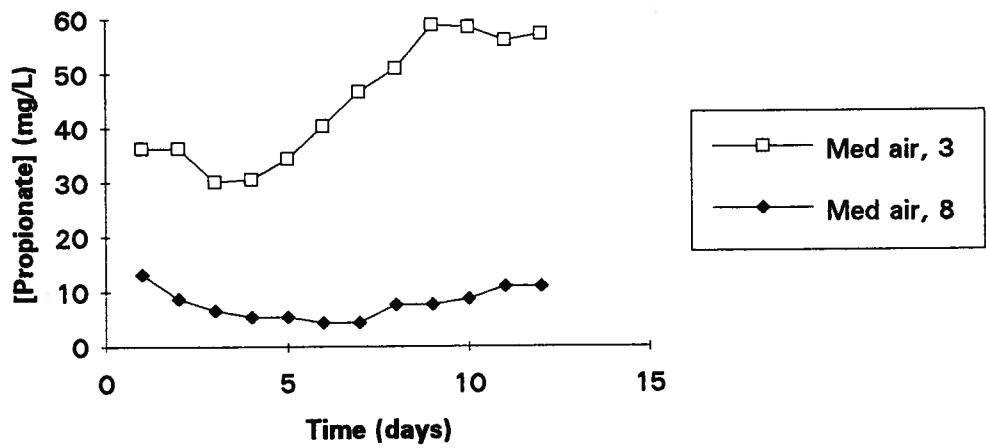


Figure B1.7: A side [Isobutyrate] with 4.5 d SRT

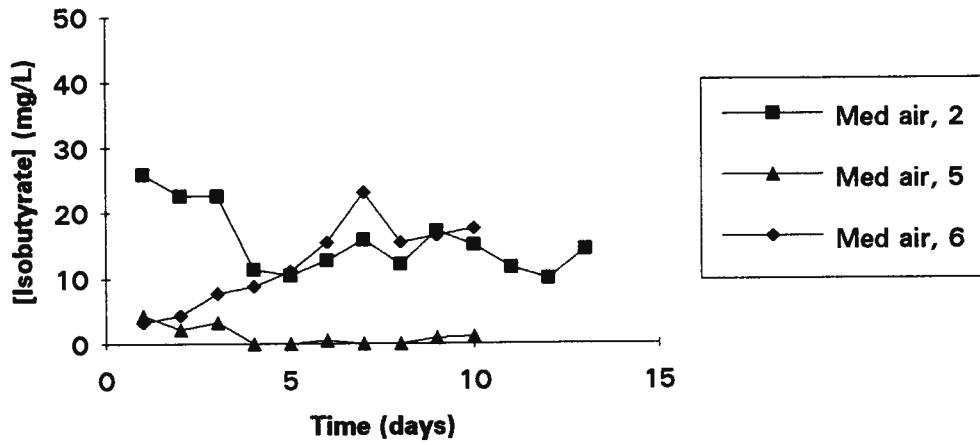


Figure B1.8: A side [Isobutyrate] with 4.5 d SRT

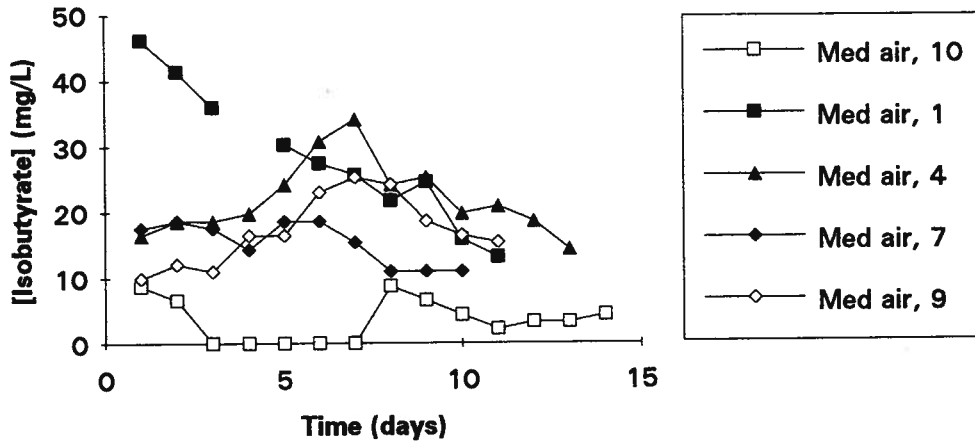


Figure B1.9: A side [Isobutyrate] with 4.5 d SRT

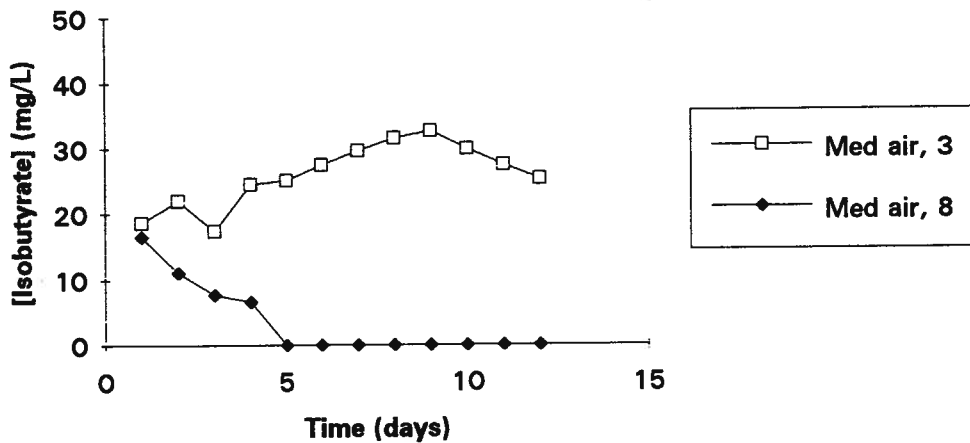


Figure B1.10: A side [Isovalerate] with 4.5 d SRT

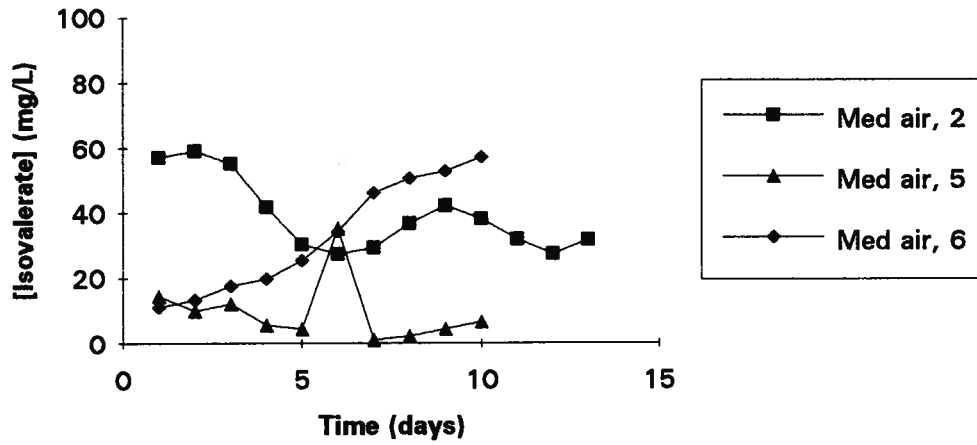


Figure B1.11: A side [Isovalerate] with 4.5 d SRT

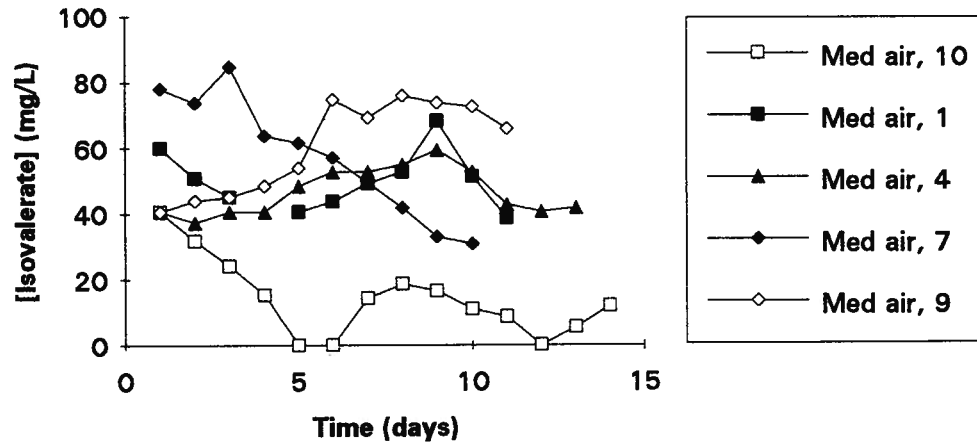


Figure B1.12: A side [Isovalerate] with 4.5 d SRT

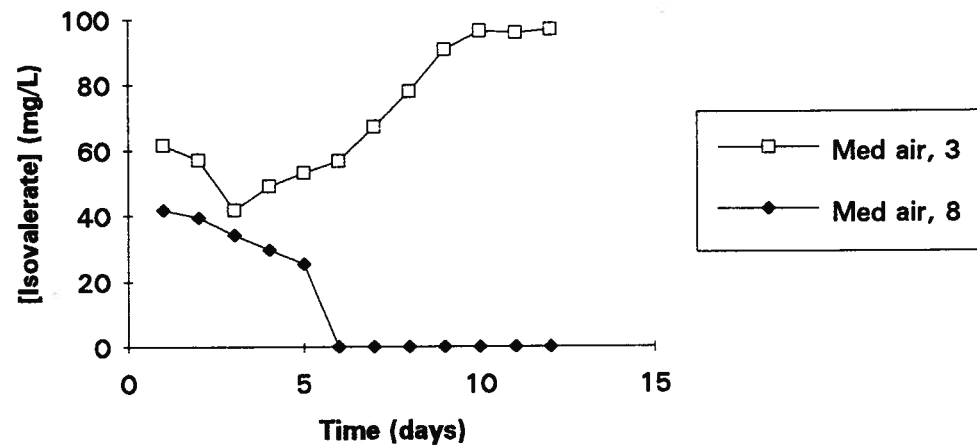


Figure B2.1: B side [Acetate] with 3 d SRT

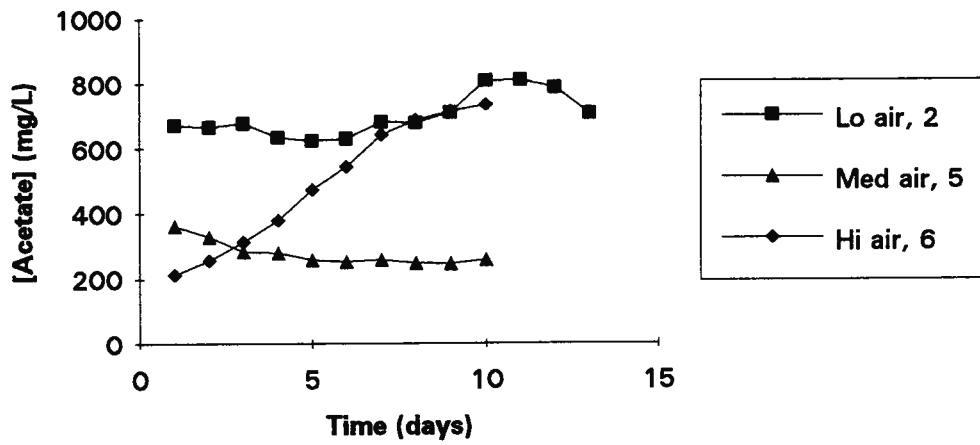


Figure B2.2: B side [Acetate] with 4.5 d SRT

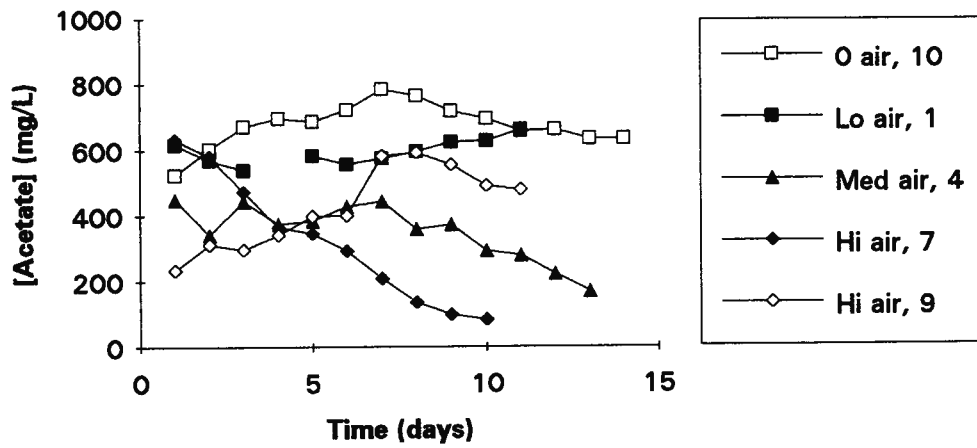


Figure B2.3: B side [Acetate] with 6 d SRT

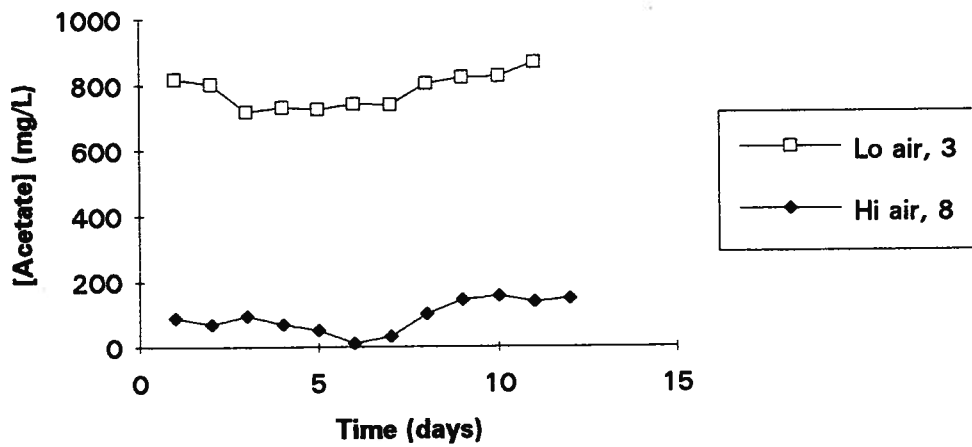


Figure B2.4: B side [Propionate] with 3 d SRT

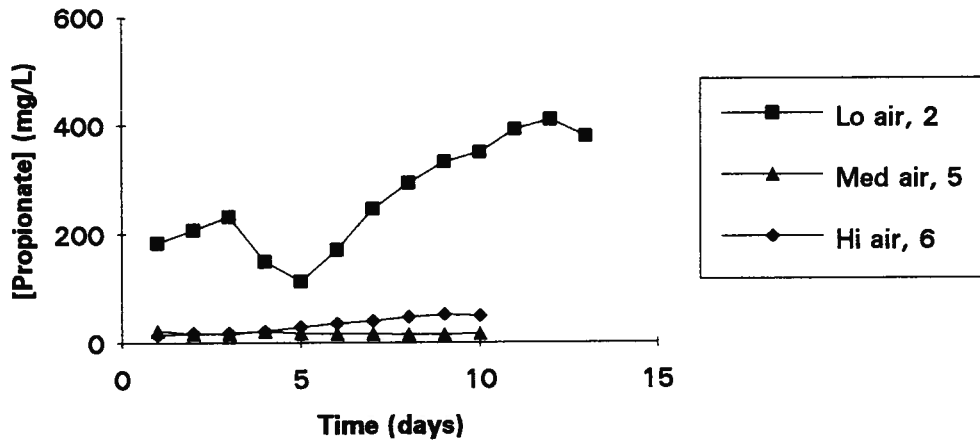


Figure B2.5: B side [Propionate] with 4.5 d SRT

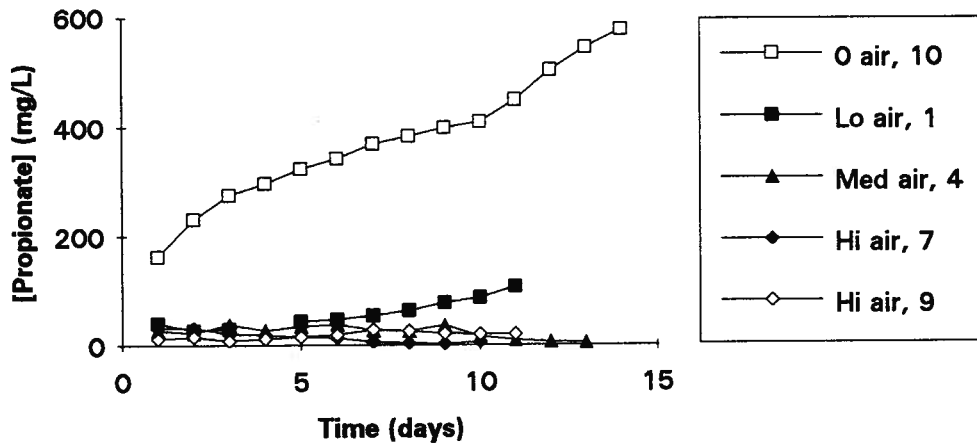


Figure B2.6: B side [Propionate] with 6 d SRT

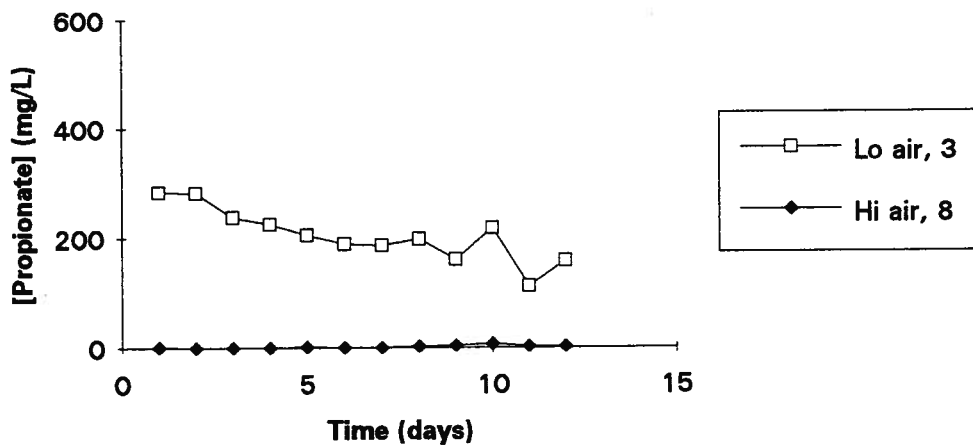


Figure B2.7: B side [Isobutyrate] with 3 d SRT

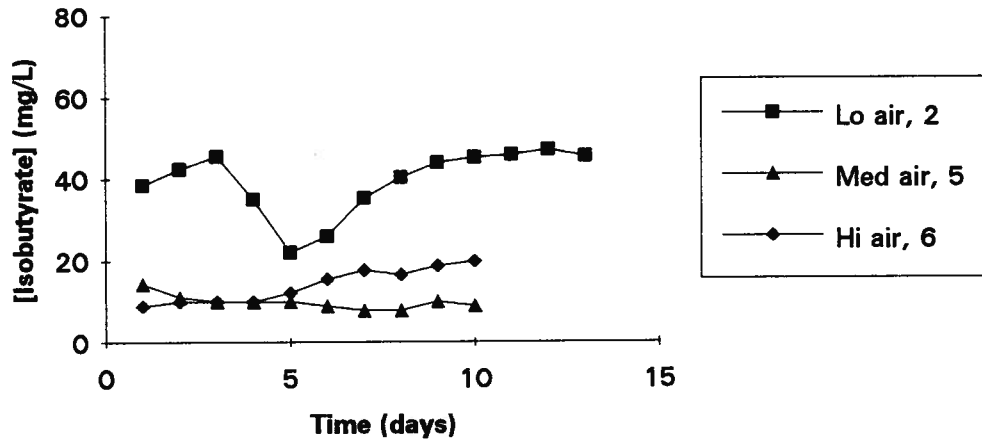


Figure B2.8: B side [Isobutyrate] with 4.5 d SRT

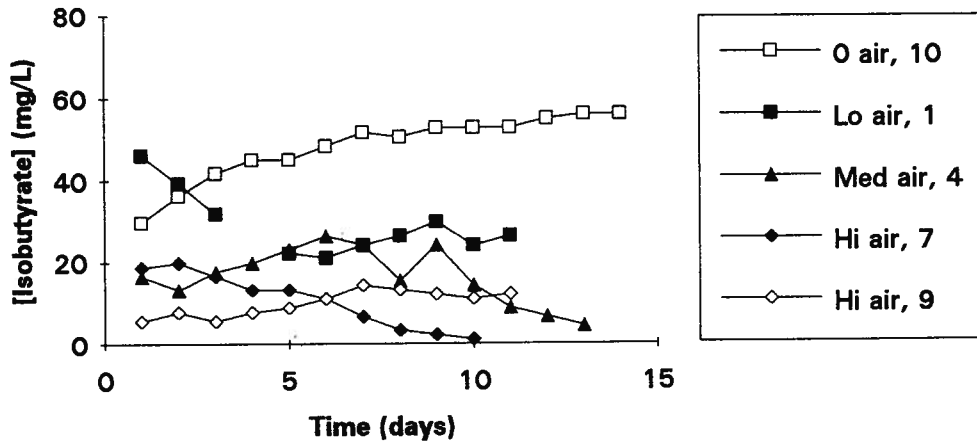


Figure B2.9: B side [Isobutyrate] with 6 d SRT

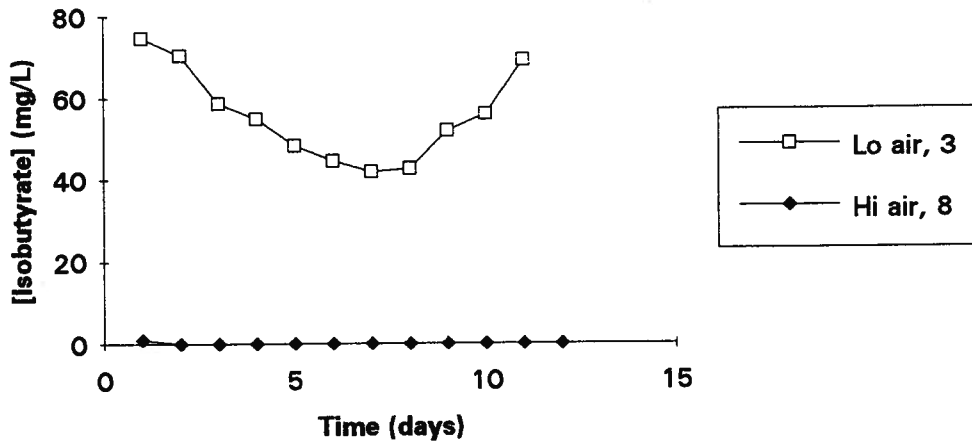


Figure B2.10: B side [Isovalerate] with 3 d SRT

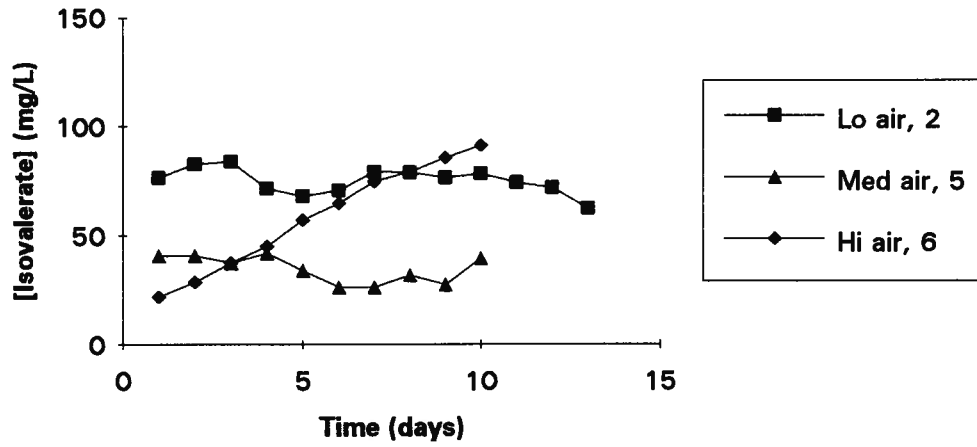


Figure 2.11: B side [Isovalerate] with 4.5 d SRT

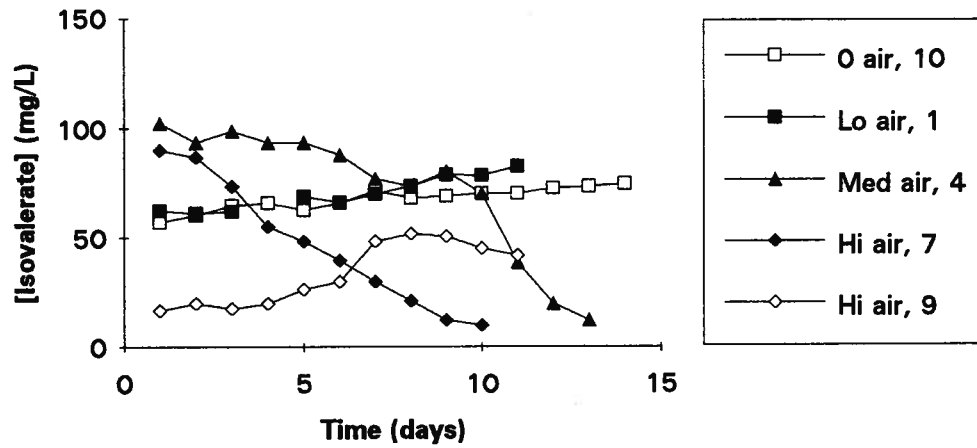


Figure B2.12: B side [Isovalerate] with 6 d SRT

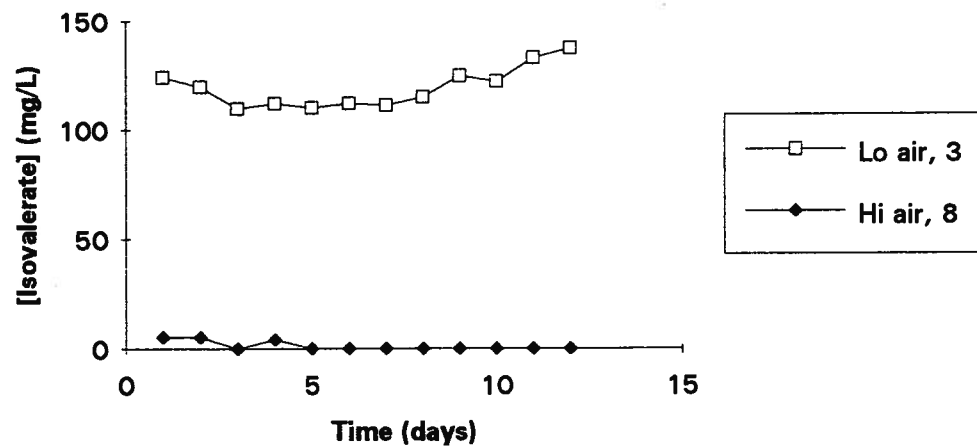


Figure B2.13: B side [Butyrate] with 3 d SRT

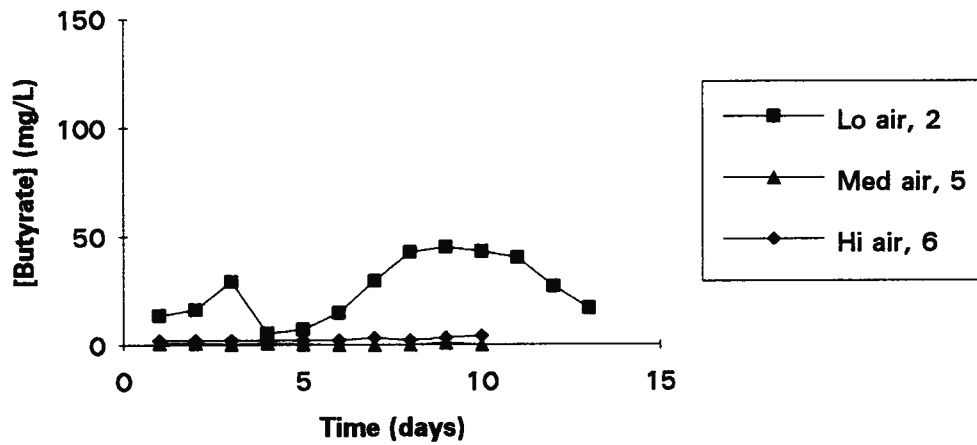


Figure B2.14: B side [Butyrate] with 4.5 d SRT

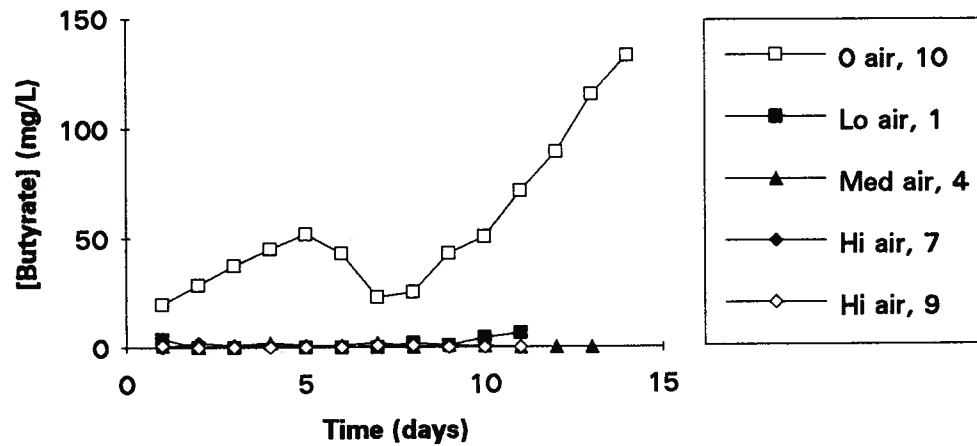


Figure B2.15: B side [Butyrate] with 6 d SRT

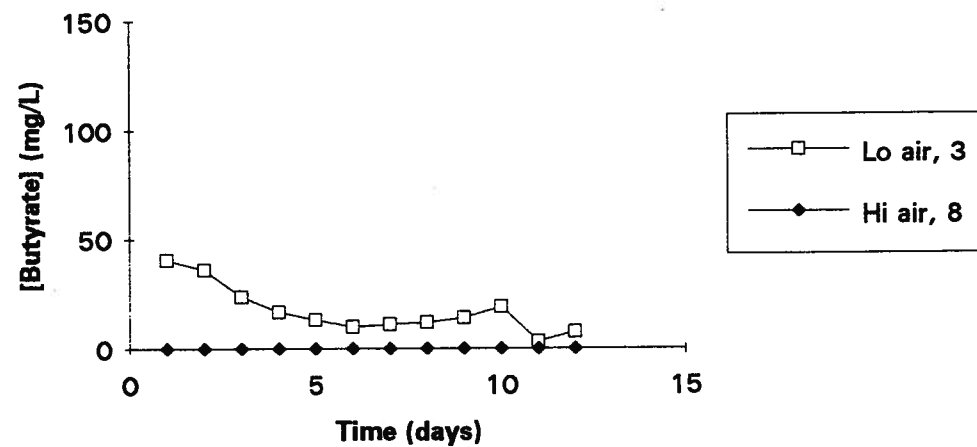


Figure B3.1: Primary [Acetate] with B side 3 d SRT

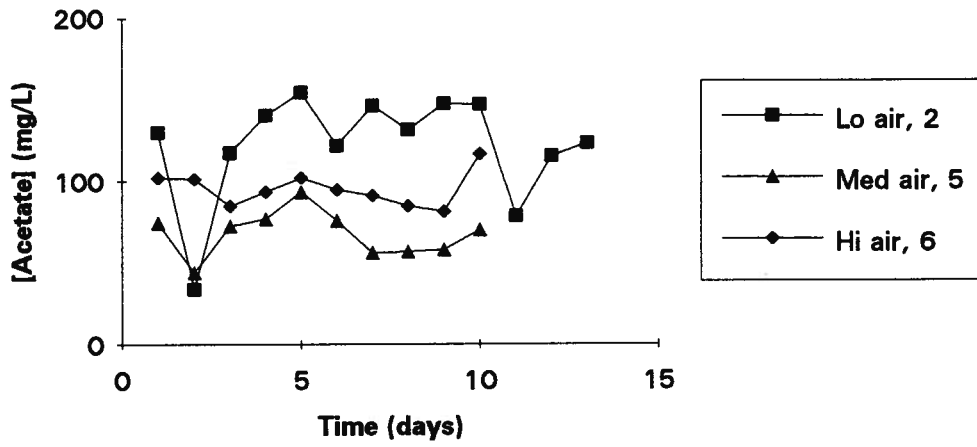


Figure B3.2: Primary [Acetate] with B side 4.5 d SRT

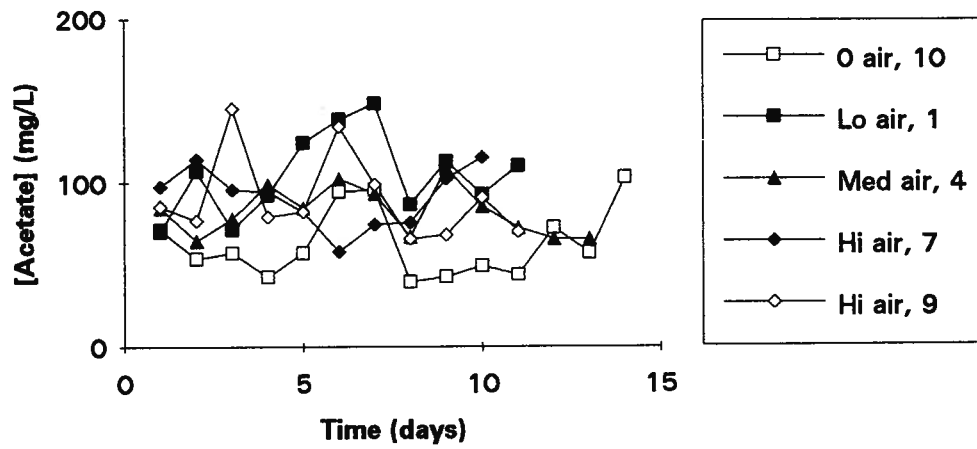


Figure B3.3: Primary [Acetate] with B side 6 d SRT

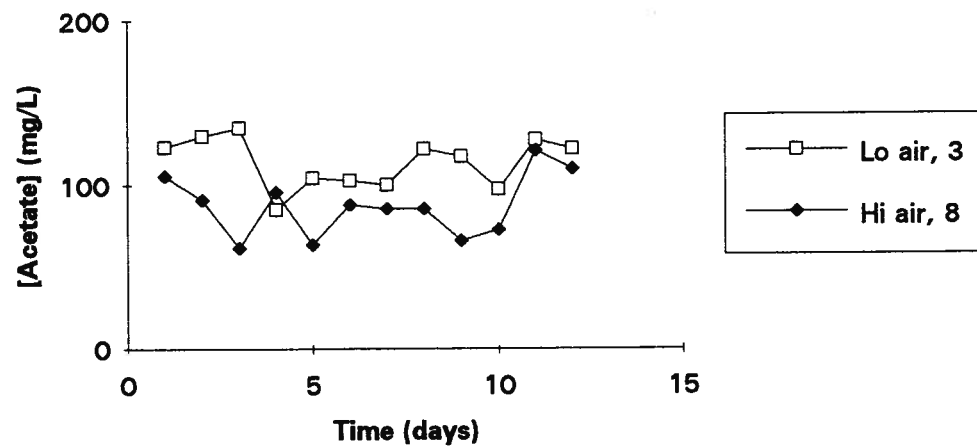


Figure B3.4: Primary [Propionate] with B side 3 d SRT

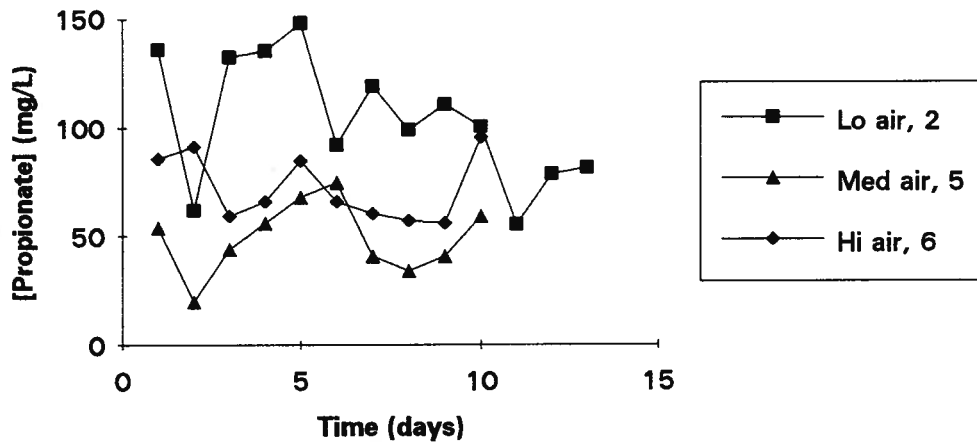


Figure B3.5: Primary [Propionate] with B side 4.5 d SRT

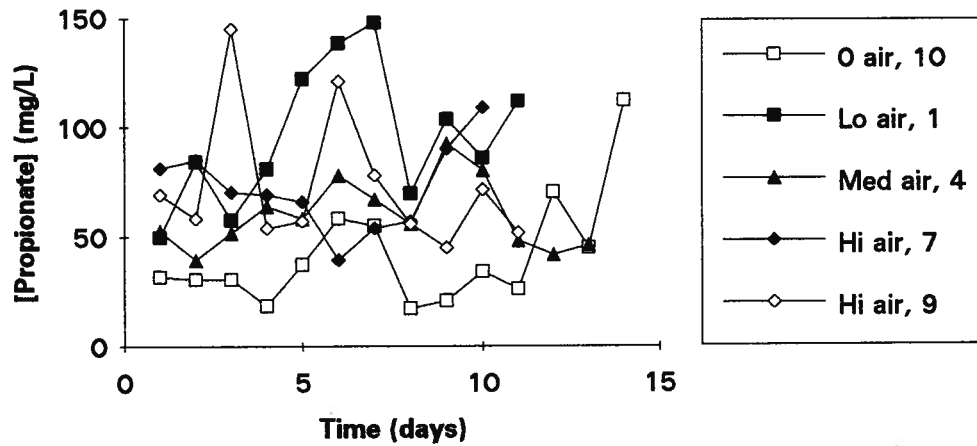


Figure B3.6: Primary [Propionate] with B side 6 d SRT

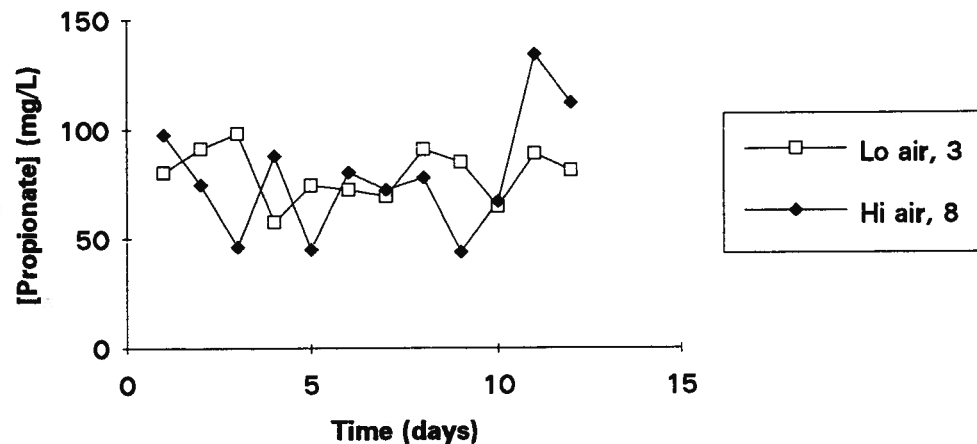


Figure B3.7: Primary [Isobutyrate] with B side 3 d SRT

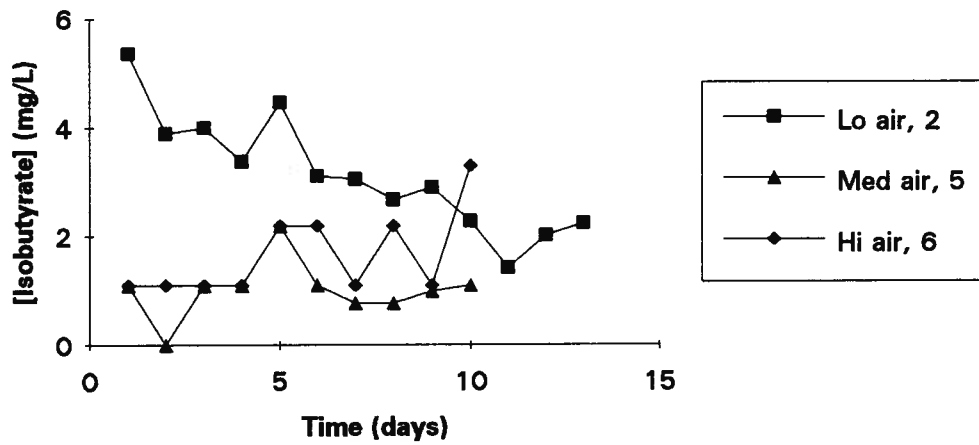


Figure B3.8: Primary [Isobutyrate] with B side 4.5 d SRT

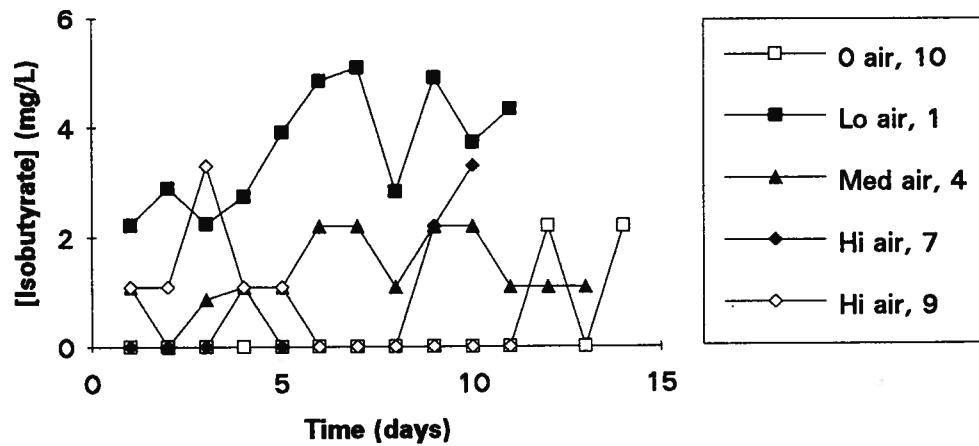


Figure B3.9: Primary [Isobutyrate] with B side 6 d SRT

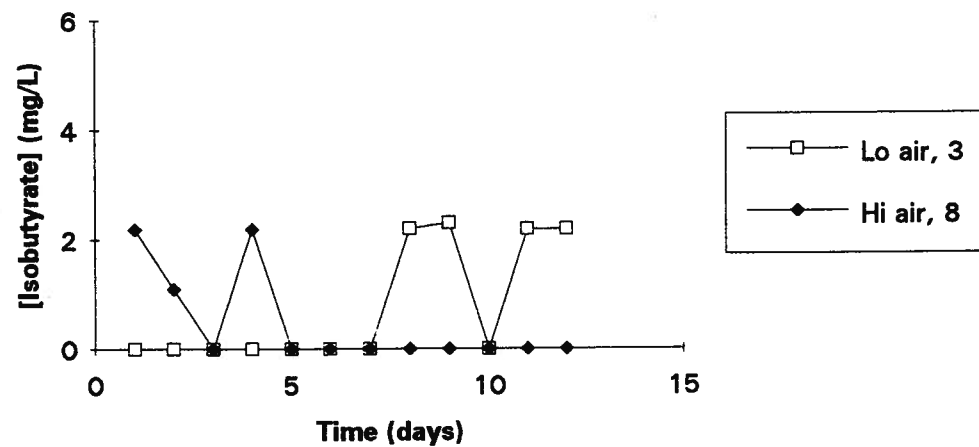


Figure B3.10: Primary [Butyrate] with B side 3 d SRT

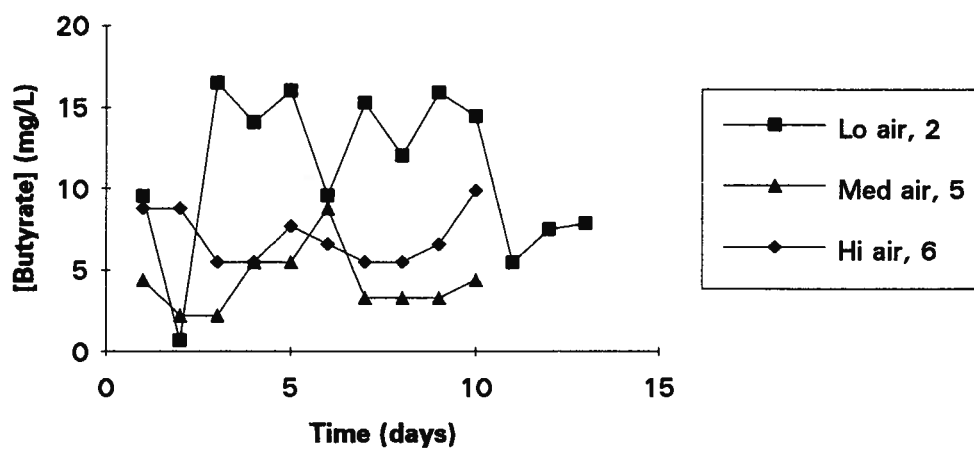


Figure B3.11: Primary [Butyrate] with B side 4.5 d SRT

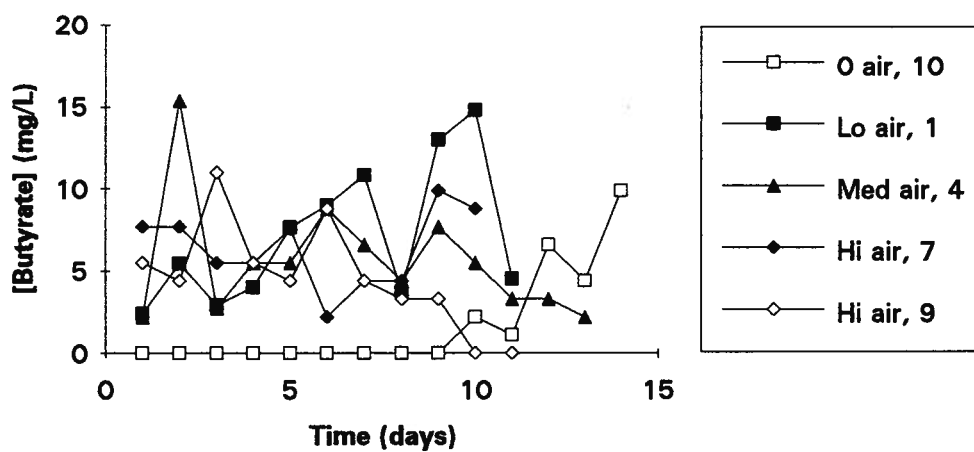


Figure B3.12: Primary [Butyrate] with B side 6 d SRT

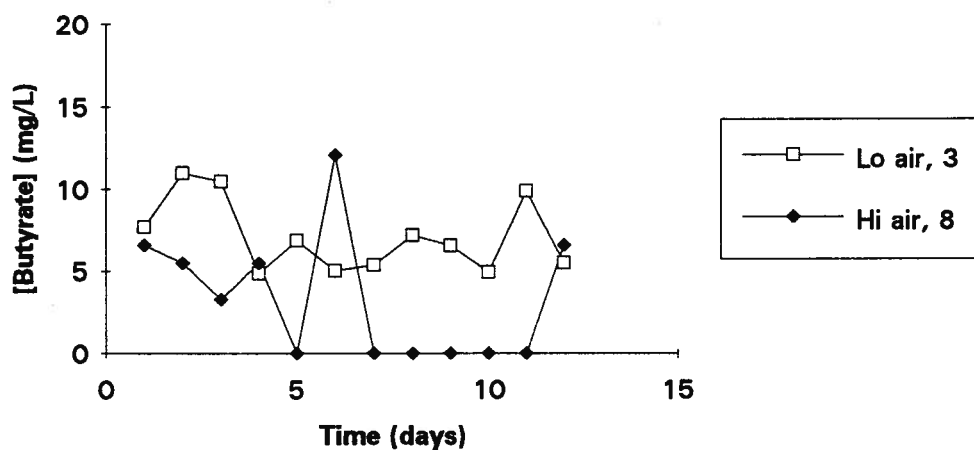


Figure B4.1: A side TOC with 4.5 d SRT

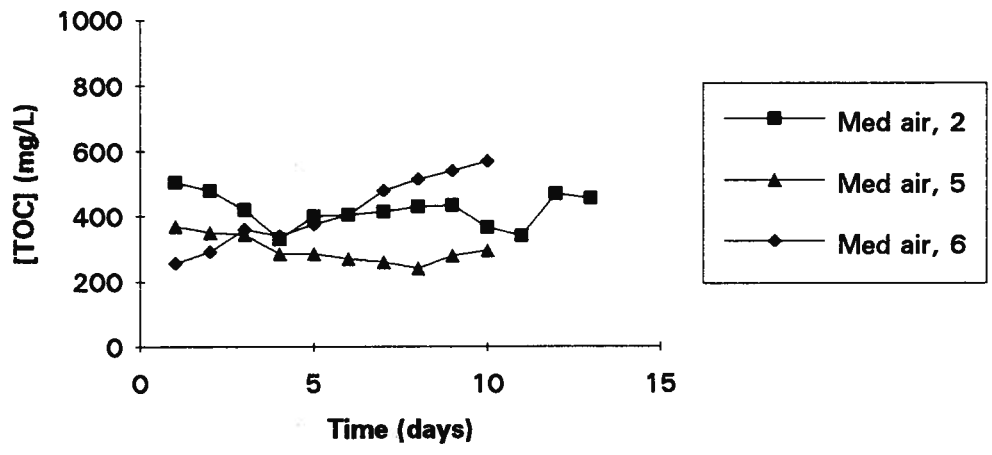


Figure B4.2: A side TOC with 4.5 d SRT

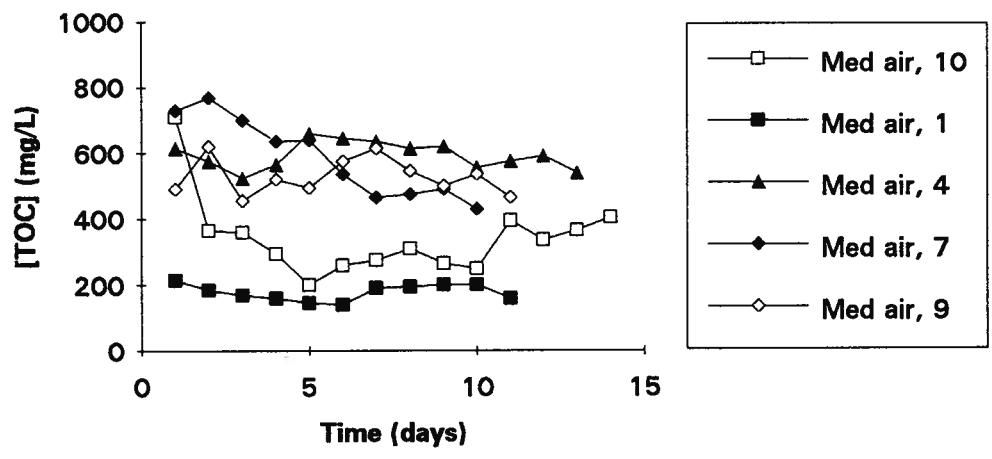


Figure B4.3: A side TOC with 4.5 d SRT

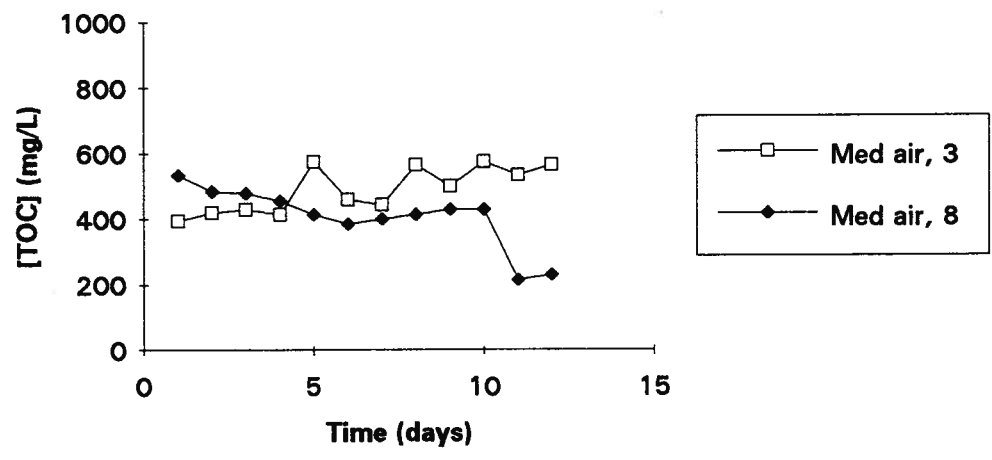


Figure B5.1: B side TOC with 3 d SRT

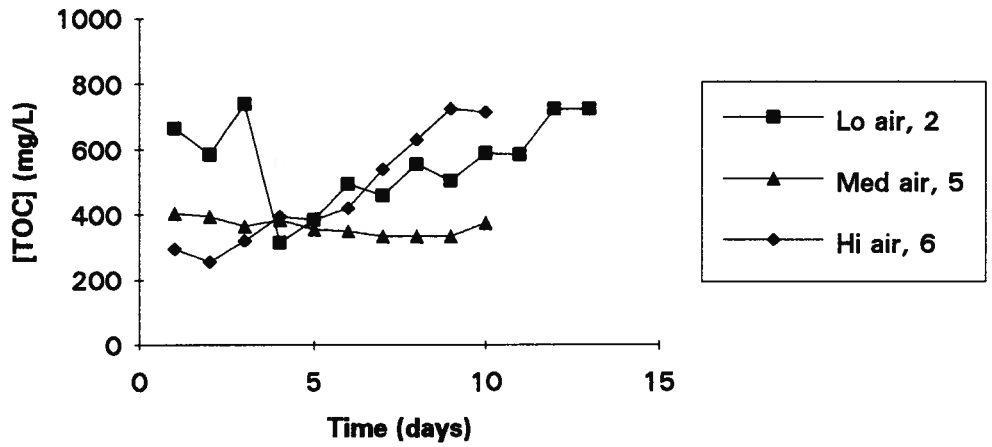


Figure B5.2: B side TOC with 4.5 d SRT

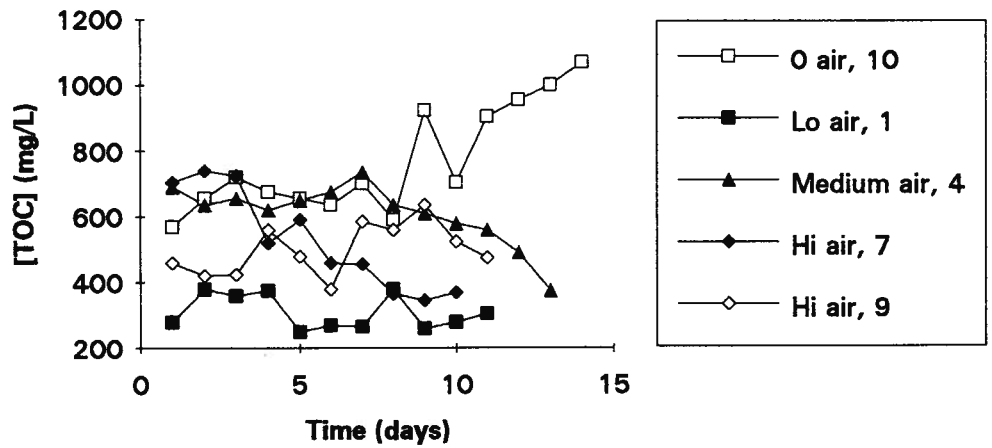


Figure B5.3: B side TOC with 6 d SRT

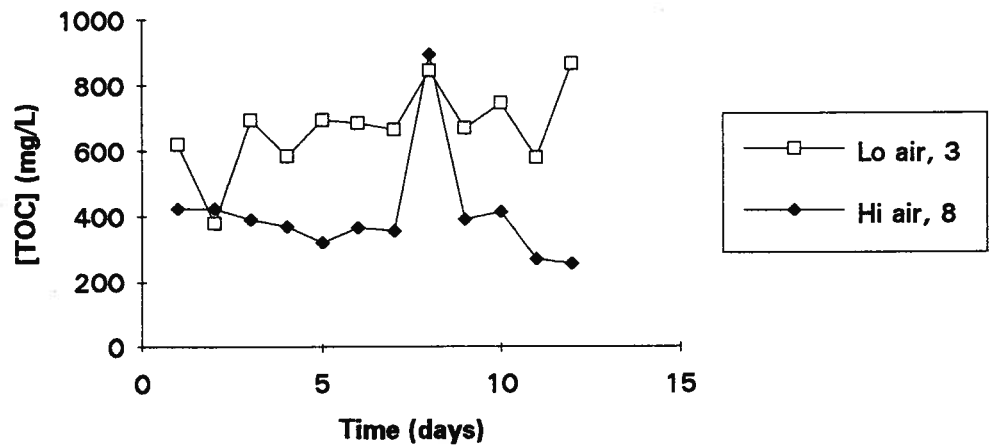


Figure B6.1: Primary TOC with B side 3 d SRT

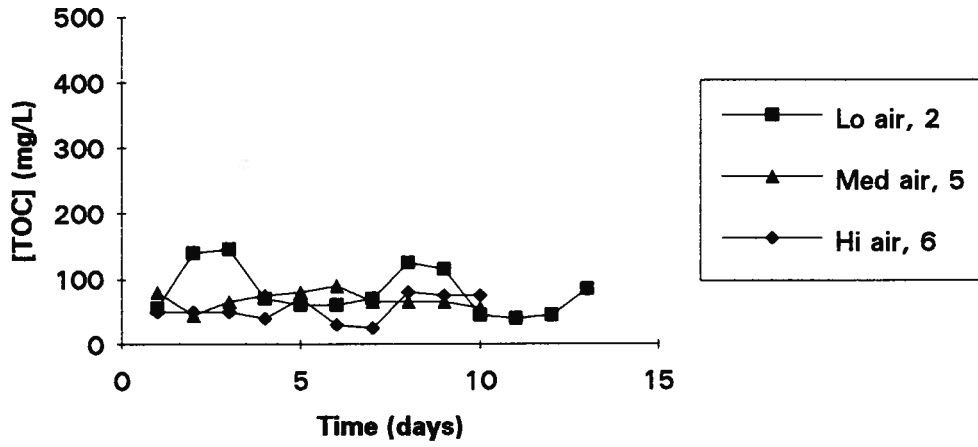


Figure B6.2: Primary TOC with B side 4.5 d SRT

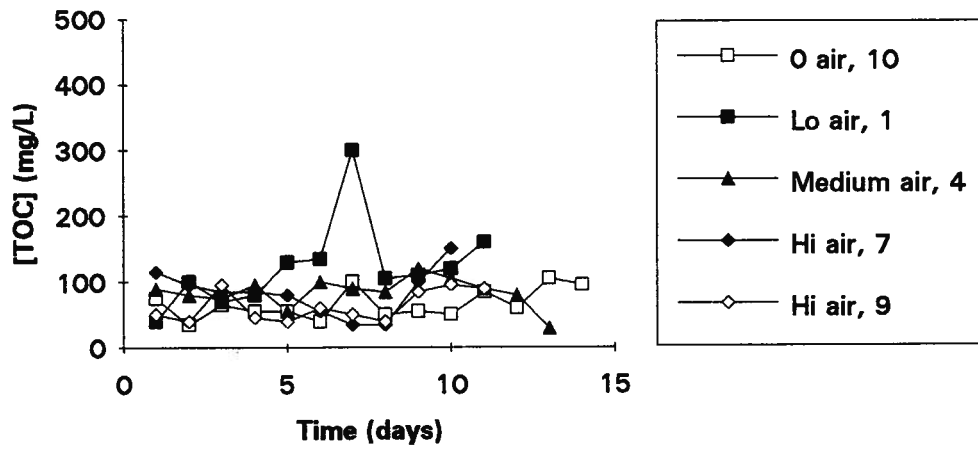


Figure B6.3: Primary TOC with B side 6 d SRT

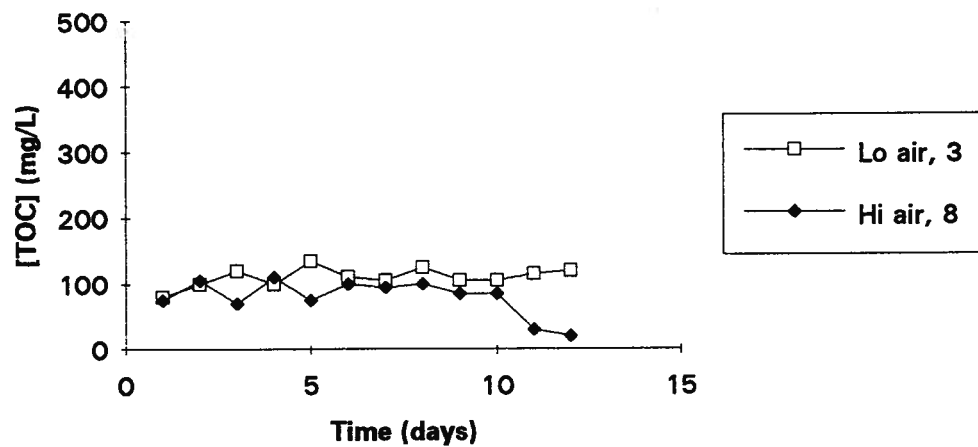


Figure B7.1: A side pH with 4.5 d SRT

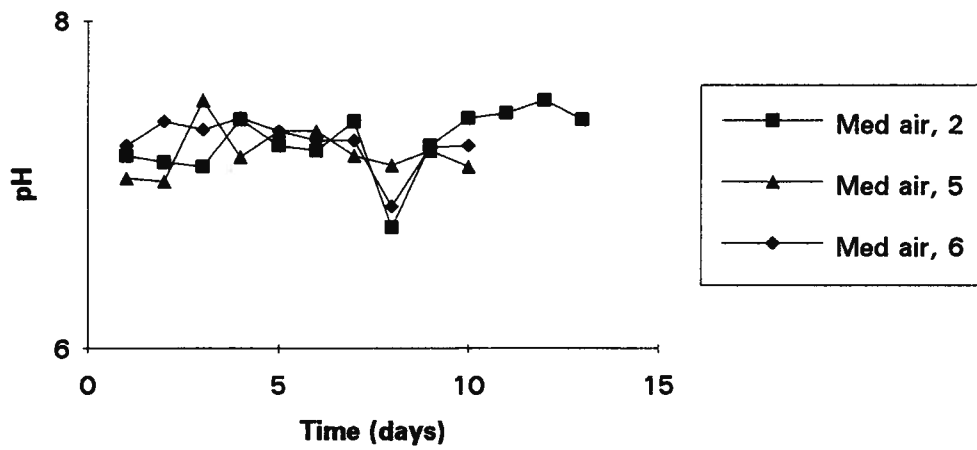


Figure B7.2: A side pH with 4.5 d SRT

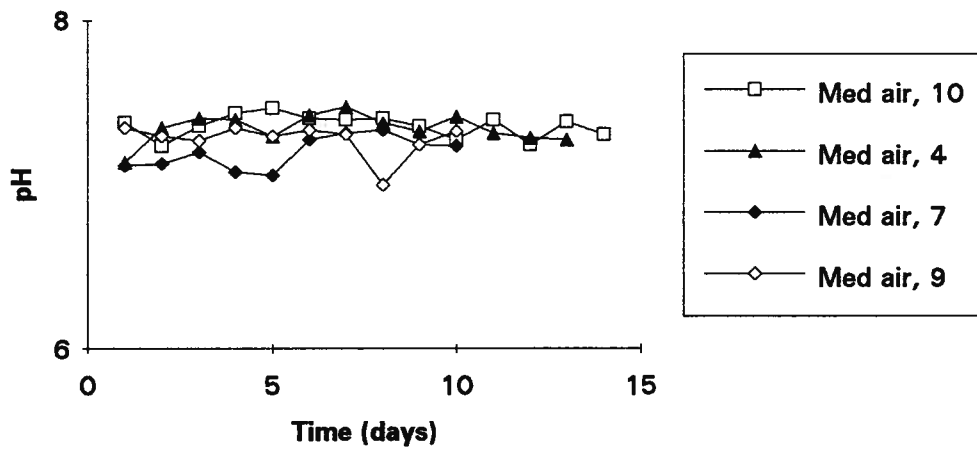


Figure B7.3: A side pH with 4.5 d SRT

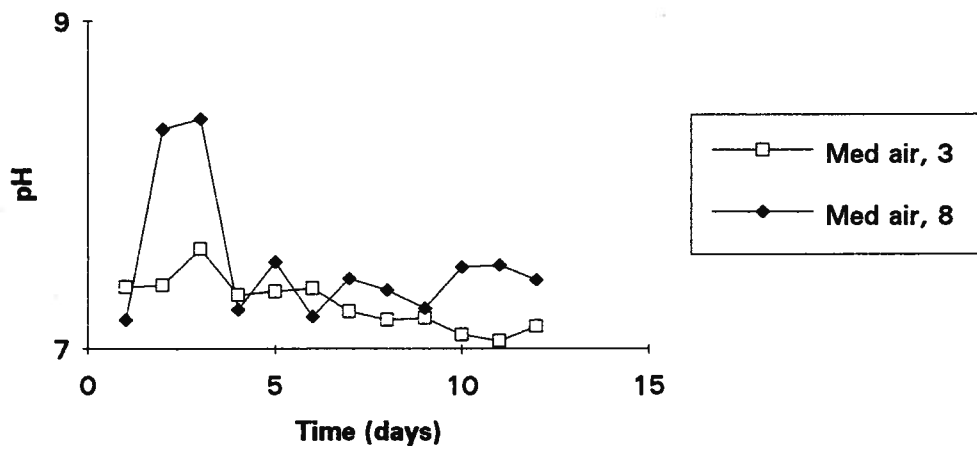


Figure B8.1: B side pH with 3 d SRT

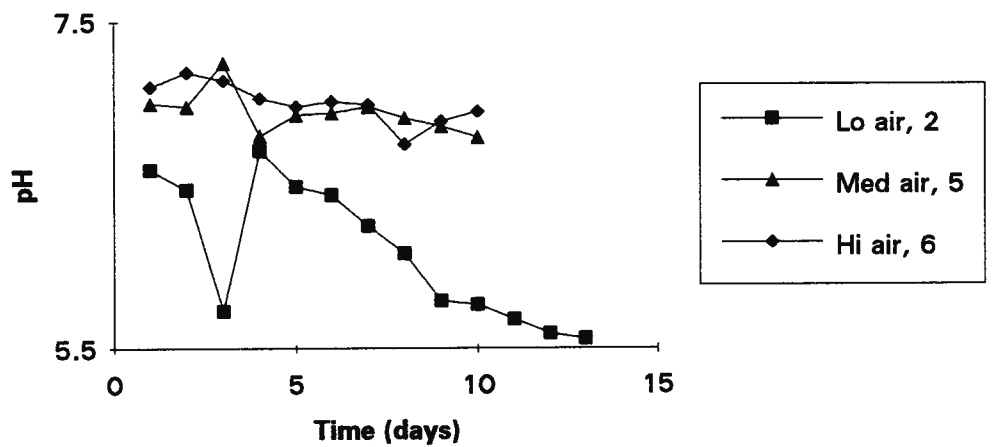


Figure B8.2: B side pH with 4.5 d SRT

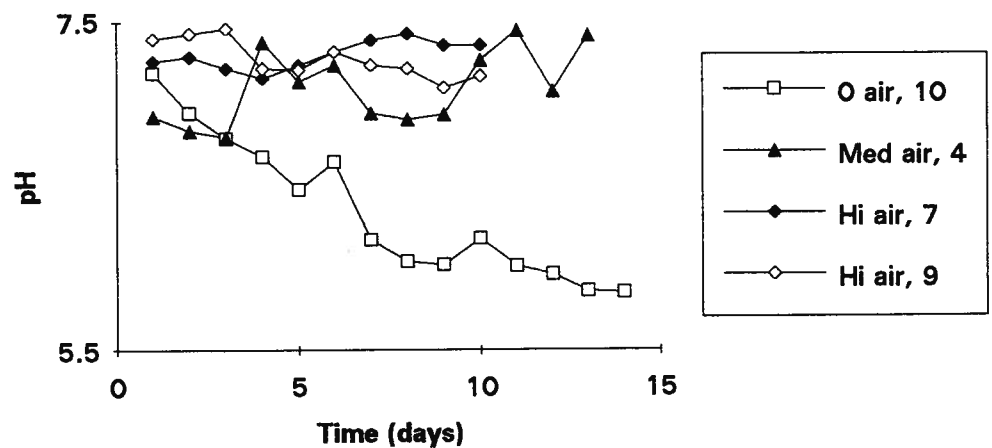


Figure B8.3: B side pH with 6 d SRT

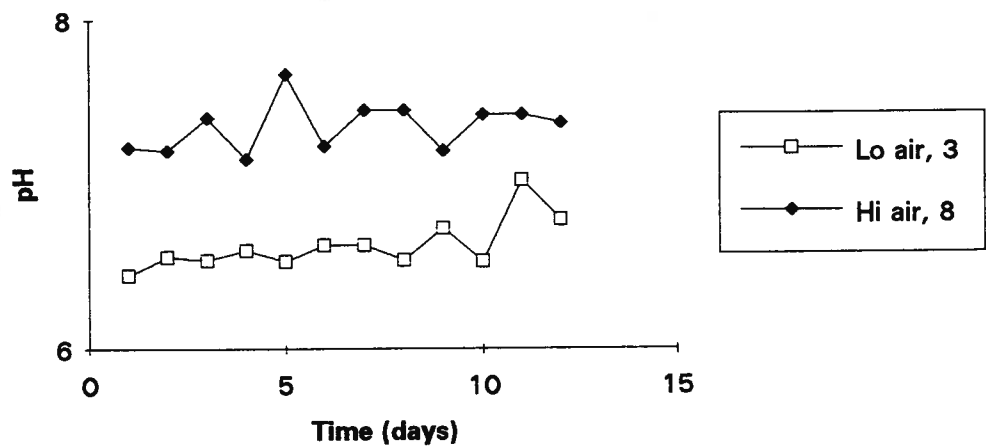


Figure B9.1: A side solids levels with B side 3 d SRT

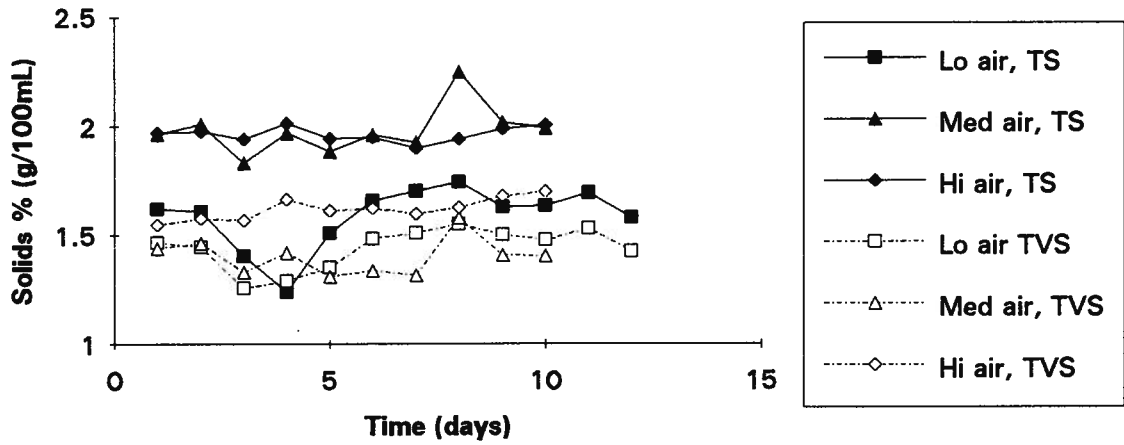


Figure B9.2: A side solids levels with B side 4.5 d SRT

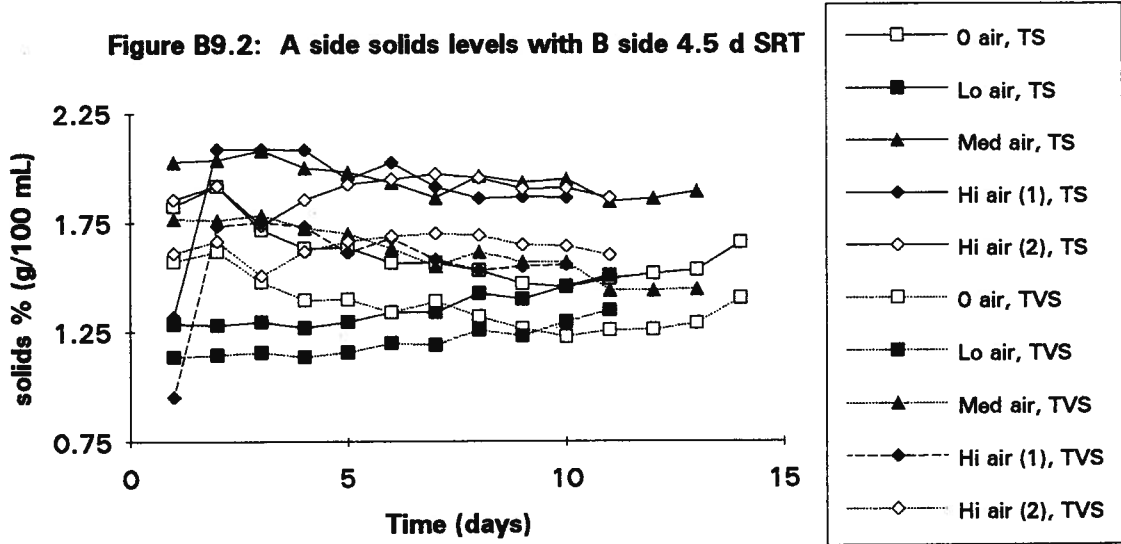


Figure B9.3: A side solids levels with B side 6 d SRT

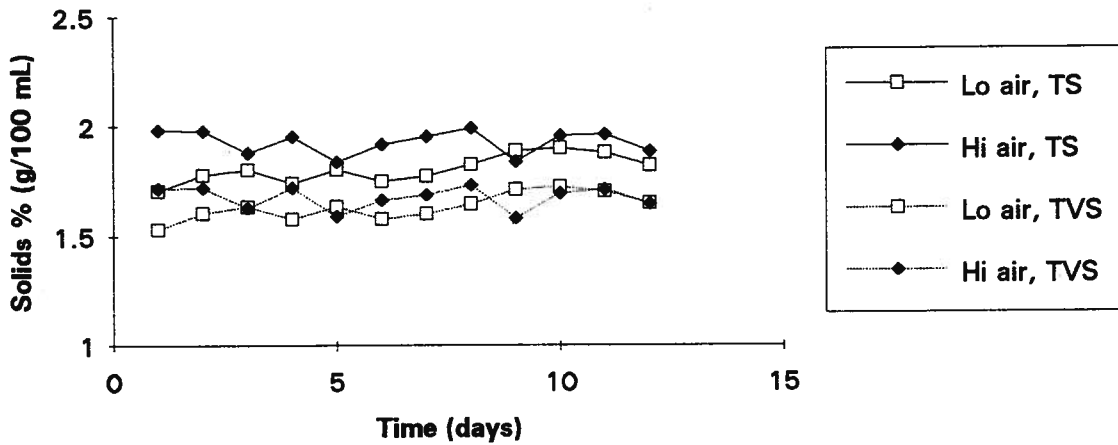


Figure B10.1: B side solids levels with 3 d SRT

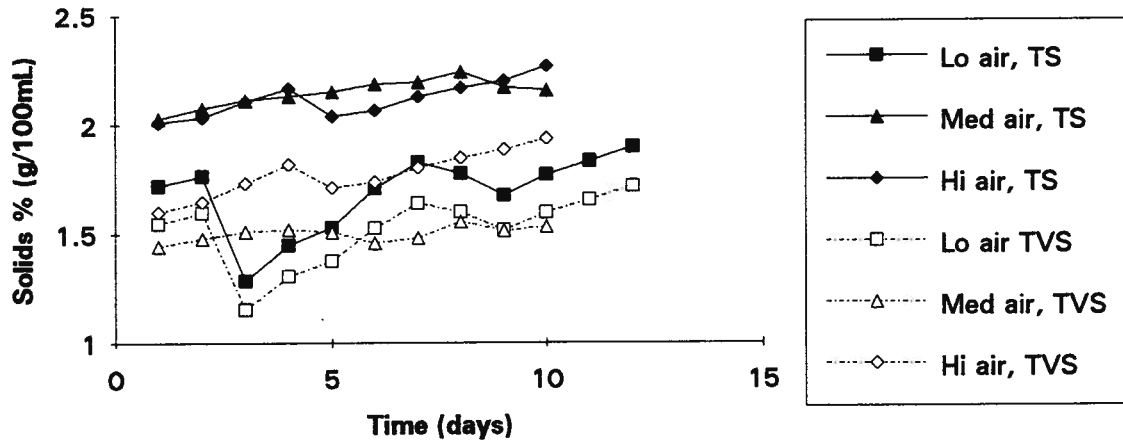


Figure B10.2: B side solids levels with 4.5 d SRT

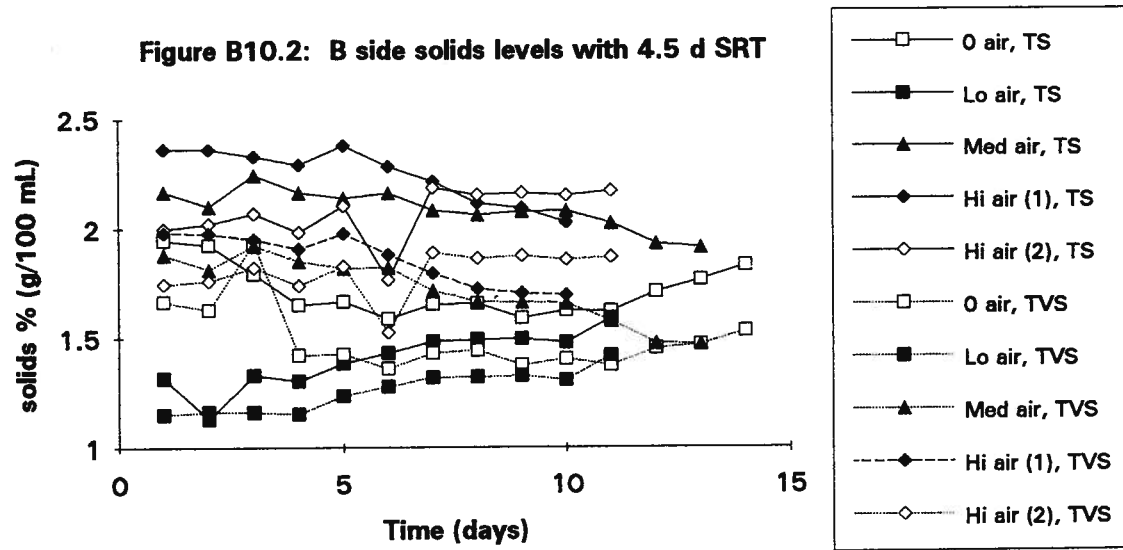


Figure B10.3: B side solids levels with 6 d SRT

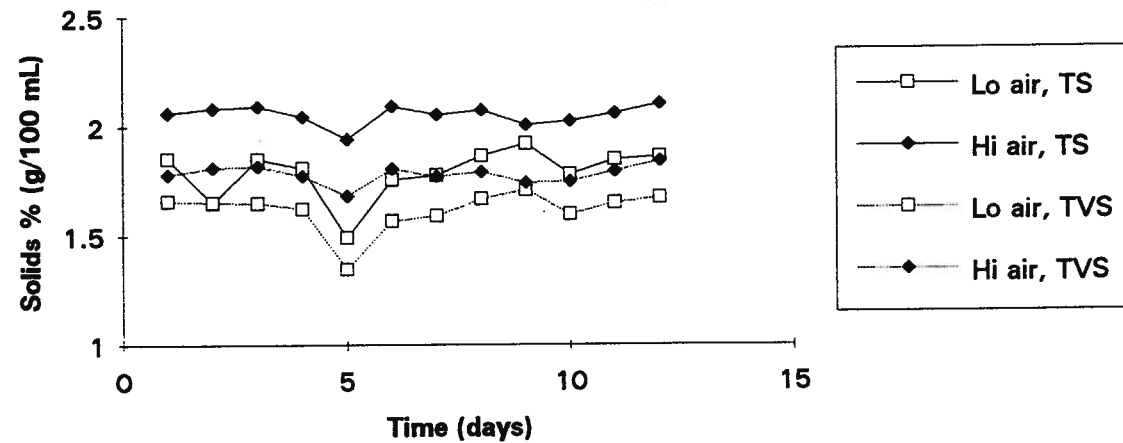


Figure B11.1: Primary solids levels with B side 3 d SRT

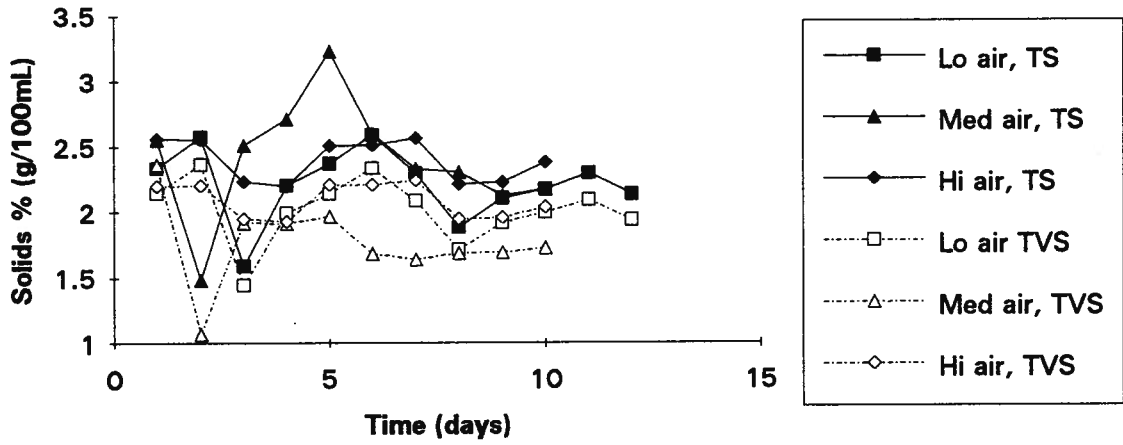


Figure B11.2: Primary solids levels with B side 4.5 d SRT

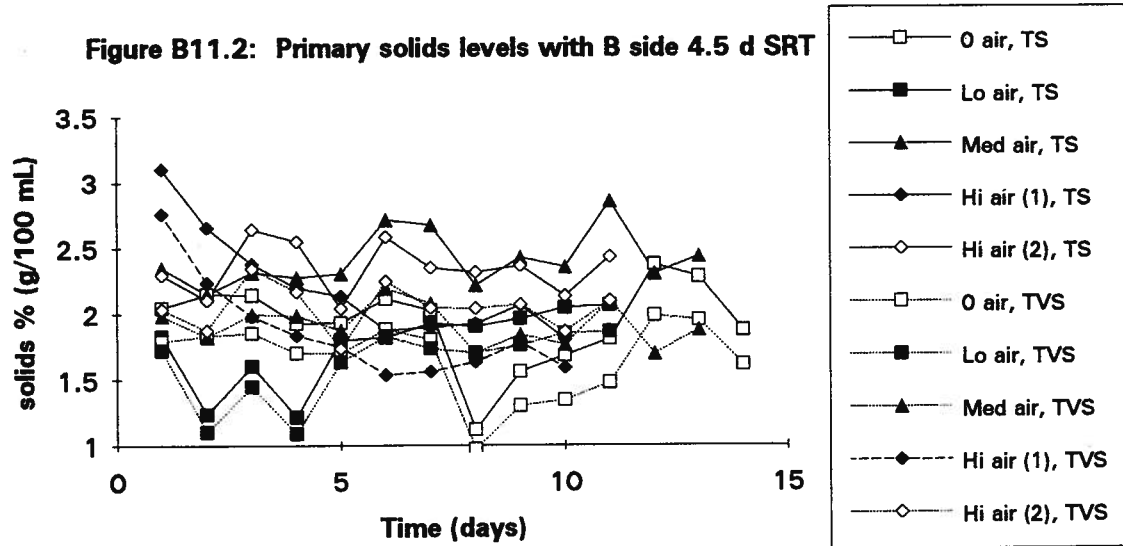


Figure B11.3: Primary solids levels with B side 6 d SRT

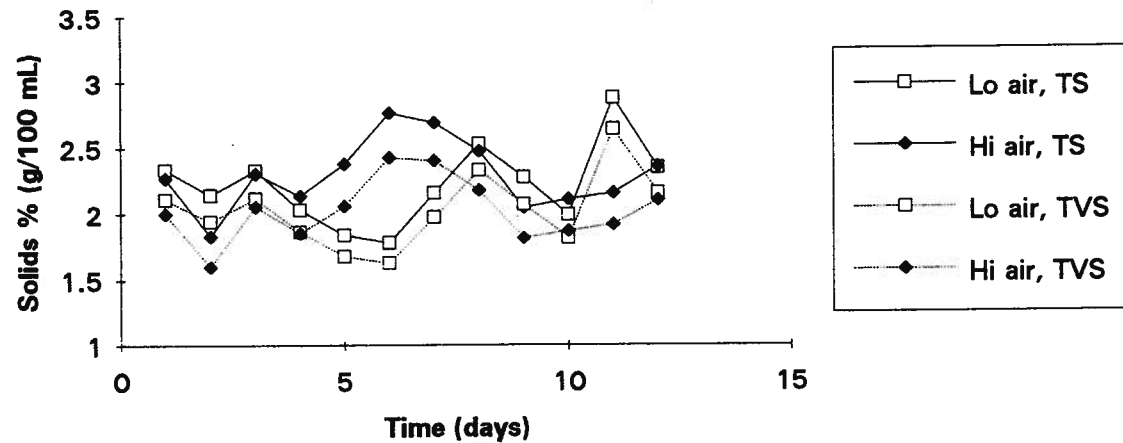


Figure B12.1: A side air flow with 4.5 d SRT

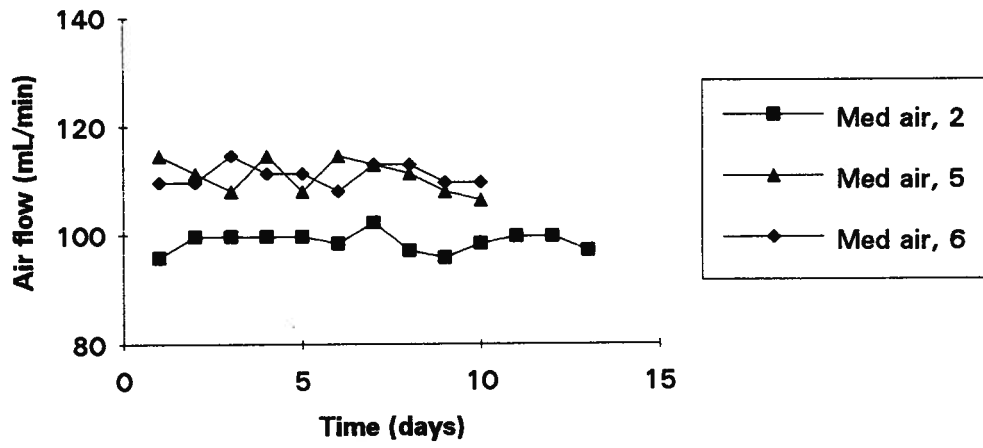


Figure B12.2: A side air flow with 4.5 d SRT

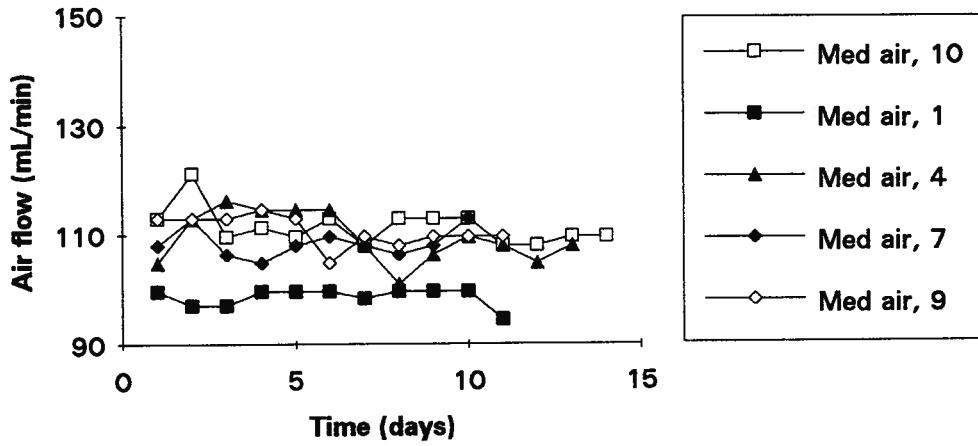


Figure B12.3: A side air flow with 4.5 d SRT

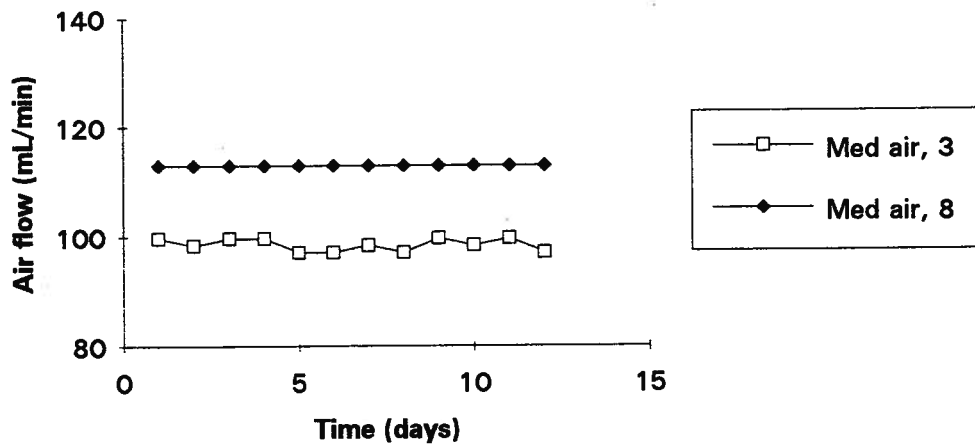


Figure B13.1: B side air flow with 3 d SRT

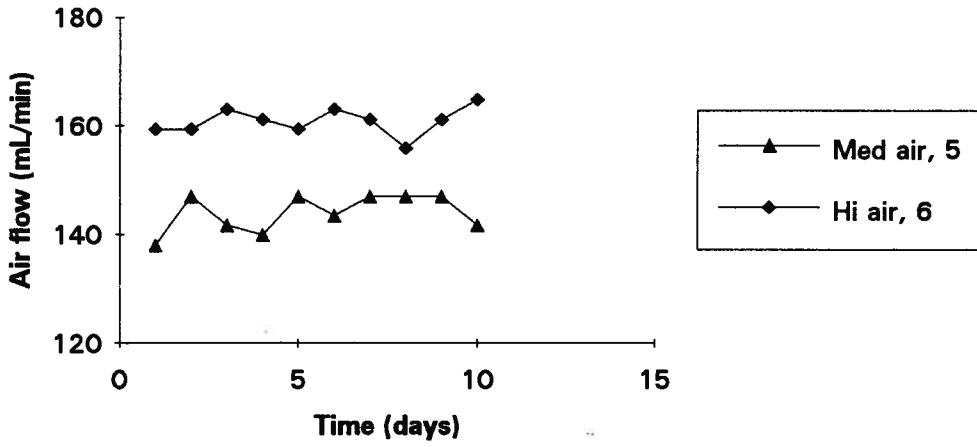


Figure B13.2: B side air flow with 4.5 d SRT

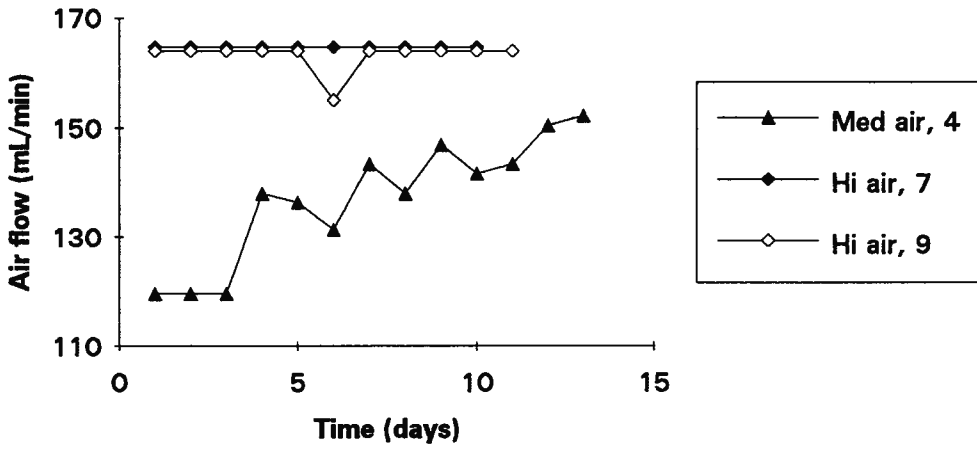


Figure B13.3: B side air flow with 6 d SRT

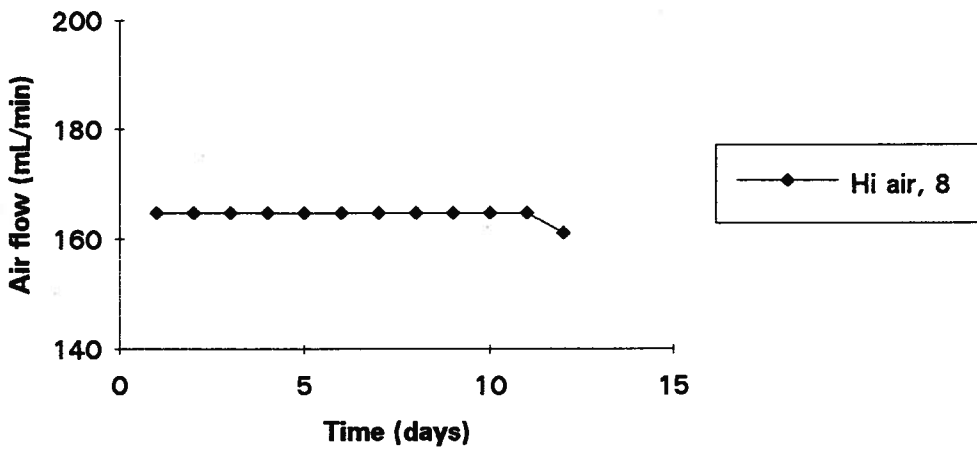


Figure B14.1: A side mixer RPM with 4.5 d SRT

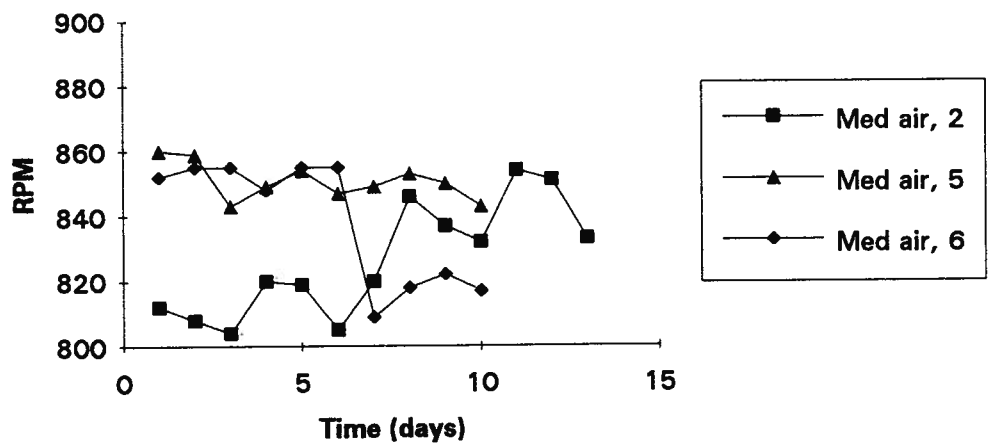


Figure B14.2: A side mixer RPM with 4.5 d SRT

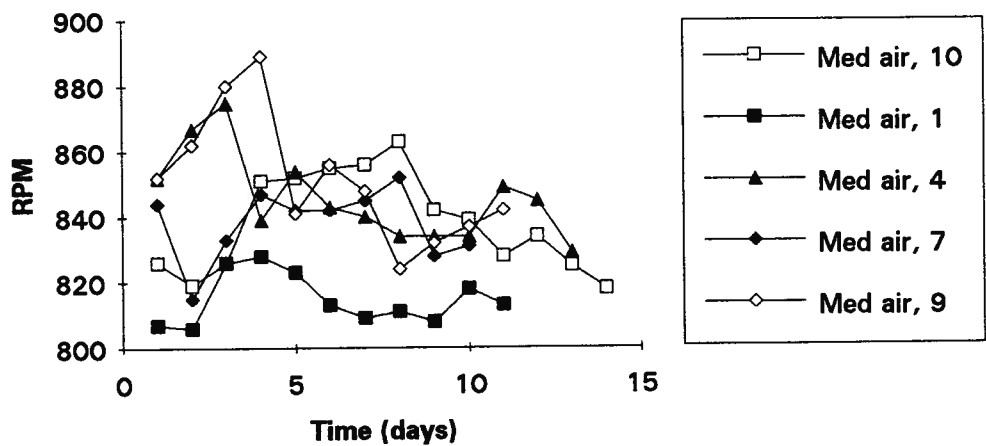


Figure B14.3: A side mixer RPM with 4.5 d SRT

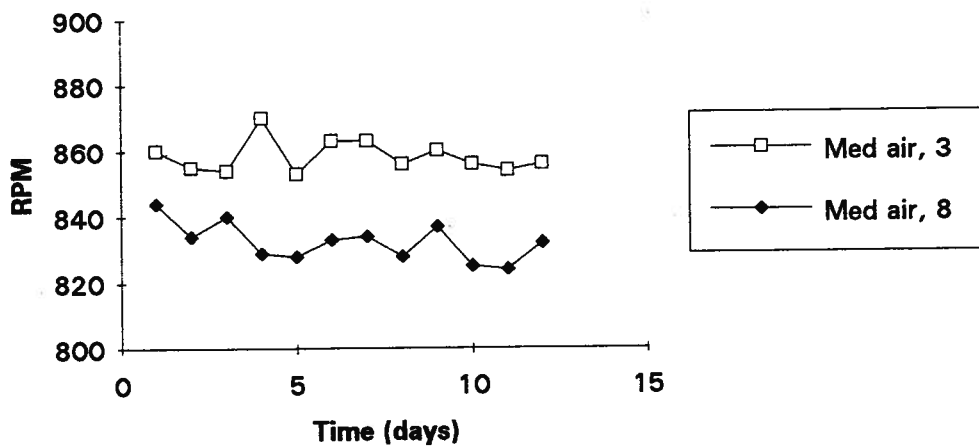


Figure B15.1: B side mixer RPM with 3 d SRT

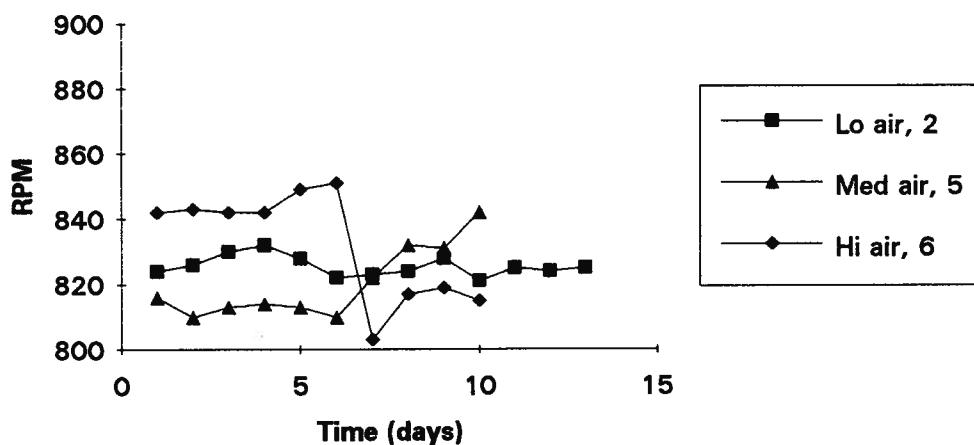


Figure B15.2: B side mixer RPM with 4.5 d SRT

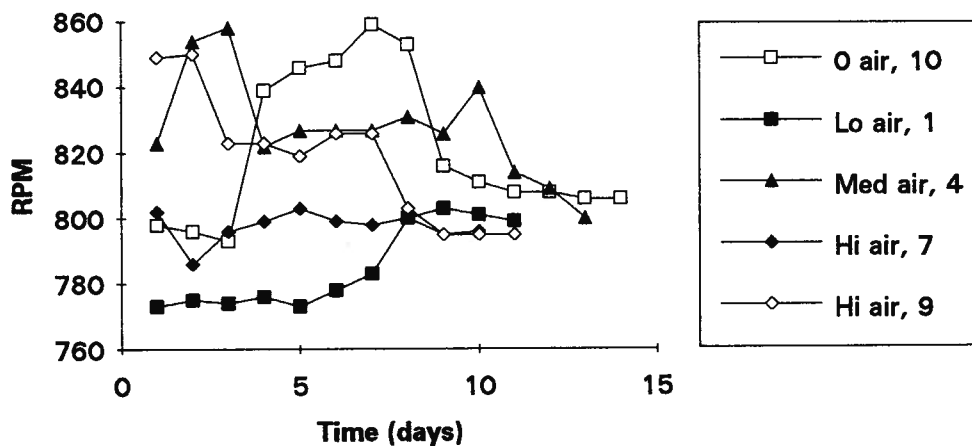


Figure B15.3: B side mixer RPM with 6 d SRT

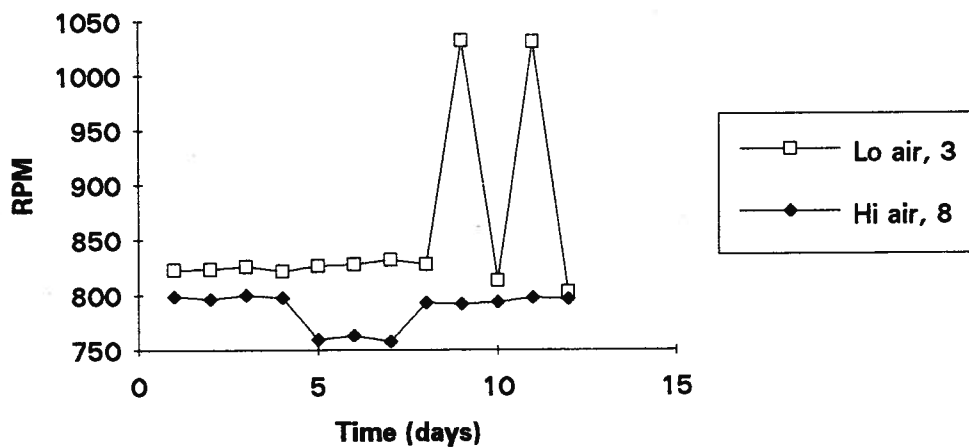


Figure B16.1: A side actual SRT for nominal B side 3 d SRT

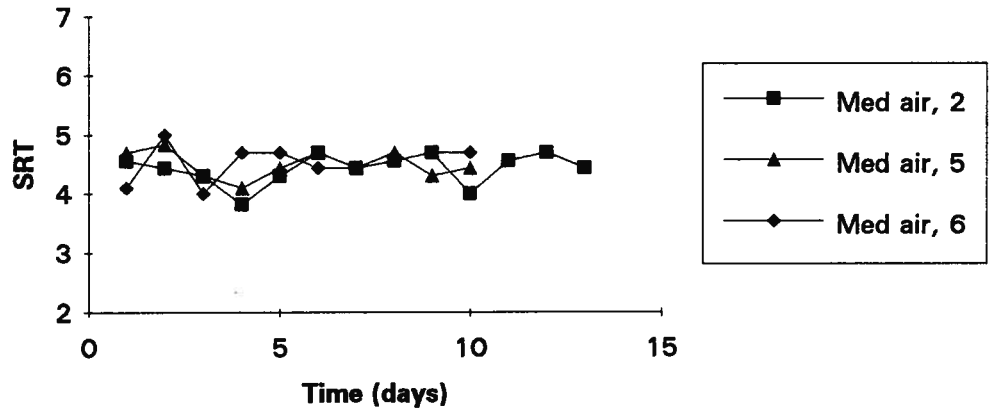


Figure B16.2: A side actual SRT for nominal B side 4.5 d SRT

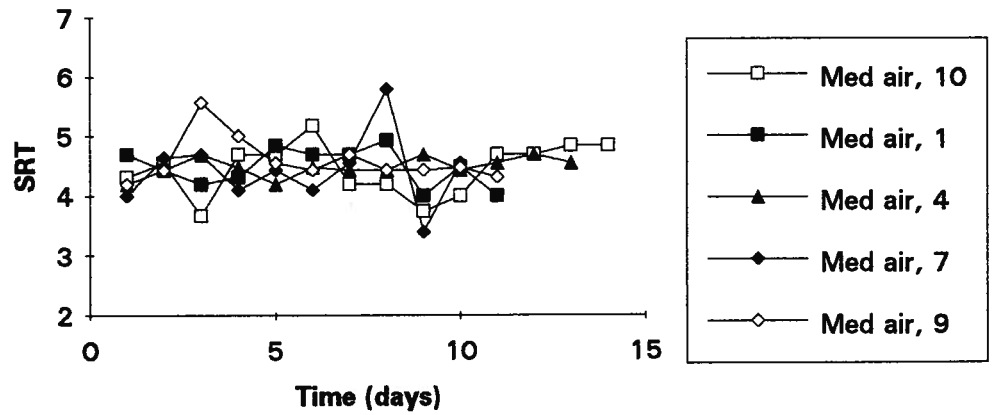


Figure B16.3: A side actual SRT for nominal B side 6 d SRT

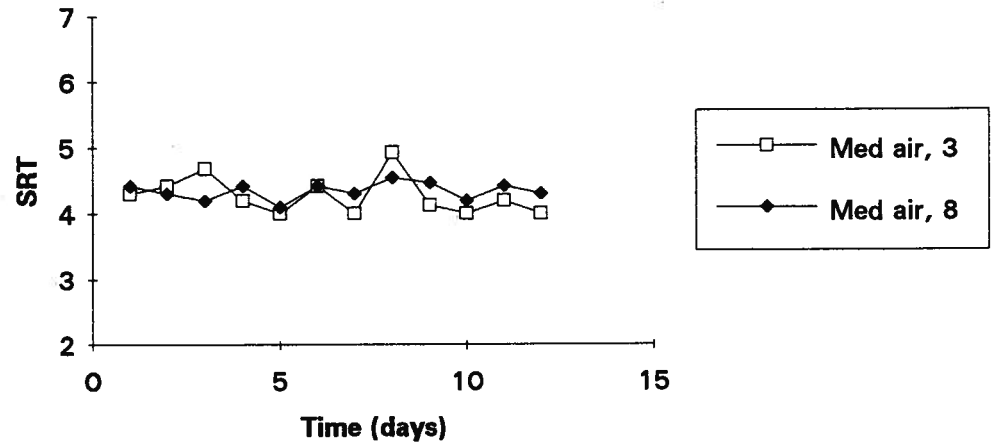


Figure B17.1: B side actual SRT for nominal B side 3 d SRT

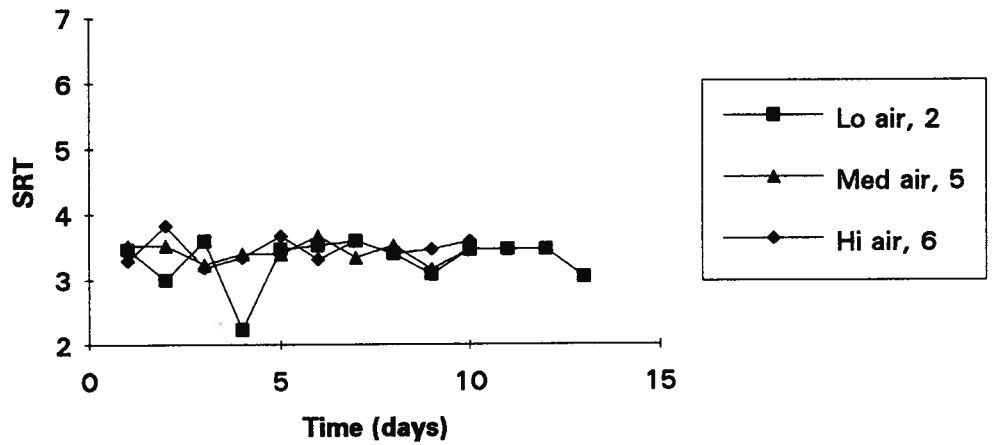


Figure B17.2: B side actual SRT for nominal B side 4.5 d SRT

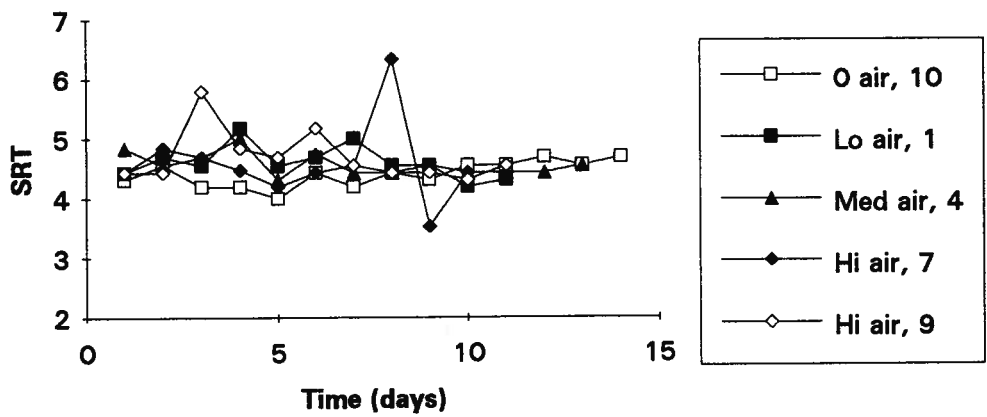


Figure B17.3: B side actual SRT for nominal B side 6 d SRT

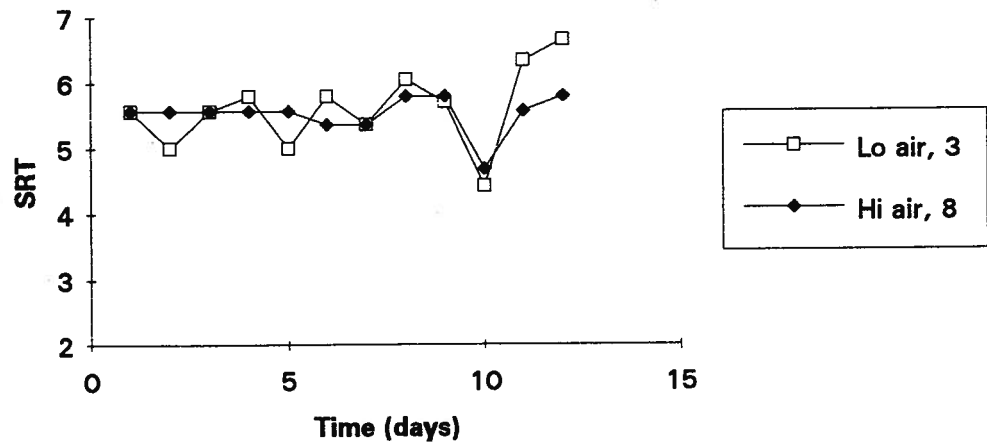


Figure B18.1: Temperature Variations, Sides A and B, Run 1

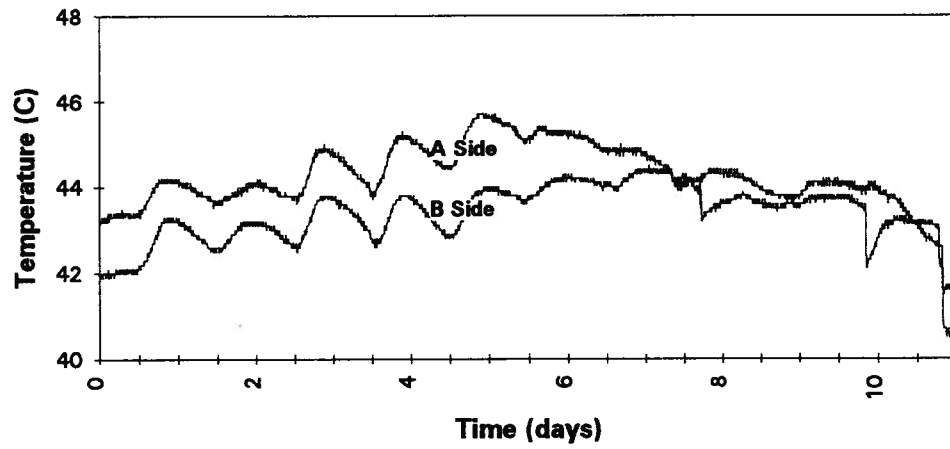


Figure B18.2: ORP Variations, Sides A and B, Run 1

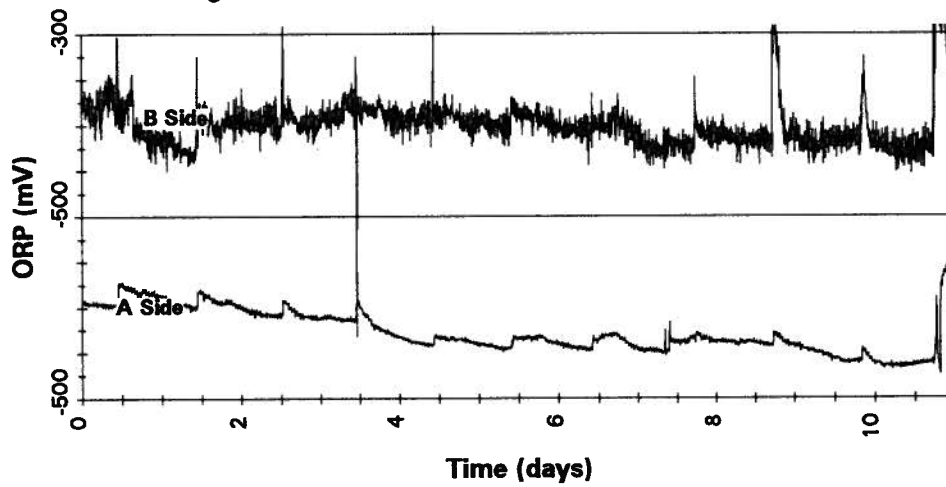


Figure B18.3: ORP FFTs, Sides A and B, Run 1

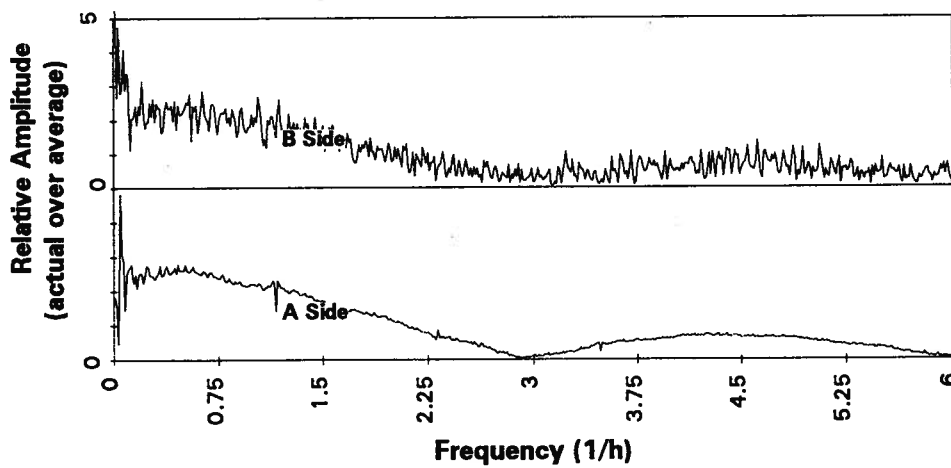


Figure B19.1: Temperature Variations, Sides A and B, Run 2

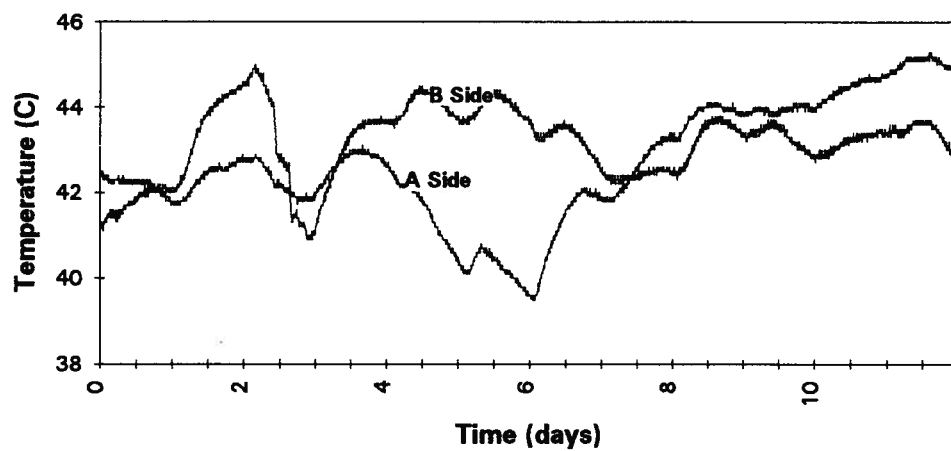


Figure B19.2: ORP Variations, Sides A and B, Run 2

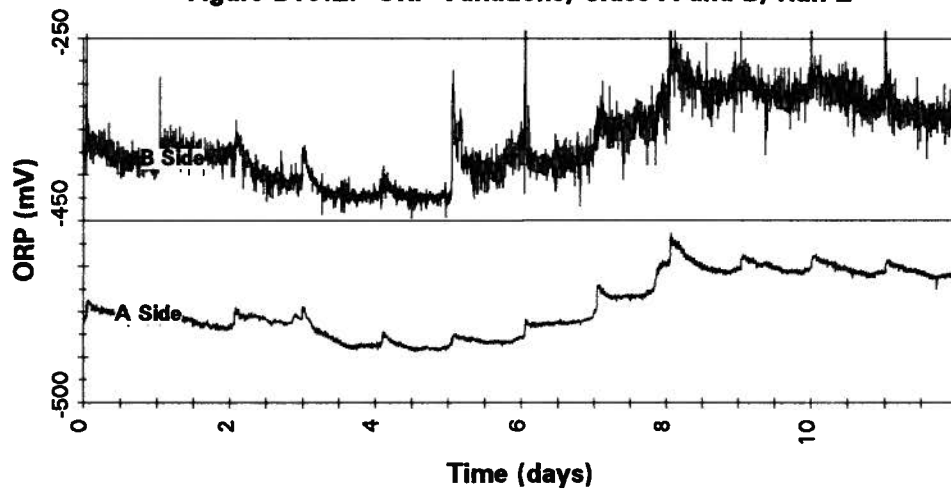
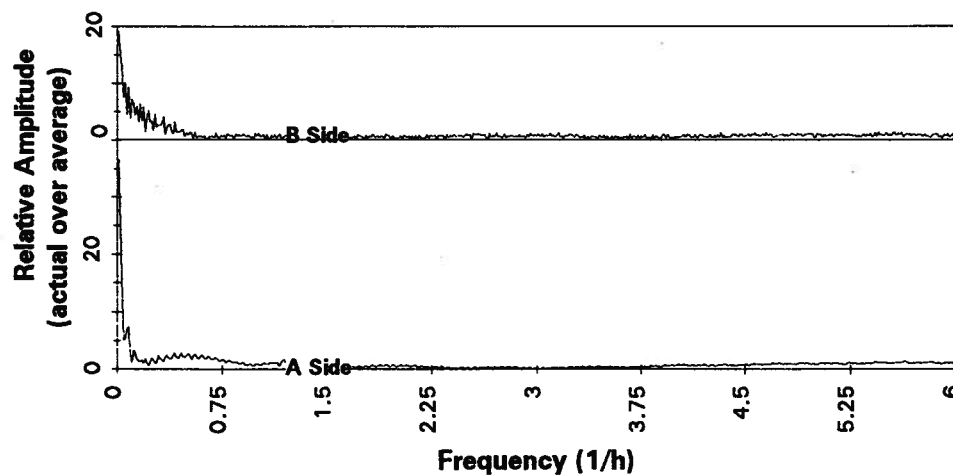
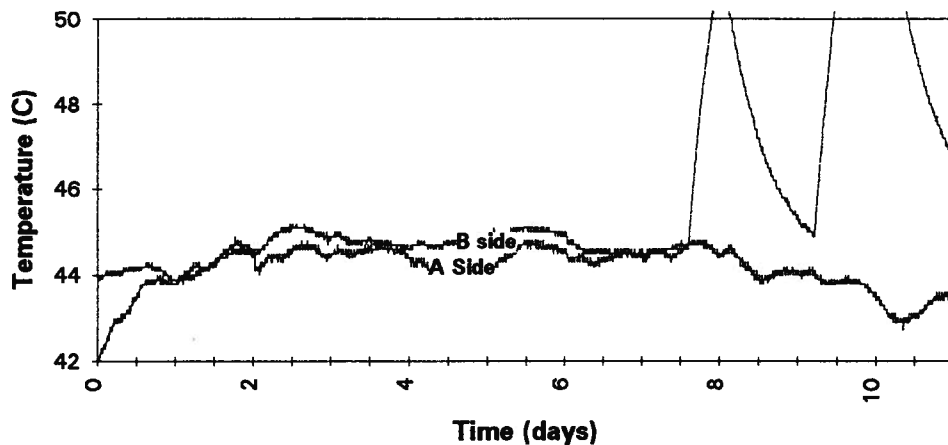


Figure B19.3: ORP FFTs, Sides A and B, Run 2



B20.1: Temperature Variations, Sides A and B, Run 3



B20.2: ORP Variations, Sides A and B, Run 3

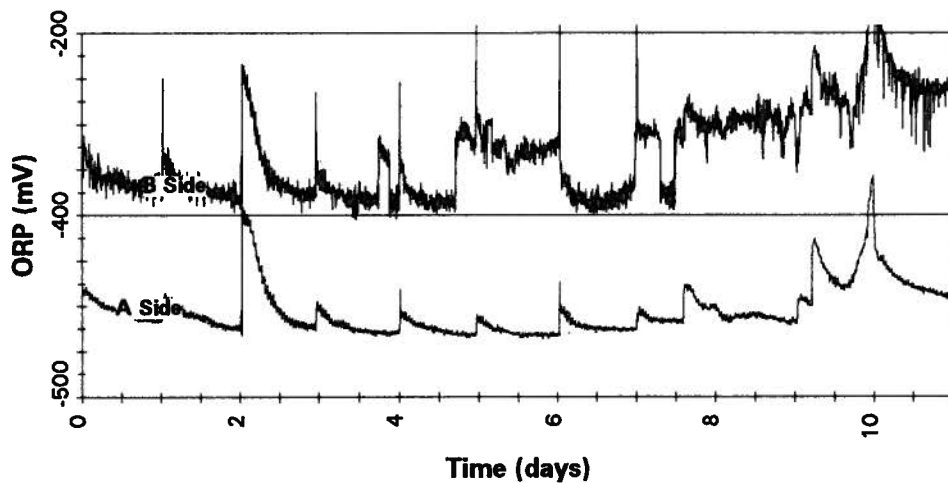


Figure B20.3: ORP FFTs, Sides A and B, Run 3

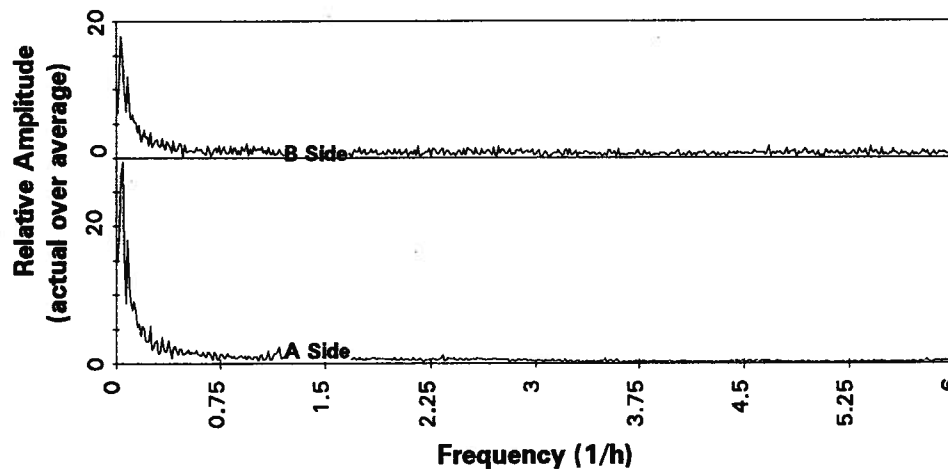


Figure B21.1: Temperature Variations, Sides A and B, Run 4

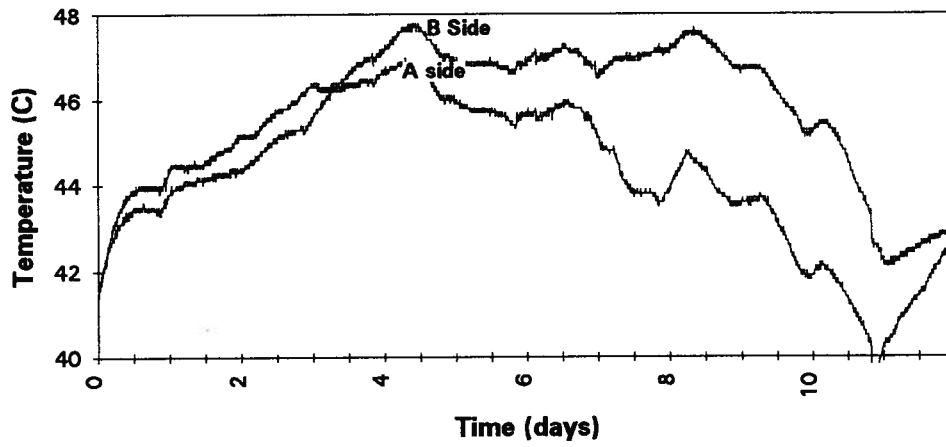


Figure B21.2: ORP Variations, Sides A and B, Run 4

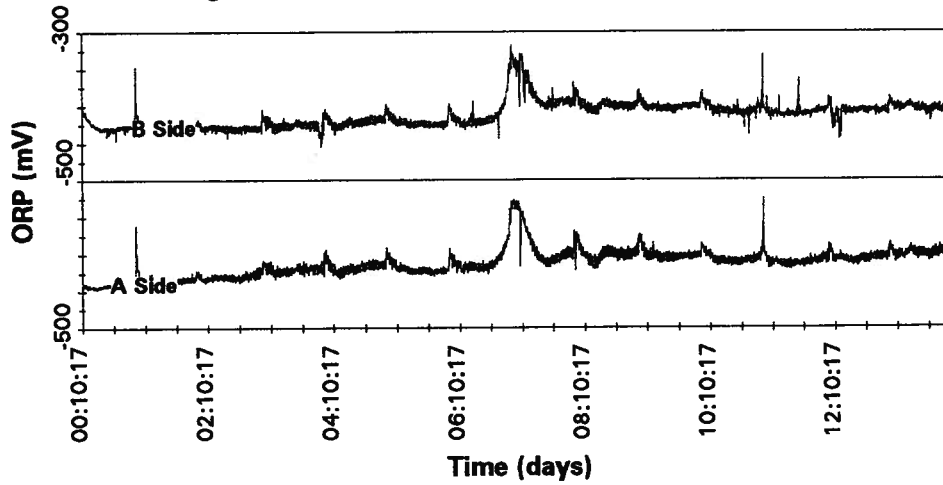


Figure B21.3: ORP FFTs, Sides A and B, Run 4

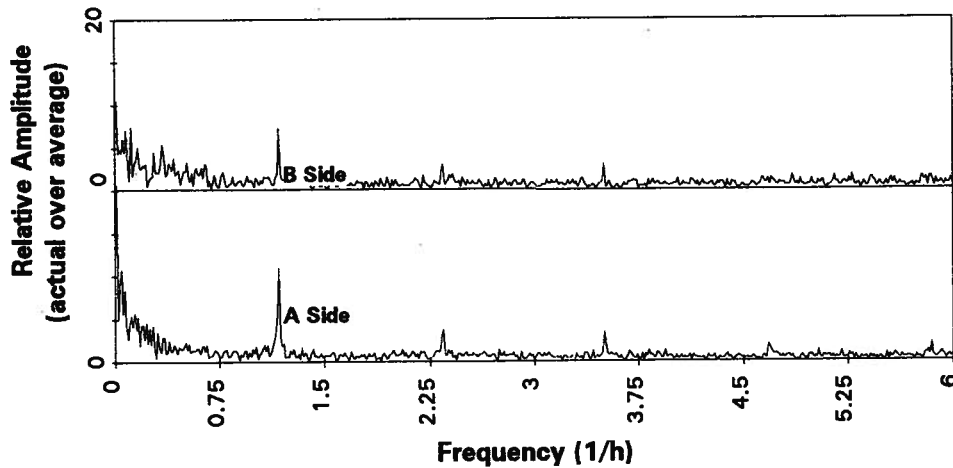


Figure B22.1: Temperature Variations, Sides A and B, Run 5

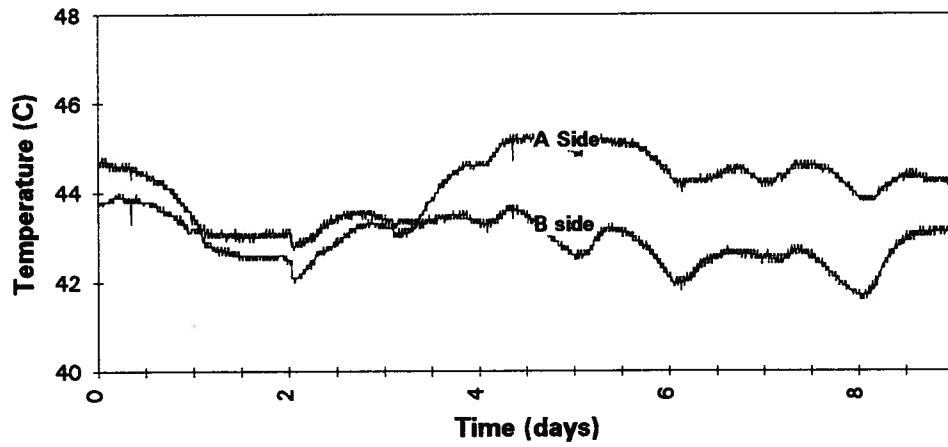


Figure B22.2: ORP Variations, Sides A and B, Run 5

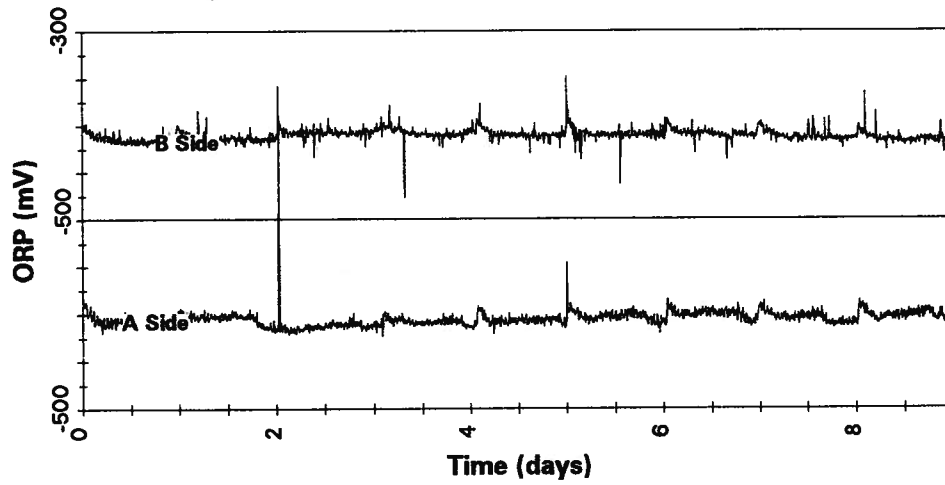


Figure B22.3: ORP FFTs, Sides A and B, Run 5

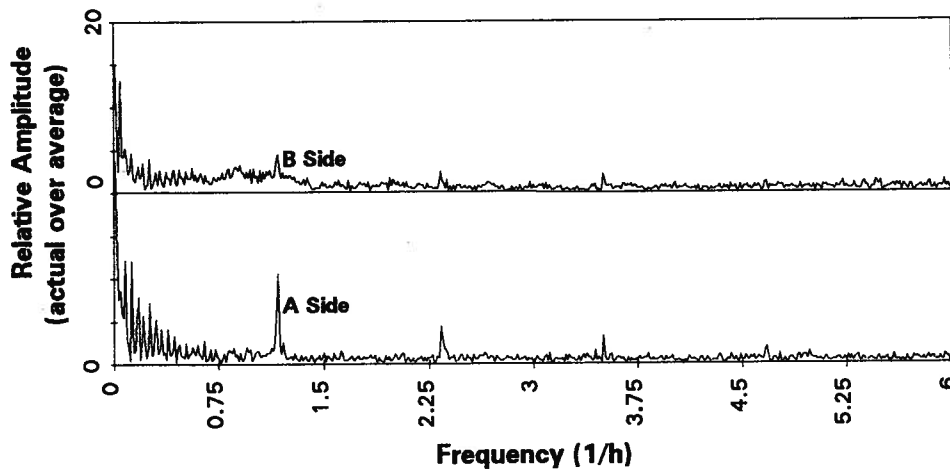


Figure B23.1: Temperature Variations, Sides A and B, Run 6

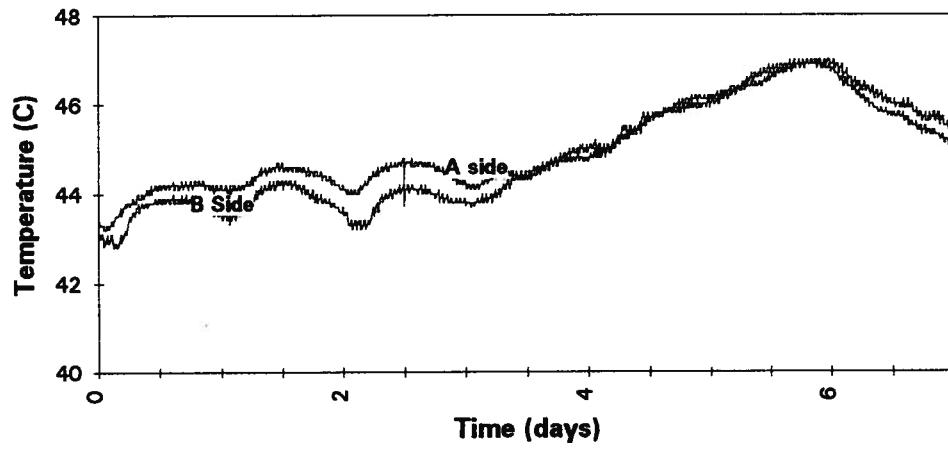


Figure B23.2: ORP Variations, Sides A and B, Run 6

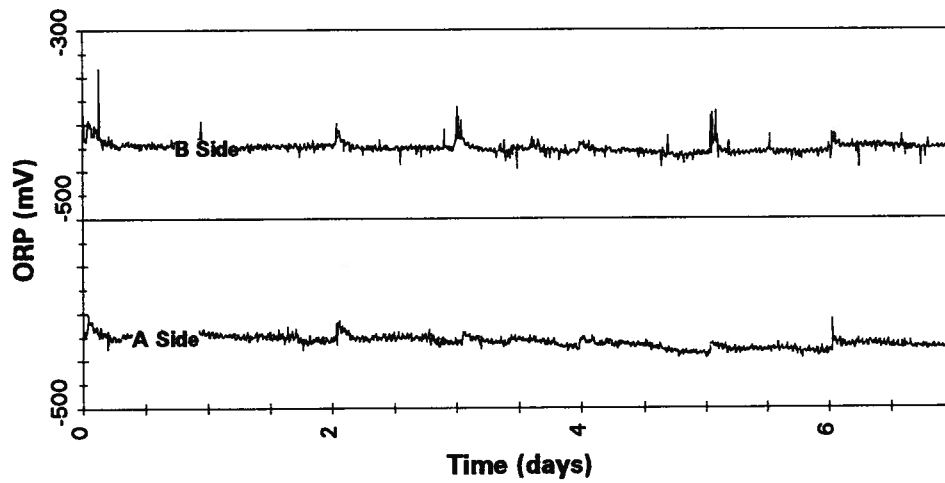


Figure B23.3: ORP FFTs, Sides A and B, Run 6

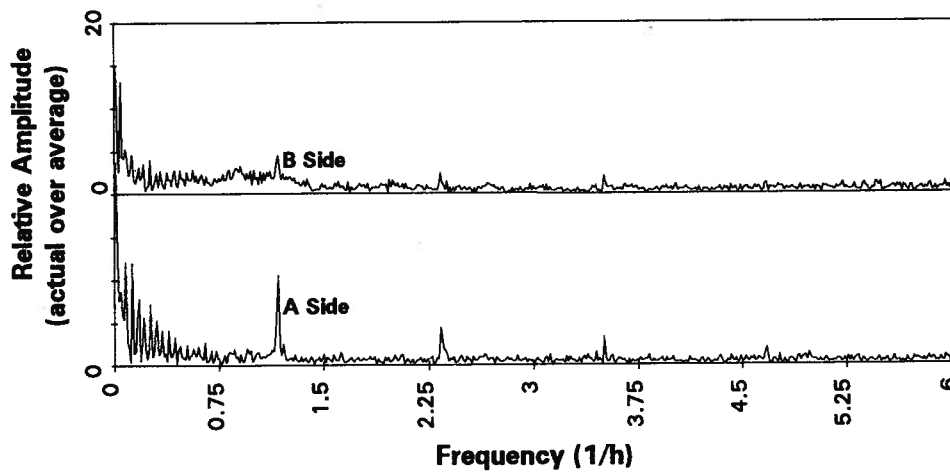


Figure B24.1: Temperature Variations, Sides A and B, Run 7

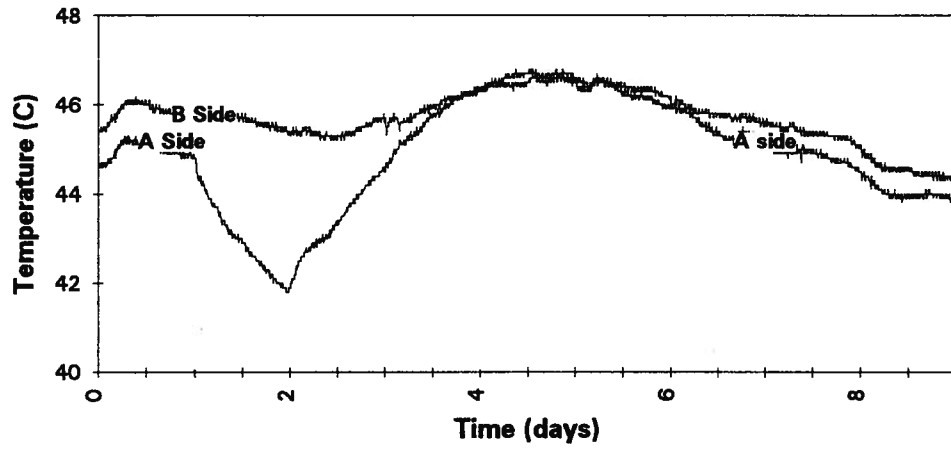


Figure B24.2: ORP Variations, Sides A and B, Run 7

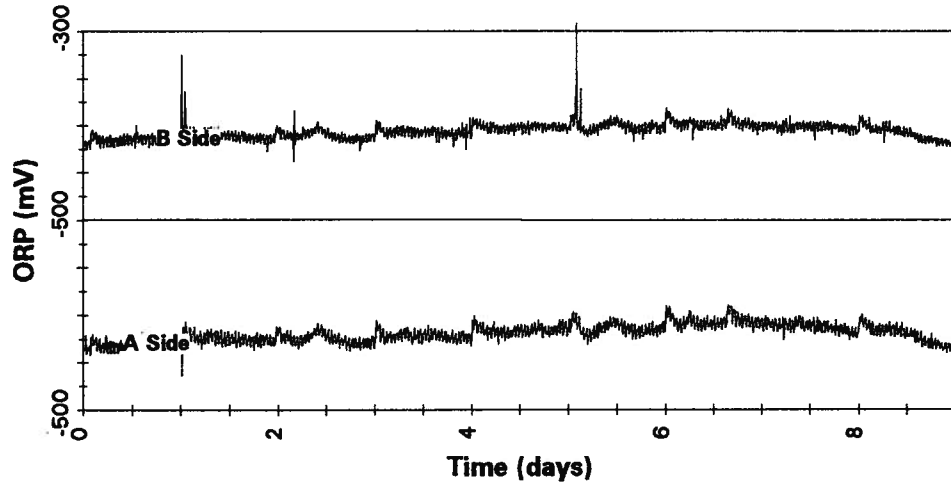


Figure B24.3: ORP FFTs, Sides A and B, Run 7

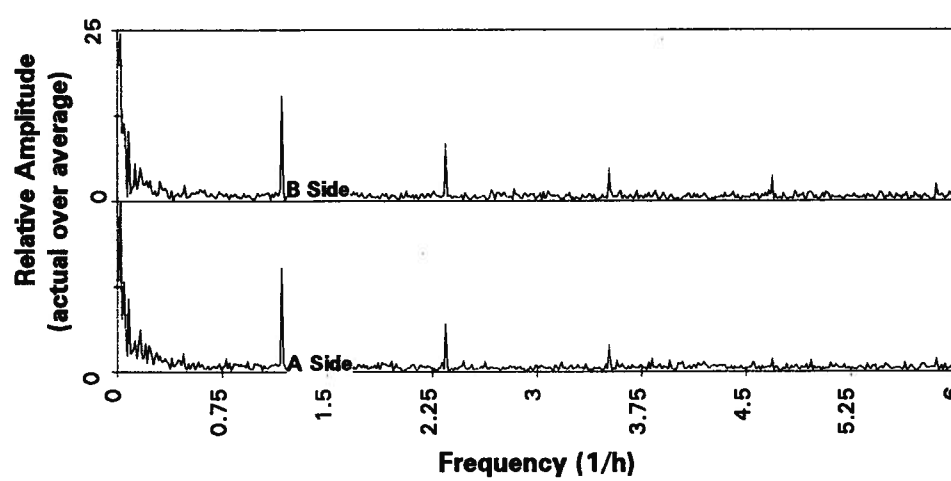


Figure B25.1: Temperature Variations, Sides A and B, Run 8

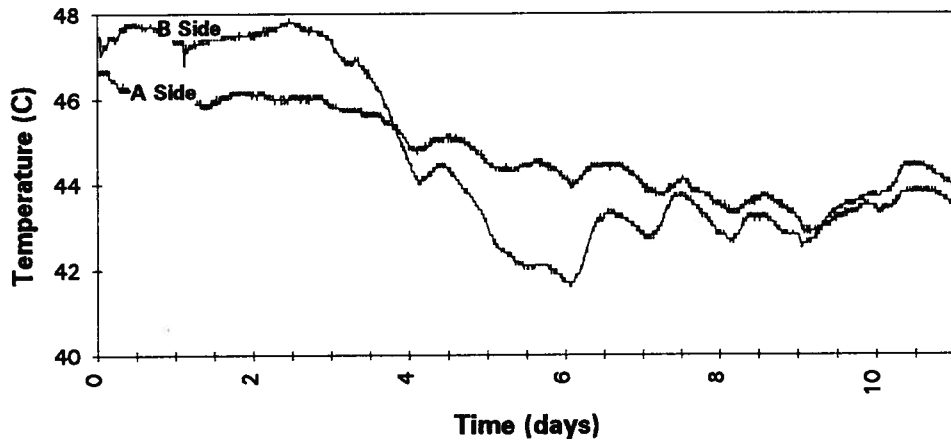


Figure B25.2: ORP Variations, Sides A and B, Run 8

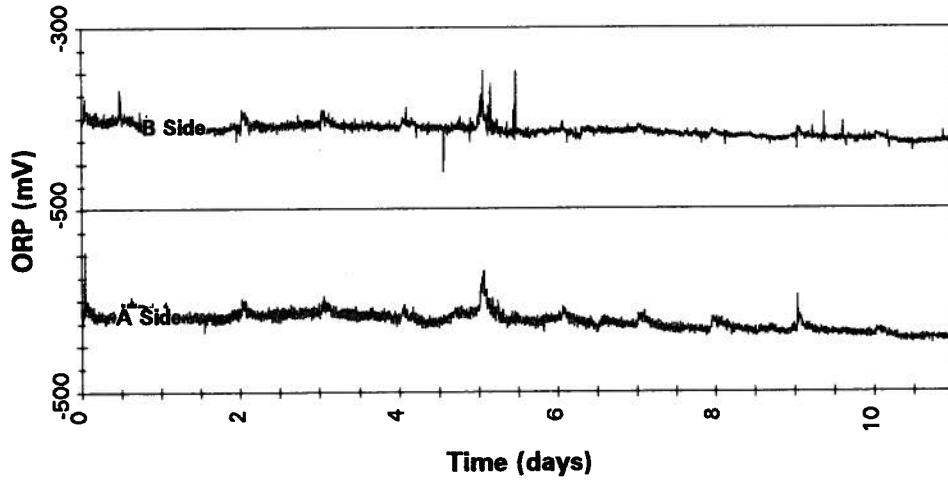


Figure B25.3: ORP FFTs, Sides A and B, Run 8

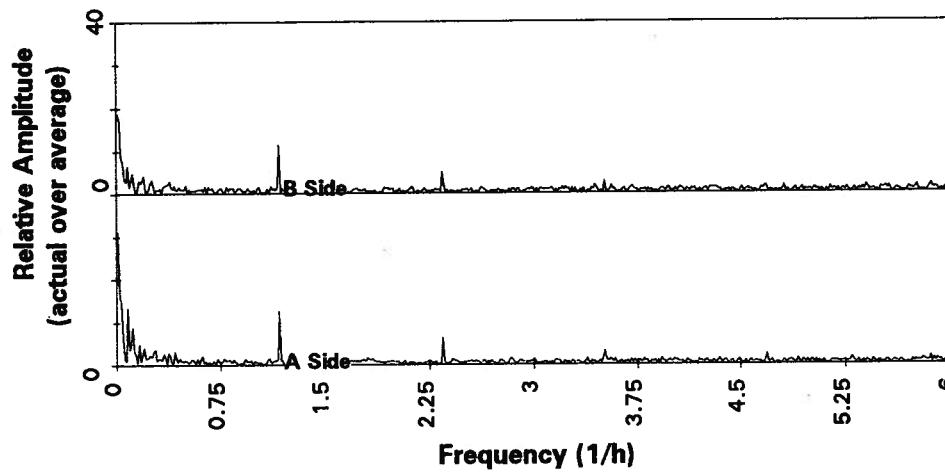


Figure B26.1: Temperature Variations, Sides A and B, Run 9

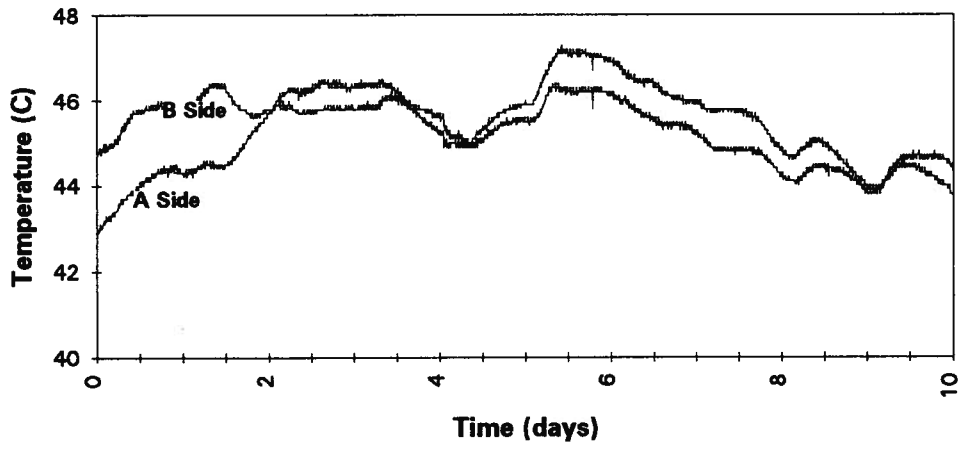


Figure B26.2: ORP Variations, Sides A and B, Run 9

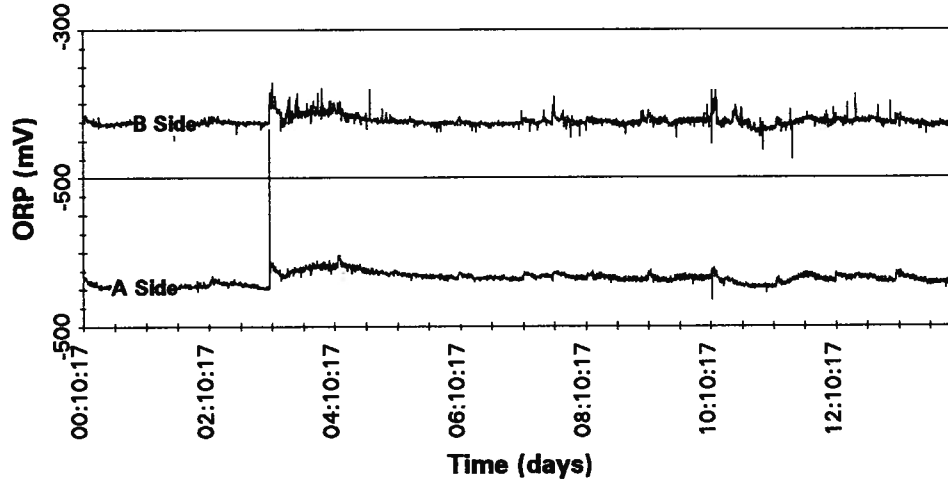


Figure B26.3: ORP FFTs, Sides A and B, Run 9

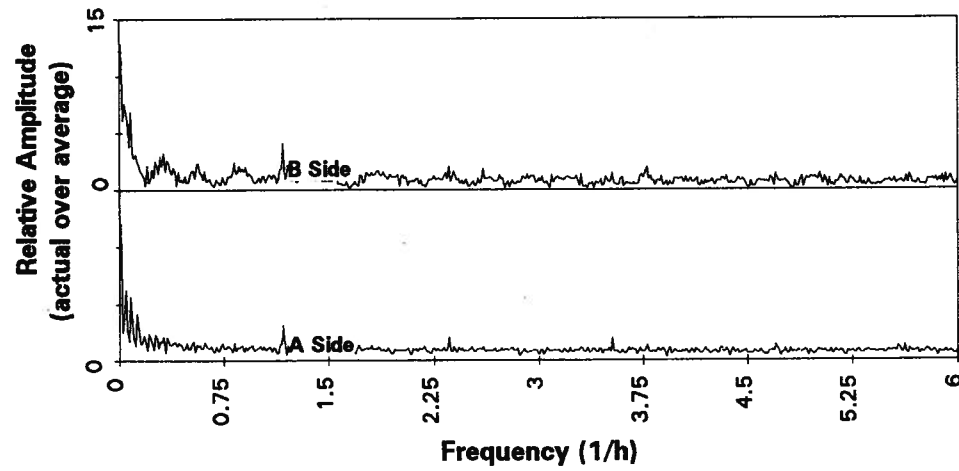


Figure B27.1: Temperature Variations, Sides A and B, Run 10

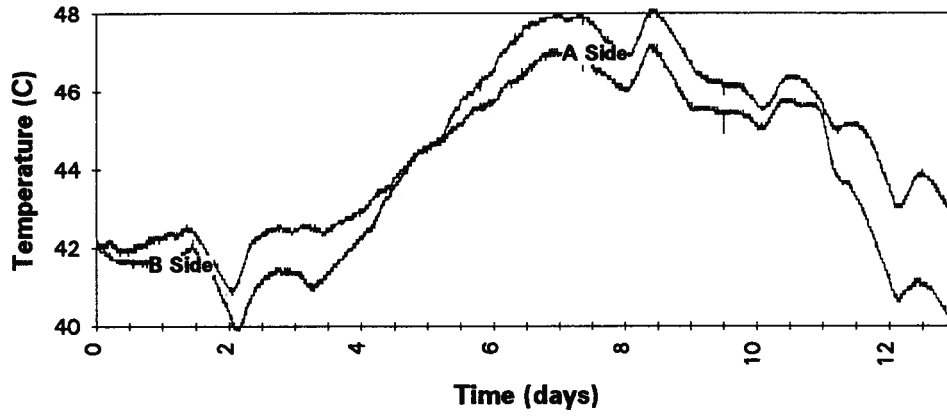


Figure B27.2: ORP Variations, Sides A and B, Run 10

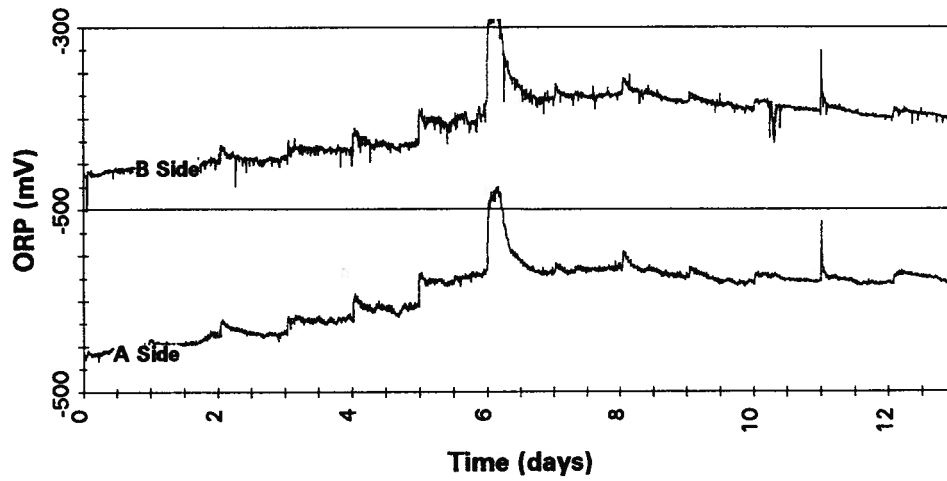
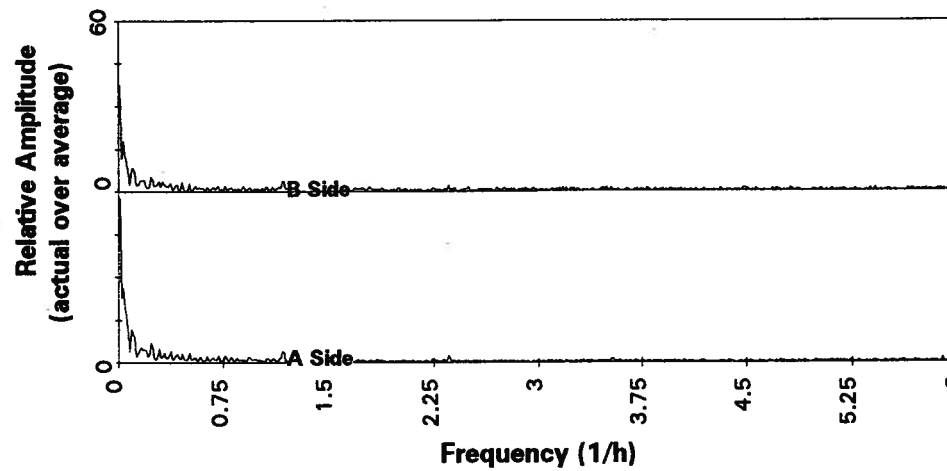


Figure 27.3: ORP FFTs, Sides A and B, Run 10



Appendix C: Preliminary Pilot Scale TAD Results

Figure C1.1: Temperature profiles over 1 SRT under the transition condition (0.28 V/V-h)	294
Figure C1.2: ORP profiles over 1 SRT under the transition condition (0.28 V/V-h)	294
Figure C2.1: Temperature profiles over 1 SRT under the aerobic condition (0.6 V/V-h)	295
Figure C2.2: ORP profiles over 1 SRT under the aerobic condition (0.6 V/V-h)	295
Figure C3.1: Temperature profiles over 1 SRT under the microaerobic condition (0 V/V-h)	296
Figure C3.2: ORP profiles over 1 SRT under the microaerobic condition (0 V/V-h)	296
Figure C4.1: [VFA] in stage 1 of TAD and total solids in primary sludge under the aerobic condition (0.6 V/V-h)	297
Figure C4.2: [VFA] in stage 1 of TAD and total solids in primary sludge under the transition condition (0.6 V/V-h)	297
Figure C4.3: [VFA] in stage 1 of TAD and total solids in primary sludge under the microaerobic condition (0.6 V/V-h)	297
Figure C5.1: [VFA] in the primary sludge under aerobic conditions (0.6 V/V-h)	298
Figure C5.2: [VFA] in the primary sludge under the transition condition (0.28 V/V-h)	298
Figure C5.3: [VFA] in the primary sludge under the microaerobic condition (0 V/V-h)	298

Figure C1.1: Temperature profiles over 1 SRT under the transition condition (0.28 V/V-h)

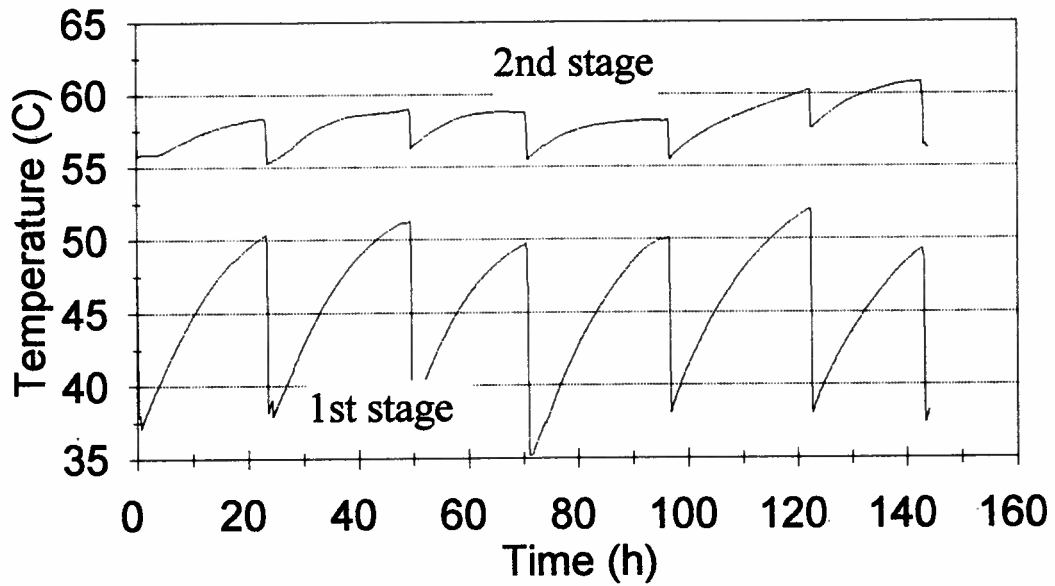
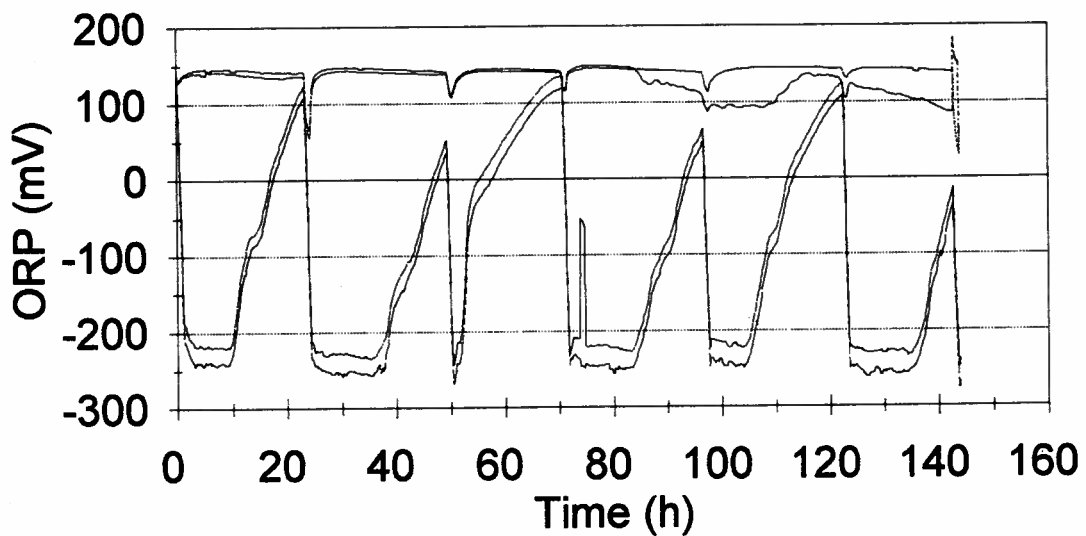


Figure C1.2: ORP profiles over 1 SRT under the transition condition (0.28 V/V-h)



— ORP 1 --- ORP 1A - · - ORP 2 · · · ORP 2A

Figure 2.1: Temperature profiles over 1 SRT under the aerobic condition (0.6 V/V-h).

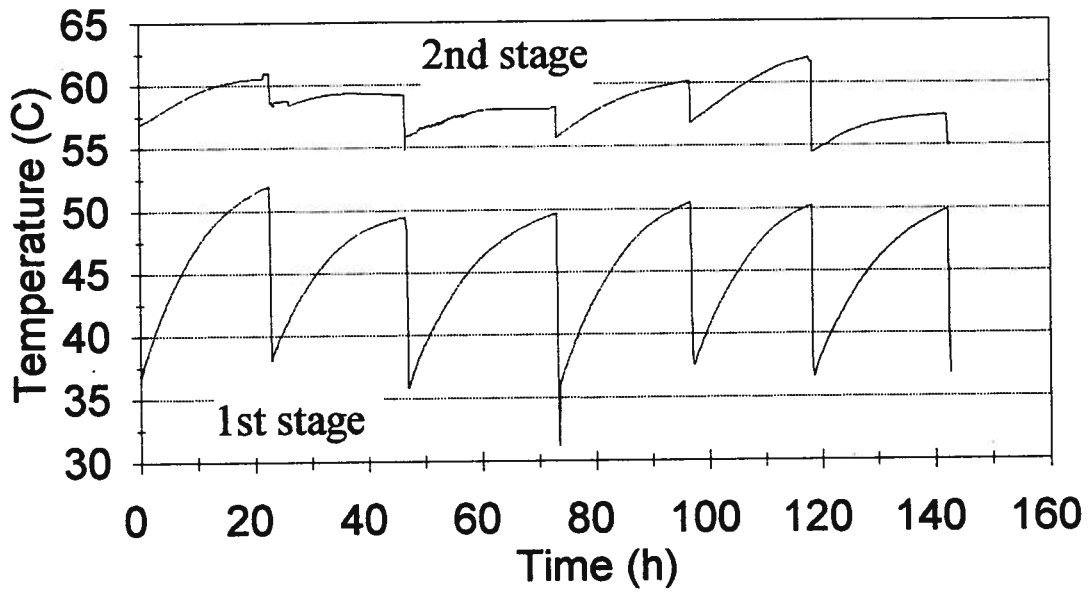
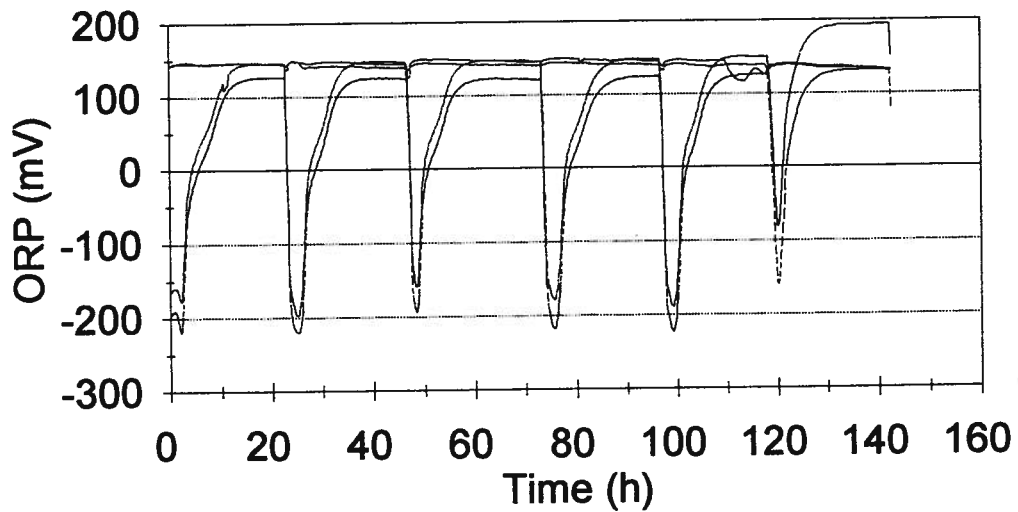


Figure 2.2: ORP profiles over 1 SRT under the aerobic condition (0.6 V/V-h).



— ORP 1 --- ORP 1A - · - ORP 2 · · · ORP 2A

Figure C3.1: Temperature profiles over 1 SRT under the microaerobic condition (0 V/V-h).

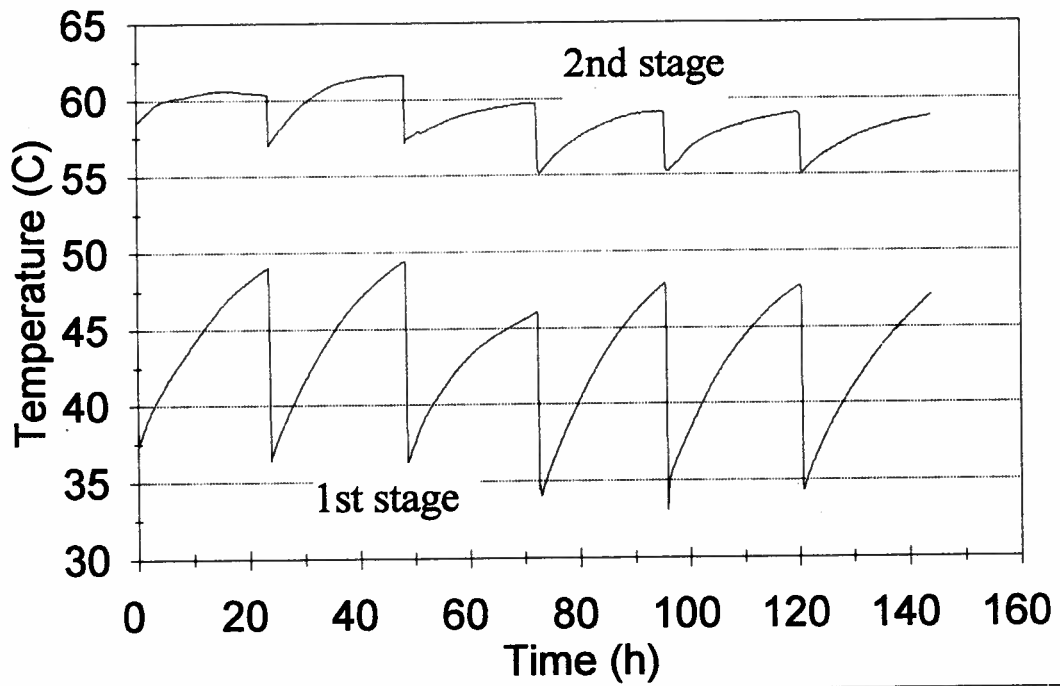
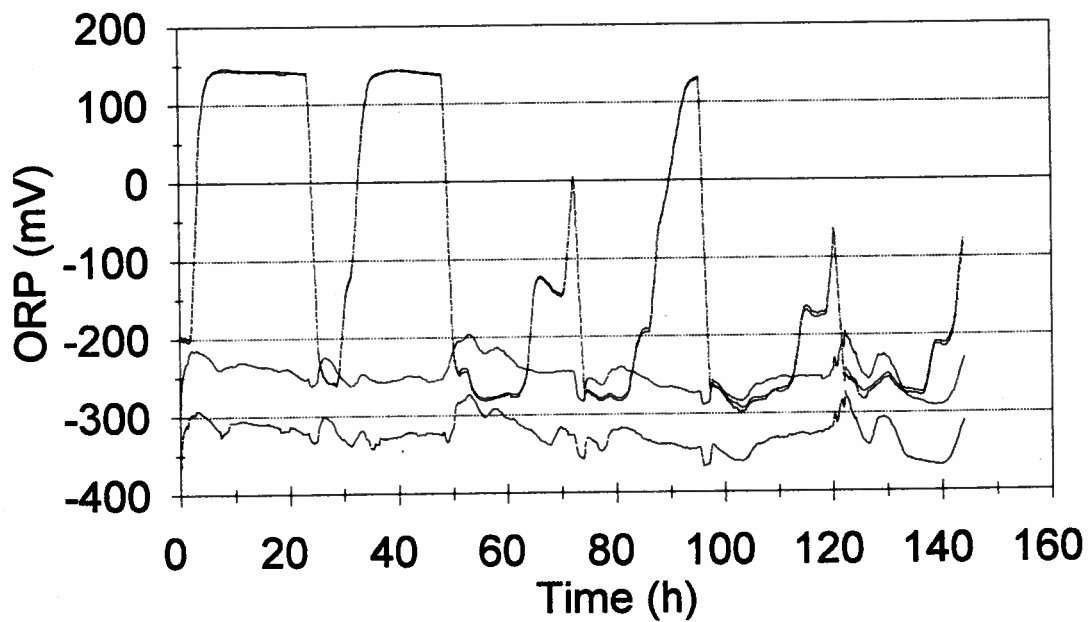


Figure C3.2: ORP profiles over 1 SRT under the microaerobic condition (0 V/V-h).



— ORP 1 --- ORP 1A - · - ORP 2 ··· ORP 2A

Figure C4.1: [VFA] in stage 1 of TAD and total solids in primary sludge under the aerobic condition (0.6 V/V-h).

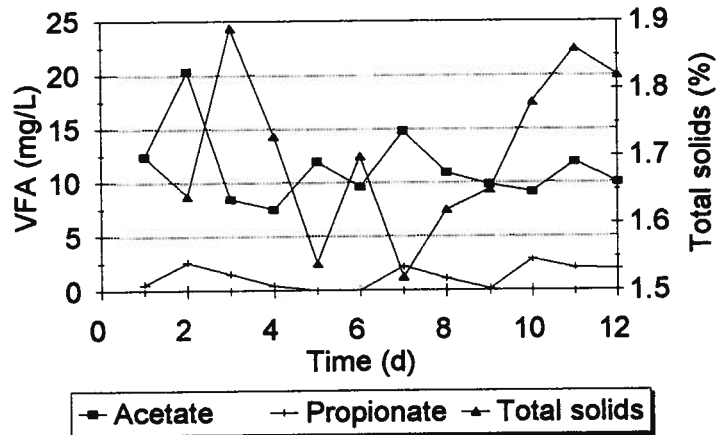


Figure C4.2: [VFA] in stage 1 of TAD and total solids in primary sludge under the transition condition (0.28 V/V-h).

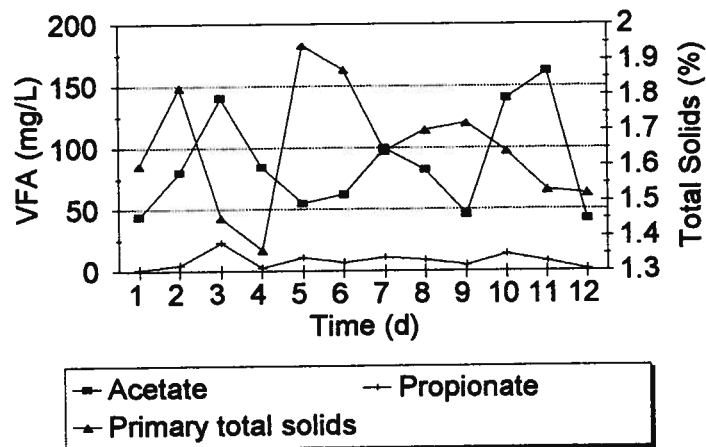


Figure C4.3: [VFA] in stage 1 of TAD and total solids in primary sludge under the microaerobic condition (0 V/V-h).

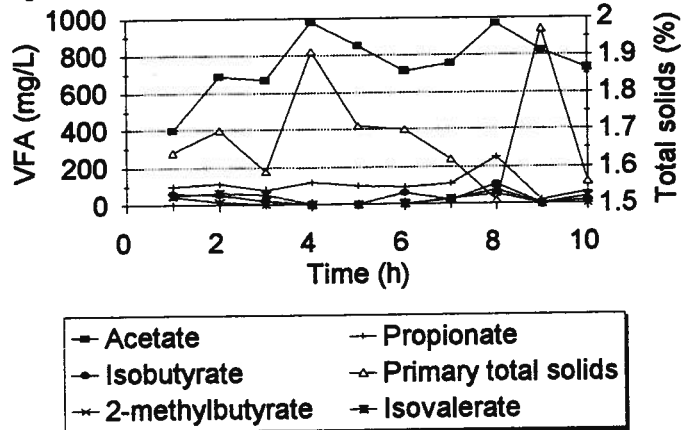


Figure C5.1: [VFA] in the primary sludge under aerobic conditions (0.6 V/V-h).

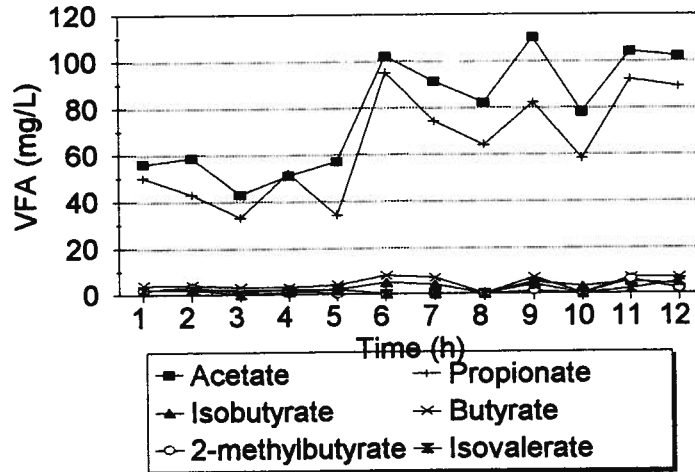


Figure C5.2: [VFA] in the primary sludge under the transition condition (0.28 V/V-h).

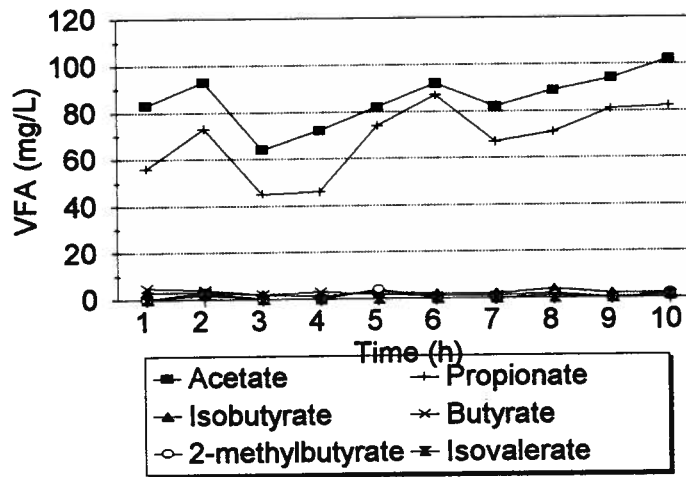
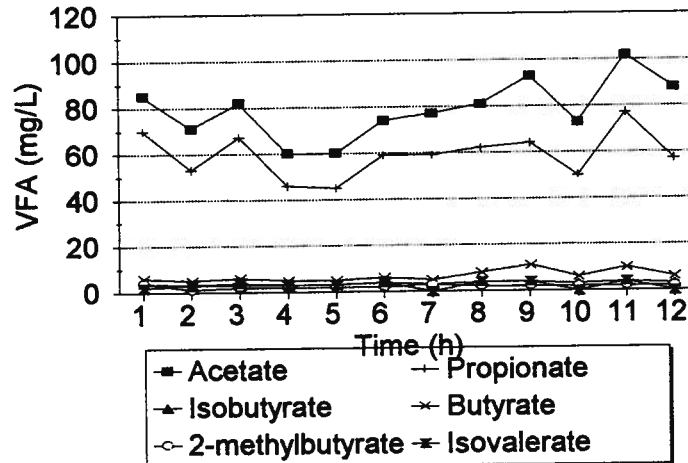


Figure C5.3: [VFA] in the primary sludge under the microaerobic condition (0 V/V-h).



Appendix D: Test Chemicals

Table D1: Chemical structure of compounds.

Compound	Structure
Acetic acid	CH_3COOH
Ethanol	$\text{CH}_3\text{CH}_2\text{OH}$
Propanol	$\text{CH}_3\text{CH}_2\text{CH}_2\text{OH}$
Propionic acid	$\text{CH}_3\text{CH}_2\text{COOH}$
Lactic acid	$\text{CH}_3\text{CHOHCOOH}$
Pyruvic acid	$\text{CH}_3\text{COCO OH}$
Butyric acid	$\text{CH}_3(\text{CH}_2)_2\text{COOH}$
Isobutyric acid	$(\text{CH}_3)_2\text{CHCOOH}$
Valeric acid	$\text{CH}_3(\text{CH}_2)_3\text{COOH}$
Isovaleric acid	$(\text{CH}_3)_2\text{CHCH}_2\text{COOH}$
Glucose	$\text{CHO}(\text{CHOH})_4\text{CH}_2\text{OH}$
Dextrin	$(\text{C}_6\text{H}_{10}\text{O}_5)_n\text{xH}_2\text{O}$
Linoleic acid	$\text{C}_{18}\text{H}_{30}\text{O}_2$
2-methylbutyric acid	$\text{CH}_3\text{CH}_2\text{CH}_2\text{CHCOOH}$
Toxicants:	
2,4-dinitrophenol	$(\text{NO}_2)_2\text{C}_6\text{H}_3\text{OH}$
Fluoride	F^-
Sodium cyanide	NaCN